NONLINEAR VIBRATIONS OF CURVED SINGLE AND DOUBLE WALLED CARBON NANOTUBES

A THESIS SUBMITTED TO
THE GRADUATE SCHOLL OF NATURAL AND APPLIED SCIENCES
OF
MIDDLE EAST TECHNICAL UNIVERSITY

BY

HAMED SAMANDARI

IN PARTIAL FULFILLMENT OF THE REQOURMENTS
FOR
THE DEGREE OF DOCTOR OF PHILOSOPHY
IN
MECHANICAL ENGINEERING

JULY 2014

© Copyright by Hamed Samandari 2014

All Rights Reserved

Approval of this thesis:

NONLINEAR VIBRATIONS OF CURVED SINGLE AND DOUBLE WALLED CARBON NANOTUBES

submitted by **HAMED SAMANDARI** in partial fulfillment of the requirements for the degree of **Doctor of Philosophy in Mechanical Engineering Department, Middle East Technical University** by,

Prof Dr. Canan Özgen _____
Dean, Graduate School of **Natural and Applied Science**

Prof. Dr. Suha Oral _____
Head of Department, **Mechanical Engineering**

Assoc. Prof. Dr. Ender Cigeroglu _____
Supervisor, **Mechanical Engineering Dept., METU**

Examining Committee Members:

Prof. Dr. Fevzi Suat Kadıoğlu _____
Mechanical Engineering Dept., METU

Assoc. Prof. Dr. Ender Cigeroglu _____
Mechanical Engineering Dept., METU

Assist. Prof. Dr. Yigit Yazicioglu _____
Mechanical Engineering Dept., METU

Assist. Prof. Dr. Mehmet Bulent Ozer _____
Mechanical Engineering Dept., TOBB

Assist. Prof. Dr. Caglar Baslamisli _____
Mechanical Engineering Dept., HACC

Date: 17/07/2014

I hereby declare that all information in this document has been obtained and presented in accordance with academic rules and ethical conduct. I also declare that, as required by these rules and conduct, I have fully cited and referenced all material and results that are not original to this work.

Name, Last name: Hamed Samandari

Signature :

ABSTRACT

NONLINEAR VIBRATIONS OF CURVED SINGLE AND DOUBLEWALLED CARBON NANOTUBES

Samandari, Hamed
Ph.D., Department of Mechanical Engineering
Supervisor: Assoc. Prof. Dr. Ender Cigeroglu

July 2014, 191 pages

In this thesis, effects of Geometric, initial curvature, and van der Waals (vdW) interlayer force nonlinearities on the variation of nonlinear natural frequency of Carbon Nanotubes (CNTs) are investigated in detail throughout several case studies. Galerkin method with a single trial function, which is the eigenfunction of the linear system, is widely used in literature in studying nonlinear vibrations of CNTs. However, eigenfunctions of the nonlinear systems can be significantly different than the eigenfunctions of the linear system. Therefore, depending on the nonlinearity, it may not be possible to capture the nonlinear characteristics by using a single trial function. Consequently, for the first time in this thesis, multiple trial functions are used to investigate the nonlinear free vibrations of CNTs. Moreover, a new solution approach– describing function method– is proposed which has the advantage of expressing the nonlinear force as a nonlinear complex stiffness matrix multiplied by displacement vector, where the off-diagonal terms of the nonlinear stiffness matrix can provide a comprehensive knowledge about the coupling between the trial functions. Depending on the boundary conditions considered, it is hard to find suitable trial functions that satisfies all the boundary conditions; hence, in order to overcome this difficulty, iterative path following method (IPFM) based on differential quadrature method (DQM) is developed which does not require trial functions. It is concluded that DQM based nonlinear solution method is very promising in solving nonlinear continuous systems, since it requires less number of gird points which results in less number of nonlinear equations compared to finite element methods.

Keywords: Nonlinear vibration, Curved carbon nanotubes, Nano resonators, Geometric nonlinearity, Van der Waals force nonlinearity

ÖZ

TEK VE ÇİFT DUVARLI KAVİSLİ KARBON NANOTÜPLERİN DOĞRUSAL OLMAYAN TİTREŞİMLERİ

Samandari, Hamed
Doktora, Makina Mühendisliği Bölümü
Tez Yöneticisi: Assoc. Prof. Dr. Ender Ciğeroğlu

Temmuz 2014, 191 sayfa

Bu tezde, geometrik, başlangıç kavisi ve van der Waals kuvvetleri kaynaklı doğrusal olmayan etkilerin (doğrusalsızlıkların) karbon nanotüplerin (KNT'lerin) doğrusal olmayan doğal frekans değişimi üzerindeki etkisi çeşitli vaka analizleri ile detaylı olarak incelenmiştir. Sınama (deneme) fonksiyonu doğrusal sistemin özfonksitonu olan tek sınama fonksiyonu kullanan Galerkin metodu literatürde karbon nanotüplerin doğrusal olmayan titreşimleri için sıklıkla kullanılmaktadır. Ancak, doğrusal olmayan sistemler için elde edilen doğrusal olmayan sistemlerin özfonksiyonları doğrusal sistemlerin özfonksiyonlarından önemli ölçüde farklı olabilmektedir. Dolayısıyla, doğrusalsızlığa bağlı olarak tek sınama fonksiyonu kullanarak doğrusal olmayan karakteristiklerin yakalanması mümkün olmayabilmektedir. Bu sebeple, ilk kez bu tez çalışmasında KNT'lerin doğrusal olmayan titreşimlerini incelemek için çoklu sınama fonksiyonu kullanılmıştır. Buna ek olarak, doğrusal olmayan kuvvetlerin doğrusal olmayan karmaşık direngenlik matrisi ve yer değiştirme vektörünün çarpımı olarak yazılabildiği yeni bir çözüm metodu – tanımlama fonksiyonu metodu – önerilmiştir. Bu doğrusal olmayan karmaşık direngenlik matrisinin köşegen dışı elemanları sınama fonksiyonları arasındaki bağlantı hakkında çok önemli bilgiler sağlamaktadır. Ele alınan sınır koşularına bağlı olarak bütün sınır koşullarını sağlayan uygun sınama fonksiyonları bulmak çok zor olmaktadır. Bu sebeple, bu zorluğu aşmak için, sınama fonksiyonu gerektirmeyen diferansiyel tümlev metodu (DTM) üzerine kurulu yinelemeli yol takibi metodu (YYTM) geliştirilmiştir . Sonlu elemanlar metoduna göre daha az sayıda nokta kullandığı için daha az sayıda doğrusal olmayan denklem elde edilmesini sağlayan DTM'in DTM tabanlı doğrusal olmayan çözüm metodunun sürekli sistemlerin çözümü için gelecek vadeden bir yöntem olduğuna kanaat getirilmiştir.

Anahtar Kelimeler: Doğrusal olmayan titreşim, Kavisli karbon nanotüpler, Nano rezonatör, Geometrik doğrusalsızlık, Van der Waals kuvvet doğrusalsızlığı

To my parents,

To my lovely wife who has supported me in many ways along this journey,

To my brother and sister, you are always with me.

ACKNOWLEDGMENTS

First and foremost, I would like to thank my supervisor, Dr. Ender Cigeroglu, for his guidance and support throughout my graduate study and during the completion of this thesis. I am really thankful to him because he believed in my abilities and gave me the support to continue and finish my graduate study. More important than anything else, he helped and advised me through a lot of personal issues.

I would like to express my appreciation to my committee members, Dr. Yigit Yazicioglu, Dr. Mehmet Bulent Ozer, Dr. Fevzi Suat Kadıoğlu and Dr. Caglar Baslamisli for their guidance and support.

I would like to gratefully acknowledge the support provided by TUBITAK (The Scientific and Technological Research Council of Turkey), grant no: 2215 - Graduate Scholarship Program for International Students.

Finally, I am extremely thankful to my family and my wife, for their love, patience, sacrifices, and support over the last few years away from them.

TABLE OF CONTENTS

ABSTRACT v
ÖZ vi
ACKNOWLEDGMENTS viii
TABLE OF CONTENTS ix
LIST OF TABLES xii
LIST OF FIGURES xiv
LIST OF SYMBOLS xxii

CHAPTERS

1. INTRODUCTION 1
   1.1. General Introduction and Applications 1
      1.1.1. Applications areas of CNTs 4
      1.1.2. Brief literature review and motivations 8
   1.2. Objectives and Scopes of this thesis 11
   1.3. Outline of Thesis 13
2. VIBRATION OF CARBON NANOTUBES: A CRITICAL REVIEW 17
   2.1. Introduction 17
   2.2. Defects in CNTs 19
   2.3. Linear vibration of carbon nanotubes 20
      2.3.1. Molecular simulations 20
      2.3.2. Euler-Bernoulli beam theorem 22
      2.3.3. Timoshenko beam theorem 25
      2.3.4. Shell theorems 26
      2.3.5. Nonlocality 27
   2.4. Nonlinear vibration of carbon nanotubes 28
   2.5. Concluding remarks 39
3. ON THE NONLINEAR VIBRATION OF DOUBLE WALLED CARBON NANOTUBES WITH CONCENTRATED MASS 43
   3.1. Introduction 43
   3.2. Equation of motion using Euler-Bernoulli beam model 44
   3.3. Solution method 46
   3.4. Results 49
      3.4.1. Effect of key parameters in the first in-phase vibration mode 51
      3.4.2. Effect of key parameters in the first out-of-phase vibration mode 54
   3.5. Effect of medium stiffness on the first out of-phase nonlinear natural frequency 56
   3.6. Concluding remarks 58
4. NONLINEAR FREE VIBRATION OF DOUBLE WALLED CARBON NANOTUBES BY USING DESCRIBING FUNCTION METHOD WITH MULTIPLE TRIAL FUNCTIONS 61
   4.1. Introduction 61
   4.2. Equation of motion using Euler-Bernoulli beam model 62
      4.2.1. Van der Waals force 63

4.2.2. Describing Function Method (DFM) 65
4.3. Solution Method 66
4.4. Solution of Nonlinear Algebraic Equations 71
4.5. Results 73
4.5.1. First in-phase natural frequency considering vdW force nonlinearity 75
4.5.2. First out-of-phase natural frequency considering vdW force nonlinearity 77
4.5.3. Geometric nonlinearity 83
4.5.4. Effect of medium stiffness 83
4.6. Concluding remarks 86
5. EFFECT OF CURVATURE NONLINEARITY ON THE VARIATION OF FUNDAMENTAL NONLINEAR NATURAL FREQUENCY 87
5.1. Introduction 87
5.2. Equation of motion using Euler Bernoulli beam model for thin tubes 88
5.3. Analytical Solutions 91
5.3.1. Single harmonic balance method 91
5.3.2. Multiple harmonic balance method 92
Case 1: first and second harmonics 93
5.4. Numerical results and discussion 96
5.4.1. Effect of number of harmonics in the presence of large deformations 97
5.4.2. Effect of number of harmonics in the presence of both large deflection and waviness 99
5.5. Concluding remarks 102
6. DIFFERENTIAL QUADRATURE METHOD, A NOVEL METHOD TO STUDY NONLINEAR VIBRATIONS OF CNTS 105
6.1. Introduction 105
6.2. Modeling 108
6.3. Generalized differential quadrature method 110
6.4. Application of DQM 111
6.5. Solution method 117
6.6. Results 120
6.6.1. Geometric nonlinearity 121
6.6.2. Effect of initial curvature on the fundamental natural frequencies of the DWCNT 124
6.6.3. Van der Waals force nonlinearity together with geometric nonlinearity 126
6.7. Effect of Medium stiffness 132
6.8. Concluding remarks 133
7. NONLINEAR FREE VIBRATION OF NONUNIFORM ROTATING CARBON NANOTUBES BASES ON ERINGEN THEORY 135
7.1. Introduction 135
7.2. Nonlocal constitutive relations 136
7.3. Modeling 138
7.4. Generalized differential quadrature method 143
7.5. Utilizing DQM 144
7.5.1. Nonlinear nonlocal boundary conditions 146
7.6. Solution method 147
7.7. Results 149

7.7.1. Linear vibration analysis and verifications 150
7.7.2. Nonlinear vibrations 154
7.8. Concluding remarks 159
8. CONCLUSIONS, CONTRIBUTIONS AND FUTURE WORKS 161
8.1. Introduction 161
8.2. Conclusions 162
8.3. Contributions 165
8.4. Future works 166
REFERENCES 169
APPENDIX A. Nonlinear equations of motion 183
APPENDIX B. Nonlinear vdW force terms 186
APPENDIX C. Permissions 187
CURRICULUM VITAE 190

LIST OF TABLES

TABLES

Table 1-1 A comparison between strength of different types of CNTs and stainless steel [8-11] 4

Table 2-1Value of frequency parameters, β_n 23

Table 2-2 A comparison between Euler and Timoshenko beam theories [85] 26

Table 2-3 Theoretical methods for studying the vibrational characteristics of CNTs, part-1 35

Table 2-4 Theoretical methods for studying the vibrational characteristics of CNTs, part-2 36

Table 2-5 Theoretical methods for studying the vibrational characteristics of CNTs, part-3 37

Table 2-6 Theoretical methods for studying the vibrational characteristics of CNTs, part-4 38

Table 3-1 Numerical Values of DWCNT Parameters [162] 50

Table 3-2 Natural frequencies of DWCNT without concentrated-mass 50

Table 4-1 Numerical values of parameters used 74

Table 4-2 First five natural frequencies and modes of the linear DWCNT 74

Table 5-1 Numerical Values of SWCNT Parameters [51]. 96

Table 6-1 Effect of the Number of Grid Points on the Linear Fundamental Frequencies of the DWCNTs with Different Boundary Conditions 121

Table 6-2 Numerical Values of Tubes Parameters 121

Table 6-3 Fundamental Linear Natural Frequencies of a Simply Supported DWCNT 121

Table 6-4 DQM and Galerkin Results at Selected Points for a H-H DWCNT 131

Table 6-5 Effect of Medium Stiffness on Fundamental Linear Natural Frequency of DWCNT 132

Table 6-6 Normalized Nonlinear Natural Frequencies at Selected Normalized Vibration Amplitudes of Outertube 133

Table 7-1 Numerical Values of tubes Parameters 149

Table 7-2 Linear natural frequencies of the non-rotating local DWCNT 150

Table 7-3 Variation of normalized 1st and 2nd linear in-phase vibration mode of DWCNT 153

LIST OF FIGURES

FIGURES

Figure 1-1 Schematic of a graphene sheet [5] 2

Figure 1-2 Graphene can be rolled up into a carbon nanotube, wrapped into a fullerene, and stacked into graphite [6]..... 2

Figure 1-3 Electro micrographs of nanotubes where it consists of a) five tubes b) two tubes c) seven tubes [7]..... 3

Figure 1-4 Naming schemes for the nanotubes..... 3

Figure 1-5 A CNT mass sensor taken from [12]..... 5

Figure 1-6 A schematic of CNT resonator, taken from [19]..... 6

Figure 1-7 Atomic Force Microscopy a) a schematic view b) a Silicon tip with CNT Probe [26]..... 6

Figure 1-8 A CNT based switch: (a) turn-on and (b) turn-off states, taken form [29]7

Figure 1-9 a) conceptual drawing of nano-actuator b) Scanning electron microscope image of nano-actuator [32]..... 7

Figure 1-10 Diagrams of two carbon nanotube gears [31] 8

Figure 1-11 Images of a carbon nanotube showing the initial curvature [54] 11

Figure 2-1 a) schematic showing the principle of measurement based on double AFM tips b) Stress vs. Strain curve, Taken from [60] 19

Figure 2-2. The network of hexagons is not disturbed hence the tube can unbend without any damage, Taken from Iijima et al. [69] 21

Figure 2-3 Typical mode shapes for SWNT and DWNT from MD approach, Taken from [3] 22

Figure 2-4 Dispersion relation of transverse wave in the (a) armchair (15,15) carbon nanotube and (b) zigzag (20,0) carbon nanotube, Taken from [108]..... 28

Figure 2-5 The MWCNT probe tip (SEM micrograph) used in the experiments by [111]. The MWCNT is approximately 7.5 μm long and 10 nm in diameter. 29

Figure 2-6 (a) The tip deflection as it approaches and retreats from surface. (b) Schematic diagrams of the tip deflection at selected point during approach and retreat, Taken from [111] 30

Figure 2-7 Frequency response of the MWCNT tip around its first natural frequency [111] 30

Figure 2-8 Fabricated nonlinear carbon nanotube resonator, Taken from [119] 32

Figure 2-9 The response spectrum of the nonlinear CNT resonator (O) before and (•) after adding a center mass [119] 32

Figure 2-10 Comparison between available data in literature for a DWCNT vibrating in the out-of-phase vibration mode 33

Figure 2-11 Bifurcation diagram of a carbon nanotube resonator near its first natural frequency, taken from [126]..... 34

Figure 3-1 Model of an embedded DWCNT. 45

Figure 3-2 First two linear mode shapes of DWCNT a) in-phase b) out-of-phase... 51

Figure 3-3 Variation of the first two linear natural frequencies against increasing concentrated-mass (position of the concentrate-mass is at the middle of the DWCNT) a) in-phase b) out-of-phase..... 51

Figure 3-4 Variation of normalized nonlinear natural frequency in the presence of only geometric nonlinearity in the first in-phase vibration mode 52

Figure 3-5 Variation of the normalized nonlinear natural frequency in the presence of only vdW force nonlinearity in the first in-phase vibration mode 53

Figure 3-6 Variation of normalized nonlinear natural frequency in the presence of both geometric and vdW force nonlinearities in the first in-phase vibration mode.. 53

Figure 3-7 Variation of the normalized nonlinear natural frequency in the presence of only vdW force nonlinearity in the first in-phase vibration mode 53

Figure 3-8 Variation of the normalized nonlinear natural frequency in the presence of only geometric nonlinearity in the first out-of-phase vibration mode 54

Figure 3-9 Variation of the normalized nonlinear natural frequency in the presence of only vdW force nonlinearity in the first out-of-phase vibration mode 55

Figure 3-10 Variation of the normalized nonlinear natural frequency in the presence both nonlinearities in the first out-of-phase vibration mode 55

Figure 3-11 Variation of the normalized nonlinear natural frequency in the presence both nonlinearities in the first out-of-phase vibration mode 56

Figure 3-12 Variation of the normalized nonlinear natural frequency for different values of medium stiffness in the first in-phase vibration mode 57

Figure 3-13 Variation of the normalized nonlinear natural frequency for different values of medium stiffness in the first out-of-phase vibration mode 57

Figure 3-14 Variation of the normalized nonlinear natural frequency in the first out-of-phase vibration mode 58

Figure 4-1 Model of an embedded DWCNT 62

Figure 4-2 Arc-length continuation method 72

Figure 4-3 First three in-phase and out-of-phase linear mode shapes of DWCNT .. 75

Figure 4-4 Variation of normalized nonlinear natural frequency of innertube vibrating in the first in-phase mode 76

Figure 4-5 Variation of normalized nonlinear natural frequency of outertube vibrating in the first in-phase mode 76

Figure 4-6 Coefficient of trial functions of outertube vibrating in the first in-phase mode 77

Figure 4-7 Variation of normalized nonlinear natural frequency of innertube vibrating in the first out-of-phase mode 78

Figure 4-8 Variation of normalized nonlinear natural frequency of outertube vibrating in the first out-of-phase mode 78

Figure 4-9 Variation of normalized nonlinear natural frequency of innertube vibrating in the first out-of-phase mode 79

Figure 4-10 Transition of mode shapes from one region to another for innertube ... 80

Figure 4-11 Normalized coefficients of trail functions of inner and outer tubes at the beginning and middle of each region 81

Figure 4-12 Variation of normalized nonlinear natural frequency of outertube for different natural frequencies 82

Figure 4-13 Comparison with data available in literature 83

Figure 4-14 amplitude frequency curve of the outertube vibrating in the first in-phase mode 84

Figure 4-15 Effect of medium stiffness on the nonlinear natural frequency for the first in-phase vibration mode 85

Figure 4-16 Effect of medium stiffness on the nonlinear natural frequency for the first out-of-phase mode 85

Figure 5-1 Model of an Embedded curved SWCNT. 90

Figure 5-2 Variation of the fundamental linear natural frequencies of the SWCNT versus waviness..... 96

Figure 5-3 Fundamental mode shape of the SWCNT when mid-center is at its positive and negative maximum values..... 97

Figure 5-4 Variation of normalized nonlinear natural frequency in the presence of only geometric nonlinearity 98

Figure 5-5 Coefficients of the first and third harmonics..... 98

Figure 5-6 Variation of the normalized nonlinear natural frequency for different values of medium stiffness in the presence of only geometric nonlinearity..... 99

Figure 5-7 Variation of the normalized nonlinear natural frequency in the presence of both geometric nonlinearity and waviness nonlinearity 100

Figure 5-8 Variation of the normalized nonlinear natural frequency in the presence of both geometric nonlinearity and waviness nonlinearity 100

Figure 5-9 Coefficient of harmonics of SWCNT vibrating in the fundamental natural frequency for different initial curvature..... 101

Figure 5-10 Variation of the normalized nonlinear natural frequency for different values of initial curvature utilizing single and multiple harmonic solutions..... 102

Figure 5-11 Variation of the normalized nonlinear natural frequency for different values of normalized medium stiffness..... 102

Figure 6-1 Model of an Embedded Curved DWCNT..... 110

Figure 6-2 Variation of Normalized Nonlinear Natural Frequency of Inner and Outer Tubes Vibrating in the First in-Phase Mode for Different End Conditions ($e = 0$) 122

Figure 6-3 Variation of Normalized Nonlinear Natural Frequency of Inner and Outer Tubes Vibrating in the First out-of-Phase Mode for Different End Conditions ($e = 0$) 123

Figure 6-4 Variation of Normalized Nonlinear Natural Frequency of Outertube Vibrating in the First Out-of-Phase Mode and the Corresponding Mode Shapes in the Middle of Each Region 124

Figure 6-5 Variation of Normalized Modal Contributions vs. Normalized Total Arc-length 124

Figure 6-6 Effect of Initial Curvature on the Variation of Normalized Nonlinear Natural Frequency of Inner and Outer Tubes Vibrating in the First In-Phase Mode a) H-H b) C-H c) C-C 125

Figure 6-7 Effect of Initial Curvature on the Variation of Normalized Nonlinear Natural Frequency of Inner and Outer Tubes Vibrating in the First out-of-Phase Mode a) H-H b) C-H c) C-C 126

Figure 6-8 Variation of Normalized Nonlinear Natural Frequency of Inner and Outer Tubes Vibrating in the First In-Phase Mode for Different End Conditions in the Presence of both vdW Force and Geometric Nonlinearities 127

Figure 6-9 Variation of Normalized Nonlinear Natural Frequency of Inner and Outer Tubes Vibrating in the First Out-of-Phase Mode for Different End Conditions in the Presence of both vdW Force and Geometric Nonlinearities ($e = 0$) 128

Figure 6-10 Variation of Normalized Nonlinear Natural Frequency of Innertube Vibrating in the First Out-of-Phase Mode a) H-H b) C-H c) C-C 128

Figure 6-11 Variation of Normalized Modal Contributions vs. Total Arc-length a) H-H b) C-H c) C-C 129

Figure 6-12 Normalized Modal Contribution of Innertube and the Mode Shapes of Inner and Outer Tubes at the End of each Region for H-H DWCNT 130

Figure 6-13 Normalized Modal Contributions of Innertube and the Mode Shapes of Inner and Outer Tubes around the Middle of each Region for C-H DWCNT 130

Figure 6-14 Normalized Modal Contributions of Innertube and the Mode Shapes of Inner and Outer Tubes around the Middle of each Region for C-C DWCNT..... 130

Figure 6-15 Comparison with Available Data in the Literature for a H-H DWCNT 131

Figure 6-16 Effect of Medium Stiffness on the Nonlinear Fundamental Natural Frequency of DWCNT vibrating in the First in-phase Vibration Mode a) Hinged-Hinged b) Clamped-Hinged c) Clamped-Clamped ($e = 0$)..... 133

Figure 7-1 Schematic view of a rotating nanotube. 138

Figure 7-2 Validation of present study, DQM, with the results reported by Lu et al. [212] and Wang et al [85] 151

Figure 7-3 Variation of mode shape of CNT with normalized nonlocal parameter μ_2 a) $\mu_1 = 0$ i.e. disregarding the nonlocality effect in BCs b) $\mu_1 = \mu_2$ including the nonlocality effect in BCs 151

Figure 7-4 Variation of normalized linear natural frequency versus normalized rotation speed a) present study with $\mu_1 = 0$ comparing to Pradhan and Murmu [207] b) present study with $\mu_1 = \mu_2$ 152

Figure 7-5 Instability plot a) 1st in-phase vibration mode b) 2nd in-phase vibration mode..... 153

Figure 7-6 Variation of normalized nonlinear natural frequency of outertube vibrating in the first in-phase mode a) Disregarding nonlinear terms in boundaries b) Including the nonlinear terms..... 155

Figure 7-7 Variation of outer tube mode shape vibrating in the 1st in-phase vibration mode at normalized vibration amplitude equal to 2.5 a) Local DWCNT b) Nonlocal DWCNT $\mu_2 = 0.4$ 155

Figure 7-8 Variation of normalized nonlinear natural frequency of outertube vibrating in the first in-phase mode at different rotation speeds a) $\mu_2 = 0$ b) $\mu_2 = 0.2$ c) $\mu_2 = 0.4$ 156

Figure 7-9 Variation of outer tube mode shape vibrating in the 1st in-phase vibration mode at different rotation speed a) local DWCNT $\mu_2 = 0$ b) nonlocal DWCNT $\mu_2 = 0.4$ 157

Figure 7-10 Variation of normalized nonlinear natural frequency of outertube with different cross sections at constant rotation speed of $\Omega = 0.4$ THz with $\mu_2 = 0.4$ vibrating in the a) 1st in-phase b) 2nd in-phase 157

Figure 7-11 Variation of normalized nonlinear natural frequency of outertube vibrating in the first in-phase mode with different hub radius rotating at constant speed of $\Omega = 0.2$ THz a) $\beta = 0$ b) $\beta = 0.3$ c) $\beta = 0.5$ 158

Figure 7-12 Variation of normalized nonlinear natural frequency of outertube vibrating in the first in-phase mode with different length to diameter ratio rotating at constant rotation speed of $\Omega = 0.2$ THz with $\mu_2 = 0.4$ a) $\beta = 0$ b) $\beta = 0.5$ 159

LIST OF SYMBOLS

$w(x,t)$	Transverse displacement
$u(x,t)$	Axial displacement
E	Young's modulus
A	Cross section area
I	Area moment of inertia
ρ	Density
L	Tube length
p_1	Linear coefficient of vdW force
p_3	Nonlinear coefficient of vdW force
k	Coefficient of medium stiffness
x	Axial coordinate
t	Temporal variable
ω	Natural frequency
M_c	Concentrated mass
L_c	Position of concentrated mass
$\mathbf{K}$	Stiffness matrix
$\mathbf{M}$	Mass matrix
$\mathbf{C}$	Viscous damping matrix
$\mathbf{H}$	Structural damping matrix
$\mathbf{f_N}$	Nonlinear force vector
$\mathbf{\Delta}$	Response dependent nonlinear matrix
$\phi(\mathrm{x})$	Linear system eigenfunction
$\mathbf{x}$ and $\mathbf{q}$	Unknown displacement vector
$Z(x)$	Initial curvature function
$e_0 a$	Nonlocal parameter

μ	Normalized nonlocal parameter
Ω	Rotation speed
c	Weighting coefficient of DQM
d	Weighting coefficient of Guass-Labatto integration method

Subscripts

i	Innertube
o	Outertube
g	Geometric nonlinearity
v	vdW force nonlinearity
L	Linear
NL	Nonlinear

Superscripts

c	Clamped end
F	Free end

Abbreviations

AFM	Atomic Force Microscopy
SEM	Scanning Electron Microscopy
BCs	Boundary Conditions
MD	Molecular Dynamics
vdW	van der Waal
DQM	Differential Quadrature Method
DFM	Describing Function Method
CNT	Carbon nanotube
SWCNT	Single Walled Carbon Nanotube
DWCNT	Double Walled Carbon Nanotube
SHBM	Single Harmonic Balance Method
MHBM	Multiple Harmonic Balance Method

CHAPTER 1

INTRODUCTION

This chapter aims at presenting a general overview of carbon nanotubes and their application areas as well the need for understanding the dynamic characteristics of carbon nanotubes.

1.1. General Introduction and Applications

In recent years, the subject area of nanotechnology has become the focus of attention of industries, scientists and researchers. Among the nano-materials, carbon nanotubes (CNTs) have received the highest amount of attentions owing to their novel mechanical, chemical, thermal, and electrical properties [1-3].

Carbon nanotubes are named based on their unique sizes. A CNT has a diameter of few nanometers while its length can be up to several millimeters. In an article in "nano letter", Wang et al [4] show that a single walled carbon nanotube can have a length to diameter ratio up to $132,000,000:1$. A CNT can be constructed by folding a sheet of graphene into a cylinder. Graphene, Figure 1-1, is a flat, two dimensional, layer of carbon atoms packed tightly in the shape of a hexagonal lattice (honeycomb lattice). A graphene sheet can be wrapped into the fullerene or nanotube, or it can be stacked into the graphite (Figure 1-2).

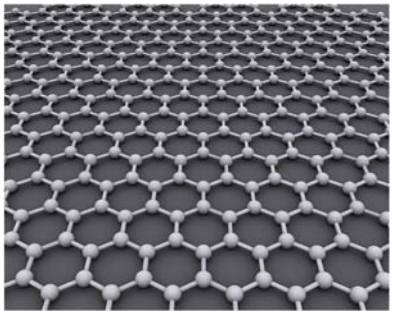

Figure 1-1 Schematic of a graphene sheet [5]

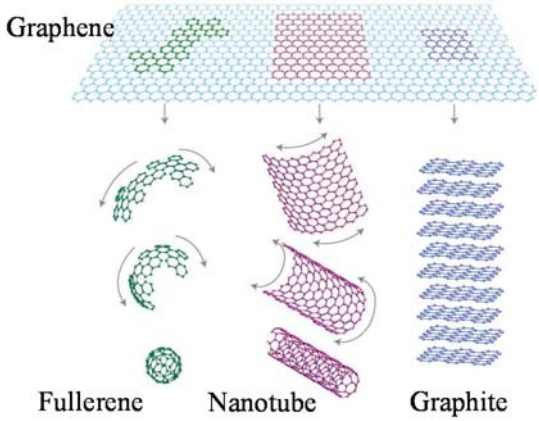

Figure 1-2 Graphene can be rolled up into a carbon nanotube, wrapped into a fullerene, and stacked into graphite [6].

In 1991, Iijima discovered carbon nanotubes while working with NEC Corporation[1] [7]. Using a high resolution Electron micrographs, he captured pictures of nanotubes for the first time (Figure 1-3). Later, studies show that CNTs can be grouped in three basic groups of zigzag, armchair, and chiral. These groups are categorized based on the ways in which a graphene sheet can be rolled into a tube. Wrapping a graphene sheet can be presented by a pair of indices (m,n). The integers show the number of unit vector along the two directions in the graphene. As shown in Figure 1-4, if $m=0$ nanotube is called zigzag, if $m=n$ nanotube is called armchair, and if $m\neq n\neq 0$ nanotube is called chiral. CNTs as well can be grouped according to the number of their walls (layers) as single walled, double walled, and multiple walled tubes.

[1] NEC Corporation is a Japanese multinational provider of information technology (IT) services and products, with its headquarters in Minato, Tokyo, Japan.

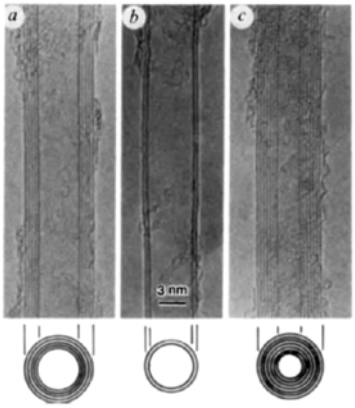

Figure 1-3 Electro micrographs of nanotubes where it consists of
a) five tubes b) two tubes c) seven tubes [7]

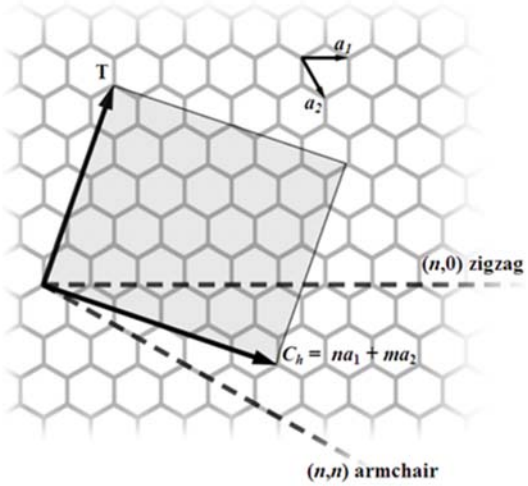

Figure 1-4 Naming schemes for the nanotubes

Studies show that, to this date, CNTs are the strongest discovered material owing to the strong "sp^2 bonds"[2] formed between the individual carbon atoms. For example a multiple walled carbon nanotube (MWCNT) can have a tensile strength around 100 GPa. It is worth noting that this strength is equal the ability to endure a weight equivalent to 10,190 kg on a cable with cross section of one millimeter. In addition to high strength, carbon nanotubes have a low density for a solid, around 1.3 g/cm^3. As a result, they have a specific strength around 48,000 $kN \cdot m \cdot kg^{-1}$ which is much higher compared to high-carbon steel's 154 $kN \cdot m \cdot kg^{-1}$. Table 1-1 represents a comparison between strength of different types of CNTs and Stainless steel. These

[2] Refer to Orbital hybridization on Chemical books for information on sp^2 bonds

approximate results are obtained based on theoretical predictions and some experiments and are given here just to provide an estimate about their properties.

Table 1-1 A comparison between strength of different types of CNTs and stainless steel [8-11]

Material	Young's modulus (TPa)	Tensile strength (GPa)
SWNT	around 1	13–53
Zigzag SWNT	0.94	94.5
Armchair SWNT	0.94	126.2
Chiral SWNT	0.92	–
MWNT	0.2–0.95	11–150
Stainless steel	0.186–0.214	0.38–1.55

In addition to unique mechanical characteristics, CNTs show an unrivaled electrical and thermal properties. For example, electrical and thermal conductivities of a SWCNT are 1000 and 20 times greater than a metal such as copper, respectively. All these unique properties give the CNTs the potential to reshape critical technologies. Nowadays, CNTs are being fabricated and used as parts in the new emerging nano-devices. CNTs have potential applications in devices such as nano-actuators, nano-motors, nano-sensors, nano-turbines, and nano shaft and gear systems. In the following section, application areas of CNTs are explored focusing on their vibratory applications.

1.1.1. Applications areas of CNTs

Carbon nano-structures have attracted many attentions in the past two decades owing to their exceptional properties and hence, new applications are introduced by researchers literally every day. CNTs play an important part in diverse fields of technology such as medical, sensor, computing, and etc., to make our lives more comfortable. Some of those applications are as follows:

- Nano sensors:

  A nano-sensor obtains data from atomic scales and transfers them to the macroscopic world where they can be measured. The detection involves in identifying the mass by measuring the changes of vibration frequencies. The very small mass of CNTs gives them the capability to even identify atoms. Figure 1-5

shows a SWCNT mass fabricated by Philippe et al [12]. They show that first natural frequency of structure shifted from 3.29 MHz to 968 KHz due to attached mass. They estimate the mass of nano-particle to be equal to 30 femtogram (30×10^{-15} gr).

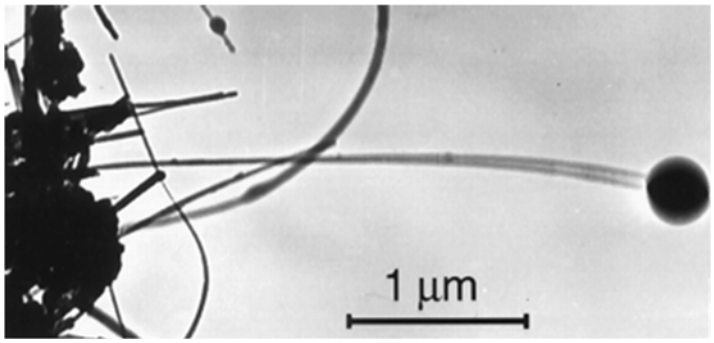

Figure 1-5 A CNT mass sensor taken from [12]

Recent studies show that the behavior of carbon nanotubes are nonlinear in nature and it is been reported that SWCNT based mass sensors can exhibit super-harmonic and sub-harmonic responses with different level of mass [13, 14]. Hence, further development in this area needs a complete understanding of the nonlinear behavior of CNTs. Moreover, recently, it is been suggested that the higher harmonics can be used to develop a more sensitive sensor.

- Tunable Oscillators (resonators):

  A resonator is a vibrating structure which is used in radio-frequency signal processing and transmitting [15, 16] and as a model system for exploring quantum phenomena in macroscopic systems [17, 18]. The sensitivity of these devices increases as their size and more importantly their mass decreases. Hence, CNTs can be the ultimate material for these applications. Furthermore, the high stiffness of CNTs gives them the ability to oscillate at gigahertz frequencies. In letter to nature, Sazonova et al [19], proposed an electrical tunable resonator. Figure 1-6 shows the resonator where the nanotubes are suspended over a hole between two metal electrodes. The gate electrode underneath the tube is used to actuate and tune the nanotube. Several studies regarding oscillators can be found in literature [20-24]. Figure 1-7a shows a schematic view of an atomic force microscopy

(AFM) used in quantum researches. The cantilever-tip vibrates due to atomic forces and its vibration is measured using a laser and quad photodiode. The resolution, sensitivity, and probing depth of an AFM depend on the structure of the probe. Recent studies [25, 26] show that probing depth of AFM can be significantly increased by utilizing carbon nanotubes (Figure 1-7b)

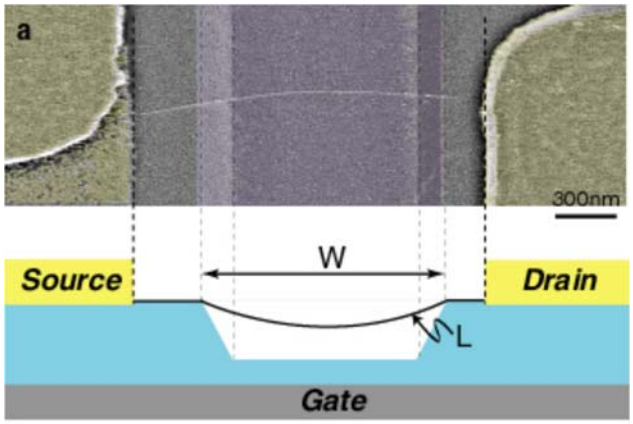

Figure 1-6 A schematic of CNT resonator, taken from [19]

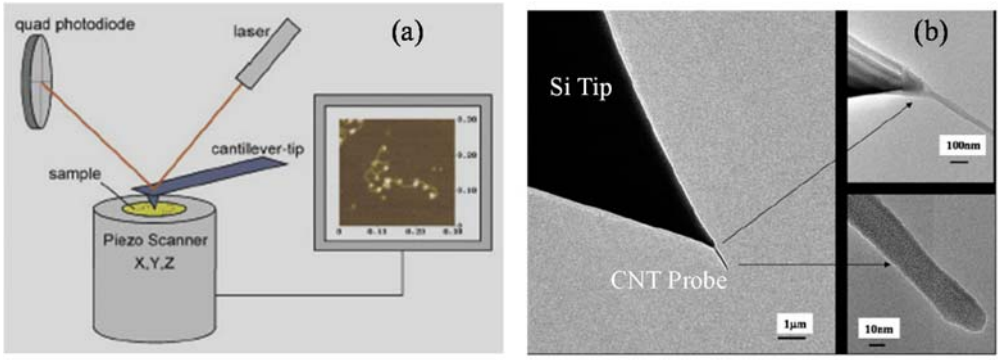

Figure 1-7 Atomic Force Microscopy a) a schematic view b) a Silicon tip with CNT Probe [26]

- Nano switches:

  Recent studies show that CNTs can be used as a switch for applications such as logic devices, memory elements, pulse generators, and current or voltage amplifiers [27, 28]. Moreover, high natural frequencies of CNTs (gigahertz regions) give them the ability to respond very fast. Figure 1-8 shows a CNT based switch where the on and off statues are shown. The researches in this area are still under development.

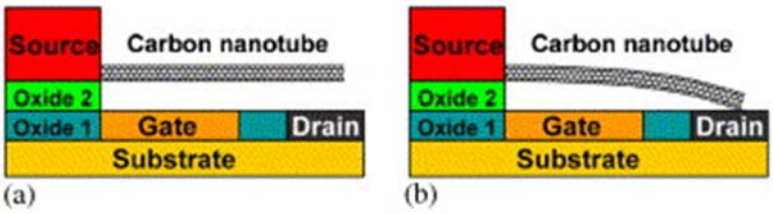

Figure 1-8 A CNT based switch: (a) turn-on and (b) turn-off states, taken form [29]

- Nano gears and nano actuators:

  The rotating nano-structures are expected to receive an extensive attention in the near future since they will be the building block of power transmission system of any nano machines. In the past few years, the feasibility of these machines have been studied by several researcher [30, 31]. For example, in letter to nature, Fennimore et al. [32] reported on the construction and successful operation of a nanoscale electromechanical actuator incorporating a rotatable metal plate. Figure 1-9 shows the schematic and electron microscope image of nano-actuator. In the presented study, a multiple walled CNT is acted as shaft. Figure 1-10 shows a typical carbon nanotube gear reported by Srivastava [31]. A laser electric field is used to power the driven gear.

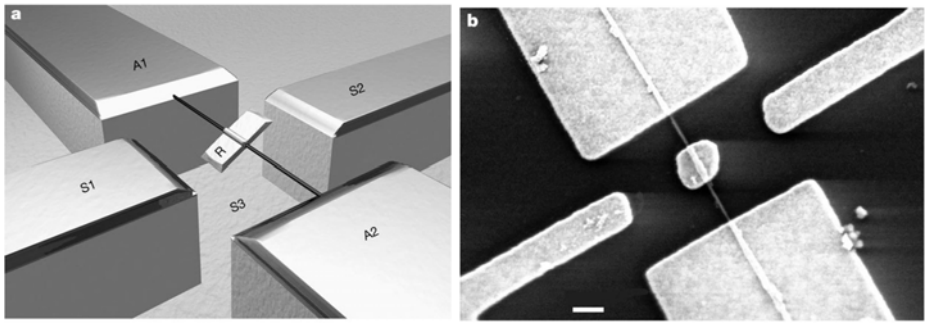

Figure 1-9 a) conceptual drawing of nano-actuator b) Scanning electron microscope image of nano-actuator [32]

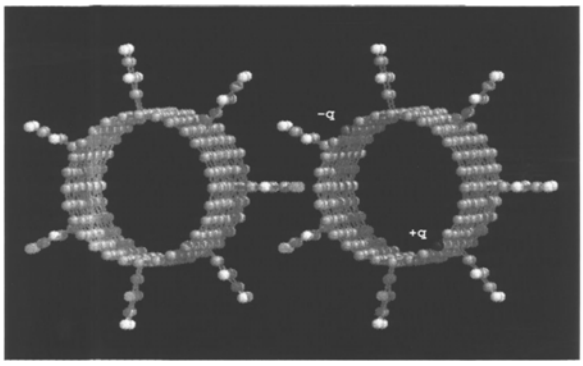

Figure 1-10 Diagrams of two carbon nanotube gears [31]

Reviewing literature, it can be concluded that CNTs will find applications in several areas. Even though, some of them are still in the prototype stages, they will be a part of our daily life in the near future. Moreover, the growth of CNTs in the past few years suggests that these application areas will not be limited to the ones mentioned here.

1.1.2. Brief literature review and motivations

In order to design a new efficient vibrating nano-scale device, researchers need detailed information about dynamic properties of the device. In contrast to macro scale structures, atomic forces play an important role in defining the mechanical characteristics of nano-structures. Hence, a clear understanding of atomic interactions are required. Furthermore, producing prototypes without having clear image of the structural properties can be very time consuming, misleading and sometimes impossible. Therefore, having a good insight of the dynamic behavior is important for the practical development of the nanomachines.

Experiments can be used to analyze the behavior of nanostructures. However doing experiment at nanoscale is a difficult task and even for some cases it is almost impossible with current technologies. Moreover, an efficient design requires several experiments in order to identify and optimize the system parameters. Therefore, molecular dynamic (MD) simulation methods have been developed. MD is a computer based simulation of physical movement of each atom and molecule in the context of a body. In this method, each atom is considered as a particle which interacts

with other particles (atoms). The forces between the particles and potential energies are defined by molecular mechanics force fields. Since a molecular system consists of a vast number of particles, it is impossible to find the solution analytically. Hence, the trajectory of particles are commonly obtained numerically by solving the Newton's equation of motion. It should be noted that the size of such atomic systems are limited due to highly time consuming computational requirements. In the past decades, MD method is used by several researches to study the dynamics of nanostructure. However, employing the molecular dynamic (MD) simulations for each case requires a huge amount of time and computational resources.

In recent years, elastic beam models [33-37] and elastic shell models [38-40] have been effectively used to predict resonant frequencies of CNTs. Using simple equations of motions offered by the continuum models, key parameters that affect the free vibration of CNTs can be easily studied. These studies [33-39] show that, compared to MD simulations, continuum modeling is more practical and useful in the analysis of CNTs in terms of computational efforts.

Even though classic continuum models can provide quick and approximate predictions, they fail to account for the size effects. Size effects are emerged from the interaction of atoms and molecules that create the material. In recent years, several research efforts have been conducted to bring in the size effects within the formulation by modifying the traditional classical continuum mechanics. One widely used size-dependent theory is the nonlocal elasticity theory presented by Eringen [41]. In the nonlocal elasticity theory, the size effects are captured by assuming that the stress at a point is a function of the strains at all points in the domain [41]. Therefore, unlike classical elasticity theory, nonlocal theory can consider long-range inter-atomic interactions; hence, it yields in the results dependent on the size of a body. Some other theories which also capture the size effects include couple stress elasticity theory, strain gradient theory, and modified couple stress theory.

In the majority of studies given in literature, the vibrational behavior of CNTs is studied by using linear models [42, 43]. Nonlinear vibrational behavior of CNTs has recently become the interest of research, where both geometric nonlinearity caused by large transverse displacement and van der Waals force nonlinearity are studied

[44-46]. Based on Donnell's cylindrical shell model, Yan et al. [39] investigated the nonlinear vibrational behavior of a double wall carbon nanotube (DWCNT) due to large deformations; whereas, Ke et al. [34] studied the same problem by using Timoshenko beam model. The effect of surrounding medium on the nonlinear vibration of the CNTs with geometric nonlinearity has been studied in [44], where single and multiple walled CNTs (MWCNTs) embedded in polymer matrix are considered.

CNTs are affected from the pressure of the medium they are embedded in and from other CNTs that are very close to them due to interlayer molecular forces. The Winkler model [47] is used to describe the surrounding pressure where the surrounding medium is assumed to act as a linear spring resulting in a pressure distribution linearly proportional to the deflection of the outermost tube. On the other hand, the interlayer force between layers of CNTs is governed by van der Waals force (vdW). The vdW force estimated by Lennard-Jones potential is inherently nonlinear [48-50]; hence, the nonlinearity of vdW force should be considered in order to accurately determine the vibrational behavior of MWCNTs. However, in the majority of the studies concerning MWCNTs, the interaction pressure between adjacent tubes of MWCNTs is linearized and assumed to depend linearly on the difference of the radial deflections. The nonlinear vibrational behavior of DWCNTs having interlayer nonlinear vdW forces between the inner and outer tubes was studied by Xu et al. [51]. Authors show that the nonlinear behavior of vdW force affected deflection amplitudes especially in the case of out-of-phase vibration mode whereas, in the case of in-phase, vibration mode this effect is very little. In the last few years, the vdW force nonlinearity has been studied by other researchers as well [52, 53].

Furthermore, recent studies show that CNTs are not straight and have a certain amount of waviness or initial curvature. The initial curvature can be introduced during fabrication or manufacturing processes because of pre-stresses and boundary effects. Figure 1-11 shows a picture of a curved SWCNT. However, in numerous recent papers, CNTs are assumed to be perfectly straight beams, and only, in few recent papers, the effect of initial curvature on linear free vibration of CNTs studied [54, 55]. Whereas, the nonlinear effect of initial curvature is not fully studied yet.

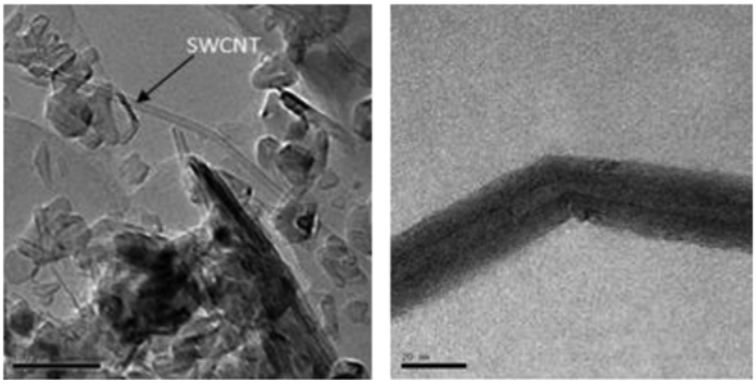

Figure 1-11 Images of a carbon nanotube showing the initial curvature [54]

1.2. Objectives and Scopes of this thesis

This thesis is going to deal with the study of the nonlinear free vibration of CNTs. Reviewing and analyzing literature, our studies show that the limited number of studies on nonlinear vibration of CNTs have serious shortfalls. A CNT can be affected by three different types of nonlinearities: Geometric nonlinearity, interlayer vdW nonlinear force, and initial curvature nonlinearity. However, in most of the recent works, the effect of each nonlinearity is studied independently from other nonlinearities without including the interaction between different types of nonlinearities. Moreover, it has been observed that, in all of the studies, single trial function assumption is used to study the system behavior where the trial function is considered to be the exact eigenfunction of the relevant linear system. However for nonlinear systems, the resulting nonlinear eigenfunctions can be significantly different from the eigenfunctions of the linear system, and depending on the nonlinearity, it may not be possible to capture the nonlinear characteristics by using a single trial function [56]. It should be noted that even for linear systems, in order to solve the eigenvalue problem, multiple trial functions are needed unless the exact eigenfunctions of the system are known.

Moreover, our studies show that even though Galerkin method is easy to implement, it requires trial functions or comparison functions that satisfy all the (geometric and natural) boundary conditions of the system. Hence, most of the researches based on Galerkin approach are limited in studying hinged-hinged beams where the trial functions are simple sine functions. Therefore, presenting a general formulation

capable of predicting the vibrational behavior of CNTs under different boundary conditions is of high importance.

Furthermore, our studies show that, in all studies regarding the nonlinear vibrations of CNTs, the boundary conditions (BCs) of CNTs have been assumed to be same as linear classic beam models. However, our insight on the problem suggests that BCs will be nonlinear and nonlocal due to inherent nonlinear characteristics of CNTs and the size effects.

Taking these shortfalls into consideration, the scopes of this thesis are defined as follows

- To get a solid understanding of the effect of different types of nonlinearities on the nonlinear free vibrations of CNTs
- To study the interactions between different types of nonlinearities
- To implement multiple trial functions to get a better approximation of the system mode shape and in the mean time, to develop a novel algorithm using describing function methods to study the coupling between the trial functions
- To develop and implement an accurate, efficient and relatively fast techniques for modeling CNTs which does not require any pre-knowledge on the system comparison functions (differential quadrature method)
- To study the effect of initial curvature and higher harmonics
- To understand the in-phase and out-of-phase natural frequencies of CNTs and how they get affected by nonlinearities
- To improve the modeling of CNTs by including the equation regarding the nonlinear nonlocal boundary conditions

Since each of these issues is going to deal with a different aspect of nonlinear vibrations of CNTs, they will be investigated throughout different case studies in independent chapters.

1.3. Outline of Thesis

This thesis is prepared in the integrated form where each chapter is a standalone article with introduction, literature review, problem definition and modeling, solution method, discussion and results, and concluding remarks. In second chapter, a comprehensive literature review is presented starting with a detailed introduction on the mechanical characteristics of CNT and methods to anticipate and measure these properties. This chapter covers a critical review on linear and nonlinear vibrations of CNTs where various simulation methods are discussed and advantage and disadvantage of each method is mentioned. More than 130 research article are cited in order to provide a deep understanding on the subject. Simulation methods such as molecular dynamic simulation, shell theories, and local and nonlocal continuous beam theories are discussed. It is observed that CNTs are affected by geometric, vdW interlayer force, initial curvature nonlinearities. The recent works in literature on these nonlinearities are summarized and discussed. This chapter, in general, provides the required knowledge to researchers with background in engineering.

In third chapter, nonlinear free vibration of a simply supported double walled carbon nanotube (DWCNT) with a concentrated-mass is investigated. The proposed model simulates behavior of nonlinear DWCNT mass sensor where concentrated mass stands for the absorbed mass of atoms or molecules. Using Galerkin method with a single trial function, a detailed numerical study on the nonlinear vibrations of double walled carbon nanotubes is presented. Nonlinearities are due to large deflection of carbon nanotubes and nonlinear interlayer van der Waals force between tubes. In this chapter, the effect of both nonlinearities and key parameters of concentrated mass on the variation of the in-phase and out-of-phase vibration modes of DWCNTs is studied.

Chapter four aims to introduce the concept of multiple trial functions. It is a common assumption in the literature to use a single trial function assumption to study nonlinear vibration of CNTs where the trial function is eigenfunction of corresponding linear system. Hence, in this Chapter, the motion of the DWCNT is represented by multiple eigenfunctions of the linear system which are referred as trial functions. Describing function method (DFM) is employed in order to represent the nonlinear forces as a multiplication of a nonlinear stiffness matrix and a displacement vector, which made

it possible to identify when it is necessary to consider multiple trial functions. The effects of number of trial functions and medium stiffness on the free vibration of DWCNTs are investigated.

Fifth chapter deals with the effect of higher harmonics on the nonlinear free vibration of a curved simply supported single walled carbon nanotube. In this chapter, multiple harmonic balance method (MHBM) in addition to Galerkin method is used to convert the nonlinear discretized differential equations of motion into a set of nonlinear algebraic equations where application of MHBM make it possible to study the effect of higher harmonics. An expression for the variation of nonlinear fundamental natural frequency of CNTs is derived analytically. The effect of higher harmonics on the natural frequency of CNTs are studied for the first time in this chapter.

Chapter six is dealing with development and implementation of an accurate and fast techniques for modeling CNTs where, at the same time, it does not require any pre-knowledge on the system comparison functions. In this chapter, differential quadrature method (DQM) as higher order finite element method is introduced. Using DQM, nonlinear vibration of a curved DWCNT embedded in an elastic medium is studied. Nonlinearities considered are due to large deflection of carbon nanotubes (geometric nonlinearity) and nonlinear interlayer van der Waals forces between inner and outer tubes. The effect of nonlinearities, end conditions, initial curvature, and stiffness of the surrounding elastic medium, and vibrational modes on the nonlinear free vibration of DWCNTs is studied in this chapter.

Chapter seven is concerned with linear and nonlinear free vibration of a nonlocal rotating double walled carbon nanotube (DWCNT). It is worth mentioning that rotating structure will be inevitable part of the power transmission system of any future nano machines. Nonlinearities are due to large deflections (geometric nonlinearity) and interlayer van der Waals force. The cross-sectional area of the CNTs are assumed to change along the axial direction. The tubes are attached to molecular hub which rotates at a constant angular speed. Hamilton principle and Euler Bernoulli beam theory are used to obtain the nonlocal equations of motion and boundary condition equations based on Eringen theorem. Results show that boundary condition equations for nonlocal cantilever beam is totally different than classic beams where it

includes nonlocal and nonlinear terms. Nonlinear nonlocal BCs are studied for the first time in this chapter.

Finally, in chapter eight, a general conclusion is presented. This chapter sums up topics of discussion in the thesis and points out main contributions of the present study and possible ideas for the future works.

CHAPTER 2

VIBRATION OF CARBON NANOTUBES: A CRITICAL REVIEW

This chapter aims at reviewing the recent studies in the literature for linear and nonlinear vibrations of carbon nanotubes. Common methods in studying vibrations of CNTs are summarized and advantage and disadvantage of each method is discussed.

2.1. Introduction

Carbon nanotubes (CNTs) have the potential to reshape critical technologies owing to their novel mechanical, chemical, thermal, electrical and electronic properties [1-3]. Nowadays, CNTs are being fabricated and used as parts in the new emerging nano devices[3]. In recent years, there has been a great interest in discovering the mechanical properties of CNTs.

The mechanical properties of CNTs are characterized by the strength of the sp^2 bonds. The most important parameter which describes the mechanical properties of a material is the Young's modulus E

$$\sigma = E\varepsilon \ , \tag{2.1}$$

where it describes the slope of stress σ vs. strain ε curve. It should be noted that the natural frequency cannot be calculated without knowing the Young's modulus. In the past decades, several experiments have been conducted to measure the Young's modulus of carbon nanotubes. However, due to small size of CNTs, it is almost impossible to measure their mechanical properties directly.

[3] A review on recent applications of CNTs is presented in previous chapter.

Even though direct measurement of the strength is impossible with current technologies, it is possible to determine the strength indirectly. One method is to measure the amplitudes of intrinsic thermal vibration of cantilevered carbon nanotubes, which is a function of temperature. In a study, Treacy et al [57] show that CNTs vibrate due to thermal effects and vibration amplitude adjusted as temperature changes. This correlation can be used to obtain Young's modulus since, for small vibration amplitudes, vibration amplitude at the tip of a cantilever beam is related to Young's modulus and the vibration energy. Using this method, Treacy et al [57] calculate a Young's modulus of 1.8 TPa (average value) for multi-walled nanotubes, and Krishnan et al [58] obtained a Young's modulus of $1.25-0.35/+0.45$ TPa for single-walled nanotubes. However, the technique is limited since the thermally excited vibrations should not be too large or too small for reliable transmission electron microscopy (TEM) detection. As a result, the sample size is restricted in this method.

Another method is to measure the exerted force by a nanotube as a function of the displacement from its equilibrium position when it is bended by the tip of an atomic force microscopy (AFM). This method provides a direct measurement of bending force vs. displacement. Then, using beam theories one can extract Young's modulus. Using this method, Wong et al. [59] calculate a Young's modulus of 1.28 ± 0.5 TPa for multi-walled carbon nanotubes.

Another approach proposed by Poncharal et al. [12] is to use an alternating electric field to excite a cantilever beam. Changing the frequency of excitation one can obtain the resonant frequency of CNTs. Knowing the resonance frequency, one can obtain Young's modulus according to the results of vibration analysis of beams. However, results provided by this method are approximates since the effects of nonlinearities are disregarded.

In 2000, Yu et al. [60] for the first time obtained the stress vs. strain diagram for carbon nanotubes using double AFM tips. Figure 2-1 shows the principle and results of measurement done by [60]. When the top cantilever is pulled upward, the lower cantilever is bent upward by a distance, while the nanotube is stretched from its initial

length of L to $L+\delta L$ due to the forces of AFM tips. Knowing the forces and bending stiffness of cantilever beam, the Stress vs. Strain curve can be obtained. A detailed review on the mechanical properties of CNTs can be found in [61-63]

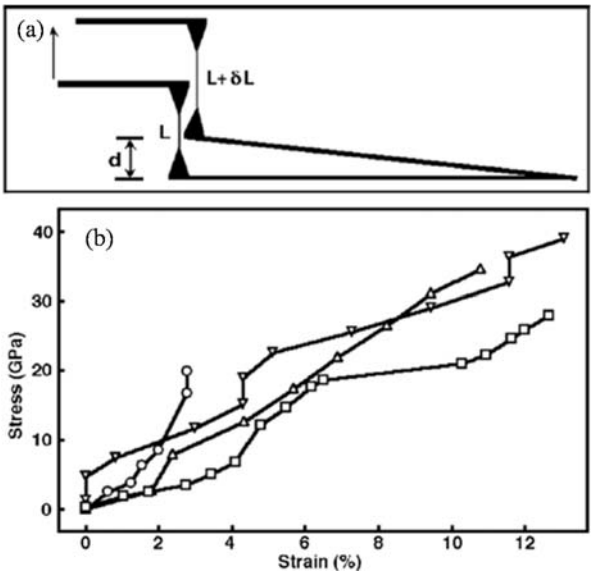

Figure 2-1 a) schematic showing the principle of measurement based on double AFM tips b) Stress vs. Strain curve, Taken from [60]

2.2. Defects in CNTs

Studies show that the material properties of any material change due to crystallographic defect. In most of cases, defects occur in the form of atomic vacancies. A high level of such defects can lower the tensile strength of the material. As a result, the theoretical strength (≈10% of the Young's modulus) is not feasible for most of the materials. However, studies show that CNTs are almost defect-free where they can achieve the theoretical strength. A perfect nanotube is a tubular structure of carbon atoms in which a carbon atom is bonded to three carbon atoms to form a hexagonal networks. In recent years, three types of native defects formed during the CNT synthesis process have been identified: isolated point defects or vacancies, topological defects, and sp^2-sp^3 hybridization defects [64]. Further information on each type of defects can be found in [65-67]. Studies confirm that the existence of few detects can change the electrical properties of the CNT from metallic to semiconducting CNT however the mechanical properties of CNTs remain without any change. The effect of defects on mechanical properties of CNTs is studied by

[68]. Using a high-resolution scanning electron microscope, authors [68] have studied both tensile strength and buckling behavior of a set of CNTs. They observed that most of the samples reach the strength of the 11% of the Young's modulus, corresponding approximately to the theoretical value of the material's strength. Their findings indicate that CNTs are remarkably free of critical defects. Hence, in the most of the studies in literature and present study, CNTs are considered to be defects free.

2.3. Linear vibration of carbon nanotubes

In the last two decades, the industrial and academic interest in CNTs have exponentially increased. Todays, CNTs are utilized in the structure of several nano devices such as sensors, oscillators, and actuators. However, the performance of these vibrating structures is directly affected by the vibrational characteristics of nanotubes; hence, it is very important to know their vibrational characteristics such as natural frequencies and mode shapes. In the past decades, experiments are used by researcher to determine the mechanical characteristics of CNTs. However doing experiment at nanoscale is a difficult task and even for some cases it is almost impossible with current technologies. Hence, in recent years, several theoretical theories have been developed in order to study vibrational behavior of CNTs. Simulation methods such as Molecular dynamics (MD) and local and nonlocal continuum models are widely used in literature. This section brought a review which covers outstanding literatures in this area.

2.3.1. Molecular simulations

Molecular dynamic (MD) simulation represents the dynamics of the system of atoms or molecules by using a discrete solution of Newton′s equations of motion. Positions and velocities of all the molecules are calculated by integrating the equations of motion numerically in time domain. The interaction between atoms is calculated using atomic potential forces which can be the classic one or obtained from solving the Schrödinger equations (known as *ab initio* method) [63]. MD simulations can provide a detailed information on the dynamics of structure and interaction of atoms.

In the past decades, MD simulation is used by several researchers to study the mechanical properties of CNTs. Iijima et al. [69] studied the bending of nanotubes under compression using molecular dynamics simulations. They investigated the large deformation and flexible properties of single and multiple walled nanotubes. They showed that the bending is completely reversible up to angles in excess of 110. Figure 2-2 represents the results reported in [69] where it shows the exceptional flexibility of carbon nanotubes at large strain.

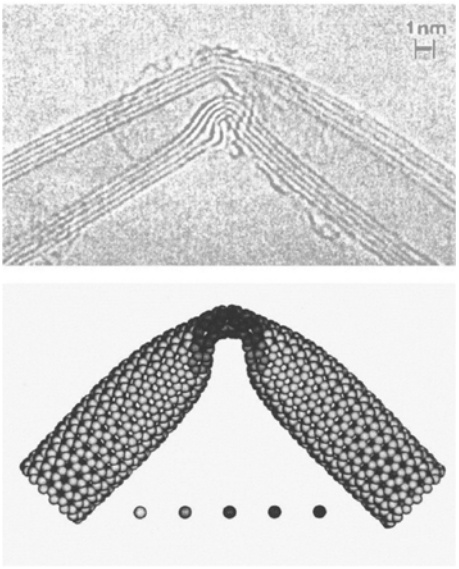

Figure 2-2. The network of hexagons is not disturbed hence the tube can unbend without any damage, Taken from Iijima et al. [69]

The bending, axial compression, and torsion of CNTs is studied in [70]. Their results shows that carbon nanotubes, when subjected to large deformations, reversibly switch into different morphological patterns. Each shape change corresponds to a sudden release of energy and a singularity in the stress–strain curve. A similar pattern was detected in works of Yakobson et al. [71].

In recent years, MD simulation is used by several researcher [72-75] to study the dynamic behavior of CNTs. For example, Li and Chou [73] investigated the natural frequencies and mode shapes of a single walled carbon nanotube (SWCNT) using MD simulations. It is worth noting that the MD simulation provides information on radial breathing modes and noncoaxial intertube modes in addition to bending modes.

Figure 2-3 shows typical mode shapes of single and double walled CNTs obtained using the MD approach.

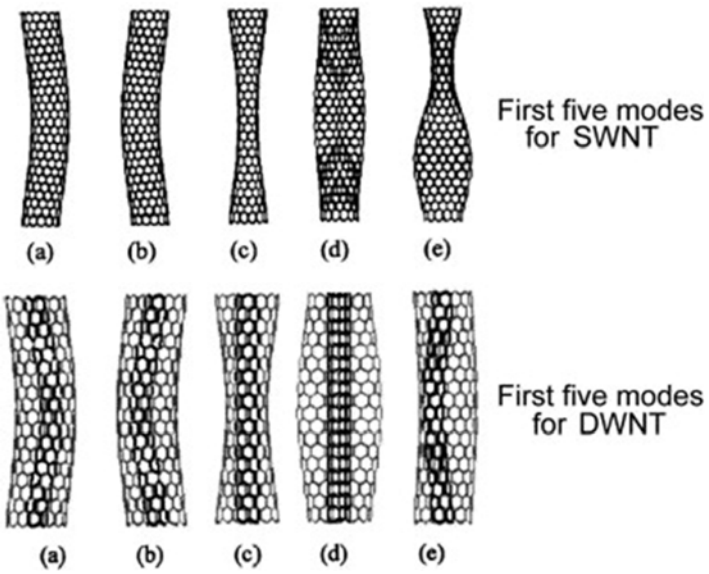

Figure 2-3 Typical mode shapes for SWNT and DWNT from MD approach, Taken from [3]

Even though MD simulations are very accurate in anticipating the dynamic and mechanical properties of CNTs, they are limited by the size of such atomic systems due to highly time consuming computational requirements. In order to perform the simulation, special high-performance computational facilities are required. Due to these limits, researchers get motivated to develop simpler approaches to study the dynamics of CNTs.

2.3.2. Euler-Bernoulli beam theorem

Recent studies show that even though the diameter of a CNT is only several times larger than the length of a bond between carbon atoms, continuum models can be used to study the dynamics of CNTs. The differential equation of motion of a uniform beam was first written by Bernoulli-Euler as follows

$$EI\frac{\partial^4 w(x,t)}{\partial x^4}+\rho A\frac{\partial^2 w(x,t)}{\partial t^2}=g(x,t)\ , \tag{2.2}$$

where E stands for the Young's modulus of elasticity, $I=\pi\left(R_{out}^4-R_{in}^4\right)/4$ is the moment of inertia, ρ is the density, A is the tube's cross section, $w(x,t)$ represents

the transverse displacement of the tube, and $g(x,t)$ stands for external forces acting on the beam. x is the axial coordinate and t is temporal variable. R_{out} and R_{in} denote outer and inner radius of the tube. It should be noted that the actual thickness of a CNT is not more than the size of one carbon atom, however it is a common assumption in the literature to consider the thickness of carbon tubes to be equal to the distance between layers of tubes (around 0.34 nm).

The Euler beam assumes that displacements are small and the cross section stays normal to central axis during bending which is valid for long thin beams. A general solution to Eq. (2.2) is

$$w(x,t) = W(x)T(t) = \left[a\cosh(\beta_n x) + b\sinh(\beta_n x) + c\cos(\beta_n x) + d\sin(\beta_n x)\right]e^{i\omega_n t} \ . \tag{2.3}$$

The constants, a , b , c , and d , are defined by the beam boundary conditions and β_n is the eigenvalue for n^{th} vibration mode which is defined by the characteristic equation. According to Euler beam theory, the natural frequencies of system are obtained as

$$f_n = \frac{\omega_n}{2\pi} = \frac{1}{2\pi}\left(\frac{\beta_n}{L}\right)^2\sqrt{\frac{EI}{\rho A}} \ . \tag{2.4}$$

Table 2-1 Shows the values of β_n for the Clamped-Clamped (C-C), Clamped-Hinged (C-H), Hinged-Hinged (H-H), and cantilever beams.

Table 2-1Value of frequency parameters, β_n

	C-C	C-H	H-H	Cantilever
$\beta_1 L$	4.7300	3.9266	3.1416	1.8751
$\beta_2 L$	7.8532	7.0686	6.2832	4.6941
$\beta_3 L$	10.9956	10.2102	9.4248	7.8548
$\beta_4 L$	14.1372	13.3518	12.566	10.9955
$\beta_5 L$	17.2787	16.4934	14.708	14.1372

For a CNT with outer radius R_{out} and inner radius R_{in} or any tubular beam, Eq. (2.4) can be simplified as

$$f_n = \frac{\beta_n^2}{\sqrt{8}\pi}\left(E\frac{R_{out}^2 + R_{in}^2}{\rho}\right)^{1/2}. \quad (2.5)$$

Eq. (2.5) have commonly been used by researchers in order to determine the frequencies of nano resonators and estimate the Young's modulus of CNTs from measured frequencies [57, 76].

CNTs are affected by the pressure of the medium which they are embedded in. The Winkler model [47] is used in literature to describe the surrounding pressure where the surrounding medium is assumed to act as a linear spring resulting in a pressure distribution linearly proportional to the deflection of outermost tube as

$$g(x,t) = -kw(x,t), \quad (2.6)$$

The negative sign in the above equation shows that the pressure $p(x,t)$ is opposite to the deflection of the tube and k is defined by the material constants of the surrounding elastic medium.

In early studies, single and multiple walled CNTs are modeled as a single continuous beam [12]. However, in this model, all the walls remain in-phase and it is not possible to study out-of-phase vibration modes. In reality tubes of carbon can interact with each other. The interlayer force between layers of CNTs is governed by van der Waals force (vdW). The vdW force estimated by Lennard-Jones potential is inherently nonlinear [48-50]. However, in the majority of the early studies concerning MWCNTs, the interaction pressure between adjacent tubes of MWCNTs is linearized and assumed to depend linearly on the difference of the radial deflections as follows

$$f(x,t) = p_1(w_o - w_i), \quad (2.7)$$

where p_1 is the interaction coefficient between the outer layer w_o and inner layer w_i. Yoon et al. [77] were one of first researchers who modified Euler-Bernoulli beam equations to study the out-of-phase vibration of MWCNTs. Their study, later followed by several researchers. The transverse vibration of an *N*-wall CNT is defined by the following *N* coupled equations of motion

$$
\begin{aligned}
EI_1 \frac{\partial^4 w_1}{\partial x^4} + \rho A_1 \frac{\partial^2 w_1}{\partial t^2} &= p_1 (w_2 - w_1) \\
EI_1 \frac{\partial^4 w_2}{\partial x^4} + \rho A_1 \frac{\partial^2 w_2}{\partial t^2} &= p_2 (w_3 - w_2) - p_1 (w_2 - w_1) \\
&\vdots \\
EI_N \frac{\partial^4 w_N}{\partial x^4} + \rho A_N \frac{\partial^2 w_N}{\partial t^2} &= p_{N-1} (w_N - w_{N-1})
\end{aligned}, \tag{2.8}
$$

$w_k \left(k = 1, 2 \cdots N\right)$ is the transverse displacement of the k^{th} tube, I_k and A_k are the moment of inertia and the cross section area of the k^{th} tube. A similar approach is used by Zhang et al.[78] to study free vibrations of double walled CNTs under compressive axial load. They show that natural frequency decreases as axial loads increases. Moreover, they found out that the amplitude ratios of the inner to the outer tubes are independent of axial load.

2.3.3. Timoshenko beam theorem

Studies show that the effects of shear deformation and rotary inertia become significant for the short beam vibrating at higher modes. In recent years, Timoshenko beam used by several researchers to study the free vibration of short CNTs (length to diameter ration smaller than ten). Ru [79], Yoon et al. [80], and Wang et al. [81] used the Timoshenko beam model for vibration analysis of MWCNTs. The buckling of MWCNTs is studied by Zang et al. [82]. A comparison between results of Timoshenko and Euler beam theories show that shear deformations get important when the length-to-diameter ratios are small and the difference is expanded for higher vibration modes. The coupled differential equations of a SWCNT is given by [83]

$$
-kAG\left(\frac{\partial \psi}{\partial x} - \frac{\partial^2 w}{\partial x^2}\right) = \rho A \frac{\partial^2 w}{\partial t^2}, \tag{2.9}
$$

$$
EI \frac{\partial^2 \psi}{\partial x^2} + kAG\left(\psi - \frac{\partial w}{\partial x}\right) = \rho I \frac{\partial^2 w}{\partial t^2}, \tag{2.10}
$$

where ψ is the slope of the deflection curve, w is the transverse deflection, E is the Young's modulus of elasticity, G is the shear modulus of elasticity, ρ is the mass density per unit volume, k is the shear correction factor which depends on the shape

of the cross-section, and A and I are the area and second moment of the cross sections.

Eliminating the ψ from Eq. (2.9) and (2.10), the coupled equations can be reduced to single differential equation as

$$EI\frac{\partial^4 w}{\partial x^4}+\rho A\frac{\partial^2 w}{\partial t^2}-\rho I\left(1-\frac{E}{kG}\right)\frac{\partial^4 w}{\partial x^2\partial t^2}+\frac{\rho^2 I}{kG}\frac{\partial^4 w}{\partial t^4}=0\,. \tag{2.11}$$

Table 2-2 shows a comparison between frequency parameters of SWCNT obtained from Euler and Timoshenko beam theories where the length ratio is considered to be equal to 10 and shear factor correction factor equal to 0.563 [84]. It can be seen that as frequency increases the differences increases. However, it is worth noting that, in most of the application cases, CNTs are only excited around the first natural frequencies. Moreover, mainly they have a length to diameter ratio greater than 10.

Table 2-2 A comparison between Euler and Timoshenko beam theories [85]

Mode number	Hinged-Hinged		Clamped-Hinged		Clamped-Clamped	
	Timoshenko	Euler	Timoshenko	Euler	Timoshenko	Euler
1	3.0929	3.1416	3.7845	3.9266	4.4491	4.7300
2	5.9399	6.2832	6.4728	7.0686	6.9524	7.8532
3	8.4444	9.4248	8.1212	10.2102	9.1626	10.9956
4	10.626	1.5660	10.880	13.3518	11.113	14.1372
5	12.541	15.708	12.707	16.4934	12.863	17.2787

2.3.4. Shell theorems

In recent years shell theories are used by researchers to study vibrations of CNTs. Shell theories have the ability to model the cross sectional deformation of the tubes as well as their bending, torsional, and extensional modes. However, shell theories cannot estimate size effects since Atomic force effects are not included in these theories. Moreover, the geometrical and mechanical parameters which are used in these studies are basically obtained from empirical or numerical studies.

Yakobson et al. [70, 71] studied similarities between macroscopic shell models and MD simulation methods. Their results show that mechanical properties of CNTs are

strongly dependent on helicity and atomic structure of the tubes. Hence, the common isotropic shell models which neglect the discrete nature of the CNT cannot predict the effects of curvature and chirality on the mechanical behavior of CNTs. Therefore, to overcome this problem, anisotropic shell models have been developed [86-88].

In the past years, several shell models have been developed by researchers to study vibration characteristics of CNTs [89-94]. A review on the validity and accuracy of cylindrical shell theories such as Donnell thin shell theory, Sanders thin shell theory, and the first-order shear deformation shell theory in predicting the critical buckling strains of axially loaded SWCNTs can be found in [94, 95]. Studies show that shallow shell theories (e.g., Donnell theory [96]) are not accurate for the CNT analysis due to the CNT non-shallow structure. Only more complex shell theories (e.g., Sanders theory [97]) are capable of reproducing the results of MD simulations.

Reviewing literature, it can be seen that shell theories are favorable in predicting the buckling behavior of CNTs where beam theories are more favorable in predicting the vibration characteristics of CNTs.

2.3.5. Nonlocality

Although classic continuum models can provide quick and approximate predictions, they fail to account for the size effects. Size effects are emerged from the non-contact interaction of atoms and molecules due to atomic forces such as van der Waals force. In recent years, several research efforts have been conducted to bring in the scale effects within the formulation by modifying the traditional classical continuum mechanics. One widely used size-dependent theory is the nonlocal elasticity theory presented by Eringen [41]. In the nonlocal elasticity theory, the small-scale effects are captured by assuming that the stress at a point is a function of the strains at all points in the domain [41]. Hence, unlike classical elasticity theory, nonlocal theory can consider long-range inter-atomic interactions where it yields in the results dependent on the size of a body. Some other theories which also capture the size effects include couple stress elasticity theory, strain gradient theory, and modified couple stress theory.

Nonlocal Euler–Bernoulli model is used by Peddieson et al. [98]. They studied the effect of nonlocality on static deflection of cantilever beams. Sudak [99] used the nonlocal elasticity for column buckling. Wang and Liew [100] studied scale effect on static deformation of micro and nano tubes using nonlocal Euler–Bernoulli and Timoshenko beam theories. In recent years, wave propagation and vibration of CNTs are studied by several researchers using beam theories [101-106]. A review on application of nonlocal theories in modeling of graphene sheet and CNTs can be found in [107].

In a study, Hu et al [108] compared the nonlocal continuum shell model and molecular dynamic simulation for wave propagation in SWCNTs and double walled carbon nanotubes (DWCNTs). Figure 2-4 shows the dispersion relations between the phase velocity and the wavenumber of the transverse wave in the armchair (15,15) SWCNT and zigzag (20,0) SWCNT. Good agreement is predicted between molecular dynamic simulations and nonlocal continuum modeling. The accuracy and limits of nonlocal theories are studied in [90, 109, 110]

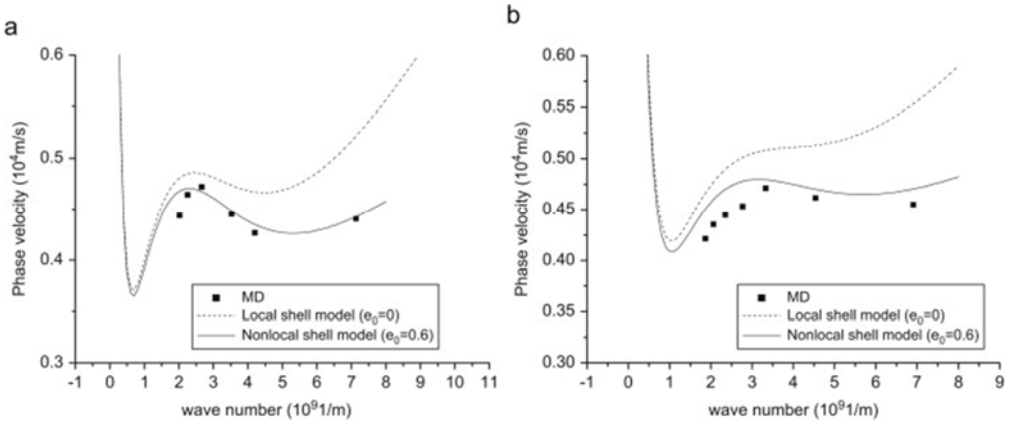

Figure 2-4 Dispersion relation of transverse wave in the (a) armchair (15,15) carbon nanotube and (b) zigzag (20,0) carbon nanotube, Taken from [108]

2.4. Nonlinear vibration of carbon nanotubes

In the past decade, linear elastic beam models and elastic shell models have been effectively used by researchers to predict resonant frequencies of CNTs. However, recent studies show that CNTs are affected by nonlinearities such as geometric nonlinearity, van der Waals interlayer nonlinear force, and initial curvature nonlinearity.

Lee at al. [111] were one of first who experimentally studied statics and nonlinear bending dynamics of a CNT used in atomic force microscopy (AFM). In AFM applications, CNT tips are considered advantageous since they have small tip radii, a high length-to-diameter aspect ratio, a well-defined atomic configuration, a high wear resistance, and significant bending flexibility [112]. Figure 2-5 shows the MWCNT probe used by Lee at al. [111]. They studied the deformation of the CNTs as it approaches and retracts from the surface (Figure 2-6). They observed that as the tip gets close the surface (from A to F), the cantilever first snaps into contact with the sample and then bends linearly from point B to C as the CNT tip gets closer to the surface. From point C the cantilever exhibits a nonlinear deflection with increasing deflection. The MWCNT buckled at point D. Furthermore, they studied the dynamics of the tip as its travel distance, Z, decreases. Figure 2-7 shows the frequency response of the tip around its first natural frequency. It can be seen that the response is linear when CNT tip is far away from the sample. As the distance between tip and sample decreases to 65 nm, the amplitude of vibration is reduced and saturates in the frequency range where it taps on the sample. Further decrease in Z develops a distinct feature where a jump in frequency can be detected.

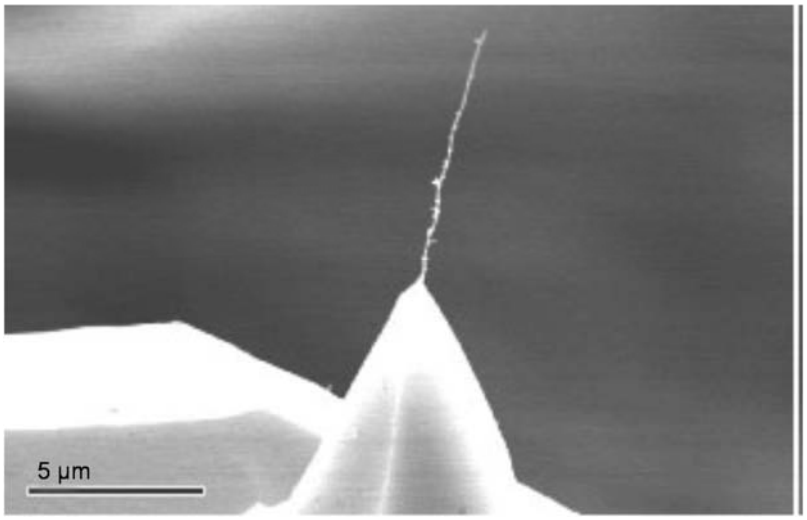

Figure 2-5 The MWCNT probe tip (SEM micrograph) used in the experiments by [111]. The MWCNT is approximately 7.5 μm long and 10 nm in diameter.

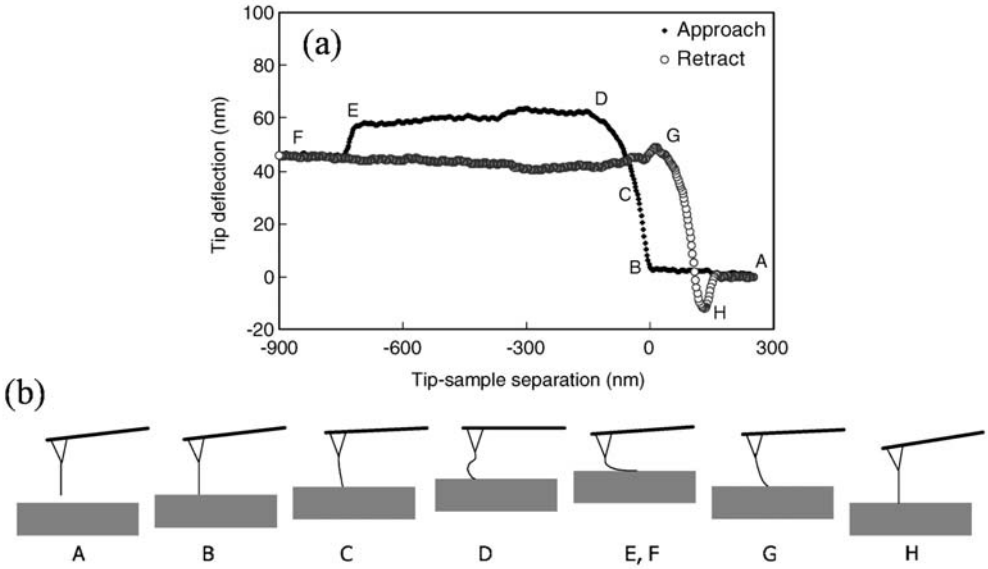

Figure 2-6 (a) The tip deflection as it approaches and retreats from surface. (b) Schematic diagrams of the tip deflection at selected point during approach and retreat, Taken from [111]

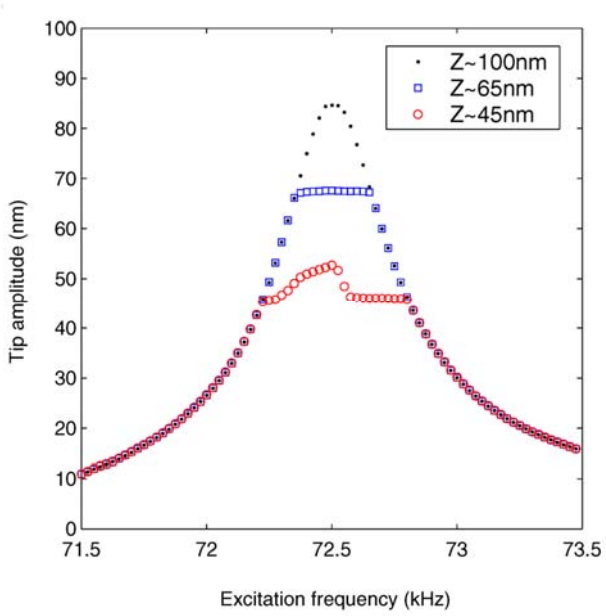

Figure 2-7 Frequency response of the MWCNT tip around its first natural frequency [111]

Later, studies confirm that deformation of CNTs are nonlinear in nature. Hence, static and dynamics properties of CNTs can accurately be anticipated only when the nonlinearities in the geometry and physics are considered. Fu et al. [113] were the first who studied the nonlinear vibrations of CNTs due to large deformations (geometric nonlinearity) using Euler-Bernoulli beam theory. Later, Based on Donnell's cylindrical shell model, Yan et al. [39] investigated the nonlinear

vibrational behavior of a double wall carbon nanotube (DWCNT) due to large deformations; whereas, Ke et al. [34] studied the same problem by using Timoshenko beam model. It is worth noting that nonlinear phenomenon such as bifurcation and chaos can only be studied when nonlinearities are considered. Moreover, since Young's modulus is measured using the vibration methods, accurate measurements can only be obtained when nonlinear effects are considered. In a similar manner, all the vibratory applications of CNTs are affected by the same fact. For example, nano mass sensors work based on the shift in natural frequency therefore the precise mass is obtained only when nonlinearities are accounted. The importance and effects of nonlinearities have been studied by several researchers [114-118] in the past few years. These studies offer understanding and strategies to deal with the nonlinear behavior of CNTs.

Recently, in nano letters, Cho et al. [119] showed that it is possible to use nonlinearity of a resonator to improve its performance. It should be noted that, in the linear operation rage, the small size of a resonator reduces its dynamic range down to the few nano meter. Whereas, the small vibration amplitudes complicate the development of the required measurement system and accordingly limits its sensitivity, especially under ambient and room temperature environments [120]. Figure 2-8 shows the scanning electron microscope (SEM) image of fabricated resonator by [119]. According to this study [119], the measurement sensitivity of the mass sensor increases 3.7 times by measuring the drop off frequency instead of the linear frequency shift. Figure 2-9 shows the frequency response of the resonator which shows a hardening behavior with a jump from higher amplitude to lower amplitude as frequency increases. The large amplitude and sharp change are favorable properties for the precision measurements. Furthermore, the large vibration amplitude indicates less susceptibility of the resonance system to the thermal noise, and a sharp transition allows for a narrow measurement bandwidth.

In the past years, several applications for CNTs are proposed where CNTs have length to diameter ratio between 10 and 20. Studies show that, in these cases, the radial relative displacement between layers of MWCNTs can play an important role. Results [22, 73] show that the out-of-phase vibration mode of MWCNTs are excited at

ultrahigh frequencies (above 1 THz) where it has a characteristic wave number just few times bigger than the diameter of CNT.

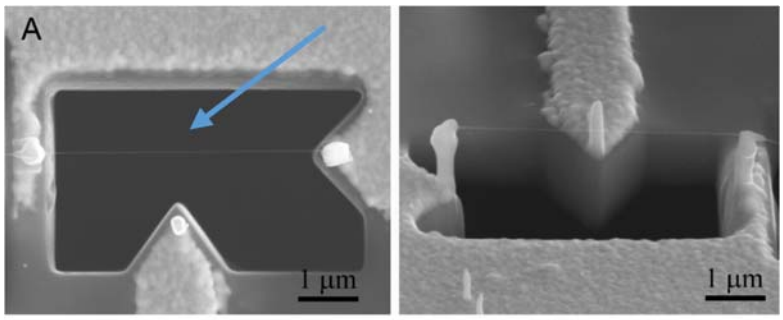

Figure 2-8 Fabricated nonlinear carbon nanotube resonator, Taken from [119]

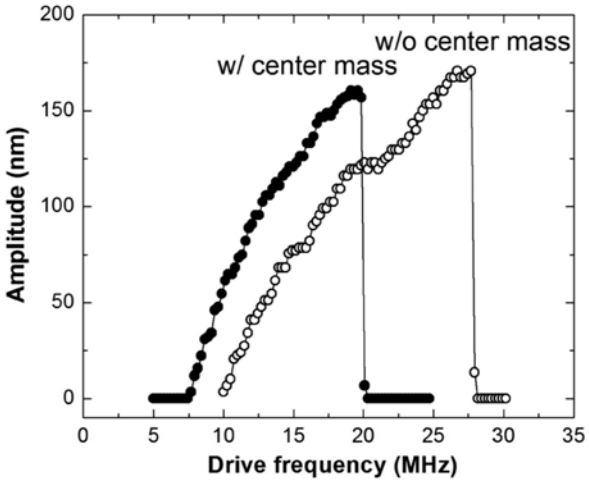

Figure 2-9 The response spectrum of the nonlinear CNT resonator (O) before and (•) after adding a center mass [119]

The distortion by out-of-phase mode could significantly affect some important physical properties) of MWNTs such as electronic and optical properties. Therefore, it is important to study the out-of-phase vibration mode. The interlayer force between layers of CNTs is governed by van der Waals force (vdW). The vdW force estimated by Lennard-Jones potential is inherently nonlinear [48-50]; hence, the nonlinearity of vdW force should be considered in order to accurately determine the vibrational behavior of MWCNTs. Xu et al. [51] were the first who study the nonlinear vibrational behavior of DWCNTs having interlayer nonlinear vdW forces between the inner and outer tubes. Authors showed that the nonlinear behavior of vdW force affected the deflection amplitudes especially in the case of out-of-phase vibration mode, whereas in the case of in-phase vibration mode this effect is very little [52, 53].

The effect of vdW force on nonlinear natural frequencies of DWCNTs is investigated by Cigeroglu and Samandari [121] using describing function method and utilizing multiple trial functions in Galerkin method. It is observed that utilization of multiple trial functions resulted in the determination of multiple nonlinear natural frequencies at the same vibration amplitude and identification of single nonlinear natural frequencies associated with different vibration amplitudes. Later, authors confirmed their results using differential quadrature method [122]. Figure 2-10 shows a comparison between different available data in literature for DWCNTs vibrating in the out-of-phase vibration mode.

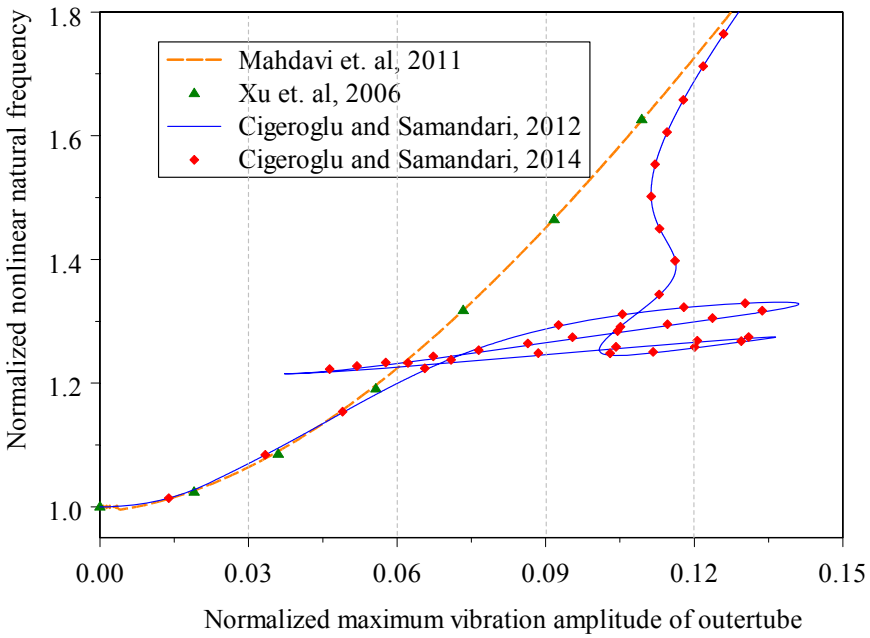

Figure 2-10 Comparison between available data in literature for a DWCNT vibrating in the out-of-phase vibration mode

Furthermore, recent studies show that CNTs are not straight and have a certain amount of waviness or initial curvature. The initial curvature can be introduced during fabrication or manufacturing processes due to the pre-stresses and boundary effects. Mehdipour et al. [123] studied the nonlinear forced vibration of a curved SWCNT embedded in Pasternak elastic foundation. They used He's Energy Balance Method to obtain the relationships of the nonlinear amplitude and frequency. Similar problem is studied by Samandari and Cigeroglu [124] using multiple harmonic balance method. They showed that the nonlinear effects of initial curvature only appear in

higher harmonics. Mohammadi et al. [125] study post buckling instability of nonlinear CNT with initial curvature embedded in elastic foundation. They show that the bifurcation diagram of a curved CNT with initial sinusoidal configuration is similar to that of a straight CNT in its nearest buckling mode.

In recent years, chaotic and non-harmonic response of CNTs attracted attention of few researchers. Mayoof and Hawwa [126] studied the possibility of a chaotic response for a curved single walled carbon nanotube near its first natural frequencies. They observed that as excitation force amplitude increases more than a certain value, period doubling occurs in which it is followed by a chaotic behavior. Figure 2-11 shows the bifurcation diagram around the first natural frequency of the CNT where it shows the maximum vibration amplitude of the CNT respect to excitation force amplitude. However, their studies [126] show that the chaotic behavior happens at high vibration amplitudes. Therefore, since in all the studies in literature on free vibration of CNTs and the present study, vibration amplitudes are limited to 3 nm, it can confidently concluded that the harmonic response assumption remains valid for these vibration amplitudes.

In the past decade, nonlinear vibrations of CNTs are studied by several researchers. Table 2-3, Table 2-4, Table 2-5, and Table 2-6 present the result of the performed investigation in this thesis on the recent literature of nonlinear vibrations of CNTs in chronological order.

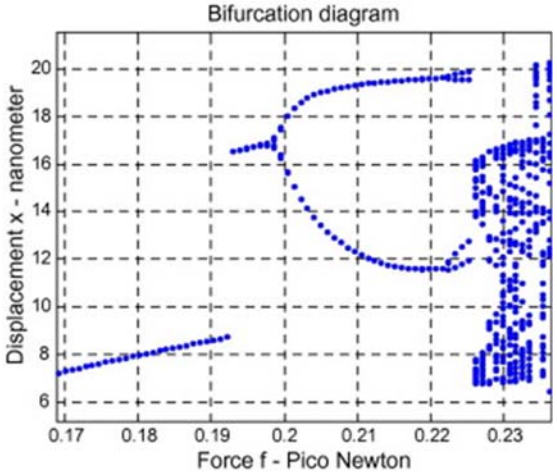

Figure 2-11 Bifurcation diagram of a carbon nanotube resonator near its first natural frequency, taken from [126]

Table 2-3 Theoretical methods for studying the vibrational characteristics of CNTs, part-1

Researcher	Year	Simulation Method	Solution method	Nonlinearity	Research summary
Lee et al. [111]	2004	Experiment and Euler beam	-	Geometric (GN)	Nonlinear frequency response is investigated where several jumps detected
Wang et al. [127]	2005	Finite element method	ABAQUS	GN	Bending moment-curvature relationship of carbon nanotubes is studied
Fu et al. [113]	2006	Euler Beam (EB)	Galerkin	GN	Relationship of nonlinear amplitude and frequency are expressed for the first time
Xu et al. [51]	2006	EB	Galerkin	van der Waals (vdW)	Effect of vdW froce on out-of-phase vibration mode is studied
Fu et al. [128]	2009	EB	Galerkin	GN	Dynamic instability of DWCNT is studied
Kuang et al. [129]	2009	EB	Galerkin	GN and vdW	Nonlinear response of a DWCNT conveying fluid is studied
Huttel et al. [130]	2009	Experiment and EB	Galerkin	GN	Nonlinear regime for a C-C CNT is studied
Ke et al. [34]	2009	Nonlocal Timoshenko beam (NTB)	Differential quadrature method (DQM)	GN	Effect of nonlocality and nonlinearity is studied
Quakad and Younis [131]	2010	EB	Galerkin	GN	Nonlinear dynamics of electrically actuated carbon nanotube is studied
Ke et al. [132]	2010	Timoshenko beam (TB)	Rayliegh Ritz	GN	Nonlinear free vibration of functionally graded carbon nanotube is studied
Hawwa and Al-Qahtani [133]	2010	EB	Galerkin	GN and vdW	Forced and choatic response of a DWCNT is studied

Table 2-4 Theoretical methods for studying the vibrational characteristics of CNTs, part-2

Researcher	Year	Simulation Method	Solution method	Nonlinearity	Research summary
Yang and Kitipornchai [46]	2010	NTB	DQM	GN	Nonlinear vibration of SWCNT, different types of Boundary conditions (BCs)
Ansari et al. [134]	2010	EB	Homotopy perturbation method	GN	onlinear vibrations of MWCNT, capability and the simplicity of Homotopy perturbation method
Cho et al. [119]	2010	Experiment and EB	Galerkin	GN	They proposed to use nonlinearity to improve efficiency of the resonator
Jannesari et al. [135]	2011	Donnell shallow shell	Series expansion	GN	They have studied the flow of a non-viscous and through SWCNT
Shen and Zhang [136]	2011	Nonlocal Euler beam (NEB)	Galerkin	GN	Postbuckling, nonlinear bending and nonlinear vibration in termal enviroment
Mahdavi et al.	2011	EB and TB	Galerkin	GN and vdW	Nonlinear vibration using different beam models, axial load effects
Yan et al. [137]	2011	EB	Multiple scales method	GN	concept of nonlinear normal modes (NNMs) to characterize the nonlinear dynamical
Wang and Shen [138]	2011	higher-order shear deformation plate theory including plate-foundation interaction	Perturbation technique	GN	Nonlinear vibration of nanotube-reinforced composite plates in thermal environments
Quakad and Younis [139]	2011	2D EB, in-plane and out-of-plane dircetion vibrations	Galerkin	GN and initial curvature (IC)	Natural frequencies and mode shapes of curved CNT resonators under electric excitation
Ansari et al. [93]	2011	Nonlocal Donnell shell theory and molecular dynamics (MD)	Rayleigh Ritz	GN	Development of the nonlocal shell model and calibration of nonlocal parameter via MD
Joshi et al. [140]	2012	EB with concentrated mass	Galerkin	GN and IC	Nonlinear vibration of a SWCNT mass sensor, time responmse, choatic response

Table 2-5 Theoretical methods for studying the vibrational characteristics of CNTs, part-3

Researcher	Year	Simulation Method	Solution method	Nonlinearity	Research summary
Yang and Lim [141]	2012	higher-order strain gradient TB	Galerkin	Nonlinear history of straining	New higher-order equations of motion and new higher-order boundary conditions & nonlocal
Quakad and Younis [142]	2012	EB	Perturbation, multiple scales	GN and IC	dynamics of electrically actuated SWCNT, verified by time integration method
Ansari and Hemmatnezhad [143]	2012	EB	Finite element	GN	large-amplitude free vibrations of DWCNT, different types of BCsMahdavi
Samandari and Cigeroglo [144]	2012	EB with concentrated mass	Galerkin and path following solution method	GN and vdW	Nonlinear in-phase and out-of-phase vibration modes, multiple solution due to concentrated mass
Farshidianfar and Soltani [145]	2012	Nonlocal Euler beam (NEB)	Perturbation, multiple scales	GN and IC	The nonlinear flow-induced vibration of a SWCNT
Cigeroglu and Samandari [121]	2012	EB	Describing function (DF) and multiple trail functions	GN and vdW	Use of DFM determines whether multiple trial functions are necessary or not
Ansari et al. [146]	2012	NEB and curvature dependent vdW force and termal effects	Incremental harmonic balance	GN	Nonlinear vibrations of MWCNT in termal enviroment
Shen and Xiang [147]	2012	carbon nanotube-reinforced composite (CNTRC) shells	Perturbation technique	GN	Nonlinear vibrations of uniformly distributed (UD) and functionally graded (FG) reinforced CNT
Samandari and Cigeroglu [124]	2012	EB	Multiple harmonic balance method (MHBM)	GN and IC	nonlinear effects of initial curvature only appears in higher harmonics
Hajnayeb and Khadem [148]	2012	EB with electrostatic actuation	Multiple scales methods	GN and vdW	Vibration and stability of a DWCNT under electrostatic actuation
Mehdipour et al. [123]	2012	EB	He's Energy Balance Method	GN and IC	nonlinear force vibration of curved SWCNT

Table 2-6 Theoretical methods for studying the vibrational characteristics of CNTs, part-4

Researcher	Year	Simulation Method	Solution method	Nonlinearity	Research summary
Rafiee et al. [149]	2012	EB	Multiple times scales with analyitical expressions	GN	rimary resonance of SWCNT, forced vibration
Ansari et al. [150]	2012	NTB in termal enviroment	Galerkin	GN and vdW	Nonlinear vibration of a DWCNT in termal enviroment, different types of BCs
Samandari and Cigeroglu [122]	2013	EB	DQM with path following solution method	GN and IC	Nonlinear vibration of a curved DWCNT
Arani et al. [151]	2013	Hamilton's principle and nonlocal-nonlinear shell theory	Galerkin and averaging methods	GN	nonlinear vibration of a DWCNT subjected to an axial fluid flow
Rafiee et al. [152]	2013	EB with termal effect	Multiple times scales method	GN	Nonlinear vibration of FGCNT reinforced composite with surface-bonded piezoelectric
Fang et al. [153]	2013	NEB	Davidon–Fletcher–Powell method	GN and vdW	nonlocal DWCNT, out-of-phase vibration mode are more sensitive to nonlocality
Zhang et al. [154]	2014	first-order shear deformation shell theory	kp-Ritz method with kernel particle function	GN	large deflection of FGCNT, CNT graded in thickness direction
Soltani et al. [155]	2014	NEB	Galerkin	GN and IC	Nonlinear vibratin under external harmonic electric force field
Souayeh and Kacem [156]	2014	EB	Galerkin	GN	nonlinear vibrations of CNT under electrostatic actuation, mass sensing applications
Kuo [157]	2014	NEB	Time integration	GN	the period-three, the chaos and the period-one are excited by the different excitation amplitudes
Cigeroglu and Samandari [158]	2014	NEB	DQM with path following alghoritm	GN and vdW and IC	Vibration of nonlocal curved DWCNT, multiple solution at same vibration amplitude

2.5. Concluding remarks

A comprehensive review on the different modeling techniques in studying linear and nonlinear vibration of CNTs is provided in this chapter. The modeling techniques for CNTs can be grouped into three major groups of atomic simulations, continuum mechanics simulations and nonlocal continuum mechanics simulations.

The atomic modeling methods include molecular dynamic (MD) and *ab initio* simulation methods. MD simulation methods relay on the basis of second Newton's law whereas *ab initio* relays on solving Schrödinger equation which is accurate and potential free method. Even though atomic methods can provide considerable amount of information to understand the behavior of a structure in nanometer scales, they are limited by the size of such atomic systems due to highly time consuming computational requirements and the complexity of the formulations. As a result, studies based on atomic simulations are mostly focused on predicting the Young' modulus and linear free vibration of CNTs where vibration amplitudes are limited to few nano meter.

In recent years, continuum modeling methods originated from continuum mechanics are used to study the mechanical properties of CNTs. In these studies the lattice structure of a CNT is replaced with a continuum medium. As a result, the continuum modeling cannot address the chirality effect of CNTs. The validity and accuracy of continuum models in predicting the buckling and bending behavior of CNT is studied by several researchers. Although the mechanical properties of CNTs are extensively depend on the chirality of CNTs, early studies show that, with a tuning, the key parameters that affect the mechanical characteristics of CNTs can be easily studied using simple equations of motions offered by the continuum models.

Furthermore, although classic continuum models can provide quick and approximate predictions, they fail in predicting the size effects. Size effects are originated by the non-contact interaction of atoms and molecules of the material. In recent years, the traditional classical continuum mechanics are modified by several researchers in order to bring in the scale effects within the formulations. The nonlocal elasticity theory presented by Eringen [41] is commonly used by researchers to study vibrations of

CNTs where it has both the accuracy and simple formulation. In the nonlocal elasticity theory, the small-scale effects are captured by assuming that the stress at a point is a function of the strains at all points in the domain [41]. Therefore, unlike the classic elasticity theory, nonlocal theory can include long-range inter-atomic interactions; thus, it yields in the results dependent on the size of a body. Some other theories which also capture the size effects include couple stress elasticity theory, strain gradient theory, and modified couple stress theory. Studies show that nonlocal continuum can be an acceptable approach to overcome the shortcomings of atomistic simulations. However, as to this date, MD simulation provides much reliable predictions, thus it can be used to verify results from other solution methods.

Comparing results in literature obtained from MD methods and continuum methods, it can be concluded that Euler-Bernoulli beam is reliable in predicating the mechanical properties of CNTs when the length to diameter ratio (aspect ratio) is higher than ten ($L/D \geq 10$) whereas Timoshenko beam is more reliable for the length to diameter ratio smaller than 10 and higher bending modes. Between shell theories, the Donnell thin shell theory is unable to include the length dependent critical strains when aspect ratio is smaller than eight whereas Sanders shell theory is accurate in predicting buckling strains and mode shapes of axially compressed CNTs with small aspect ratios.

Recent theoretical and experimental studies show that the deformation of CNTs is nonlinear in nature and it is possible for CNTs to go through large deformations in their elastic region. Studies show that nonlinear natural frequency changes considerably as vibration amplitude increases more than few nano meter. Therefore, it is very important to include the nonlinearity in identifying of the mechanical properties of CNTs. Furthermore, depending on the geometry, phenomenon such as jump and chaos is detected for CNTs theoretically and experimentally. Geometric nonlinearity of CNTs is studied by several researchers in the past few years using different methodologies. Most of these studies are concentrated on understanding the effect of geometric nonlinearity so that its effect can be filtered out for the linear applications. However, for linear operation, the small size of a CNT reduces its dynamic range down to the few nano meter which limits its sensitivity, especially

under ambient and room temperature environments. Recently, it is been suggested by researchers to improve the efficiency of a CNT resonator using its nonlinear characteristics. It is worth noting that nowadays nonlinearities have been successfully used in application such as energy harvesting to improve their efficiency and bandwidth. Hence, the nonlinear characteristics of a CNT resonator can be integrated into the ongoing development of nano scale electromechanical systems to extend their operation limits.

In early studies, tubes of CNT are considered as single beam where interlayer displacement between layers of nanotubes is disregarded. However, with introducing applications such as atomic force probe and mass sensor which have aspect ratio around 10 to 20, the interlayer displacement gets important. The interlayer force between layers of CNTs is governed by van der Waals force (vdW). The vdW force estimated by Lennard-Jones potential is inherently nonlinear. Studies show that nonlinear natural frequency increases as vibration amplitude increases due to vdW force when the CNTs vibrate in the out-of-phase vibration mode. Moreover, the highly nonlinear behavior of the tubes resulted in identification of single nonlinear natural frequencies associated with different vibration amplitudes.

The subject area of carbon nanotube structures is developed in the past few years considerably; however, it is still in its early stages and new applications, literally every day, are introduced by researchers. Furthermore, studies show that these structures are strongly nonlinear. Hence, it is clear for authors that future studies will be directed toward understanding the nonlinear vibration behavior of these structures in practice as well as using potential capacities of the nonlinearities in order to extend their operational capabilities.

CHAPTER 3

ON THE NONLINEAR VIBRATION OF DOUBLE WALLED CARBON NANOTUBES WITH CONCENTRATED MASS[4]

Mechanical resonators are commonly used as a tool to detect small quantities of the adsorbed mass through shifts in the natural frequency. Recent advances in lithography and materials synthesis have enabled the fabrication of nanoscale mechanical resonators. These resonators can be used in application such as atomic probes or atomic mass sensors.

In this chapter, nonlinear free vibration of a simply supported double walled carbon nanotube (DWCNT) with a concentrated-mass is investigated. The proposed model simulates behavior of a nonlinear DWCNT mass sensor where the concentrated mass stands for the absorbed mass. Furthermore, for the first time in this chapter, the effect of both geometric and van der Wall force nonlinearities on the variation of nonlinear natural frequency of CNTs is studied.

3.1. Introduction

In recent years, vibrational behavior of CNTs studied by a number of researchers [44, 159, 160] where, the continuum mechanics approach is used [161, 162]. Using simple equations of motions offered by the continuum models, key parameters that affect the free vibration of CNTs can be easily studied. In the majority of these studies [42, 43], linear models are used to study the vibrational behavior of CNTs. However, it is observed from the experiments that CNTs show nonlinear behavior as their vibration

[4] A version of this chapter is published in the proceeding of the 15th International Conference on Machine Design and Production, June 19 - 22, 2012, Pamukkale, Denizli, Turkey as "Nonlinear Free Vibration Analysis of Double Walled Carbon Nanotubes with a Concentrated-Mass".

amplitude passes a certain value. As a result, in order to consider a more realistic model for CNTs, nonlinear continuum beam models are developed.

Fu et al [44] were the first who studied the nonlinear vibration of carbon nanotubes caused by large deflections. They showed that the nonlinear natural frequency of carbon nanotubes increases considerably as the vibration amplitude increases. Later, their work followed by several researchers. However, reviewing literature, it can be observed that in the majority of the studies concerning nonlinear vibrations of MWCNTs, the interaction pressure between adjacent tubes is linearized and is assumed to depend linearly on the difference of the radial deflections. It should be noted that the interlayer force between layers of CNTs is governed by nonlinear van der Waals force (vdW) as estimated by Lennard-Jones potential [48-50]. Therefore, the nonlinearity of vdW force should be considered in order to determine the vibrational behavior of MWCNTs accurately. It is worth mentioning that the nonlinear vibrational behavior of DWCNTs considering only nonlinear interlayer vdW forces between adjacent tubes was studied in [52, 159, 163]. However, in all of these studies, the effect of geometric nonlinearity is disregarded. Hence, in this chapter for the first time, considering the effect of both geometric and vdW force nonlinearities, nonlinear free vibrations of a DWCNT with a concentrated-mass is studied. Galerkin method is used to discretize the continuous partial differential equation of motion and harmonic balance method is used to convert the nonlinear discretized differential equation of motion into a set of nonlinear algebraic equations which are solved by a nonlinear equation solver [164, 165].

3.2. Equation of motion using Euler-Bernoulli beam model

A DWCNT with a concentrated mass is shown in Figure 3-1, where L, A, E, I, ρ, M_c, L_c and k are the length of the CNT, cross-sectional area, Young's modulus, area moment of inertia, density, mass of the concentrated mass, position of the concentrated mass and the stiffness per unit length of elastic medium, respectively. It is worth noting that, in case of DWCNT, two concentric tubes will interact with each other due to the molecular van der Waals pressure. This pressure acting on the two adjacent tubes depends on the difference between the transverse deflections of the

inner and outer tubes. The free vibration equation of embedded nanotubes considering both geometric and vdW force nonlinearities are [123, 166, 167][5]

$$\begin{aligned} EI_i \frac{\partial^4 w_i}{\partial x^4} + \rho A_i \frac{\partial^2 w_i}{\partial t^2} &= \left[\frac{EA_i}{2L} \int_0^L \left(\frac{\partial w_i}{\partial x} \right)^2 dx \right] \frac{\partial^2 w_i}{\partial x^2} + f(x,t), \\ EI_o \frac{\partial^4 w_o}{\partial x^4} + \left(\rho A_o + M_c \delta(x - L_c) \right) \frac{\partial^2 w_o}{\partial t^2} + k w_o &= \left[\frac{EA_o}{2L} \int_0^L \left(\frac{\partial w_o}{\partial x} \right)^2 dx \right] \frac{\partial^2 w_o}{\partial x^2} - f(x,t) \end{aligned}, \tag{3.1}$$

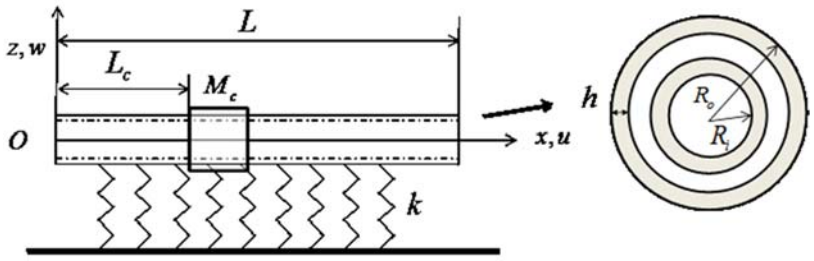

Figure 3-1 Model of an embedded DWCNT.

where i and o indicate the inner and outer tubes, respectively, $\delta(x)$ is the Dirac delta function. $f(x,t)$ is the nonlinear van der Waals force, which is given by [168, 169] as follows

$$f(x,t) = p_1 (w_o - w_i) + p_3 (w_o - w_i)^3, \tag{3.2}$$

and

$$\begin{aligned} p_1 &= \left. \frac{\partial^2 U}{\partial \delta^2} \right|_{\delta = \delta_0} 2R_i = -48 K R_i \\ p_3 &= \left. \frac{\partial^4 U}{\partial \delta^4} \right|_{\delta = \delta_0} 2R_i = -3984 K R_i \end{aligned}. \tag{3.3}$$

$K = -61.665$ meV/atom, R_i is the inner tube radius, and δ_0 is the equilibrium interlayer spacing which has a value of 0.34 nm. For equilibrium spacing, i.e. $\delta = \delta_0$,

[5] The derivation for the nonlinear equation of motion due to stretching of mid-plan is given in Appendix A

the vdW force is equal to zero. U is the interlayer potential per unit area, which can be expressed in terms of the interlayer spacing δ as

$$U(\delta) = K\left[\left(\frac{\delta_0}{\delta}\right)^4 - 0.4\left(\frac{\delta_0}{\delta}\right)^{10}\right]. \tag{3.4}$$

Note that $\delta - \delta_0 = w_o - w_i$ [163]. From Eq. (3.3), it can be observed that the value of p_3 is approximately two orders of magnitude larger than the value of p_1. Substituting Eq. (3.2) into Eq. (3.1) results in the following nonlinear partial differential equations of motion for the DWCNT

$$EI_i \frac{\partial^4 w_i}{\partial x^4} + \rho A_i \frac{\partial^2 w_i}{\partial t^2} = \left[\frac{EA_i}{2L}\int_0^L \left(\frac{\partial w_i}{\partial x}\right)^2 dx\right]\frac{\partial^2 w_i}{\partial x^2} + p_1\left(w_o - w_i\right) + p_3\left(w_o - w_i\right)^3, \tag{3.5}$$

$$EI_o \frac{\partial^4 w_o}{\partial x^4} + \left(\rho A_o + M_c \delta\left(x - L_c\right)\right)\frac{\partial^2 w_o}{\partial t^2} + k w_o = \left[\frac{EA_o}{2L}\int_0^L \left(\frac{\partial w_o}{\partial x}\right)^2 dx\right]\frac{\partial^2 w_o}{\partial x^2} - p_1\left(w_o - w_i\right) - p_3\left(w_o - w_i\right)^3. \tag{3.6}$$

3.3. Solution method

In order to discretize the partial differential equations given by Eqs. (3.5) and (3.6), Galerkin methods is used where the following form of solution is assumed

$$w_k(x,t) = \phi_{k,r}(x) W_{k,r}(t). \tag{3.7}$$

Subscript $k = i, o$ stand for innertube and outertube, respectively. $W_{k,r}(t)$ is the r^{th} generalized coordinate and $\phi_r(x)$ is the r^{th} eigen-function of simply supported linear CNT. The boundary conditions for simply supported CNT can be given as follows

$$w_k(0,t) = w_k(L,t) = 0, \tag{3.8}$$

$$\left.\frac{d^2 w_k}{dx^2}\right|_{x=0} = \left.\frac{d^2 w_k}{dx^2}\right|_{x=L} = 0. \tag{3.9}$$

Mass normalized eigen-functions of a simply supported CNT can be expressed as follows

$$\phi_{k,r}(x)=\sqrt{\frac{2}{\rho A_k L}}\sin\left(\frac{r\pi x}{L}\right),\ r=1,2,\cdots. \tag{3.10}$$

Substituting Eq. (3.7) into Eqs. (3.5) and (3.6), multiplying both sides by $\phi_{k,s}(x)$ and integrating over the domain, the discretized nonlinear ordinary differential equations of motion in $W_{k,r}(t)$ is obtained as follows

$$\begin{aligned}\frac{d^2W_{i,r}(t)}{dt^2}+\frac{EI_i\pi^4r^4}{\rho A_i L^4}W_{i,r}(t)+\frac{EA_i\pi^4r^2}{4L^4}W_{i,r}^3(t)-\frac{p_1}{\rho A_i}\left[W_{o,r}(t)-W_{i,r}(t)\right]\\ -\frac{p_3}{\rho A_i}\left[f_{k,1}-3f_{k,2}+3f_{k,3}-f_{k,4}\right]=0\end{aligned}, \tag{3.11}$$

$$\begin{aligned}\left(1+\frac{2M_c}{\rho A_0 L}\sin\left(\frac{r\pi L_c}{L}\right)^2\right)\frac{d^2W_{o,r}(t)}{dt^2}+\left(\frac{EI_o\pi^4r^4}{\rho A_0L^4}+\frac{k}{\rho A_0}\right)W_{o,r}(t)+\frac{EA_o\pi^4r^2}{4L^4}W_{o,r}^3(t)\\ +\frac{p_1}{\rho A_o}\left[W_{o,r}(t)-W_{i,r}(t)\right]+\frac{p_3}{\rho A_o}\left[f_{k,1}-3f_{k,2}+3f_{k,3}-f_{k,4}\right]=0\end{aligned}, \tag{3.12}$$

where

$$f_{k,1}=\int_0^L\left(\left(\phi_{o,r}(x)W_{o,r}(t)\right)^3\phi_{k,s}(x)\right)dx, \tag{3.13}$$

$$f_{k,2}=\int_0^L\left(\left(\phi_{o,r}(x)W_{o,r}(t)\right)^2\left(\phi_{i,r}(x)W_{i,r}(t)\right)\phi_{k,s}(x)\right)dx, \tag{3.14}$$

$$f_{k,3}=\int_0^L\left(\left(\phi_{o,r}(x)W_{o,r}(t)\right)\left(\phi_{i,r}(x)W_{i,r}(t)\right)^2\phi_{k,s}(x)\right)dx, \tag{3.15}$$

$$f_{k,4}=\int_0^L\left(\left(\phi_{i,r}(x)W_{i,r}(t)\right)^3\phi_{k,s}(x)\right)dx. \tag{3.16}$$

It should be noted that two nonlinear ordinary differential equation of motions are obtained for each eigenfunctions, where the nonlinear terms are expressed by $f_{k,j}$. In

this study only the undamped nonlinear natural frequency of DWCNTs is investigated; hence, any form of damping, structural and viscous damping, are neglected. Assuming a harmonic solution in the following form

$$W_{k,r}(t) = a_{k,r}\sin(\omega_r t), \tag{3.17}$$

and substituting it into Eq. (3.11) and (3.12), the following set of nonlinear algebraic equations is obtained

$$\begin{aligned}&\left[-\omega_r^2 a_{i,r} + \frac{EI_i\pi^4 r^4}{\rho A_i L^4}a_{i,r} + \frac{EA_i\pi^4 r^2}{4L^4}a_{i,r}^3 - \frac{p_1}{\rho A_i}\left[a_{o,r} - a_{i,r}\right]\right.\\ &\left.-\frac{p_3}{\rho A_i}\left[g_{k,1} - 3g_{k,2} + 3g_{k,3} - g_{k,4}\right]\right]\sin\omega_r t + O(\text{higher harmonics}) = 0\end{aligned}, \tag{3.18}$$

$$\begin{aligned}&\left[-\omega_r^2\left(1 + \frac{2M_c}{\rho A_0 L}\sin\left(\frac{r\pi L_c}{L}\right)^2\right)a_{o,r} + \left(\frac{EI_o\pi^4 r^4}{\rho A_0 L^4} + \frac{k}{\rho A_0}\right)a_{o,r} + \frac{EA_i\pi^4 r^2}{4L^4}a_{o,r}^3\right.\\ &\left.+\frac{p_1}{\rho A_0}\left[a_{o,r} - a_{i,r}\right] + \frac{p_3}{\rho A_0}\left[g_{k,1} - 3g_{k,2} + 3g_{k,3} - g_{k,4}\right]\right]\sin(\omega_r t) + O(\text{higher harmonics}) = 0\end{aligned}, \tag{3.19}$$

where

$$g_{k,1} = \frac{3a_{o,r}^3}{4}\int_0^L\left(\phi_{o,r}^3(x)\phi_{k,s}(x)\right)dx, \tag{3.20}$$

$$g_{k,2} = \frac{3a_{o,r}^2 a_{i,r}}{4}\int_0^L\left(\phi_{o,r}^2(x)\phi_{i,r}(x)\phi_{k,s}(x)\right)dx, \tag{3.21}$$

$$g_{k,3} = \frac{3a_{o,r}a_{i,r}^2}{4}\int_0^L\left(\phi_{o,r}(x)\phi_{i,r}^2(x)\phi_{k,s}(x)\right)dx, \tag{3.22}$$

$$g_{k,4} = \frac{3a_{i,r}^3}{4}\int_0^L\left(\phi_{i,r}^3(x)\phi_{k,s}(x)\right)dx. \tag{3.23}$$

Disregarding the effect of higher harmonic terms, a set of two nonlinear algebraic equations is derived for the r^{th} eigenfunction as follow

$$\left(\mathbf{K} - \omega_r^2\cdot\mathbf{M}\right)\cdot\mathbf{x}_r + \boldsymbol{\alpha}\cdot\mathbf{x}_r^3 + \mathbf{g}_N(\mathbf{x}_r) = 0, \tag{3.24}$$

where

$$\mathbf{M}=\begin{bmatrix}1 & 0\\ 0 & 1+\dfrac{2M_c}{\rho A_0 L}\sin\left(\dfrac{r\pi l}{L}\right)^2\end{bmatrix}, \tag{3.25}$$

$$\mathbf{K}=\begin{bmatrix}\dfrac{EI_i\pi^4 r^4}{\rho A_i L^4}+\dfrac{c_1}{\rho A_i} & -\dfrac{c_1}{\rho A_i}\\ -\dfrac{c_1}{\rho A_o} & \dfrac{EI_o\pi^4 r^4}{\rho A_0 L^4}+\dfrac{c_1}{\rho A_o}\end{bmatrix}, \tag{3.26}$$

$$\boldsymbol{\alpha}=\begin{bmatrix}\dfrac{EA_i\pi^4 r^2}{4L^4} & 0\\ 0 & \dfrac{EA_o\pi^4 r^2}{4L^4}\end{bmatrix}, \tag{3.27}$$

$$\mathbf{g}_N(\mathbf{x})=\begin{Bmatrix}-c_3\cdot\left(g_{i,1}-3g_{i,2}+3g_{i,3}-g_{i,4}\right)\\ c_3\cdot\left(g_{o,1}-3g_{o,2}+3g_{o,3}-g_{o,4}\right)\end{Bmatrix}, \tag{3.28}$$

$$\mathbf{x}_r=\begin{Bmatrix}a_{i,r}\\ a_{o,r}\end{Bmatrix},\quad \mathbf{x}_r{}^3=\begin{Bmatrix}a_{i,r}{}^3\\ a_{o,r}{}^3\end{Bmatrix}. \tag{3.29}$$

In order to solve the resulting nonlinear algebraic equations given by Eq. (3.24), Newton's method with Homotopy continuation and Arc-length continuation is used, details of which can be found in [165].

3.4. Results

In this section, nonlinear free vibration of simply supported DWCNT with a concentrated-mass is investigated. The material and geometric parameters of the simply supported DWCNT used in this study are given in Table 3-1 [163]. It is worth to present characteristics of the linear system before investigating the effects of nonlinearities.

Natural frequencies of the linear system without the concentrated-mass are given in Table 3-2 together with the modal coefficients of the inner and outer tubes. Since the equation of motion is composed of two partial differential equations, there exist two

natural frequencies corresponding to the in-phase, and out-of-phase vibration modes. In the former case, inner and outer tubes move in the same direction; whereas, for the latter case, they vibrate in opposite directions. The coefficient of mode shape of each CNT is as well given in the table, where a sign difference indicates the out-of-phase mode, which are also plotted in Figure 3-2. The effect of concentrated mass on the natural frequencies of the DWCNT, is presented in Figure 3-3. It is observed that as the mass ratio increases, the linear natural frequency decreases for both natural frequencies, which is an expected result.

Table 3-1 Numerical Values of DWCNT Parameters [163]

Parameter	value
Inner radius of innertube	0.35 nm
Outer radius of outertube	1.4 nm
Density of tubes	2.3 gr/cm^3
Young modulus of tubes	1 TPa
Thickness of tubes	0.34 nm

In the following section, the effect of concentrated-mass on the first in-phase and out-of-phase nonlinear natural frequencies of a DWCNT is studied considering the effect of mass ratio and the position of the concentrated-mass. In addition to these, as a final case study, the effect of medium stiffness on the nonlinear natural frequency is investigated. It should be noted that the nonlinear natural frequency is normalized with respect to the corresponding linear natural frequency, ω_l, of the simply supported DWCNT with a concentrated-mass , and the vibration amplitude, a_k, is normalized with respect to $r=\sqrt{I_i/A_i}$.

Table 3-2 Natural frequencies of DWCNT without concentrated-mass

Eigen-functions		$\sin\frac{\pi x}{l}$
In-phase frequency [THz]		0.4673
Coefficient of Mode Shape	Innertube	1
	Outertube	0.997
Out-of-phase frequency [THz]		7.8852
Coefficient of Mode Shape	Innertube	1
	Outertube	-0.502

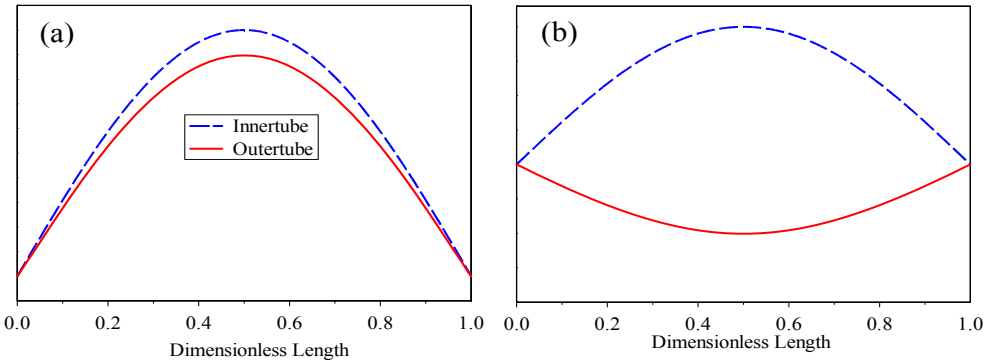

Figure 3-2 First two linear mode shapes of DWCNT a) in-phase b) out-of-phase

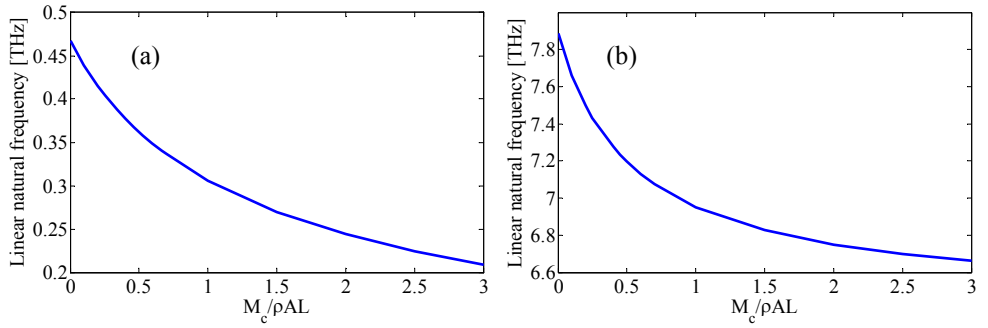

Figure 3-3 Variation of the first two linear natural frequencies against increasing concentrated-mass (position of the concentrate-mass is at the middle of the DWCNT) a) in-phase b) out-of-phase

3.4.1. Effect of key parameters in the first in-phase vibration mode

In Figure 3-4, the variation of the normalized nonlinear natural frequency of the first in-phase vibration mode, considering only the geometric nonlinearity, is presented for different ratios of the concentrated-mass to total CNT mass. Position of the concentrated mass is kept constant at the middle of the outertube. It is observed that the normalized nonlinear natural frequency is not affected by the variation of the mass ratio. It is worth noting that as the mass ratio increases, the nonlinear natural frequency decreases; however its variation after normalizing with respect to the linear natural frequency is the same for all mass ratios. On the other hand, in Figure 3-5, the variation of normalized nonlinear natural frequency is plotted in presence of only vdW force nonlinearity considering different mass ratios. It is seen that the slope of the normalized nonlinear natural frequency decreases as the mass ratio increases. It should be noted that the deviation of the nonlinear natural frequency from the linear one in the presence of only vdW force nonlinearity is negligible. This is an expected

result, since vdW force nonlinearity depends on the relative motion between the inner and outer tubes and in case of in-phase vibration modes, this difference is very small.

Considering both the geometric and vdW force nonlinearities, the variation of the normalized nonlinear natural frequency is given in Figure 3-6 for different values of mass ratio. Since the effect of vdW force nonlinearity is small in comparison to geometric nonlinearity in the first in-phase mode, it can be seen that the variation of the normalized nonlinear natural frequency is identical to the results given in Figure 3-4. Similar results can be obtained if the effect of position of the concentrated-mass is studied. For instance, the variation of the normalized nonlinear natural frequency in the first in phase mode is given in Figure 3-7 in existence of only vdW force nonlinearity. It is observed that as the concentrated mass moves away from the center of the outertube the normalized nonlinear natural frequency increases.

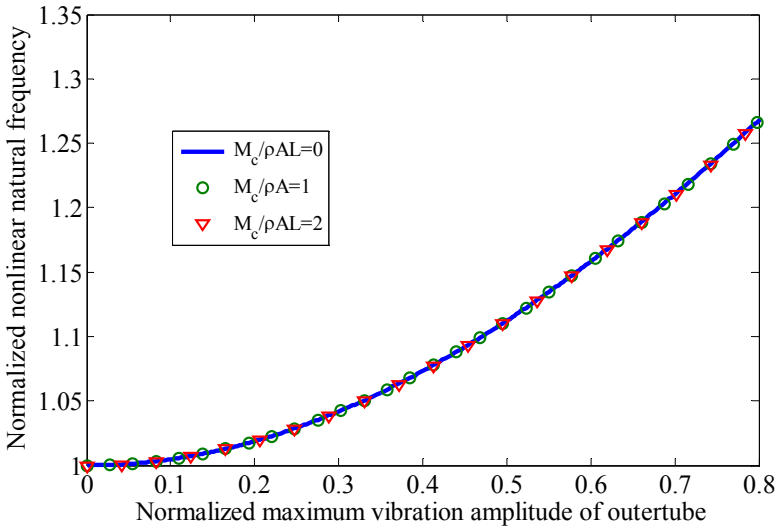

Figure 3-4 Variation of normalized nonlinear natural frequency in the presence of only geometric nonlinearity in the first in-phase vibration mode

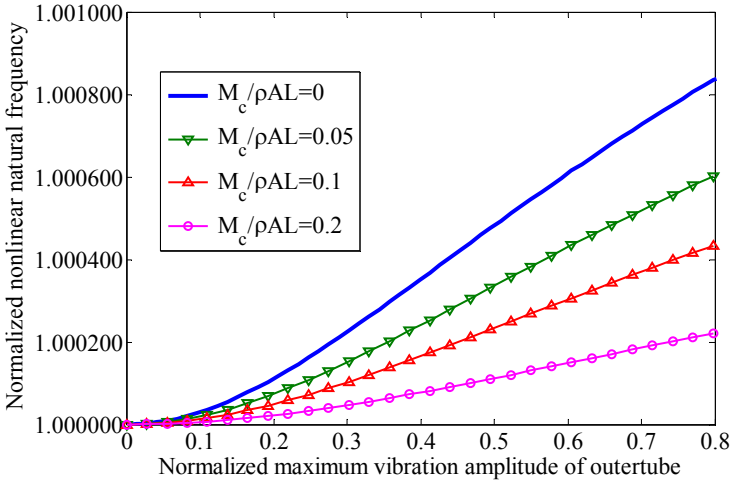

Figure 3-5 Variation of the normalized nonlinear natural frequency in the presence of only vdW force nonlinearity in the first in-phase vibration mode

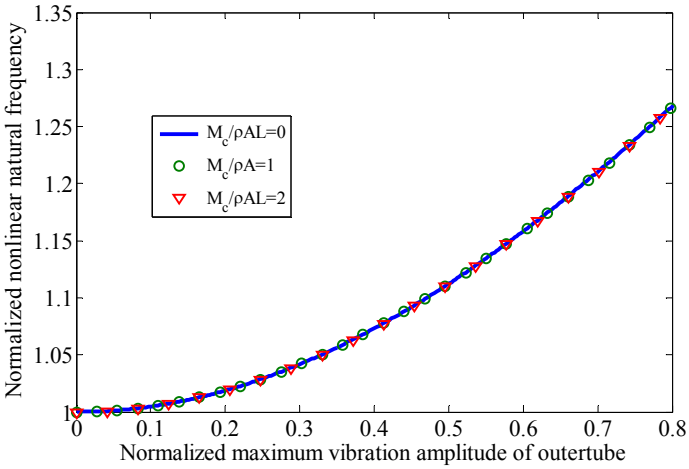

Figure 3-6 Variation of normalized nonlinear natural frequency in the presence of both geometric and vdW force nonlinearities in the first in-phase vibration mode

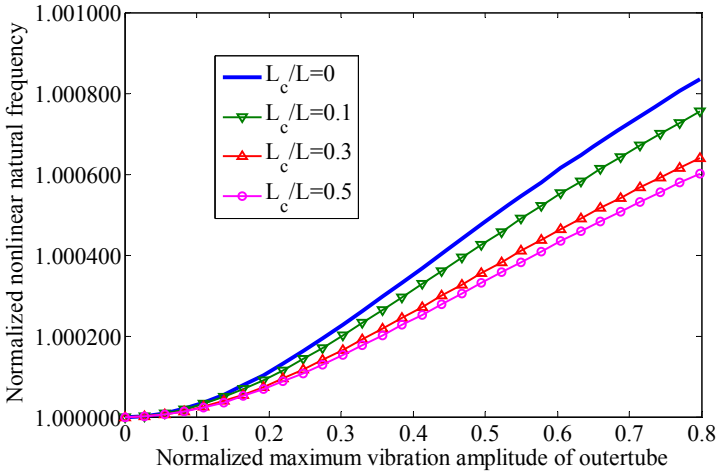

Figure 3-7 Variation of the normalized nonlinear natural frequency in the presence of only vdW force nonlinearity in the first in-phase vibration mode

3.4.2. Effect of key parameters in the first out-of-phase vibration mode

In Figure 3-8 to Figure 3-10, the variation of the normalized nonlinear natural frequency is given for the first out-of-phase vibration mode considering different mass ratios in presence of only geometric nonlinearity, only vdW force nonlinearity and both of nonlinearities keeping the concentrated mass at the middle of the outertube, respectively. It can be observed that in the first out-of-phase vibration mode, as the mass ratio increases the effect of the nonlinearity increases as well. A similar effect is observed for the case with only vdW force nonlinearity; whereas, in this case, the variation of the nonlinear natural frequency is significantly high. Therefore, considering both nonlinearities the effect of geometric nonlinearity is not visible. This is an expected result, since vdW force nonlinearity depends on the relative motion between the inner and outer tubes and in the case of out-of-phase vibration mode, this difference is significant. Similar behavior can be identified for position effect of concentrated-mass where it can be observed that as position of the concentrated-mass gets closer to the maximum point of vibration amplitude (i.e. the midpoint), the effect of the nonlinearity increases (Figure 3-11).

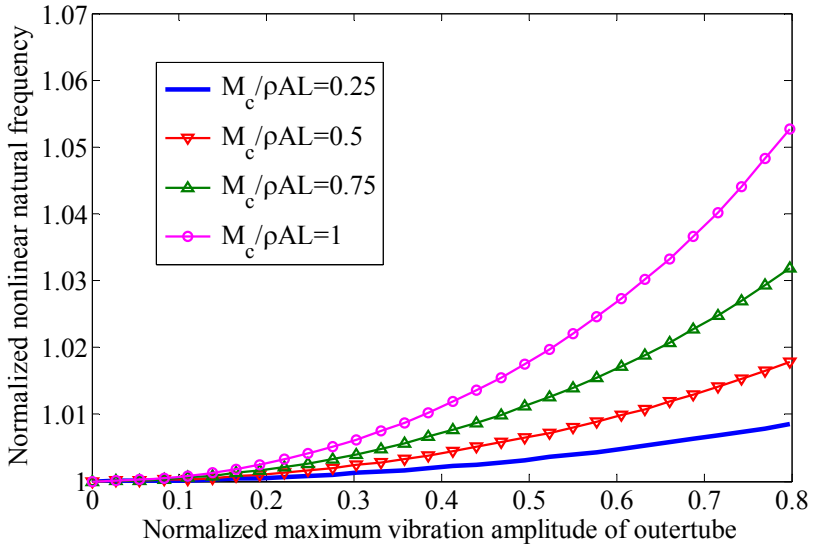

Figure 3-8 Variation of the normalized nonlinear natural frequency in the presence of only geometric nonlinearity in the first out-of-phase vibration mode

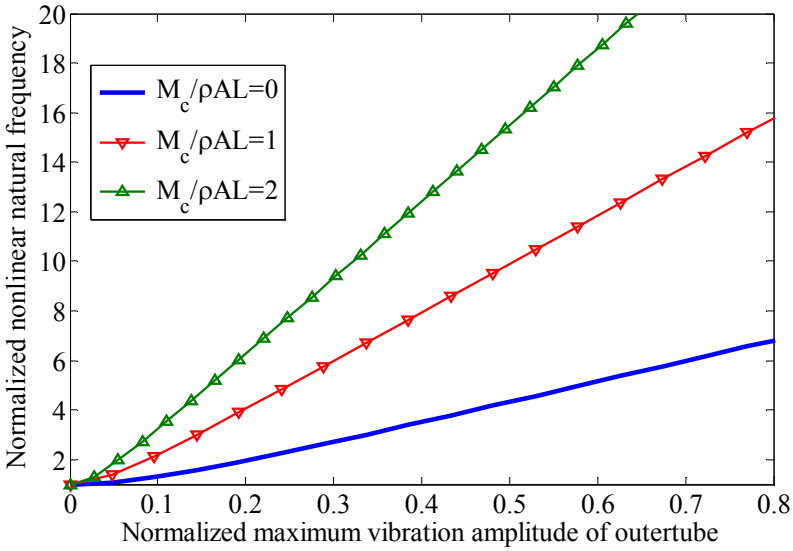

Figure 3-9 Variation of the normalized nonlinear natural frequency in the presence of only vdW force nonlinearity in the first out-of-phase vibration mode

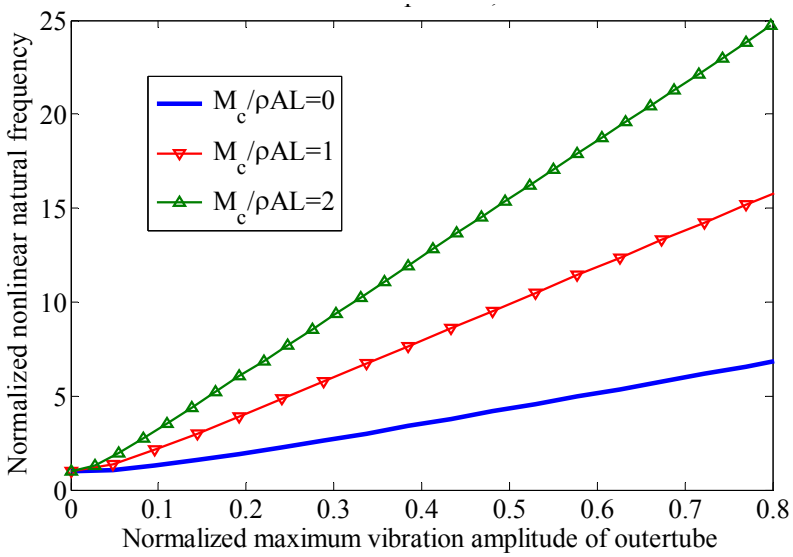

Figure 3-10 Variation of the normalized nonlinear natural frequency in the presence both nonlinearities in the first out-of-phase vibration mode

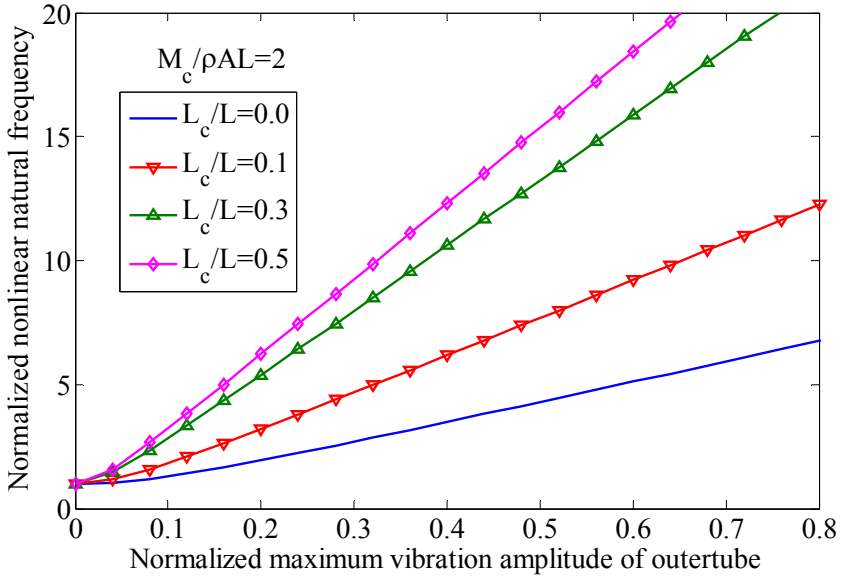

Figure 3-11 Variation of the normalized nonlinear natural frequency in the presence both nonlinearities in the first out-of-phase vibration mode

3.5. Effect of medium stiffness on the first out of-phase nonlinear natural frequency

Figure 3-12 and Figure 3-13 show the variation of the nonlinear natural frequency of the outertube against the normalized maximum vibration amplitude for different values of medium stiffness vibrating in the first out-of-phase mode. In these analyses, the concentrated mass is kept at the midpoint of the outertube with a mass ratio of 2.5. It is seen that as the medium stiffness, k , increases, the nonlinear frequency tends to approach the linear one. Moreover, it is observed in the first out-of-phase mode that the normalized nonlinear natural frequency curves can be represented by two lines having different slopes. As the medium stiffness increases the break point shifts to a higher vibration amplitude and further increase of the medium stiffness results in a turning point where multiple solutions at a single vibration amplitude can be observed. It should be noted that the turning point is not detected for the case with no concentrated-mass. In Figure 3-14, for constant medium stiffness of $1.2\text{x}10^{12}$ N/m^2, the variation of nonlinear natural frequency against normalized maximum vibration amplitude is given for several mass ratios. The break point moves towards left and the slope of the curves increases as the mass ratio increases. The slope of the part after the break point increases and at a certain value it becomes nearly perpendicular to x

axis. Increasing the mass ratio more than this value results in a turning point; hence, multiple solutions at a single vibration amplitude exist.

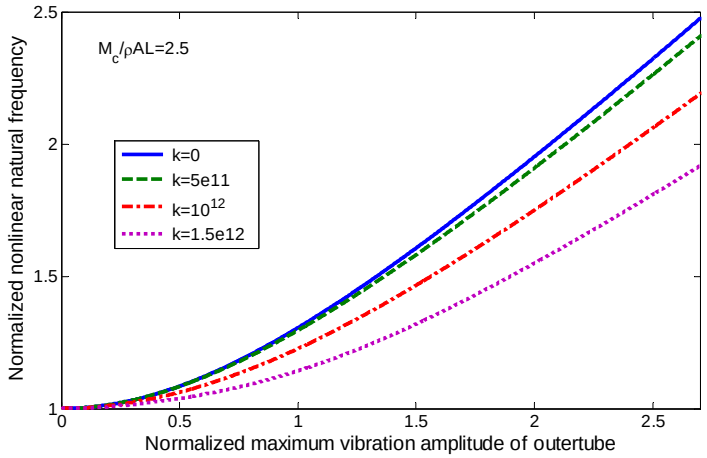

Figure 3-12 Variation of the normalized nonlinear natural frequency for different values of medium stiffness in the first in-phase vibration mode

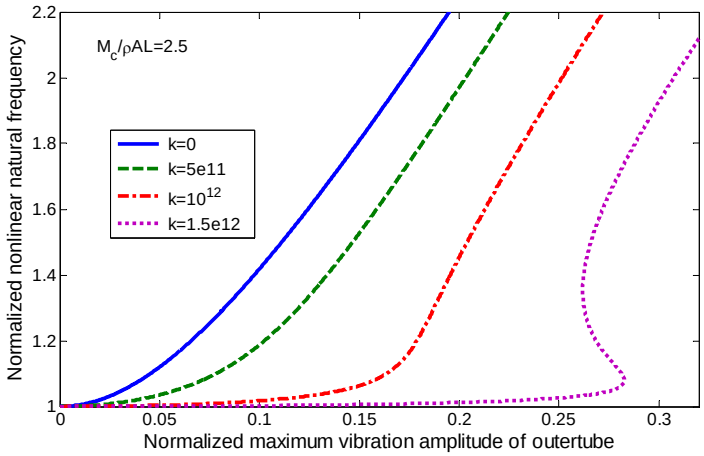

Figure 3-13 Variation of the normalized nonlinear natural frequency for different values of medium stiffness in the first out-of-phase vibration mode

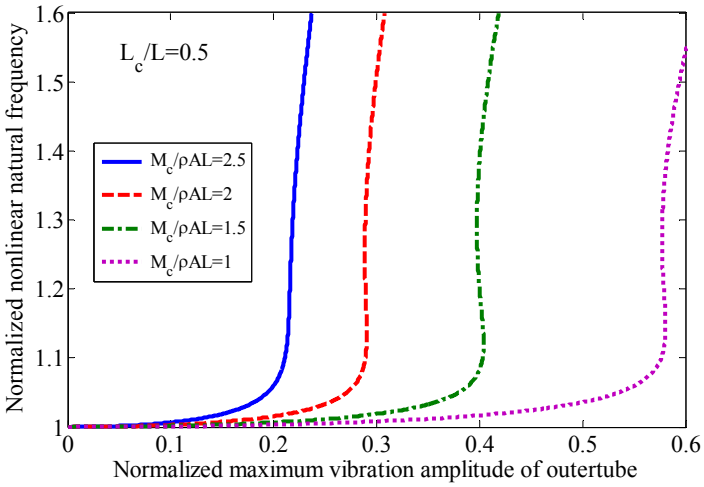

Figure 3-14 Variation of the normalized nonlinear natural frequency in the first out-of-phase vibration mode

3.6. Concluding remarks

In this chapter, nonlinear free vibration of a simply supported double walled carbon nanotube is investigated where geometric and vdW force nonlinearities are included in the analyses. Galerkin method is used to discretize the continuous differential equation of motion. The discretized ordinary differential equation of motion is converted into a set of nonlinear algebraic equations by using harmonic balance method with a single harmonic term. The resulting nonlinear algebraic equations are solved by using a nonlinear equation solver. Results show that, in the first in-phase vibration mode, the normalized nonlinear natural frequency of DWCNT is not affected by the concentrated-mass where only geometric nonlinearity exists. On the other hand, for the case of vdW force nonlinearity, the normalized nonlinear natural frequency is affected; but, this effect is very small. Moreover, it can be seen that in the presence of vdW force nonlinearity, as mass ratio increases or the position of concentrated-mass gets closer to the maximum point of vibration amplitude of DWCNT (i.e. the midpoint), the curves tend towards the linear natural frequency of system. However, for the case of vdW force nonlinearity the change in the normalized nonlinear natural frequency is very small.

Similarly, the first out-of-phase mode of DWCNT is studied, where It is observed that as the mass ratio increases, the slope of the normalized nonlinear frequency curves increases in the case of geometric and vdW force nonlinearities; however, the effect

of vdW force nonlinearity is significantly higher than the effect of geometric nonlinearity. Moreover, the effect of medium stiffness in presence of geometric and vdW force nonlinearities is investigated. Results show that for the increasing values of medium stiffness, the nonlinear natural frequency of the in-phase and out-of-phase vibration modes tends to the linear natural frequency of the system. However, for the case of out-of-phase vibration mode, the curve can be represented by two lines having different slopes. Increase of medium stiffness or the decrease of mass ratio shifts the break point at higher vibration amplitudes and at specific medium stiffness and mass ratio a turning point, which resulted in multiple nonlinear natural frequencies at a single vibration amplitude, is observed. Moreover, this phenomenon cannot be obtained when there is no concentrated mass on the DWCNT. Since nano sensors works on the basis of shifts in natural frequency due to absorbed nanoparticle, results of the present study can be used in the development of nonlinear nano mass sensors.

CHAPTER 4

NONLINEAR FREE VIBRATION OF DOUBLE WALLED CARBON NANOTUBES BY USING DESCRIBING FUNCTION METHOD WITH MULTIPLE TRIAL FUNCTIONS[6]

This Chapter deals with implementing describing function method (DFM) with multiple trial functions in order to get a better approximation of the system mode shape. Using DFM, nonlinear free vibration of double walled carbon nanotubes (DWCNTs) embedded in an elastic medium with both geometric nonlinearity and interlayer van der Waals force nonlinearity are studied. The motion of the DWCNT is represented by multiple eigenfunctions of the linear system which are referred as trial functions.

4.1. Introduction

Reviewing the literature on nonlinear vibrations of CNTs it has been observed that, in all of the studies, single trial function assumption is used to study the system behavior where the trial function is considered to be the exact eigenfunction of the relevant linear system. However for nonlinear systems, the resulting nonlinear eigenfunctions can be significantly different than the eigenfunctions of the linear system, and depending on the nonlinearity, it may not be possible to capture the nonlinear characteristics by using a single trial function [56]. It should be noted that even for linear systems, in order to solve the eigenvalue problem, multiple trial functions are needed unless the exact eigenfunctions of the system are known.

---

[6] A version of this chapter is published in the Physica E: Low-dimensional Systems and Nanostructures as "Nonlinear Free Vibration of Double Walled Carbon Nanotubes by Using Describing Function Method with Multiple Trial Functions"

In this chapter, multiple trial functions are used to investigate the nonlinear free vibrations of DWCNTs. In addition to this, a new solution approach, describing function method (DFM), is proposed to solve the resulting system of nonlinear differential equations. DFM [170-174], in comparison to solution methods like variational approach [175], or differential quadrature method [34, 176, 177], has the advantage of expressing the nonlinear force as a nonlinear stiffness matrix multiplied by a displacement vector, where the off-diagonal terms of the nonlinear stiffness matrix can provide a comprehensive knowledge about the coupling between the trial functions. Using DFM, nonlinear differential equations of motion are converted into a set of nonlinear algebraic equations, which is solved numerically by using Newton's method [164, 165] with Homotopy continuation [178, 179] or Arc-Length continuation [165, 180]. In the following section, equation of motion for DWCNTs is obtained and the basics of DFM are presented.

4.2. Equation of motion using Euler-Bernoulli beam model

Consider a CNT of length L, cross-sectional area A, area moment of inertia I, Young's modulus E, and density ρ embedded in an elastic medium having a stiffness per unit length of k as shown in Figure 3-1. Free vibration of a CNT embedded in elastic medium, considering the geometric nonlinearity due to large deformations, is governed by [166, 167]

$$EI\frac{\partial^4 w}{\partial x^4}+\rho A\frac{\partial^2 w}{\partial t^2}=\left[\frac{EA}{2L}\int_0^L\left(\frac{\partial w}{\partial x}\right)^2 dx\right]\frac{\partial^2 w}{\partial x^2}+p(x,t), \tag{4.1}$$

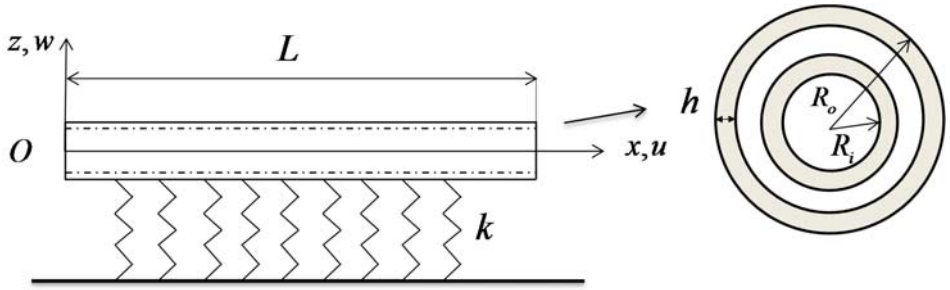

Figure 4-1 Model of an embedded DWCNT

where $w(x,t)$ is the transverse displacement and $p(x,t)$ is the interaction pressure per unit axial length between the tube and the surrounding medium, which can be identified by the Winkler-like model [47, 181] as

$$p(x,t) = -kw(x,t). \tag{4.2}$$

The negative sign in the above equation shows that the pressure $p(x,t)$ is opposite to the deflection of the tube and k is defined by the material constants of the surrounding elastic medium. Substituting Eq. (4.2) into Eq (4.1), gives

$$EI\frac{\partial^4 w}{\partial x^4} + \rho A\frac{\partial^2 w}{\partial t^2} + kw = \left[\frac{EA}{2L}\int_0^L \left(\frac{\partial w}{\partial x}\right)^2 dx\right]\frac{\partial^2 w}{\partial x^2}. \tag{4.3}$$

In case of DWCNT, two concentric tubes will interact with each other due to the molecular van der Waals pressure. This pressure acting on the two adjacent tubes depends on the difference between the transverse deflections of the inner and outer tubes. Assuming that the tubes are vibrating in the same plane; the coplanar transverse motion of an embedded DWCNT is described by the following coupled nonlinear partial differential equations.

$$\begin{aligned} EI_i\frac{\partial^4 w_i}{\partial x^4} + \rho A_i\frac{\partial^2 w_i}{\partial t^2} &= \left[\frac{EA_i}{2L}\int_0^L \left(\frac{\partial w_i}{\partial x}\right)^2 dx\right]\frac{\partial^2 w_i}{\partial x^2} + f(x,t), \\ EI_o\frac{\partial^4 w_o}{\partial x^4} + \rho A_o\frac{\partial^2 w_o}{\partial t^2} + kw_o &= \left[\frac{EA_o}{2L}\int_0^L \left(\frac{\partial w_o}{\partial x}\right)^2 dx\right]\frac{\partial^2 w_o}{\partial x^2} - f(x,t), \end{aligned} \tag{4.4}$$

where $f(x,t)$ is the van der Waals force, i and o indicate the inner and outer tubes, respectively.

4.2.1. Van der Waals force

Van der Waals (vdW) forces are composed of weak attractive forces between atoms, molecules, and surfaces, in addition to other intermolecular forces [80, 182]. The vdW force per unit area for two originally concentric tubes is given in [168, 169] as

$$F = \frac{\partial U}{\partial \delta}. \tag{4.5}$$

U is the interlayer potential per unit area, which can be expressed in terms of the interlayer spacing δ as

$$U(\delta) = K\left[\left(\frac{\delta_0}{\delta}\right)^4 - 0.4\left(\frac{\delta_0}{\delta}\right)^{10}\right], \tag{4.6}$$

Where $K = -61.665$ meV/atom, and $\delta_0 = 0.34$ nm is the equilibrium interlayer spacing. For equilibrium spacing, i.e. $\delta = \delta_0$, the vdW force, F, is equal to zero. Moreover, since the vdW force per unit area is an odd function of the interlayer spacing, the Taylor series expansion of F about $\delta = \delta_0$ can be written as follows

$$F = \left.\frac{\partial^2 U}{\partial \delta^2}\right|_{\delta=\delta_0} \left(w_o - w_i\right) + \frac{1}{6}\left.\frac{\partial^4 U}{\partial \delta^4}\right|_{\delta=\delta_0} \left(w_o - w_i\right)^3. \tag{4.7}$$

The change in the inter-tube spacing is given by $\delta - \delta_0 = w_o - w_i$ [163], then the van der Waals force per unit length of the CNT is

$$f(x,t) = p_1\left(w_o - w_i\right) + p_3\left(w_o - w_i\right)^3, \tag{4.8}$$

where

$$\begin{aligned} p_1 &= \left.\frac{\partial^2 U}{\partial \delta^2}\right|_{\delta=\delta_0} 2R_i = -48\,K\,R_i, \\ p_3 &= \left.\frac{\partial^4 U}{\partial \delta^4}\right|_{\delta=\delta_0} 2R_i = -3984K\,R_i. \end{aligned} \tag{4.9}$$

where R_i is the inner tube radius. It can be observed that the value of coefficient p_3 is approximately two orders of magnitude larger than the value of p_1. Substituting Eq. (4.8) into Eq. (4.4) results in the following nonlinear partial differential equation for the DWCNT

$$EI_i \frac{\partial^4 w_i}{\partial x^4} + \rho A_i \frac{\partial^2 w_i}{\partial t^2} = \left[\frac{EA_i}{2L} \int_0^L \left(\frac{\partial w_i}{\partial x} \right)^2 dx \right] \frac{\partial^2 w_i}{\partial x^2} + p_1 \left(w_o - w_i \right) + p_3 \left(w_o - w_i \right)^3, \tag{4.10}$$

$$EI_o \frac{\partial^4 w_o}{\partial x^4} + \rho A_o \frac{\partial^2 w_o}{\partial t^2} + k w_o = \left[\frac{EA_o}{2L} \int_0^L \left(\frac{\partial w_o}{\partial x} \right)^2 dx \right] \frac{\partial^2 w_o}{\partial x^2} - p_1 \left(w_o - w_i \right) - p_3 \left(w_o - w_i \right)^3. \tag{4.11}$$

4.2.2. Describing Function Method (DFM)

Describing Function Method was developed by Tanrikulu et al. [173] which is the generalization of the method developed by Budak and Özgüven [170] for all type of nonlinearities. Using DFM, it is possible to convert nonlinear differential equations of motion into a set of nonlinear algebraic equations [170, 172]. DFs are used to represent nonlinear functions by quasi linear describing functions with amplitude dependent gains. In this method, a sinusoidal input to the nonlinear function is applied then the fundamental component of output is considered; hence, describing function is defined as the ratio of the output to the input. Using the method described in [172], the nonlinear force vector is replaced by a response dependent matrix multiplied by a displacement vector. In this section, harmonic response analysis of nonlinear multiple degrees of freedom (mdof) systems using DFM, reported in [172], is briefly summarized, then the method is applied to nonlinear free vibration problem of DWCNTs defined by Eqs. (4.10) and (4.11).

Equation of motion of a nonlinear structure in the absence of external forcing can be written as follows

$$\mathbf{M} \cdot \ddot{\mathbf{y}} + \mathbf{C} \cdot \dot{\mathbf{y}} + i\mathbf{H} \cdot \mathbf{y} + \mathbf{K} \cdot \mathbf{y} + \mathbf{f}(\mathbf{y}, \dot{\mathbf{y}}, \ddot{\mathbf{y}}, \cdots) = \mathbf{0}, \tag{4.12}$$

where $\mathbf{f}$ and $\mathbf{y}$ represent the internal nonlinear force and displacement vectors, and $\mathbf{M}$, $\mathbf{K}$, $\mathbf{C}$, $\mathbf{H}$, and i are the mass matrix, stiffness matrix, viscous damping matrix, structural damping matrix and imaginary number, respectively. Assuming single harmonic motion, the above equation of motion can be written as

$$\left(\mathbf{K} - \omega^2 \mathbf{M} + i\omega \mathbf{C} + i\mathbf{H} \right) \cdot \mathbf{x} + \mathbf{f}_N(\mathbf{x}) = \mathbf{0}, \tag{4.13}$$

where $\mathbf{x}$ and $\mathbf{f}_N$ are the complex displacement amplitude vector, and complex nonlinear internal forcing vector, respectively. Using describing functions, it is possible to write $\mathbf{f}_N(\mathbf{x})$ as a multiplication of a displacement dependent complex matrix, $\mathbf{\Delta}$ and complex displacement vector $\mathbf{x}$, where

$$\mathbf{\Delta}_{kk} = \nu_{kk} + \sum_{\substack{j=1 \\ j\neq k}}^{n} \nu_{kj} \quad \text{and} \quad \Delta_{kj} = -\nu_{kj}\,, \tag{4.14}$$

$$\nu_{kj} = \frac{i}{\pi \left\| x_k - x_j \right\|} \int_0^{2\pi} n_{kj}\, \mathrm{e}^{-i\psi}\, d\psi\,. \tag{4.15}$$

where ν_{kj} is the harmonic input describing function and can be described as the equivalent linear complex stiffness for internal nonlinear force and n_{kj} is the nonlinear force acting between the k^{th} and the j^{th} coordinates. Using DFM the effect of nonlinear forces and the locations of the nonlinear elements can be easily identified [183].

In the next section using multiple trial functions and Galerkin method, partial differential equations of motion defined by Eqs. (4.10) and (4.11) are discretized into a set of nonlinear ordinary differential equations. Then, using DFM, the set of nonlinear ordinary differential equations is converted into a set of nonlinear algebraic equations. Finally, the resulting set of nonlinear algebraic equations is solved by using Newton's method.

4.3. Solution Method

For the discretization of the partial differential equations given by Eqs. (4.10) and (4.11), using multiple trial functions the following form of solution is assumed

$$w_k(x,t) = \sum_{r=1}^{n} W_{k,r}(t)\,\phi_r(x)\,. \tag{4.16}$$

Here, n is the number of trial functions considered in the expansion, subscript $k = i, o$ stand for innertube and outertube, respectively. $W_{k,r}(t)$ is the r^{th} generalized coordinate and $\phi_r(x)$ is the r^{th} trial function which is a comparison function satisfying all geometric and natural boundary conditions. In this paper, free vibration analysis of a simply supported DWCNT is considered and the boundary conditions for simply supported case can be given as follows:

$$w_k(0,t) = w_k(L,t) = 0, \tag{4.17}$$

$$\left.\frac{d^2 w_k}{dx^2}\right|_{x=0} = \left.\frac{d^2 w_k}{dx^2}\right|_{x=L} = 0, \tag{4.18}$$

Where $k = i, o$. The trial functions considered are the eigenfunctions of the linear system which are given as

$$\phi_r(x) = \sin\left(\frac{r\pi x}{L}\right),\ r = 1, 2, \cdots, n. \tag{4.19}$$

Substituting Eq. (4.19) into Eqs. (4.10) and (4.11), multiplying both sides by $\phi_s(x)$ and integrating over the domain, the discretized nonlinear ordinary differential equations of motion in terms of $W_{k,r}(t)$ are obtained as follows

$$\begin{aligned}\rho A_i \frac{d^2 W_{i,r}(t)}{dt^2} + \frac{EI_i \pi^4 r^4}{L^4} W_{i,r}(t) + \frac{EA_i \pi^4 r^2}{4L^4} W_{i,r}(t)\left[\sum_{s=1}^{n} s^2 W_{i,s}^2(t)\right] \\ - p_1\left[W_{o,r}(t) - W_{i,r}(t)\right] - p_3\left[f_1 - 3f_2 + 3f_3 - f_4\right] = 0\end{aligned}, \tag{4.20}$$

$$\begin{aligned}\rho A_o \frac{d^2 W_{o,r}(t)}{dt^2} + \left(\frac{EI_o \pi^4 r^4}{L^4} + k\right) W_{o,r}(t) + \frac{EA_o \pi^4 r^2}{4L^4} W_{o,r}(t)\left[\sum_{s=1}^{n} s^2 W_{o,s}^2(t)\right] \\ + p_1\left[W_{o,r}(t) - W_{i,r}(t)\right] + p_3\left[f_1 - 3f_2 + 3f_3 - f_4\right] = 0\end{aligned}, \tag{4.21}$$

$$f_1 = \frac{2}{L}\int_0^L \left(\left(\sum_{m=1}^{n} W_{o,r}(t)\sin\left(\frac{m\pi x}{L}\right)\right)^3 \sin\frac{r\pi x}{L}\right) dx, \tag{4.22}$$

$$f_2 = \frac{2}{L}\int_0^L \left(\left(\sum_{m=1}^{n} W_{o,r}(t) \sin(\frac{m\pi x}{L}) \right)^2 \left(\sum_{s=1}^{n} W_{i,s}(t) \sin(\frac{s\pi x}{L}) \right) \sin\frac{r\pi x}{L} \right) dx , \tag{4.23}$$

$$f_3 = \frac{2}{L}\int_0^L \left(\left(\sum_{m=1}^{n} W_{o,r}(t) \sin(\frac{m\pi x}{L}) \right) \left(\sum_{s=1}^{n} W_{i,s}(t) \sin(\frac{s\pi x}{L}) \right)^2 \sin\frac{r\pi x}{L} \right) dx , \tag{4.24}$$

$$f_4 = \frac{2}{L}\int_0^L \left(\left(\sum_{s=0}^{n} W_{i,s}(t) \sin(\frac{s\pi x}{L}) \right)^3 \sin\frac{r\pi x}{L} \right) dx . \tag{4.25}$$

The total number of nonlinear ordinary differential equations of motion obtained from Eqs. (4.20) and (4.21) is $2n$, where the nonlinear terms are expressed by the last three terms in Eqs. (4.20) and (4.21). In this study, only the undamped nonlinear free vibration of DWCNTs are investigated; hence, any form of damping, structural and viscous damping, are neglected. Assuming a harmonic solution in the following form

$$W_{k,r}(t) = a_{k,r} \sin(\omega t) , \tag{4.26}$$

and substituting it into Eqs. (4.20) and (4.21), and applying DFM the following set of nonlinear algebraic equations are obtained:

$$\left(\mathbf{K} - \omega^2 \mathbf{M}\right) \cdot \mathbf{x} + \mathbf{f}_N(\mathbf{x}) = \mathbf{0} , \tag{4.27}$$

$$\mathbf{M}_{2n\times 2n} = Identity, \tag{4.28}$$

$$\mathbf{K}_{2n\times 2n} = \left[\begin{array}{ccc:ccc} \frac{EI_i\pi^4}{\rho A_i l^4} + \frac{p_1}{\rho A_i} & & 0 & -\frac{p_1}{\rho A_i} & & 0 \\ & \ddots & & & \ddots & \\ 0 & & n^4\frac{EI_i\pi^4}{\rho A_i l^4} + \frac{p_1}{\rho A_i} & 0 & & -\frac{p_1}{\rho A_i} \\ \hdashline -\frac{p_1}{\rho A_o} & & 0 & \frac{EI_o\pi^4}{\rho A_o l^4} + \frac{p_1}{\rho A_o} & & 0 \\ & \ddots & & & \ddots & \\ 0 & & -\frac{p_1}{\rho A_o} & 0 & & n^4\frac{EI_o\pi^4}{\rho A_o l^4} + \frac{p_1}{\rho A_o} \end{array}\right] , \tag{4.29}$$

$$\mathbf{x}=\left\{\begin{array}{c} a_{i,1} \\ \vdots \\ a_{i,n} \\ \hline a_{o,1} \\ \vdots \\ a_{o,n} \end{array}\right\}. \tag{4.30}$$

The mass matrix is an identity matrix which is diagonal. However, the linear stiffness matrix has some off diagonal terms. The stiffness matrix given by Eq. (4.29) can be divided into four square matrices as indicated. The diagonal terms in the off-diagonal matrices are due to coupling between inner and outer tubes due to linear vdW forces. It should be noted that, since the exact eigenfunctions of the linear system are used in the expansion theorem, there is no off-diagonal terms in the four sub-matrices which indicates that there is no coupling between the trial functions employed.

In DWCNTs considered, two major sources of nonlinearity exist: geometric nonlinearity, and vdW force nonlinearity. By using DFM, the nonlinear force vector, $\mathbf{f}_N(\mathbf{x})$, can be expressed as

$$\mathbf{f}_N(\mathbf{x})=\boldsymbol{\Delta}_g(\mathbf{x})\cdot\mathbf{x}+\boldsymbol{\Delta}_v(\mathbf{x})\cdot\mathbf{x}, \tag{4.31}$$

where $\boldsymbol{\Delta}_g$, and $\boldsymbol{\Delta}_v$ are geometric nonlinearity matrix and vdW force nonlinearity matrix. Using Eqs. (4.14) and (4.15), the geometric nonlinearity matrix, $\boldsymbol{\Delta}_g(\mathbf{x})$, can be written as follows by omitting the functional dependence on $\mathbf{x}$ for brevity

$$\boldsymbol{\Delta}_g=\frac{3E\pi^4}{16\rho l^4}\sum_{r=1}^{n}\left[\begin{array}{ccc:ccc} r^2\left|a_{i,r}\right|^2 & & 0 & & & \\ & \ddots & & & \mathbf{0} & \\ 0 & & n^2r^2\left|a_{i,r}\right|^2 & & & \\ \hdashline & & & r^2\left|a_{o,r}\right|^2 & & 0 \\ & \mathbf{0} & & & \ddots & \\ & & & 0 & & n^2r^2\left|a_{o,r}\right|^2 \end{array}\right]. \tag{4.32}$$

Investigating the geometric nonlinearity matrix given by Eq. (4.32), it can be seen that $\mathbf{\Delta}_g$ is a diagonal matrix. Therefore, it can be concluded that considering only geometric nonlinearity, there is no coupling between the trial functions of inner or outer tubes. Consequently, in the absence of vdW force, each pair of nonlinear equations defined by Eq. (4.27) can be solved independent from other pairs; hence, using multiple trial functions or a single trial function does not affect the nonlinear natural frequencies.

The second source of nonlinearity considered in DWCNTs is due to the interlayer vdW force which has a cubic form. Similar to the geometric nonlinearity matrix, the elements of the vdW force nonlinearity matrix can be obtained from Eqs. (4.14) and (4.15). An example nonlinearity matrix considering three trial functions is given in Eq. (4.33). Nonlinear stiffness matrix for higher number of trial functions can be calculated in a similar manner.

$$\mathbf{\Delta}_v = \frac{9c_3}{16\rho}\left[\begin{array}{ccc|ccc} \frac{1}{A_i}\begin{bmatrix} k_{n1} & 0 & k_{n4} \\ 0 & k_{n2} & 0 \\ k_{n5} & 0 & k_{n3} \end{bmatrix} & & & \frac{-1}{A_i}\begin{bmatrix} k_{n1} & 0 & k_{n4} \\ 0 & k_{n2} & 0 \\ k_{n5} & 0 & k_{n3} \end{bmatrix} & & \\ \hline \frac{-1}{A_o}\begin{bmatrix} k_{n1} & 0 & k_{n4} \\ 0 & k_{n2} & 0 \\ k_{n5} & 0 & k_{n3} \end{bmatrix} & & & \frac{1}{A_0}\begin{bmatrix} k_{n1} & 0 & k_{n4} \\ 0 & k_{n2} & 0 \\ k_{n5} & 0 & k_{n3} \end{bmatrix} & & \end{array}\right], \tag{4.33}$$

where $k_{ni}(i=1,2,...,5)$ are given in Appendix A. The nonlinear stiffness matrix is divided into four square matrices as shown in Eq. (4.33). Similar to the linear case, the off-diagonal matrices indicates the coupling between the inner and outer tubes whereas the off-diagonal elements in the four square matrices indicate coupling between the trial functions used in the expansion process. For the case of three trial functions, Eq. (4.33), it can be observed that due to the nonzero k_{n4} and k_{n5}, there is coupling between the 1st and 3rd trial functions of the innertube and similarly there is coupling between the 1st and 3rd trial functions of the outertube as well. It is worth noting that the second trial function is not coupled with any other trial functions. This property is repeated for higher number of trial functions where even trial functions are not coupled with any other trial function. Therefore, it can be concluded that even trial functions do not affect the natural frequencies associated with odd trial functions.

Consequently, nonlinear equations associated with even numbered trail functions can be solved independent of the other equations.

In this study, since the first in-phase and out-of-phase nonlinear natural frequencies of a simply supported DWCNT is investigated, only the odd trial functions are considered and in the following sections, the term for r^{th} trial function stands for the r^{th} odd trial function.

4.4. Solution of Nonlinear Algebraic Equations

In this study, in order to solve the resulting nonlinear algebraic equations, Newton's method with Homotopy continuation and Arc-length continuation is used. The nonlinear equation of motion given in Eq. (4.27) can be written as a residual vector function as

$$\mathbf{r}(\mathbf{y},\lambda)=\left[\begin{array}{c|ccc|ccc|c} & & \mathbf{K}-\omega^2\mathbf{M} & & & & & 0 \\ \hline \phi_1(x^*) & \phi_3(x^*) & \cdots & \phi_{2n-1}(x^*) & 0 & \cdots & 0 & 0 \end{array}\right]\left\{\begin{array}{c}\mathbf{x}\\ \hline \omega\end{array}\right\}+\left\{\begin{array}{c}\mathbf{f}_N(\mathbf{x})\\ \hline 0\end{array}\right\}-\left\{\begin{array}{c}\mathbf{0}\\ \hline \lambda\end{array}\right\}=\mathbf{0}\,, \quad (4.34)$$

Where $\mathbf{y}=\left(\mathbf{x}^T \mid \omega\right)^T$, and λ is the vibration amplitude at $x=x^*$, which is used to follow the solution path as described by the bottom row of Eq. (4.34). It should be noted that since the even numbered trial functions are not coupled with other equations, only odd numbered trial functions are used in Eq. (4.34). Moreover, in this formulation innertube vibration amplitude is used to follow the path, which can be replaced with outertube by simply switching the trial functions on the left of bottom row with the zeros in the middle of the bottom row. Solution of this nonlinear algebraic equation set can be obtained by utilizing Newton's method [165], for which an iteration step is given as follows

$$\mathbf{y}_{k+1}=\mathbf{y}_k-\left[\frac{\partial\mathbf{r}(\mathbf{y},\lambda)}{\partial\mathbf{y}}\right]^{-1}\Bigg|_{\mathbf{y}_k,\lambda_k}\cdot\mathbf{r}(\mathbf{y}_k,\lambda_k), \quad (4.35)$$

where $\partial\mathbf{r}(\mathbf{y},\lambda)/\partial\mathbf{y}$ is the Jacobian matrix. Newton's method converges to the correct solution quadratically if the initial guess is sufficiently close to the actual solution.

However, convergence problems arise when a solution is around a turning point, since the Jacobian matrix becomes singular. Moreover, in order to follow the solution branch even it reverses its direction, continuation parameter λ has to be replaced with another parameter for which it is possible to follow the path. Therefore, an additional parameter, arc- length parameter, is added to the vector of unknowns, which results in a nonsingular Jacobian matrix at the turning points.

The new arc length parameter can be defined as the radius of a fictitious *n*-dimensional sphere centered at the previous converged solution point. The new solution will be searched on the surface of this sphere rather than at the next vibration amplitude. A graphical explanation is given in Figure 4-2, where the fictitious *n*-dimensional sphere becomes a circle in the two-dimensional case. It should be noted that, there exists two solutions, which are the intersection points of the solution path and the circle as shown in Figure 4-2. Therefore, in order not follow the solution path backwards, an initial guess close to the next solution point should be used.

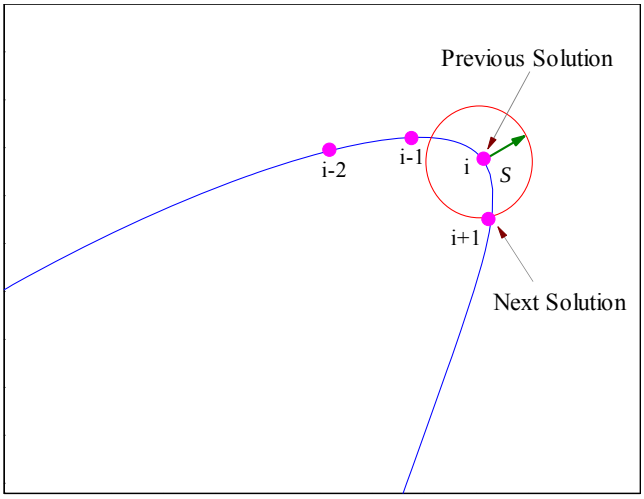

Figure 4-2 Arc-length continuation method

Since vibration amplitude, λ, becomes an unknown, a new equation is needed in order to obtain the solution. This new equation is the equation of the *n*-dimensional sphere centered at the previous solution point which can be given as follows

$$\Delta\mathbf{q}_{(i)}{}^{T} \cdot \Delta\mathbf{q}_{(i)} = s^2 . \tag{4.36}$$

Here, $\mathbf{q}_{(i)}$ is the new vector of unknowns at the i^{th} solution point which is given as

$$\mathbf{q}_{(i)} = \left\{ \begin{array}{c} \mathbf{y}_{(i)} \\ \hline \lambda_{(i)} \end{array} \right\}, \tag{4.37}$$

and

$$\Delta\mathbf{q}_{(i)} = \mathbf{q}_{(i)} - \mathbf{q}_{(i-1)}. \tag{4.38}$$

Therefore the new equation added to the system can be written as

$$h(\mathbf{y}_{(i)}, \lambda_{(i)}) = \Delta\mathbf{q}_{(i)}{}^{T} \cdot \Delta\mathbf{q}_{(i)} - s^2 = 0. \tag{4.39}$$

Therefore, Newton's iteration for the new system of equations becomes

$$\mathbf{q}_{(i)_{k+1}} = \mathbf{q}_{(i)_k} - \left[\begin{array}{c|c} \dfrac{\partial \mathbf{r}(\mathbf{y},\lambda)}{\partial \mathbf{y}} & \dfrac{\partial \mathbf{r}(\mathbf{y},\lambda)}{\partial \lambda} \\ \hline \dfrac{\partial h(\mathbf{y},\lambda)}{\partial \mathbf{y}} & \dfrac{\partial h(\mathbf{y},\lambda)}{\partial \lambda} \end{array} \right]^{-1}\Bigg|_{\mathbf{y}_{(i)_k}, \lambda_{(i)_k}} \cdot \left\{ \begin{array}{c} \mathbf{r}(\mathbf{y}_{(i)_k}, \lambda_{(i)_k}) \\ \hline h(\mathbf{y}_{(i)_k}, \lambda_{(i)_k}) \end{array} \right\}, \tag{4.40}$$

where the last row of the new Jacobian matrix can be obtained as follows,

$$\left[\begin{array}{c|c} \dfrac{\partial h(\mathbf{y},\lambda)}{\partial \mathbf{y}} & \dfrac{\partial h(\mathbf{x},\lambda)}{\partial \lambda} \end{array} \right]\Bigg|_{\mathbf{y}_{(i)_k}, \lambda_{(i)_k}} = \left[2\Delta\mathbf{q}_{(i)_k} \right]^{T}. \tag{4.41}$$

4.5. Results

In this section, nonlinear free vibration of simply supported DWCNTs is investigated by using multiple trial functions. In order to present the results in a proper form, the nonlinear natural frequency is normalized with respect to the corresponding linear natural frequency of the simply supported DWCNT, ω_1, and the deflections, $w_k(x,t)$, are normalized with respect to $\sqrt{I_i/A_i}$. The material and geometric parameters of the simply supported DWCNT used in this study are given in Table 4-1.

The first 5 natural frequencies of the linear system and the corresponding eigenfunctions are given in Table 4-2. Since the equation of motion is composed of two partial differential equations, for every eigenfunction, two natural frequencies exist: in-phase, and out-of-phase. In the former case, inner and outer tubes move in the same direction; whereas for the latter case, they vibrate in opposite directions. The coefficient of mode shape of each CNT is as well given in the table, where a sign difference indicates an out-of-phase mode. The first three in-phase and out-of-phase mode shapes of the system are given in Figure 4-3.

Table 4-1 Numerical values of parameters used

Parameter	Value
Inner radius of innertube	0.35 nm
Outer radius of outertube	1.4 nm
Density of tubes	2.3 gr/cm^3
Young modulus of tubes	1 TPa
Thickness of tubes	0.34 nm

Table 4-2 First five natural frequencies and modes of the linear DWCNT

Eigen-functions		$\sin\frac{\pi x}{l}$	$\sin\frac{2\pi x}{l}$	$\sin\frac{3\pi x}{l}$	$\sin\frac{4\pi x}{l}$	$\sin\frac{5\pi x}{l}$
In-phase frequency [THz]		0.4673	1.8595	4.0817	6.7209	9.2723
Coefficient of Mode shape	Inner tube	1	1	1	1	1
	Outer tube	0.997	0.949	0.761	0.424	0.182
Out-of-phase frequency [THz]		7.8852	8.0299	8.6772	10.5567	14.3868
Coefficient of Mode shape	Inner tube	1	1	1	1	1
	Outer tube	-0.502	-0.527	-0.657	-1.179	-2.744

In the following section, the effect of using multiple trial functions on the first in-phase and out-of-phase vibration modes of a DWCNT is investigated by presenting the variation of normalized nonlinear natural frequency with respect to the normalized maximum vibration amplitude. Firstly, only vdW force nonlinearity is considered and the effect of using multiple trial functions is investigated. Later, the same study is repeated considering only the geometric nonlinearity. Finally, considering both nonlinearities and multiple trial functions, the effect of medium stiffness on the nonlinear natural frequency of simply supported DWCNTs is investigated.

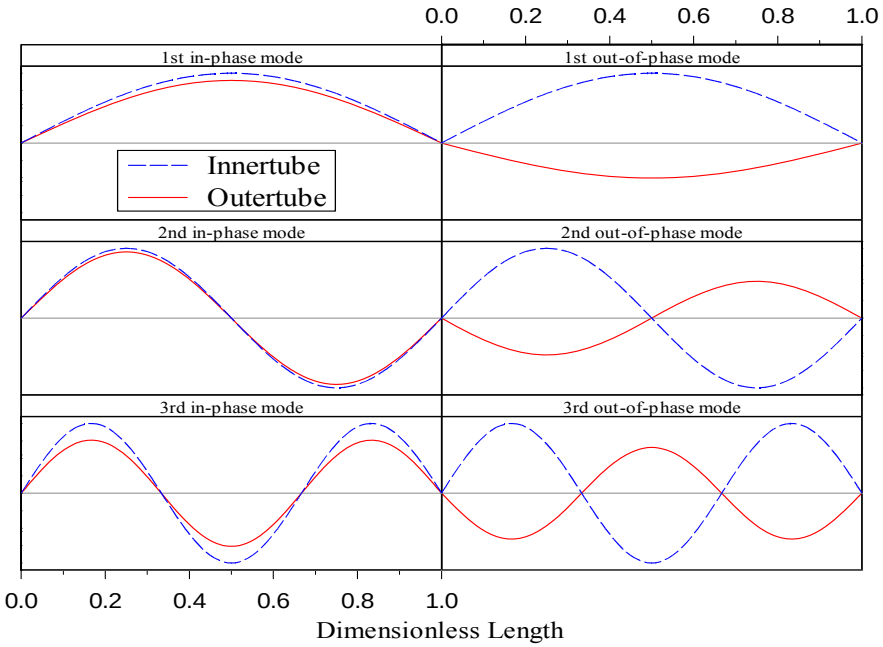

Figure 4-3 First three in-phase and out-of-phase linear mode shapes of DWCNT

4.5.1. First in-phase natural frequency considering vdW force nonlinearity

In Figure 4-4 and Figure 4-5, variation of normalized nonlinear natural frequency for the first in-phase vibration mode of inner and outer tubes are given for the cases utilizing different number of trial functions. It should be noted that, even trial functions do not affect other natural frequencies; therefore, the solutions are obtained by utilizing different number of odd trial functions. Results show that for the first in-phase vibration mode, increasing the number of trial functions used in the solution more than two does not affect the nonlinear natural frequency.

In Figure 4-6, amplitudes of the coefficients of trial functions used in the expansion are plotted for the outer tube where the contribution of each trial function can be clearly seen. It is observed that majority of the contribution is due to the first trial function. This is an expected result, since vdW force nonlinearity depends on the relative motion between the inner and outer tubes and in case of in-phase vibration modes, this difference changes slightly during free vibration. As a result of this, the nonlinear coupling terms are not strong enough to affect the natural frequency significantly.

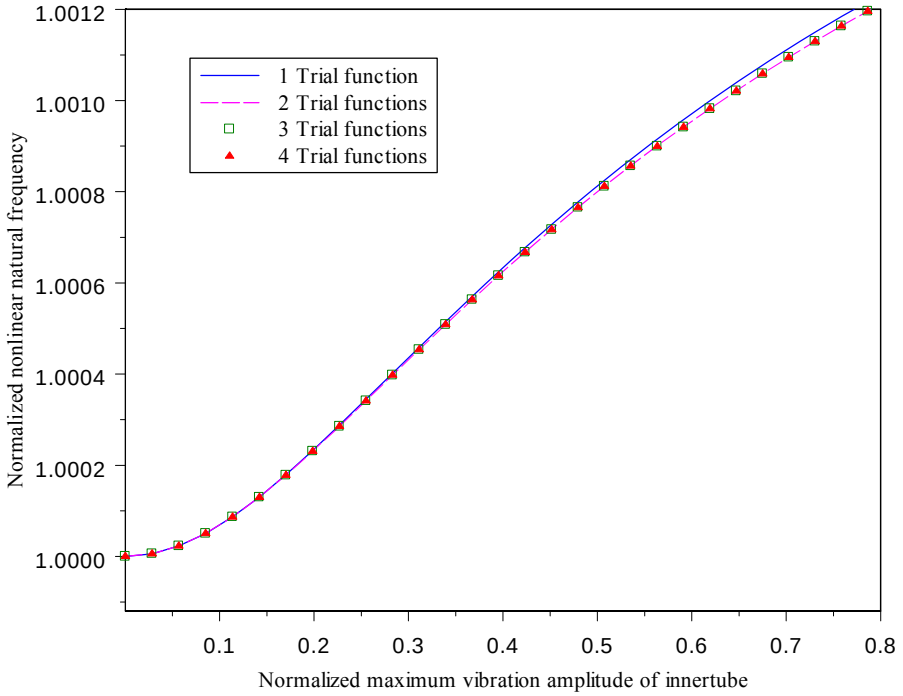

Figure 4-4 Variation of normalized nonlinear natural frequency of innertube vibrating in the first in-phase mode

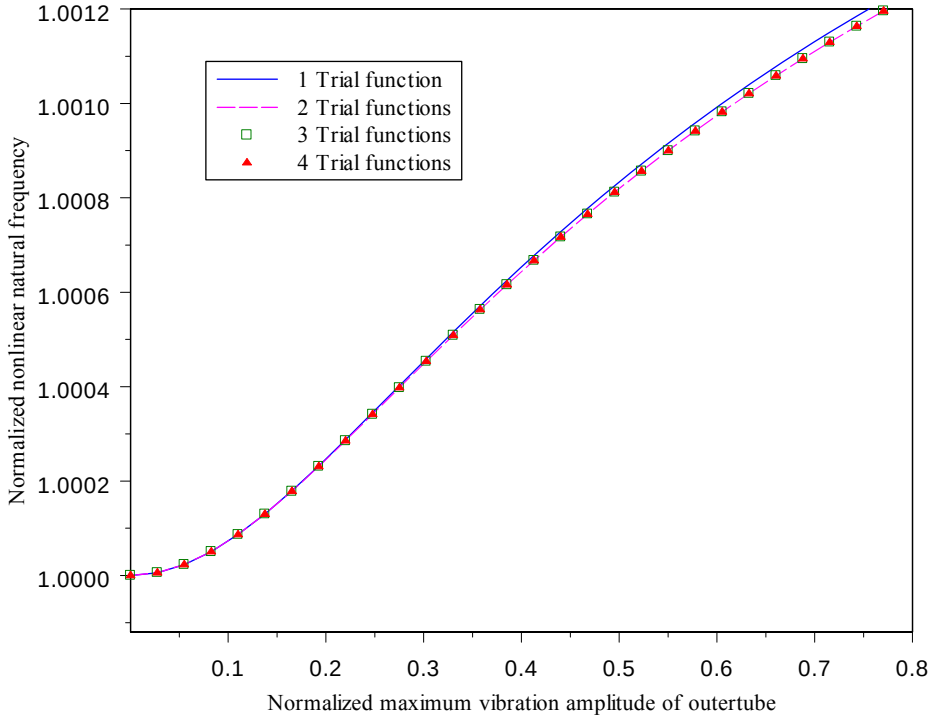

Figure 4-5 Variation of normalized nonlinear natural frequency of outertube vibrating in the first in-phase mode

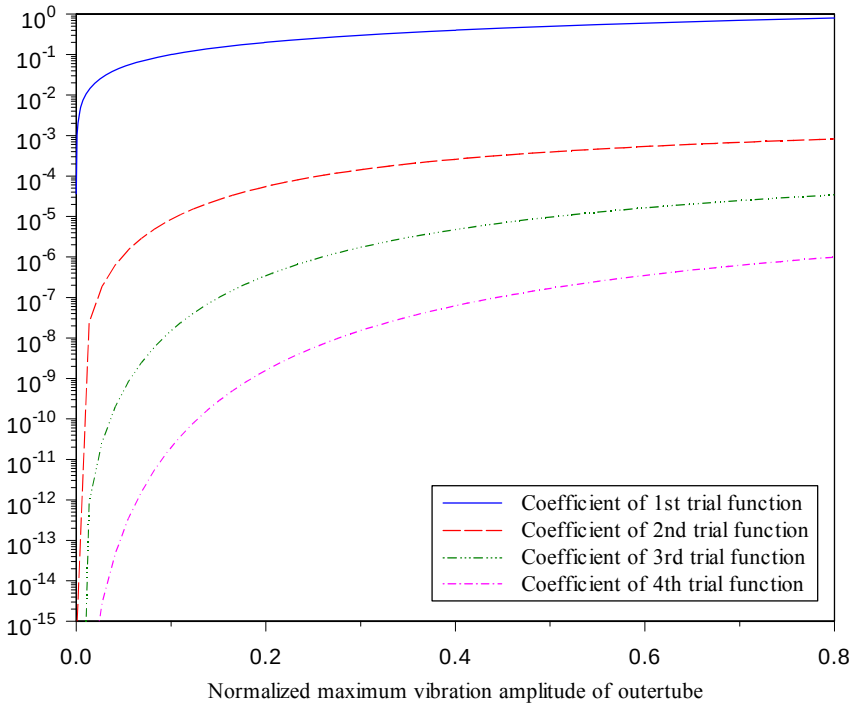

Figure 4-6 Coefficient of trial functions of outertube vibrating in the first in-phase mode

4.5.2. First out-of-phase natural frequency considering vdW force nonlinearity

In Figure 4-7 and Figure 4-8, variation of normalized nonlinear natural frequency of the innertube and the outertube for the first out-of-phase vibration mode are given utilizing different number of trial functions, respectively. Results show that, as the number of trial functions used in the expansion is increased more than two, nonlinear natural frequency vs. vibration amplitude curves change considerably. It is observed that for the case of three and more trial functions, and for increasing vibration amplitude, multiple natural frequencies for a single maximum vibration amplitude are observed. Similarly, for some nonlinear natural frequencies, multiple maximum vibration amplitudes can be obtained. It should be noted that since the free vibration of the DWCNT is expressed in terms of multiple trial functions, the maximum vibration amplitude does not occur at the same point on the CNT, which is not the case if a single trial function is used in the expansion.

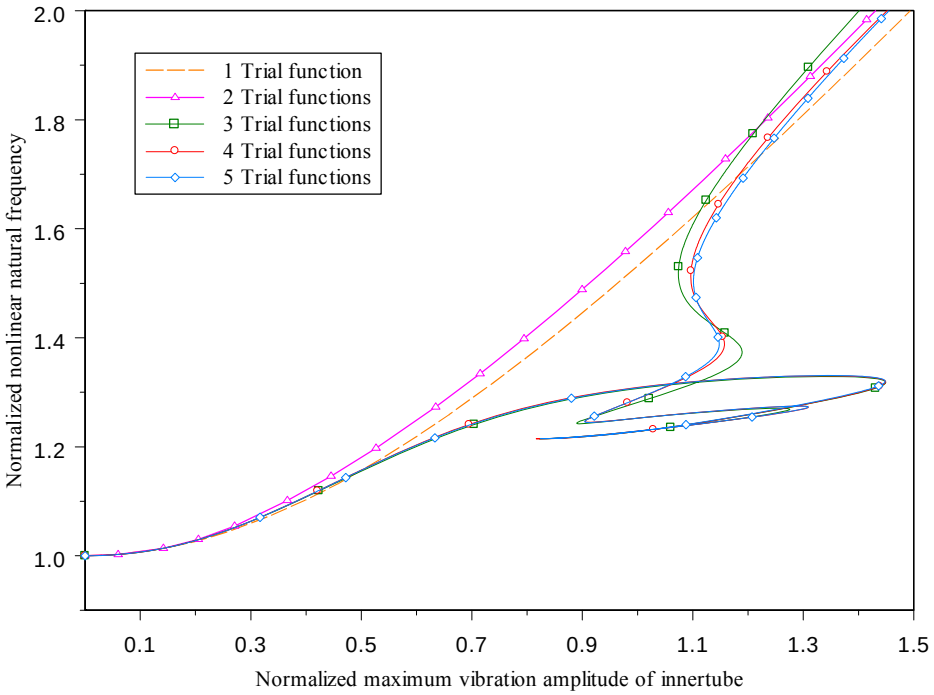

Figure 4-7 Variation of normalized nonlinear natural frequency of innertube vibrating in the first out-of-phase mode

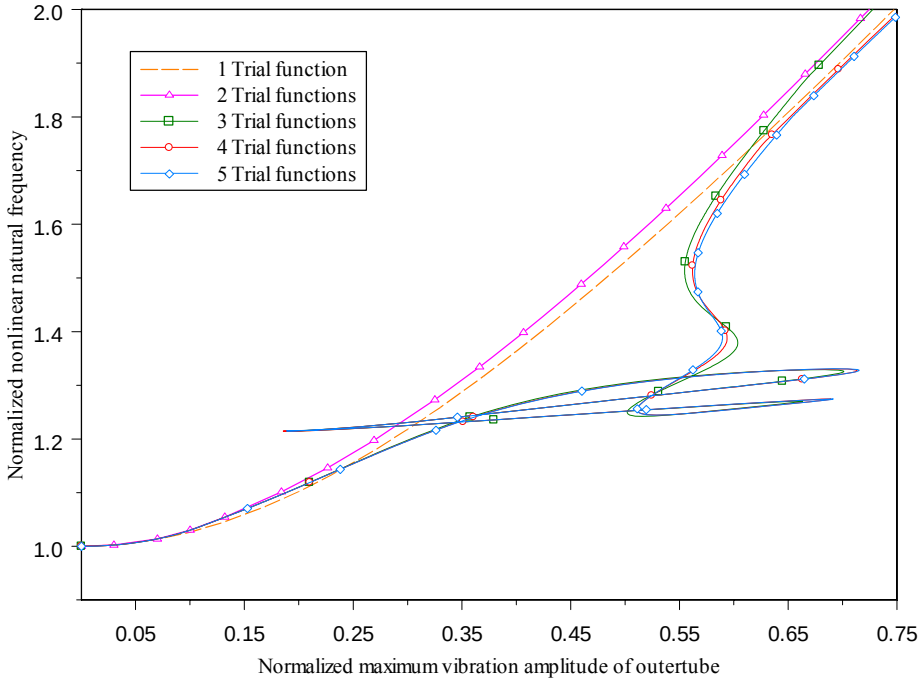

Figure 4-8 Variation of normalized nonlinear natural frequency of outertube vibrating in the first out-of-phase mode

In Figure 4-9, variation of the normalized nonlinear natural frequency using three trial functions is given, where the curve is divided into 7 different regions indicated by different markers and colors. In the first region, the first trial function has the dominant value; whereas, in the second region, the first and the third trial functions are dominant. As the number of regions increases, the characteristics of the nonlinear mode shapes also change. Example mode shapes calculated at the midpoint of each region are presented in Figure 4-10. It is observed that, in the first and the last regions, the first (out-of-phase) trial function is dominant, whereas, in between them a combination of the first three trial functions exist. Studying the mode shapes presented, it can be concluded that most of the contribution is due to the first and the third (odd) trial functions.

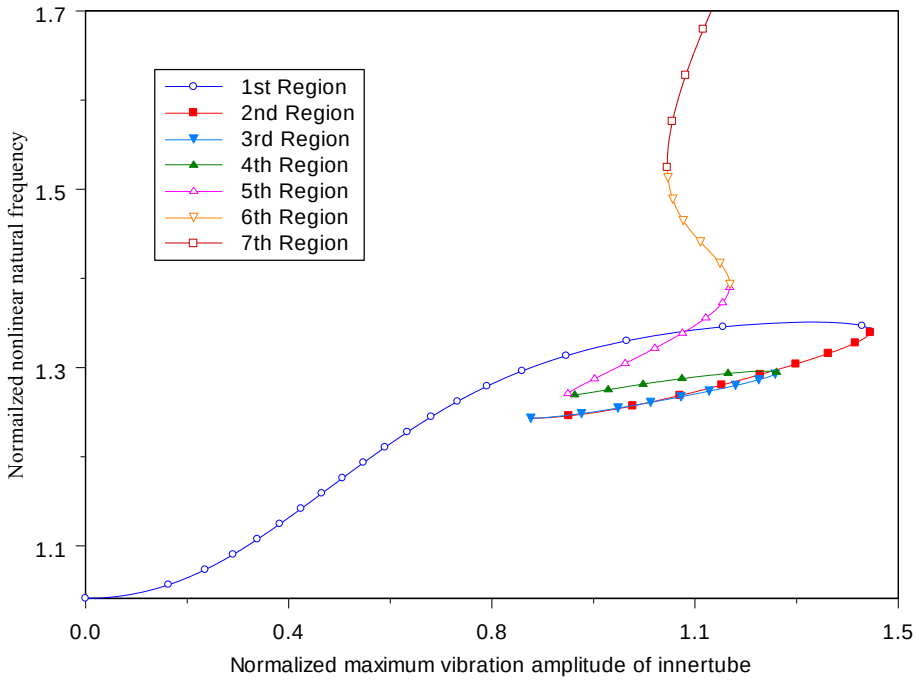

Figure 4-9 Variation of normalized nonlinear natural frequency of innertube vibrating in the first out-of-phase mode

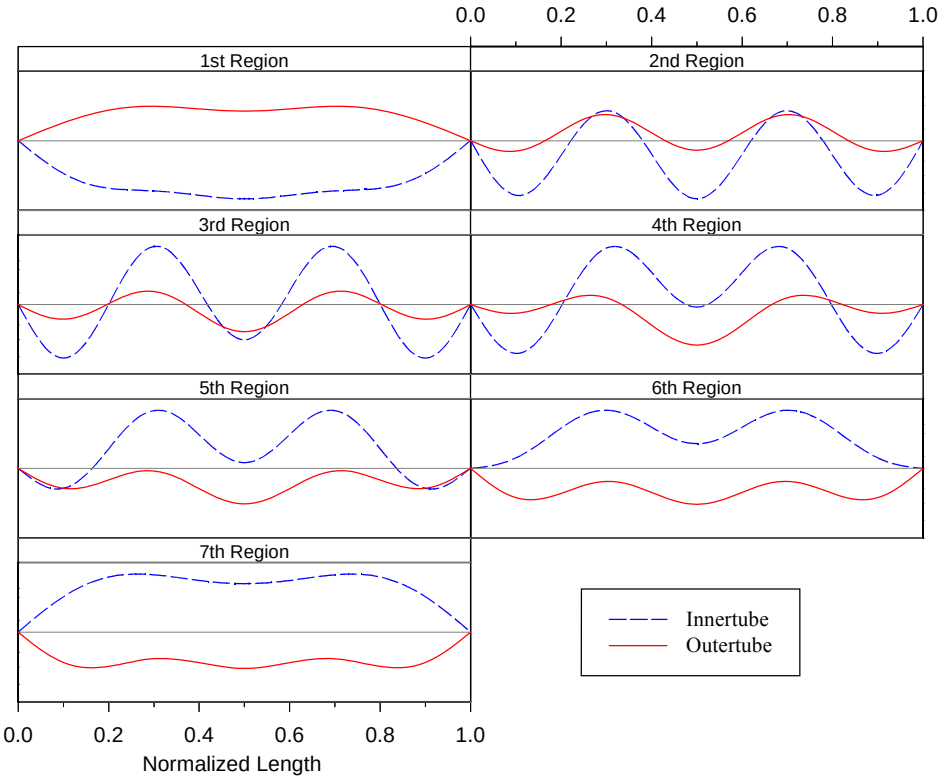

Figure 4-10 Transition of mode shapes from one region to another for innertube

Coefficients of trial functions for the outertube, which are used in the solution expansion, are presented in Figure 4-11 in a bar chart due to their complex behavior as a result of multiple solutions. It is clearly observed that, in addition to the variation of the nonlinear natural frequency of the CNT, mode shape of the CNT also changes as a function of the maximum vibration amplitude. The results obtained in Figure 4-10 are supported and clarified by the coefficients given in Figure 4-11. It is observed that in the first region, the first (out-of-phase) trial function is dominant. However, as we proceed towards higher regions the contribution of the third (in-phase) trial function gets larger in addition to the first (out-of-phase) trial function. There exist a contribution from the second (out-of-phase) trial function which reaches to the same order as the first and third trial functions in the middle of the 4th and starting of the 5th regions. Proceeding further in the regions, the first (out-phase) trial function becomes dominant again and the effect of other trial functions are ceased. In addition to these, interestingly, at the end of the 2nd region the DWCNT vibrates as if it is vibrating in the third (odd) in-phase vibration mode, since, the only contribution is due to the third (odd) trial function.

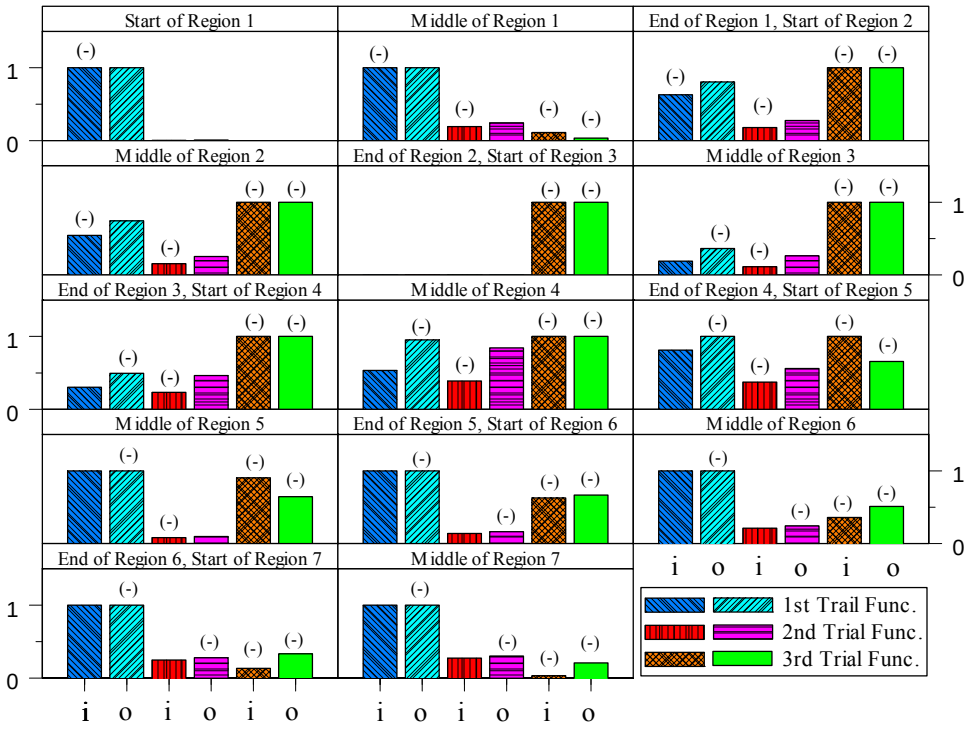

Figure 4-11 Normalized coefficients of trail functions of inner and outer tubes at the beginning and middle of each region

In Figure 4-12, variation of normalized nonlinear natural frequency of DWCNT obtained for different vibration modes are presented for inner and outer tubes. It should be noted that, since the point of the maximum vibration amplitude is not the same for inner and outer tubes, the variation of the normalized nonlinear natural frequencies are different as well. It can be observed that in-phase natural frequencies change slightly with respect to the normalized vibration amplitude; whereas, out-of-phase natural frequencies increase significantly as the normalized maximum vibration amplitude increases. Therefore, it is possible for the curve of one out-of-phase nonlinear natural frequency to reach and intersect a curve of an in-phase natural frequency as seen in Figure 4-12. When the enlarged region in Figure 4-12 is studied it is observed that one particular intersection of the out-of-phase natural frequency with the in-phase natural frequency for inner and outer tubes occurs at the same normalized nonlinear natural frequency as indicated by the horizontal line and the black circles. This particular point corresponds to the case where the DWCNT vibrates as if it is in the third (odd) vibration mode or third in-phase vibration mode as depicted by the coefficients of the trial functions presented in Figure 4-11.

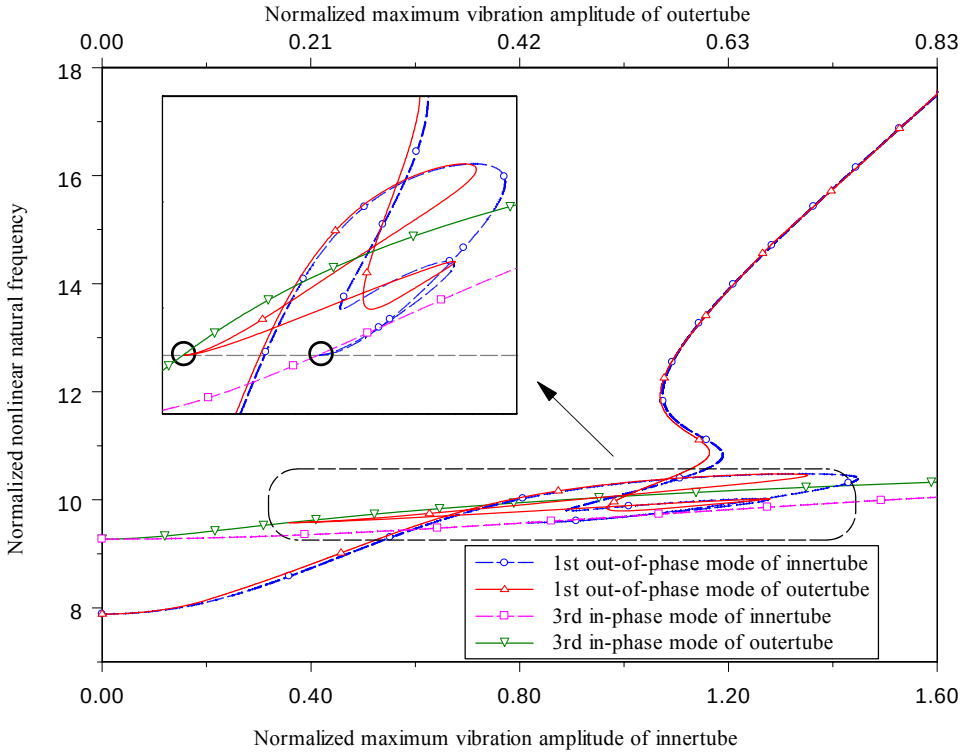

Figure 4-12 Variation of normalized nonlinear natural frequency of outertube for different natural frequencies

In Figure 4-13, results obtained by the proposed method are compared with the results available in literature, where the parameters of the DWCNT can be obtained from [184, 185]. It can be seen that the data given in literature and the results obtained from the proposed method using single trial function are identical. However, when multiple trial functions are utilized, significant difference between the results obtained by the proposed method and the data available in literature is observed, especially at the region where multiple solutions exist. For the regions where a single solution is present, the difference between the results is moderate; however, it increases as the maximum vibration amplitude increases.

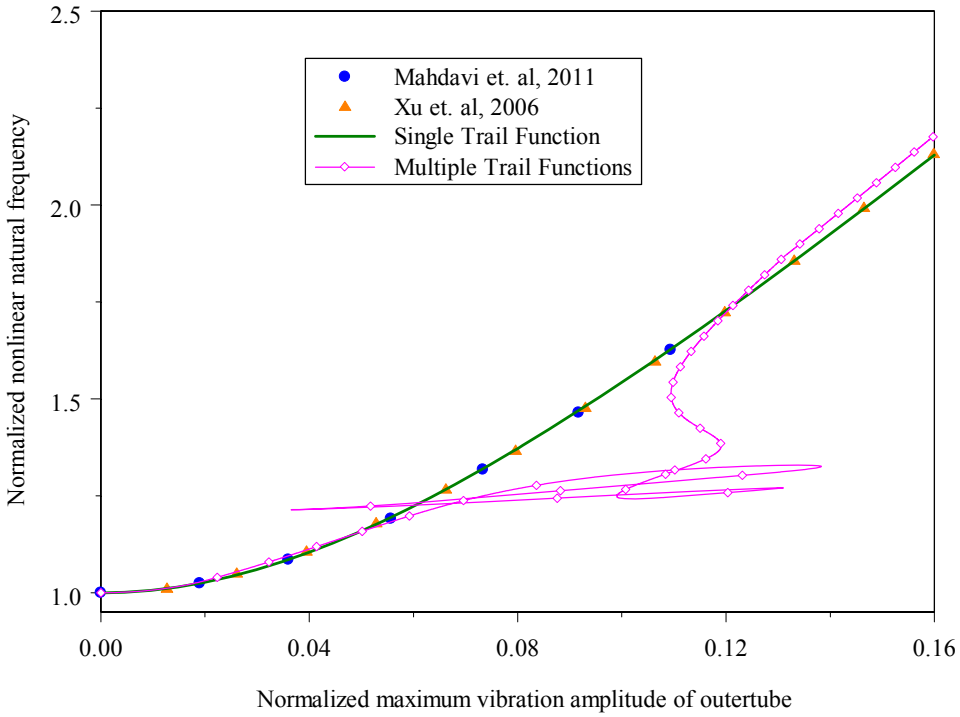

Figure 4-13 Comparison with data available in literature

4.5.3. Geometric nonlinearity

In Figure 4-14 considering just geometric nonlinearity, the variation of the normalized nonlinear natural frequency of the first in-phase vibration mode is given utilizing one and six trial functions. It is observed that using multiple trial functions does not affect the nonlinear natural frequencies, which is an expected result as observed from the nonlinearity matrix determined by DFM in Section 3. For geometric nonlinearity, in Eq. (4.32), no coupling between the trial functions is observed. This is also true for the out-of-phase modes as well, where the same results are obtained. From the nonlinearity matrixes obtained and the results shown, it can be concluded that if only geometric nonlinearity is considered, single trial function is sufficient to obtain the nonlinear free vibration frequencies of CNTs.

4.5.4. Effect of medium stiffness

In this final case study, considering geometric and vdW force nonlinearity, the effect of medium stiffness on the nonlinear natural frequency of DWCNTs using multiple trial functions is investigated. Figure 4-15 shows the variation of normalized

nonlinear natural frequency of the outertube for the first in-phase vibration mode considering different values of medium stiffness. It is seen that as the medium stiffness, k, increases, the nonlinear free vibration frequency tends to approach to the linear one. The same analysis is performed for the first out-of-phase vibration mode of DWCNT, the results of which are given in Figure 4-16. It is observed that as the medium stiffness per length, k, increases, the nonlinear natural frequency of DWCNT approaches to the linear one. Moreover, in the maximum vibration amplitude range considered, multiple solutions are not observed for medium stiffness per length of 2×10^{11} N/m^2 and larger.

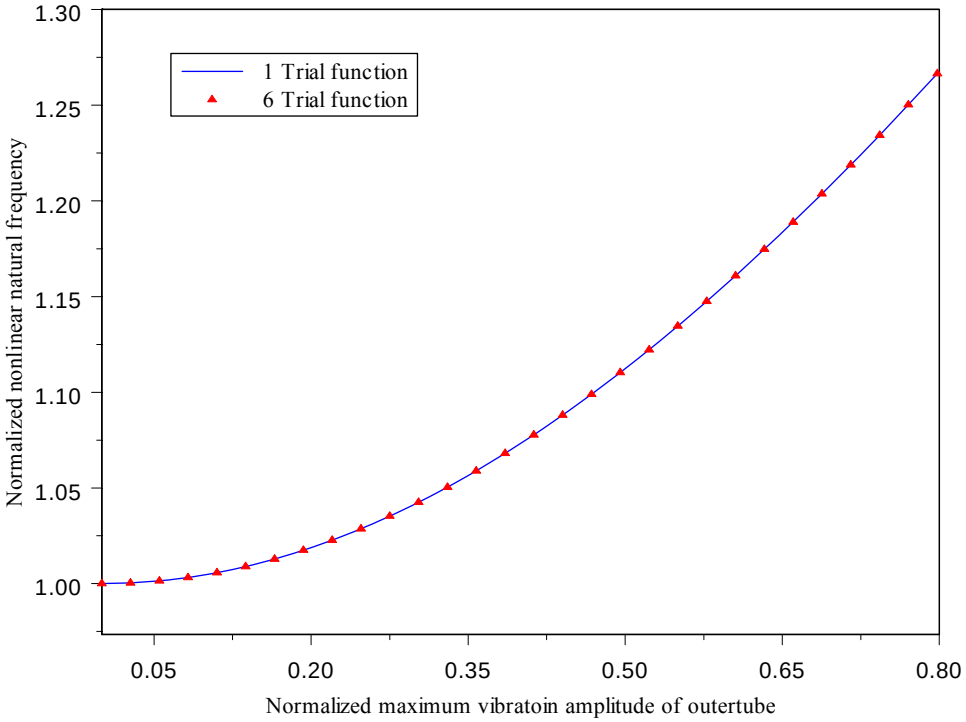

Figure 4-14 amplitude frequency curve of the outertube vibrating in the first in-phase mode

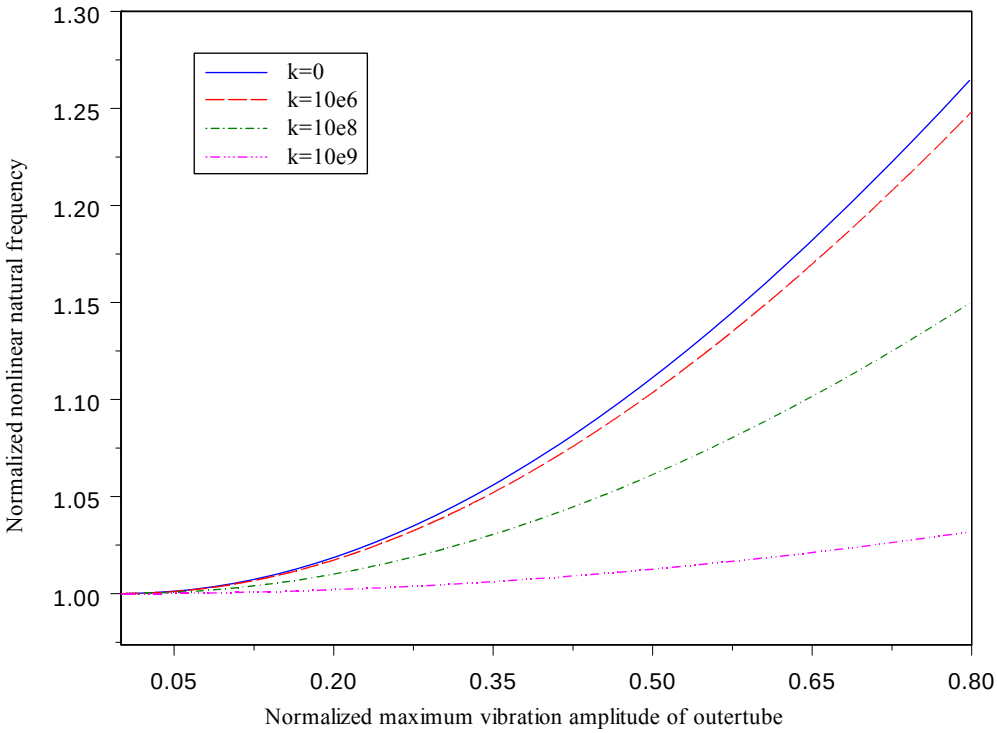

Figure 4-15 Effect of medium stiffness on the nonlinear natural frequency for the first in-phase vibration mode

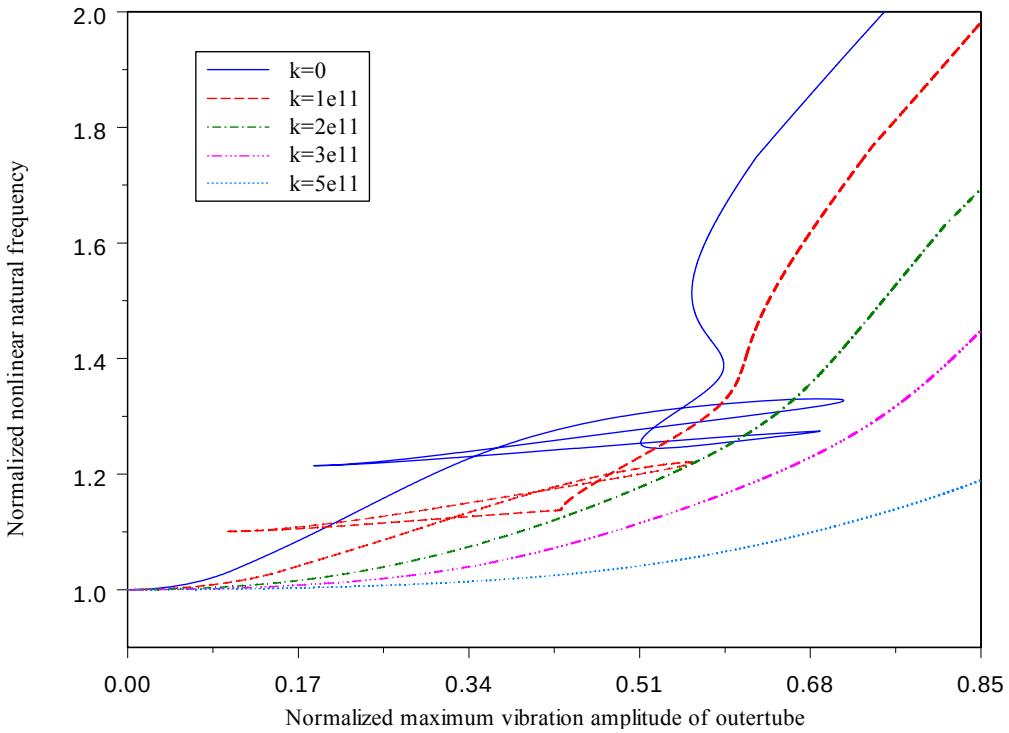

Figure 4-16 Effect of medium stiffness on the nonlinear natural frequency for the first out-of-phase mode

4.6. Concluding remarks

Nonlinear free vibration of a DWCNT is studied in this chapter using DFM with multiple trial functions where geometric and interlayer vdW force nonlinearities are considered. Application of DFM made it possible to observe the coupling between the trial functions used in the modal expansion process. The nonlinearity matrices obtained show that for simply supported CNTs considering geometric nonlinearity, a single trial function is sufficient to obtain the nonlinear natural frequencies. On the other hand, in case of vdW force nonlinearity, multiple trial functions are necessary, especially for the out-of-phase modes for which the nonlinear effects are more significant. These findings are also verified with the numerical results obtained.

It is observed that for the first out-of-phase vibration mode with vdW force nonlinearity, utilizing three or more trial functions resulted in multiple solutions where a single nonlinear natural frequency is associated with multiple vibration modes and a single maximum vibration amplitude is associated with multiple nonlinear natural frequencies. Moreover, the variation of the nonlinear mode shape of the DWCNT for different maximum vibration amplitudes is presented. It is revealed from the results that nonlinear vibration modes of the DWCNT is composed of several trial functions which can never be captured if a single trial function is used in the modal expansion. Furthermore, the effect of medium stiffness is studied and it is observed that as the medium stiffness increases normalized nonlinear natural frequencies decrease and approach to the linear one for in-phase and out-of-phase vibration modes. Moreover, for the case of out-of-phase vibration mode, increasing the medium stiffness above a certain value, multiple solutions disappear and there exists a single nonlinear natural frequency for every vibration amplitude.

It can be concluded that in order to determine the nonlinear natural frequencies of DWCNTs with nonlinear interlayer vdW forces accurately, multiple trial functions should be considered in the modal expansion. Moreover, using DFM, it is possible to identify if a specific type of nonlinearity requires multiple trial functions by studying the nonlinearity matrix obtained.

CHAPTER 5

EFFECT OF CURVATURE NONLINEARITY ON THE VARIATION OF FUNDAMENTAL NONLINEAR NATURAL FREQUENCY[7]

This chapter deals with nonlinear free vibration of a curved single walled carbon nanotube. In the previous chapters, geometric and vdW force nonlinearities are studied in detail. This chapter mainly concern about the effect of initial curvature nonlinearity on the variation of nonlinear natural frequency of CNTs. Recent experiments show that it is possible to detect a peak at system higher harmonics for the curved CNTs going through large deflections. Hence, in this chapter, multiple harmonic balance method (MHBM) in addition to Galerkin method is used to convert the nonlinear discretized differential equations of motion into a set of nonlinear algebraic equations where application of MHBM make it possible to study the effect of higher harmonics. It is worth mentioning that in this chapter single trial function assumption is used in Galerkin method since, according to previous chapter results, a single trial function is sufficient to obtain the nonlinear natural frequencies in the presence of only geometric nonlinearity. An expression for the variation of nonlinear fundamental natural frequency of CNTs is derived analytically.

5.1. Introduction

Recent studies show that even though CNTs are commonly assumed to be straight, in reality they are not straight and they are curved structures. Studies confirmed that the initial curvature in CNTs can be formed during the fabrication or due to boundary

[7] A version of this chapter is published in the proceeding of the 2012 Space Elevator Conference, August 25-27, 2012, Seattle, Washington, USA as "Effect of Waviness on the Variation of Nonlinear Fundamental Natural Frequency of Single Wall Carbon Nanotube by Using Multiple Harmonic Balance Method"

conditions. The effect of initial curvature on the nonlinear free vibration of a SWCNT is studied numerically by Mehdipour et al. [123]. They observed that as initial curvature increases, the normalized nonlinear natural frequency increases. However, reviewing literature, it has been observed that that, in the all few studies on the nonlinear effect of initial curvature, single harmonic assumption is used where the effect of higher harmonics is disregarded. However, for nonlinear systems higher harmonics of the system can be excited; hence, in order to capture system behavior accurately, terms corresponded to higher harmonics of the system are needed to be considered. Furthermore, some nonlinearities, it may not be possible to capture the nonlinear characteristics of the system using a single harmonic.

In this chapter, nonlinear fundamental natural frequency of a curved simply supported single walled carbon nanotube is studied considering the higher harmonics of the system. Galerkin method is used to convert the partial differential equations (PDEs) of motion into a set of ordinary differential equations (ODEs). In order to consider the effect of higher harmonics, multiple harmonic balance method is utilized which transforms nonlinear ODEs of motion into a set of nonlinear algebraic equations. Considering different number of harmonics, several case studies are defined, where, in each case, an expression for the variation of nonlinear fundamental natural frequency of CNTs is derived analytically. Using these expressions the effect of higher harmonics in the presence of waviness and geometric nonlinearities is investigated.

5.2. Equation of motion using Euler Bernoulli beam model for thin tubes

Figure 5-1 shows the schematic diagram of a SWCNT embedded in an elastic medium. The equation of motion of an embedded nanotube considering both geometric and waviness nonlinearities is given as [123, 166, 167]

$$EI\frac{\partial^4 w}{\partial x^4}-k_p\frac{\partial^2 w}{\partial x^2}+\rho A\frac{\partial^2 w}{\partial t^2}+kw=\frac{EA}{L}\int_0^L\left[\frac{\partial Z}{\partial x}\frac{\partial w}{\partial x}+\frac{1}{2}\left(\frac{\partial w}{\partial x}\right)^2\right]dx\cdot\left(\frac{\partial^2 w}{\partial x^2}+\frac{\partial^2 Z}{\partial x^2}\right) \tag{5.1}$$

where L, A, E, I and ρ are the length, cross-sectional area, Young's modulus, area moment of inertia and density of the CNT, respectively. k_p and k are the torsional stiffness and the bending stiffness per unit length of the elastic medium, respectively. In this chapter, it is assumed that the waviness of the tube follow the first eigenfunction of the linear simply supported beam as described by $Z(x) = e\sin(\pi x/L)$ [126], where e is the amplitude of the initial waviness (curvature).

The partial differential equation of motion is subjected to the following boundary conditions, which correspond to a simply supported beam

$$w(0,t) = w(L,t) = 0, \tag{5.2}$$

$$\left.\frac{d^2w}{dx^2}\right|_{x=0} = \left.\frac{d^2w}{dx^2}\right|_{x=L} = 0. \tag{5.3}$$

The partial differential equation of motion given by Eq (5.1) is discretized using Galerkin method. The following form of solution is assumed

$$w(x,t) = \phi_r(x)W_r(t), \tag{5.4}$$

where $W_r(t)$ is the r^{th} generalized coordinate and $\phi_r(x)$ is the r^{th} eigenfunction of simply supported linear CNT. For simply supported CNT, the mass normalized eigenfunctions can be expressed as follows

$$\phi_r(x) = \sqrt{\frac{2}{\rho AL}}\sin\left(\frac{r\pi x}{L}\right),\ r = 1,2,\cdots. \tag{5.5}$$

Since, in this study, the fundamental natural frequency of CNT is studied, $\phi_r(x)$ is assumed to be the fundamental eigenfunction of the simply supported CNT which can be obtained by substituting $r = 1$ in Eq.(5.5).

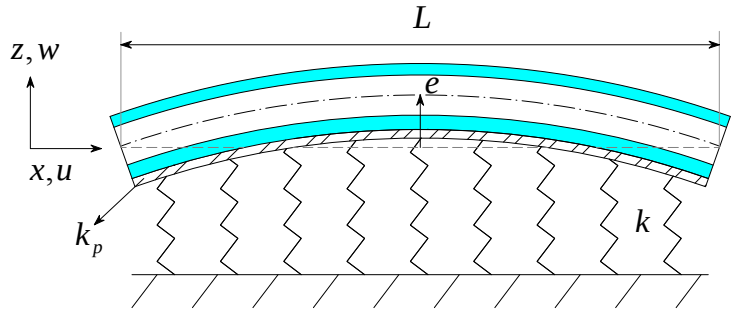

Figure 5-1 Model of an Embedded curved SWCNT.

Substituting Eq. (5.5) and Eq. (5.4) into Eq. (5.1), multiplying both sides by $\phi_1(x)$ and integrating over the domain, the discretized nonlinear ordinary differential equation of motion in $W_1(t)$ is obtained as follows

$$\frac{d^2W_1(t)}{dt^2} + \alpha_1 W_1(t) + \alpha_2 W_1(t)^2 + \alpha_3 W_1(t)^3 = 0, \tag{5.6}$$

where

$$\alpha_1 = \frac{EI\pi^4}{\rho AL^4} + \frac{k_p\pi^2}{\rho AL^2} + \frac{1}{2}\frac{E\pi^4}{\rho L^4}e + \frac{k}{\rho A}, \tag{5.7}$$

$$\alpha_2 = \frac{3}{4}\frac{E\pi^4}{\rho L^4}e, \tag{5.8}$$

$$\alpha_3 = \frac{1}{4}\frac{E\pi^4}{\rho L^4}. \tag{5.9}$$

In Eq. (5.6), α_1 denotes the square of the fundamental natural frequency of the corresponding linear system, which also includes the effect of initial curvature, α_2 represents the nonlinear effect of initial curvature, and α_3 characterizes the effect of mid-plane stretching and geometric nonlinearity. It is worth noting that, in Eq. (5.6), cubic nonlinearity is due to large deformation of the CNT, whereas quadratic nonlinearity is due to the initial curvature nonlinearity.

To facilitate theoretical formulations, the following dimensionless quantities are introduced

$$r=\sqrt{\frac{I}{A}},\quad \bar{W}_1(t)=\frac{W_1(t)}{r},\quad \omega_l=\sqrt{\frac{EI\pi^4}{\rho AL^4}},\quad e_n=\frac{e}{r},\quad k_n=\frac{kL^4}{EI\pi^4},\quad k_{pn}=\frac{k_pL^2}{EI\pi^2}. \tag{5.10}$$

Therefore, Eq. (5.6) can be rewritten in dimensionless form as

$$\frac{d^2\bar{W}_1(t)}{dt^2}+\omega_l^2\cdot\left(1+\frac{1}{2}e_n+k_n+k_{pn}\right)\bar{W}_1(t)+\left(\frac{3}{4}\omega_l^2\cdot e_n\right)\bar{W}_1(t)^2+\left(\frac{1}{4}\omega_l^2\right)\bar{W}_1(t)^3=0 \tag{5.11}$$

5.3. Analytical Solutions

In this study, harmonic balance method (HBM), a very effective and convenient method, is utilized to convert the discretized the ordinary differential equation of motion in time domain to a set of algebraic equation. [144, 186-188] According to HBM, the steady state solution of a differential equation can be expressed as summation of multiple harmonics as follows

$$\bar{W}(t)=\sum_m a_m\cos\left(m\omega_n t\right), \tag{5.12}$$

where a_m is the amplitude of the m^{th} harmonic, and ω_n is the fundamental natural frequency of the CNT. By substituting the assumed solution into differential equation and equating the coefficient of each harmonic to zero, a set of algebraic equations relating a_m and ω_n is obtained. Although HBM is very easy to apply, the accuracy of results depends on the number of harmonics used the solution. [189]

On the basis of the number of harmonics, HBM can be grouped in two major categories: single harmonic balance method (SHBM) and multiple harmonic balance method (MHBM). For weakly nonlinear systems, SHBM can be used without introducing any considerable error. However, in presence of highly nonlinear sources, MHBM should be used to track system behavior [189].

5.3.1. Single harmonic balance method

According to SHBM, the steady solution of a differential equation can be expressed by the fundamental harmonic as follows

$$\bar{W}(t) = a_1 \cos(\omega_n t), \tag{5.13}$$

where a_1 stands for the normalized maximum vibration amplitude of the CNT. Substituting Eq. (5.13) into Eq. (5.11) and disregarding higher harmonics, the following nonlinear algebraic equation is obtained

$$-\omega_n^2 + \omega_l^2 + \frac{1}{2}\omega_l^2 \cdot e_n + \omega_l^2 \cdot k_n + \omega_l^2 \cdot k_{pn} + \frac{3}{16}\omega_l^2 a_1^2 = 0, \tag{5.14}$$

From Eq. (5.14), ω_n can be obtained as follows, where only the positive value is considered to be the acceptable solution

$$\omega_n = \omega_l \sqrt{1 + \frac{1}{2}e_n + k_n + k_{pn} + \frac{3}{16}a_1^2}\,. \tag{5.15}$$

In Eq. (5.15), it can be seen that the nonlinear fundamental natural frequency is a function of the maximum vibration amplitude, a_1. Moreover, it is observed that, for the case of single harmonic, the term associated with the nonlinear effect of initial curvature is not incorporated in equation and only the term associated with large deflection, $3/16 a_1^2$, is included. Although the nonlinear natural frequency is affected by waviness in Eq. (5.15), it should be noted that the term $e/2$ corresponds to the linear effect of waviness and does not represent the quadratic nonlinearity associated with the initial curvature nonlinearity.

5.3.2. Multiple harmonic balance method

In the previous case, it is observed that the nonlinear effect of initial curvature cannot be studied when a single harmonic solution is assumed. Hence, the effect of higher harmonics on the variation of nonlinear natural frequency of the CNT is studied. Three case studies are defined. In the first case, the first and the second harmonics are considered, whereas, in the second case, the first and the third harmonics are considered. In case three, both the second and the third harmonics in addition to fundamental harmonic are considered.

Case 1: first and second harmonics

In this case, the steady state solution of the system is expressed as follows

$$\bar{W}(t) = a\cos(\omega_n t) + a_2\cos(2\omega_n t)\ , \tag{5.16}$$

where a_1 and a_2 are the coefficients of the first and the second harmonics, respectively. Substituting Eq. (5.16) into Eq. (5.11) and considering the terms corresponded to the first and the second harmonics, the following nonlinear set of algebraic equations is obtained for $a_2 \neq 0$

$$-\omega_n^2 + \left(1 + \frac{1}{2}e_n + k_n + k_{pn}\right)\omega_l^2 + \frac{3}{4}\omega_l^2 e_n a_2 + \frac{3}{16}\omega_l^2 a_1^{\,2} + \frac{3}{8}\omega_l^2 a_2^{\,2} = 0\,, \tag{5.17}$$

$$-4\omega_n^2 + \left(1 + \frac{1}{2}e_n + k_n + k_{pn}\right)\omega_l^2 + \frac{3}{8}\omega_l^2 a_1^{\,2}\left(1 + \frac{e_n}{a_2}\right) + \frac{3}{16}\omega_l^2 a_2^{\,2} = 0\,, \tag{5.18}$$

From Eqs. (5.17) and (5.18), ω_n can be respectively obtained as follows, where only the positive value is considered to be the acceptable solution,

$$\omega_n = \omega_l\sqrt{\left(1 + \frac{1}{2}e_n + k_n + k_{pn}\right) + \frac{3}{4}e_n a_2 + \frac{3}{16}a_1^{\,2} + \frac{3}{8}a_2^{\,2}}\,, \tag{5.19}$$

$$\omega_n = \frac{1}{2}\omega_l\sqrt{\left(1 + \frac{1}{2}e_n + k_n + k_{pn}\right) + \frac{3}{8}a_1^{\,2}\left(1 + \frac{e_n}{a_2}\right) + \frac{3}{16}a_2^{\,2}}\,. \tag{5.20}$$

In Eq. (5.17), $3/4\,\omega_l^2 e_n a_2$ corresponds to the nonlinear effect of waviness and the last two terms stand for the geometric nonlinearity. A similar interpretation can be done for Eq. (5.18). By equating the nonlinear natural frequencies obtained from Eqs. (5.19) and (5.20) the following relation is obtained

$$6e_n a_1^{\,2} - 24a_2 e_n^{\,2} - 48a_2\left(k_n + k_{pn}\right) - 48a_2 - 6a_2 a_1^{\,2} - 21a_2^{\,3} - 48e_n a_2^{\,2} = 0\,. \tag{5.21}$$

Eq. (5.21) expresses the variation of the second harmonic with respect to the first harmonic.

Case 2: first and third harmonics

In this case, the steady state solution of system is considered to include the first and third harmonic of the system as follows

$$\bar{W}(t) = a_1 \cos(\omega_n t) + a_3 \cos(3\omega_n t), \tag{5.22}$$

where a_1 and a_3 are the coefficients of the first and the third harmonics, respectively. Following a similar procedure, the following nonlinear set of algebraic equations is obtained for $a_3 \neq 0$:

$$\omega_n = \omega_l \sqrt{\left(1 + \frac{1}{2}e_n + k_n + k_{pn}\right) + \frac{3}{16}\left(a_1^2 + a_1 a_3 + 2a_3^2\right)}, \tag{5.23}$$

$$\omega_n = \frac{1}{3}\omega_l \sqrt{\left(1 + \frac{1}{2}e_n + k_n + k_{pn}\right) + \frac{3}{16}\left(a_3^2 + 2a_1^2\right) + \frac{1}{16}\frac{a_1^3}{a_3}}. \tag{5.24}$$

In Eqs. (5.23) and (5.24), the waviness term does not depend to vibration amplitude, a_i; hence, even though the third harmonic of system is considered, the present formulation fails to capture the nonlinear effect of initial curvature. Therefore, it can be concluded, in order to capture the quadratic nonlinearity of initial curvature, the second harmonic (even harmonics) of system should be considered. Furthermore, comparing the magnitude of coefficient of second and third harmonics in their corresponding closed form formulations, it is observed that the third harmonic (odd harmonic) has higher priority in comparison to the second harmonic (even harmonic) in capturing the effect of geometric nonlinearity. By equating the nonlinear natural frequencies obtained from Eqs. (5.23) and (5.24) the following relation is obtained:

$$a_1^3 - 64a_3 e_n^2 - 128a_3 k_n - 128a_3 - 128a_3 k_{pn} - 21a_3 a_1^2 - 51a_3^3 - 27a_1 a_3^2 = 0 \tag{5.25}$$

Eq. (5.25) expresses the variation of the third harmonic with respect to the first harmonic.

Case 3: first, second, and third harmonics

In this case it is assumed that the solution contains the first, the second, and the third harmonics as follows

$$\bar{W}(t) = a_1 \cos(\omega_n t) + a_2 \cos(2\omega_n t) + a_3 \cos(3\omega_n t), \tag{5.26}$$

where a_1, a_2 , and a_3 are the coefficients of the first, the second, and the third harmonics, respectively. Substituting Eq. (5.26) into equation (5.11) and collecting the coefficients of each harmonic, the following set of nonlinear equations is obtained

$$-\omega_n^2 + \left(1 + \frac{1}{2}e_n + k_n + k_{pn}\right)\omega_l^2 + \frac{3}{4}e_n\omega_l^2\left(a_2 + \frac{a_2 a_3}{a_1}\right) + \frac{3}{16}\omega_l^2\left(a_1^2 + 2a_2^2 + 2a_3^2 + a_1 a_3 + \frac{a_2 a_3^2}{a_1}\right) = 0, \tag{5.27}$$

$$-4\omega_n^2 + \left(1 + \frac{1}{2}e_n + k_n + k_{pn}\right)\omega_l^2 + \frac{3}{8}e_n\omega_l^2\left(\frac{a_1^2}{a_2} + \frac{2a_1 a_3}{a_2}\right) + \frac{3}{16}\omega_l^2\left(a_2^2 + 2a_1^2 + 2a_3^2 + 2a_1 a_3\right) = 0, \tag{5.28}$$

$$-9\omega_n^2 + \left(1 + \frac{1}{2}e_n + k_n + k_{pn}\right)\omega_l^2 + \frac{3}{4}e_n\omega_l^2\frac{a_2 a_1}{a_3} + \frac{3}{16}\omega_l^2\left(a_3^2 + 2a_2^2 + 2a_1^2 + \frac{a_1 a_2^2}{a_3} + \frac{a_1^3}{a_3}\right) = 0. \tag{5.29}$$

From Eqs. (5.27) to (5.29) , ω_n can be respectively obtained as follows, where only the positive value is considered to be the acceptable solution

$$\omega_n = \omega_l\sqrt{\left(1 + \frac{1}{2}e_n + k_n + k_{pn}\right) + \frac{3}{4}e_n\left(a_2 + \frac{a_2 a_3}{a_1}\right) + \frac{3}{16}\left(a_1^2 + 2a_2^2 + 2a_3^2 + a_1 a_3 + \frac{a_2 a_3^2}{a_1}\right)} \tag{5.30}$$

$$\omega_n = \frac{1}{2}\omega_l\sqrt{\left(1 + \frac{1}{2}e_n + k_n + k_{pn}\right) + \frac{3}{8}e_n\left(\frac{a_1^2}{a_2} + \frac{2a_1 a_3}{a_2}\right) + \frac{3}{16}\left(a_2^2 + 2a_1^2 + 2a_3^2 + 2a_1 a_3\right)} \tag{5.31}$$

$$\omega_n^2 = \frac{1}{3}\omega_l\sqrt{\left(1 + \frac{1}{2}e_n + k_n + k_{pn}\right) + \frac{3}{4}e_n\frac{a_2 a_1}{a_3} + \frac{3}{16}\left(a_3^2 + 2a_2^2 + 2a_1^2 + \frac{a_1 a_2^2}{a_3} + \frac{a_1^3}{a_3}\right)} \tag{5.32}$$

By equating these equations, solutions for the variation of the second and third harmonics with respect to the first harmonic can be obtained as follows

$$\begin{aligned} &384a_2 e_n^2 a_1 + 768a_2 a_1 + 768a_2 k_n a_1 + 288a_2 a_3^2 a_1 + 192a_2^3 a_3 + 768a_2 k_{pn} a_1 + 768e_n a_2^2 a_1 + 96a_2 a_1^3 \\ &+336a_2^3 a_1 + 768e_n a_2^2 a_3 + 96a_2 a_1^2 a_3 - 192e_n a_1^2 a_3 - 96e_n a_1^3 = 0, \end{aligned} \tag{5.33}$$

$$\begin{aligned} &1024a_3 e_n^2 a_1 + 2048a_1 a_3 + 2048a_3 k_n a_1 + 816a_3^3 a_1 + 432a_2^2 a_3^2 + 2048a_3 k_{pn} a_1 + 1728e_n a_1 a_2 a_3 \\ &+336a_1^3 a_3 + 768a_1 a_2^2 a_3 + 1728e_n a_2 a_3^2 + 432a_3^2 a_1^2 - 48a_2^2 a_1^2 - 16a_1^4 - 192e_n a_2 a_1^2 = 0 \end{aligned} \tag{5.34}$$

5.4. Numerical results and discussion

In this section, nonlinear free vibration of simply supported curved SWCNT is investigated. The material and geometric parameters of the CNT used in this study are given in Table 5-1 [51].

Table 5-1 Numerical Values of SWCNT Parameters [51].

Parameter	value
Inner radius of innertube	0.7 nm
Outer radius of outertube	0.8 nm
Density of tubes	2.3 gr/cm^3
Young modulus of tubes	1 TPa
Thickness of tubes	0.1 nm

It is worth studying the characteristics of the linear system before examining the effects of nonlinearities. The natural frequency of the linear system can be obtained as

$$\bar{\omega}_l^2 = \left(1 + \frac{1}{2}e_n^2 + k_n + k_{pn}\right)\omega_l^2, \tag{5.35}$$

The effect of waviness on the variation of the linear natural frequencies of the SWCNT, is presented in Figure 5-2. It is observed that the linear natural frequency increases as the waviness increases, which is an expected result. The mode shape of the system is given in Figure 5-3 in the presence of initial curvature.

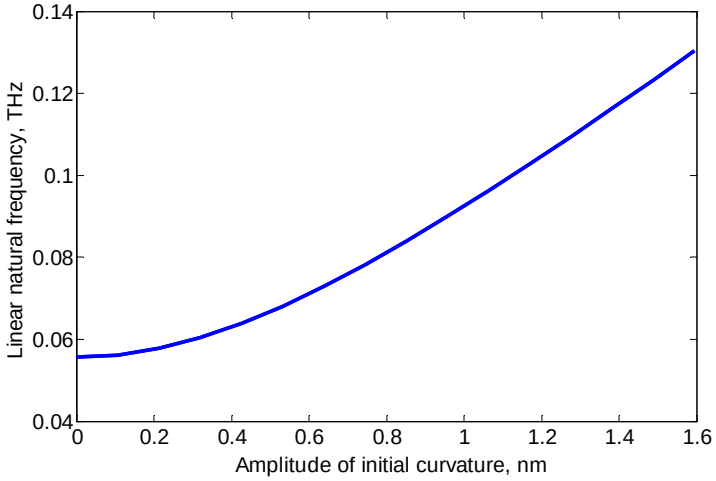

Figure 5-2 Variation of the fundamental linear natural frequencies of the SWCNT versus waviness

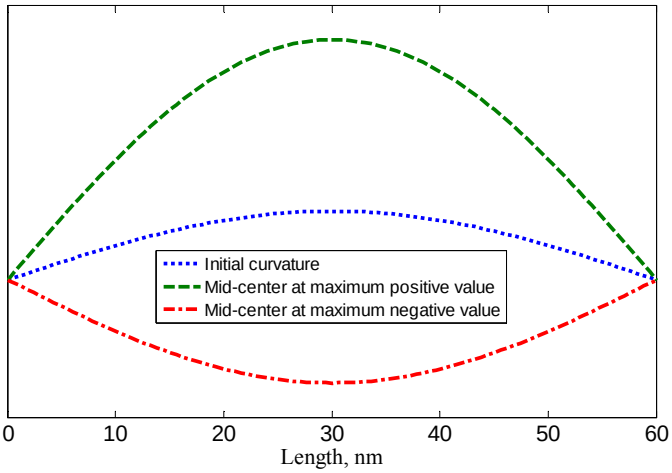

Figure 5-3 Fundamental mode shape of the SWCNT when mid-center is at its positive and negative maximum values

In the following section, the effect of large deformation and waviness on the variation of first nonlinear natural frequency of a simply supported SWCNT is studied considering the effect of number of harmonics used in the HBM. In addition to these the effect of medium stiffness on the nonlinear natural frequency of the SWCNT is studied. It should be noted that the variation of nonlinear natural frequency is normalized with respect to the corresponding linear natural frequency, $\bar{\omega}_l$, of the simply supported curved SWCNT, and the maximum vibration amplitude is normalized with respect to $r = \sqrt{I/A}$.

5.4.1. Effect of number of harmonics in the presence of large deformations

In Figure 5-4, the variation of the normalized nonlinear natural frequency of the SWCNT is presented considering only the geometric nonlinearity where effect of higher harmonics is studied. The waviness, e_n, is considered to be equal to zero. Results show that in the absence of waviness, including the second harmonic in the solution expansion does not affect the nonlinear natural frequency. On the other hand, it is seen that the variation of the normalized nonlinear natural frequency decreases as the third harmonic is included in solution expansion. In Figure 5-5, amplitudes of the coefficients of harmonics are plotted for the case of multiple harmonics where the contribution of each trial function can be clearly seen. It is observed that when

normalized maximum vibration amplitude is small, majority of the contribution comes from the first harmonic, but the contribution of the third coefficient increases as vibration amplitude increases. It should be noted that the coefficient of second harmonic is zero so it does not affect system behavior at all in the presence of only geometric nonlinearity.

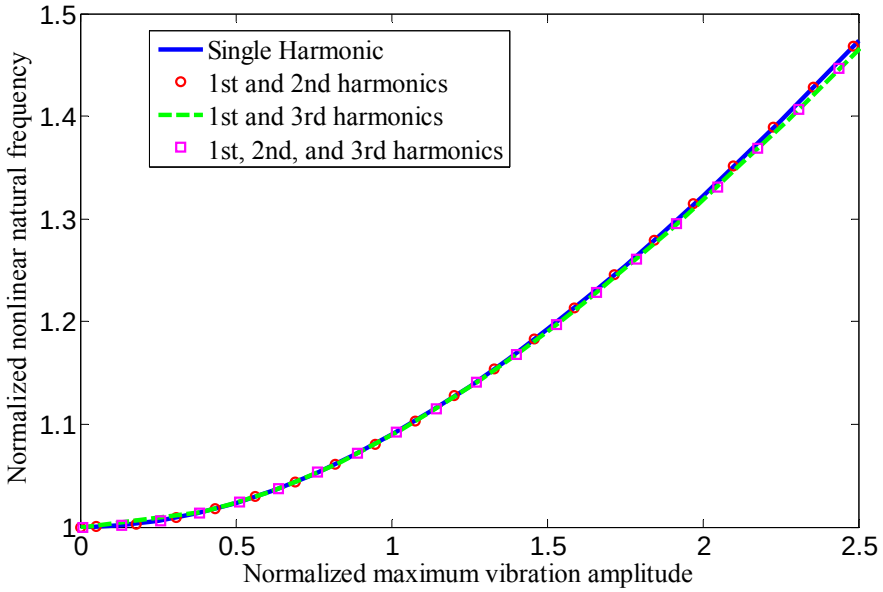

Figure 5-4 Variation of normalized nonlinear natural frequency in the presence of only geometric nonlinearity

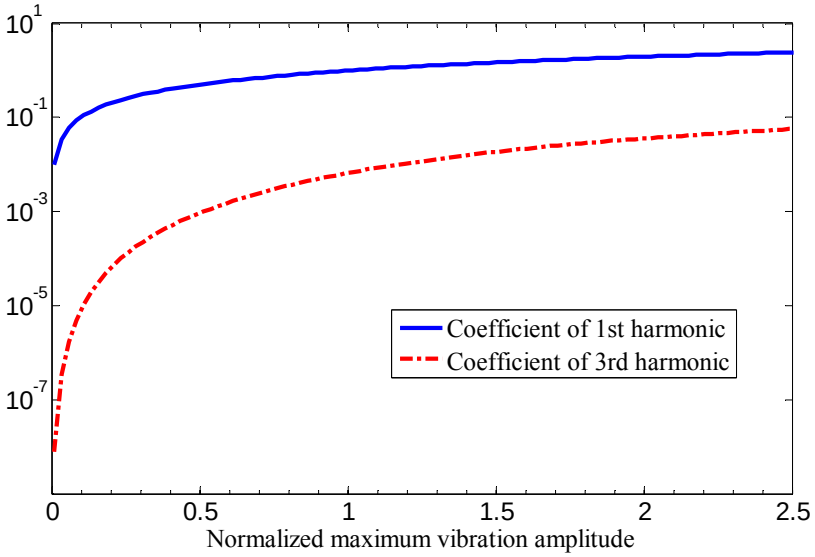

Figure 5-5 Coefficients of the first and third harmonics

Figure 5-6 shows the variation of the nonlinear natural frequency against the normalized maximum vibration amplitude for different values of medium stiffness

vibrating in the first vibration mode. It is seen that as the normalized medium stiffness, k_n, increases, the normalized nonlinear frequency tends to approach the linear one. Moreover, it is observed that, as the medium stiffness increases, the normalized nonlinear natural frequency for single harmonic and multiple harmonic solutions converge to each other. This is an expected result, since the effect of geometric nonlinearity decreases as medium stiffness increases. Since the torsional stiffness resulted in a term similar to medium stiffness in the equation of motion, similar results can be obtained if the effect of torsional stiffness is studied.

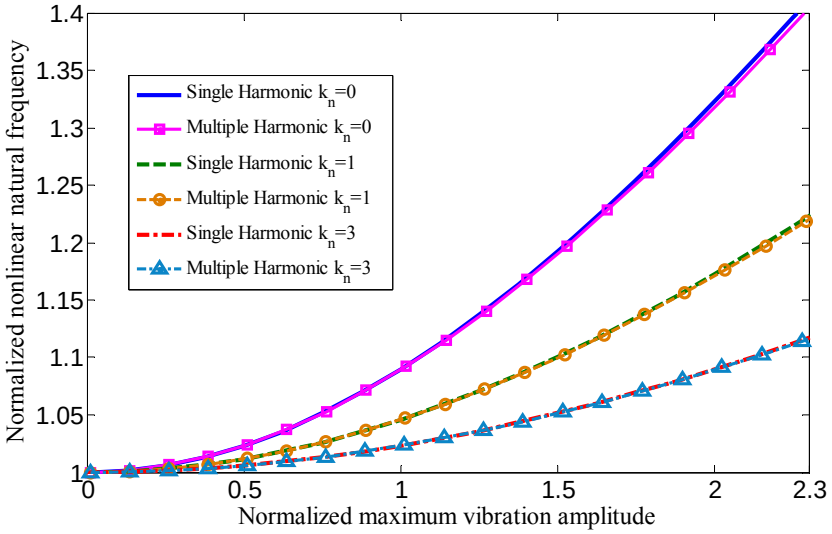

Figure 5-6 Variation of the normalized nonlinear natural frequency for different values of medium stiffness in the presence of only geometric nonlinearity

5.4.2. Effect of number of harmonics in the presence of both large deflection and waviness

In Figure 5-7 and Figure 5-8, the variation of normalized nonlinear natural frequency is given for different value of initial curvature where the effect of higher harmonics is studied in the presence of both initial curvature and geometric nonlinearities. It is observed that, in the presence of initial curvature, the system response is mainly affected by the second harmonic of system and including the third harmonic in solution expansion does not affect the results. Furthermore, it can be seen that the effect of second harmonics becomes more dominant as value of initial curvature increases (Figure 5-8) where it cannot be disregarded.

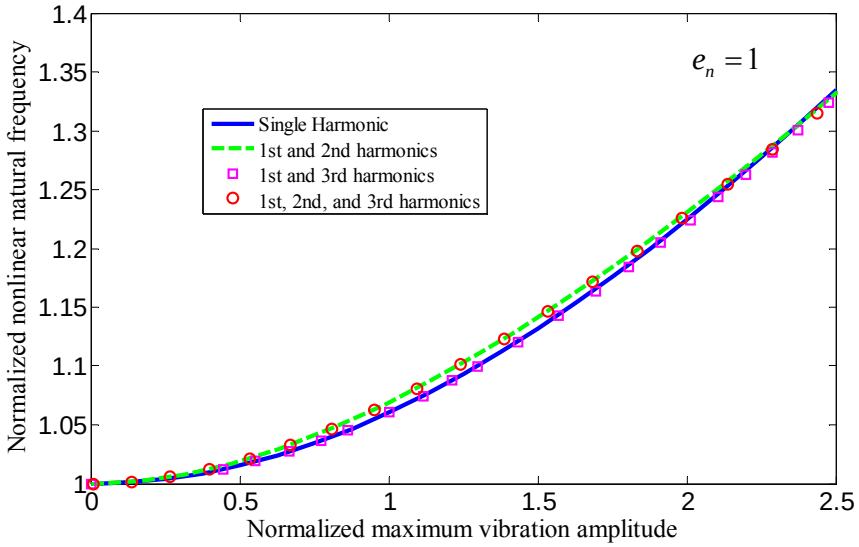

Figure 5-7 Variation of the normalized nonlinear natural frequency in the presence of both geometric nonlinearity and waviness nonlinearity

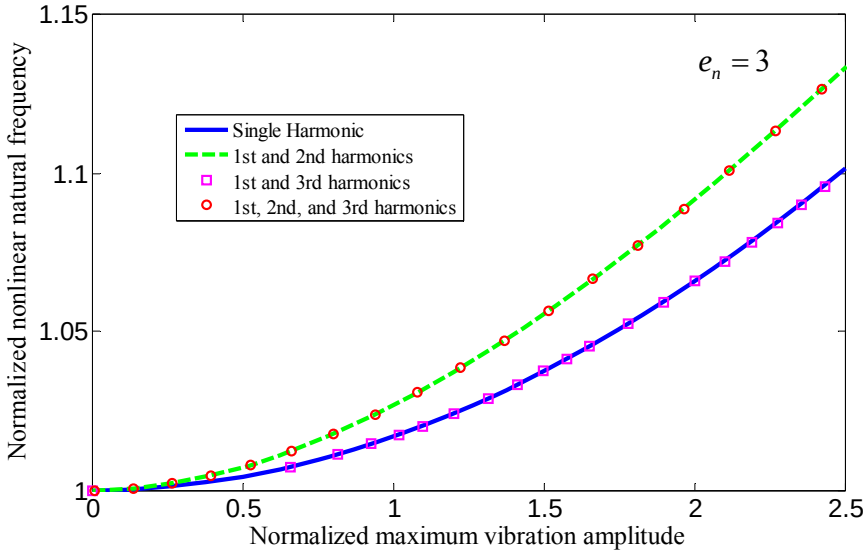

Figure 5-8 Variation of the normalized nonlinear natural frequency in the presence of both geometric nonlinearity and waviness nonlinearity

The coefficients of the first three harmonics are presented in Figure 5-9. It is observed that the coefficient all the harmonic increases slightly and reaches to a constant value as the maximum vibration amplitude increases. Increasing waviness only effects the third harmonic, which is two orders of magnitude less than the first harmonic

In Figure 5-10, the variation of normalized nonlinear natural frequency is presented for different values of initial curvature utilizing single and multiple harmonics in solution expansion. It is observed that the normalized nonlinear natural frequency

decreases as waviness increases. Moreover, it can also be observed that the difference between the single and multiple harmonics solutions increases as initial curvature increases.

As a final case study, considering both geometric and waviness nonlinearities, the effect of medium stiffness on the variation of normalized nonlinear natural frequency of SWCNT is investigated using single and multiple harmonics where $e_n = 3$. Figure 5-11 shows the variation of the normalized nonlinear natural frequency considering different values of medium stiffness. It is observed that, as the normalized medium stiffness, k_n, increases, the normalized nonlinear natural frequency tends to approach to the linear one. It is worth noting that, for similar initial curvature, single harmonic solution estimates a lower normalized nonlinear frequency compared to the multiple harmonics solution.

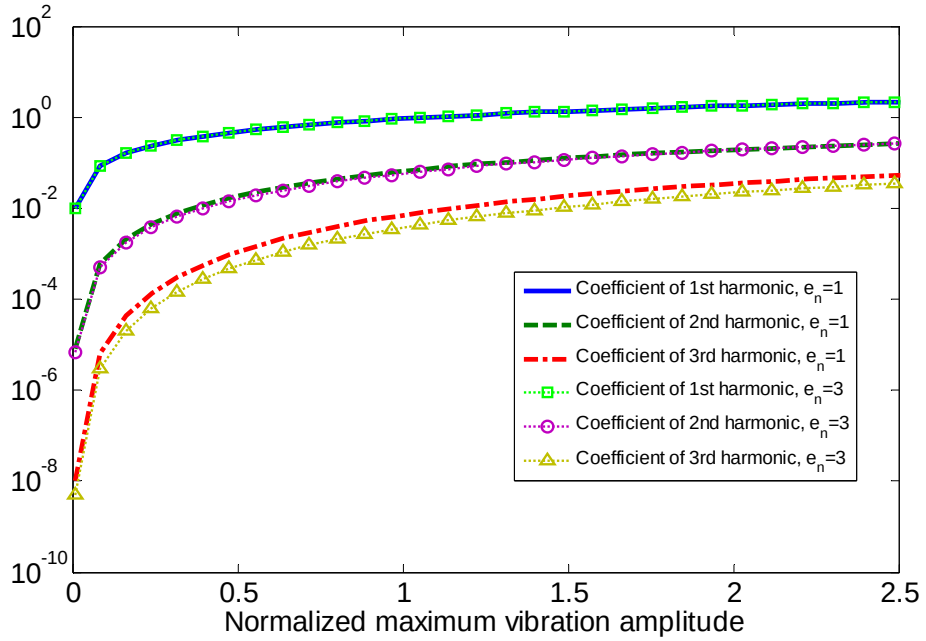

Figure 5-9 Coefficient of harmonics of SWCNT vibrating in the fundamental natural frequency for different initial curvature

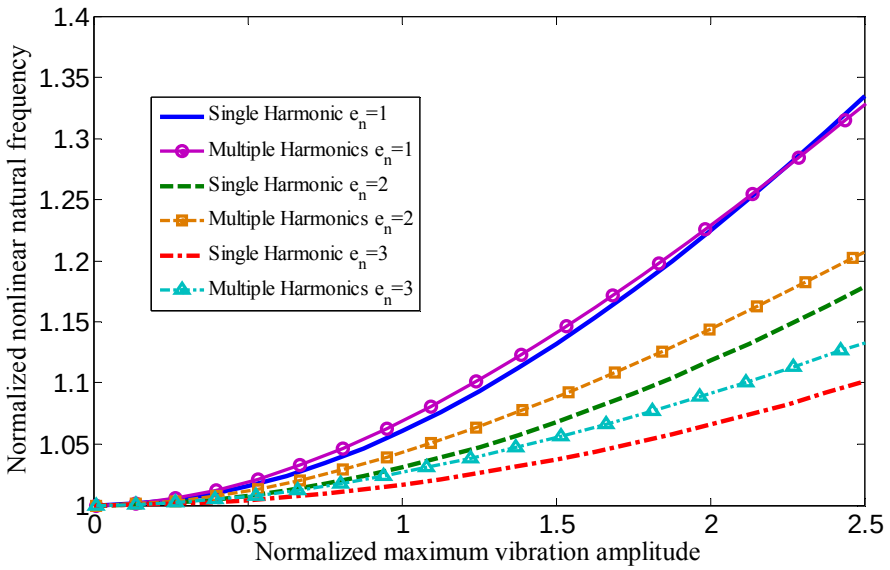

Figure 5-10 Variation of the normalized nonlinear natural frequency for different values of initial curvature utilizing single and multiple harmonic solutions

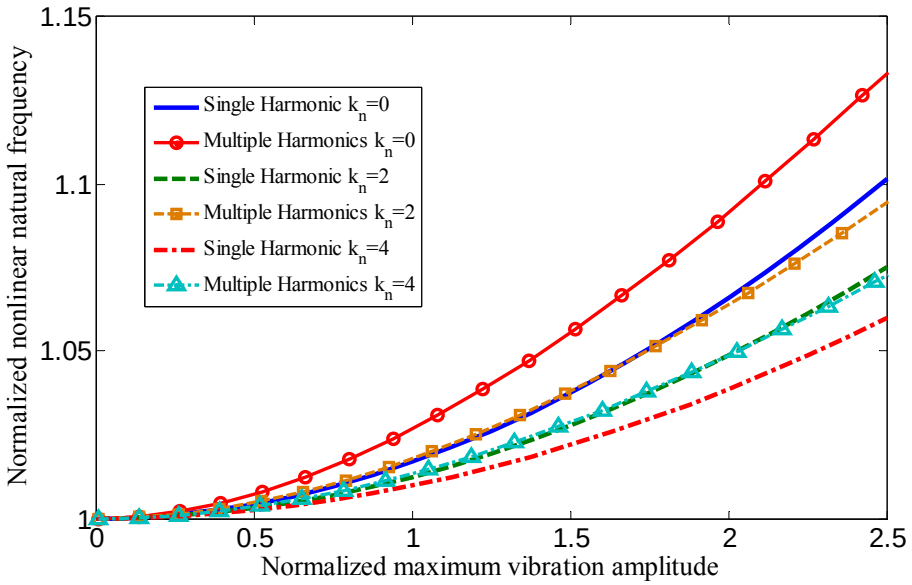

Figure 5-11 Variation of the normalized nonlinear natural frequency for different values of normalized medium stiffness

5.5. Concluding remarks

In this chapter, the variation of normalized nonlinear fundamental natural frequency of a curved SWCNT is investigated where the effect of higher harmonics is studied in detail. Galerkin method is used to discretize the equation of motion. Multiple

harmonic balance method is utilized to convert the discretized ordinary differential equations of motion into nonlinear algebraic equations and study the effect of higher harmonics. On the basis of the number of harmonics used in the solution expansion, several case studies are defined in order to explore the effect of higher harmonics on the variation of normalized nonlinear natural frequency in the presence of geometric and waviness nonlinearities. In each case, a closed form expression for the variation of the nonlinear fundamental natural frequency of CNTs is obtained analytically.

Results show that in the case of only geometric nonlinearity, the variation of nonlinear natural frequency is only affected by odd harmonics, however, the effect is not significant. On the other hand, in the case of both waviness and geometric nonlinearities, it is observed that the variation of normalized nonlinear natural frequency is affected by even harmonics as well. Our further studies show that the effect of waviness on the natural frequency can be classified in two categories named as: linear effect, and nonlinear effect. It is observed that the single harmonic approach is enough to detect linear effect of waviness on the variations of the nonlinear fundamental natural frequency, however, in order to detect the nonlinear effect of waviness, higher even harmonics should be considered. Moreover, it is observed that as medium stiffness increases the difference between solutions of single harmonic and multiple harmonic solutions decreases.

CHAPTER 6

DIFFERENTIAL QUADRATURE METHOD, A NOVEL METHOD TO STUDY NONLINEAR VIBRATIONS OF CNTS[8]

Depending on nonlinearity, common solution methods such as Galerkin require a set of multiple comparison functions to anticipate the system behavior. The effect of trial functions on the system response is studied in detail in chapter 4. However, these solution methods are limited to simple cases such as simply supported beams where the comparison functions have simple known forms. The objective of this chapter is to overcome the shortfalls of solution methods such as Galerkin by developing and implementing an accurate, efficient and relatively fast techniques for modeling CNTs which does not require any pre-knowledge on the system comparison functions, i.e. differential quadrature method. The method is introduced through its application in studying nonlinear free vibration analysis of curved double-walled carbon nanotubes (DWNTs) embedded in an elastic medium. Nonlinearities considered are due to large deflection of carbon nanotubes (geometric nonlinearity) and nonlinear interlayer van der Waals forces between inner and outer tubes.

6.1. Introduction

After the discovery of carbon nanotubes (CNTs) by Iigima [7], considerable attention has been devoted to carbon nanotubes (CNTs), since they have the ability to revolutionize critical technologies owing to their remarkable physical, mechanical, and electrical properties [61, 190-196].

---

[8] A version of this chapter is submitted to be published in Physica E as "Nonlinear Free Vibrations of Curved Double Walled Carbon Nanotubes Using Differential Quadrature Method"

Recent theoretical and experimental studies show that the deformation of CNTs is nonlinear in nature where they are affected by geometric and vdW force nonlinearities. Therefore, in order to accurately predict the vibrational behavior of CNTs, the nonlinear effect of both geometric and vdW force should be considered [51, 184, 197]. The effect of nonlinearities on nonlinear natural frequencies of DWCNTs is investigated in chapter 4 using describing function method and utilizing multiple trail functions in Galerkin method. It is observed that utilization of multiple trial functions resulted in the determination of multiple nonlinear natural frequencies at the same vibration amplitude and identification of single nonlinear natural frequencies associated with different vibration amplitudes. However, Even though Galerkin method is easy to implement, it requires trial functions or comparison functions that satisfy all the (geometric and natural) boundary conditions of the system. Hence, Galerkin approach is used only for studying hinged-hinged beams where the trial functions are simple sine functions. Therefore, presenting a general formulation capable of predicting the vibrational behavior of CNTs under different boundary conditions is of high importance. Recently, finite element method (FEM) is proposed to study the free vibration of CNTs where solution method such as Galerkin method is not applicable. Applicability of FEM in studying the free vibration of CNTs is investigated by Ansari et al. [143] in the presence of only geometric nonlinearity. Using FEM, authors were able to study the effect of boundary conditions on nonlinear natural frequencies for the first time. Even though classic FEMs can predict vibrational behavior of CNTs, they are disadvantaged in terms of computational time since they require higher number of grid points which results in large number of nonlinear equations. In order to overcome this difficulty differential quadrature method is utilized in this study.

The differential quadrature method (DQM) is a well-developed numerical method for quick solutions of linear and nonlinear partial differential equations. DQM developed by Bellman and Casti [198] is a discrete approach to directly solve the governing equations of various engineering problems. Different from conventional methods such as finite difference (FD) and finite element (FE) methods, DQM requires less grid points to obtain an acceptable accuracy. A comprehensive review on the DQM can be found in [199]. Owing to its efficiency and accuracy, DQM has the potential

to be used in variety of application areas. Applicability of DQM for micro and nanoscale beams and tubes is studied by Civalek et al. [200] and Wang et al. [201] for linear systems. Later, considering the nonlocal effect and temperature effects, same problem has been solved by Zhen and Fang [202]. Based on Eringen's nonlocal elasticity theory and von Kármán geometric nonlinearity, the nonlinear free vibration of a DWCNT is studied by Ke et al. [34] where a direct iterative method is used to solve the resulting system of equations. They studied the effect of system parameters on variation of nonlinear natural frequency of a DWCNT vibrating in the first in-phase vibration mode where different types of boundary conditions are considered. Later, benefiting from the advantages of DQM, Janghorban and Zare [203] studied the linear free vibration of functionally graded carbon nanotubes with variable thickness, where material properties are assumed to be graded in the longitudinal direction and a similar problem using different beam theories is studied by Ansari et al. [204].

The number of nonlinear studies on vibrations of CNTs having different end conditions is rare in literature due to the limitation of Galerkin method explained formerly. In addition to this, it is observed that only geometric nonlinearity is studied in these studies and nonlinear van der Waals effects between the layers of CNTs are neglected, since existence of vdW force complicates the solution. Therefore, to the best of author's knowledge, this is the first study which considers nonlinear free vibrations of curved double walled carbon nanotubes (DWCNTs) with different types of boundary conditions, where in addition to geometric nonlinearity, nonlinear interlayer van der Waals (vdW) force is also included. Differential quadrature method is used to discretize the partial differential equations of motion resulting in a system of nonlinear ordinary differential equations. The main advantage of DQM, in comparison to solution methods like variational approach [175], or Galerkin method [184, 197], is its inherent simplicity in formulation, where different end conditions can be easily adopted. Using DQM and considering a harmonic solution in time, nonlinear differential equations of motion are converted into a set of nonlinear algebraic equations, which is solved by the developed iterative path following method (IPFM).

6.2. Modeling

Consider a DWCNT of length L, cross-sectional areas A_i, A_o, area moment of inertias I_i, I_o, Young's modules E_i, E_o, and densities embedded in an elastic medium having a stiffness per unit length of k as shown in Figure 6-1, where i and o indicate the inner and outer tubes, respectively,. Assume that the transverse displacements of nanotubes are $w_i(x,t), w_o(x,t)$ where x and t are the spatial coordinate and the temporal variable. Equations of motion for free vibration of embedded curved DWCNTs considering geometric, initial curvature, and vdW force nonlinearities are given as [123, 166, 167]

$$E_i I_i \frac{\partial^4 w_i}{\partial x^4} + \rho_i A_i \frac{\partial^2 w_i}{\partial t^2} = \frac{E_i A_i}{L} \int_0^L \left[\frac{dZ}{dx} \frac{\partial w_i}{\partial x} + \frac{1}{2} \left(\frac{\partial w_i}{\partial x} \right)^2 \right] dx \cdot \left(\frac{\partial^2 w_i}{\partial x^2} + \frac{d^2 Z}{dx^2} \right) + p_v(x,t), \tag{6.1}$$

$$E_o I_o \frac{\partial^4 w_o}{\partial x^4} + \rho_o A_o \frac{\partial^2 w_o}{\partial t^2} = \frac{E_o A_o}{L} \int_0^L \left[\frac{dZ}{dx} \frac{\partial w_o}{\partial x} + \frac{1}{2} \left(\frac{\partial w_o}{\partial x} \right)^2 \right] dx \cdot \left(\frac{\partial^2 w_o}{\partial x^2} + \frac{d^2 Z}{dx^2} \right) + p_m(x,t) - p_v(x,t). \tag{6.2}$$

$Z(x)$ is the initial curvature (waviness) of the cylindrical tubes. $p_m(x,t)$ is the contact force between the surrounding medium and the tube which can be identified by Winkler-like model [47, 181] and $p_v(x,t)$ is the nonlinear vdW force. According to Winkler-like model theory, the interaction between surfaces can be simulated as a linear spring resulting in a pressure distribution linearly proportional to the relative displacement between the surfaces as

$$p_m(x,t) = -k w_o(x,t). \tag{6.3}$$

The negative sign in the above equation indicates that the pressure is opposite to the deflection of the tube and k is defined by the material constants of the surrounding elastic medium. On the other hand, vdW force is composed of attractive forces between atoms, molecules, and surfaces which only come into action when the

relative displacements are comparable with the atom sizes [80, 182]. The vdW force per unit area for two originally-concentric tubes is given in [168, 169] as

$$p_v(x,t) = p_1(w_o - w_i) + p_2(w_o - w_i)^3, \tag{6.4}$$

where $p_1 = 2r_i \left.\frac{\partial^2 U}{\partial \delta^2}\right|_{\delta=\delta_0}$, $p_2 = 2r_i \frac{1}{6}\left.\frac{\partial^4 U}{\partial \delta^4}\right|_{\delta=\delta_0}$, r_i is innertube radius, and U is potential energy expressed in terms of the interlayer spacing r_i as follows [121, 184]

$$U(\delta) = K_{IL}\left[\left(\frac{\delta_0}{\delta}\right)^4 - 0.4\left(\frac{\delta_0}{\delta}\right)^{10}\right], \tag{6.5}$$

where $K_{IL} = 0.4089101874\ \text{J/m}^2$, and $\delta_0 = 0.34\ \text{nm}$ is the equilibrium interfacial spacing. Substituting Eqs. (6.3) and (6.4) into Eqs. (6.1) and (6.2), the following nonlinear partial differential equations for the DWCNT are obtained:

$$E_i I_i \frac{\partial^4 w_i}{\partial x^4} + \rho_i A_i \frac{\partial^2 w_i}{\partial t^2} = \frac{E_i A_i}{L}\int_0^L \left[\frac{dZ}{dx}\frac{\partial w_i}{\partial x} + \frac{1}{2}\left(\frac{\partial w_i}{\partial x}\right)^2\right] dx \cdot \left(\frac{\partial^2 w_i}{\partial x^2} + \frac{d^2 Z}{dx^2}\right), \\ + p_1(w_o - w_i) + p_2(w_o - w_i)^3 \tag{6.6}$$

$$E_o I_o \frac{\partial^4 w_o}{\partial x^4} + \rho_o A_o \frac{\partial^2 w_o}{\partial t^2} = \frac{E_o A_o}{L}\int_0^L \left[\frac{dZ}{dx}\frac{\partial w_o}{\partial x} + \frac{1}{2}\left(\frac{\partial w_o}{\partial x}\right)^2\right] dx \cdot \left(\frac{\partial^2 w_o}{\partial x^2} + \frac{d^2 Z}{dx^2}\right). \\ -kw_o - p_1(w_o - w_i) - p_2(w_o - w_i)^3 \tag{6.7}$$

It is assumed that the waviness of the tubes, $Z(x)$, follow the first eigenfunction of the linear system, i.e. , $Z(x) = e \cdot \phi_1(x)$, where $\phi_1(x)$ is the first eigenfunction of the linear CNT. For instance, $Z(x) = e \cdot \sin(\pi x / L)$ [126] for the case of simply supported tubes, where e is the amplitude of the initial waviness.

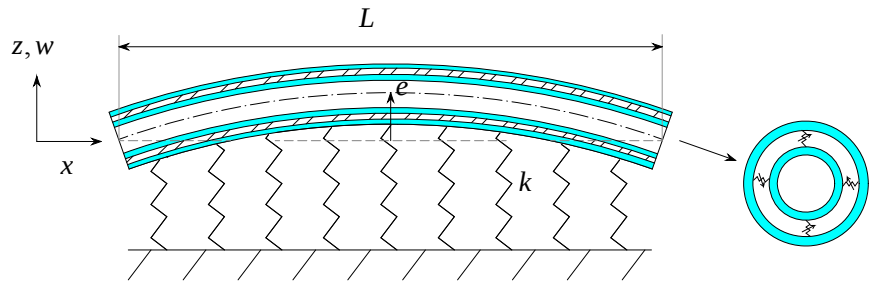

Figure 6-1 Model of an Embedded Curved DWCNT

6.3. Generalized differential quadrature method

Generalized differential quadrature method (GDQM) approximates the derivatives of a function with respect to a spatial variable at a given discrete point by a weighted linear summation of function values at all the discrete points in the computational domain. For example, the n^{th} derivative of a function $W_r(x)$ at the m^{th} point, x_m, can be estimated b

$$ {}_mW_r^{(n)} = \sum_{s=1}^{N} c_{m,s}^{(n)} {}_sW_r, \qquad j = 1,2,...,N . \tag{6.8} $$

In the generalized differential quadrature method [205], the global Lagrange interpolation polynomial is used to calculate the weighting coefficients, where Eq. (6.8) is considered to be exact for a test function of

$$ g_s(x) = \frac{l(x)}{(x - x_s)\cdot l^{(1)}(x_s)}, \quad s = 1,2,...,N , \tag{6.9} $$

$l(x)$ is the Lagrange interpolating polynomial and $l^{(1)}(x)$ is its first derivative which are defined as follows

$$. l(x) = \prod_{s=1}^{N}(x - x_s), \quad l^{(1)}(x_j) = \prod_{s=1, s\neq j}^{N}(x_j - x_s) . \tag{6.10} $$

Thus, differentiating Eq. (6.9), weighting coefficients, $c_{i,j}^{(1)}(i,j = 1,2,...,N)$, can be computed analytically as

$$c_{\mathrm{m,s}}^{(1)} = \begin{cases} \dfrac{l^{(1)}(x_m)}{(x_m - x_s)\cdot l^{(1)}(x_s)} & \text{for} \quad s \neq m \\ -\sum\limits_{s=1,s\neq m}^{N} c_{\mathrm{m,s}}^{(1)} & \text{for} \quad s = m \end{cases}. \tag{6.11}$$

The weighting coefficients for higher order derivatives can be found likewise. A recurrence relationship can be obtained for higher order derivatives as follows

$$c_{\mathrm{m,s}}^{(\mathrm{n})} = \begin{cases} n\cdot\left(c_{\mathrm{m,s}}^{(1)}\cdot c_{\mathrm{m,m}}^{(\mathrm{n}-1)} - \dfrac{c_{\mathrm{m,s}}^{(\mathrm{n}-1)}}{x_m - x_s} \right) & s \neq m \\ -\sum\limits_{s=1,s\neq m}^{N} c_{\mathrm{m,s}}^{(\mathrm{n})} & s = m \end{cases}. \tag{6.12}$$

Since the positions of the sampling points play a significant role in the accuracy of DQM [206], Gauss–Lobatto quadrature points are used which result in minimum error.

6.4. Application of DQM

Assuming a separable solution as $w_r(x,t) = W_r(x)\cdot T(t)$ and using Eq. (6.8), the partial differential equation of motion given by Eqs. (6.6) and (6.7) can be discretized at m^{th} point as

$$\begin{aligned} E_i I_i \left\{ \sum_{s=1}^{N} c_{m,s}^{(4)}\, {}_sW_i \right\} T(t) + \rho_i A_i\, {}_mW_i \frac{d^2T(t)}{dt^2} = \frac{E_i A_i}{L} \Bigg\{ \sum_{n=1}^{N} d_n \Bigg(\left.\frac{dZ}{dx}\right|_{x=x_n} \left\{ \sum_{s=1}^{N} c_{n,s}^{(1)}\, {}_sW_i \right\} \cdot T(t) + \\ \frac{1}{2}\left\{ \sum_{s=1}^{N} c_{n,s}^{(1)}\, {}_sW_i \right\}^2 \cdot T^2(t) \Bigg) \Bigg\} \cdot \left(\left\{ \sum_{s=1}^{N} c_{m,s}^{(2)}\, {}_sW_i \right\} T(t) + \left.\frac{d^2Z}{dx^2}\right|_{x=x_m} \right) \\ + p_1\left({}_mW_o - {}_mW_i \right)\cdot T(t) + p_2\left({}_mW_o - {}_mW_i \right)^3 \cdot T^3(t), \end{aligned}$$

, (6.13)

$$E_o I_o \left\{\sum_{s=1}^{N} c_{m,s}^{(4)}\, {}_sW_o\right\} T(t) + \rho_o A_o\, {}_mW_o \frac{d^2T(t)}{dt^2} = \frac{E_o A_o}{L}\left\{\sum_{n=1}^{N} d_n \left(\left.\frac{dZ}{dx}\right|_{x=x_n} \left\{\sum_{s=1}^{N} c_{n,s}^{(1)}\, {}_sW_o\right\} T(t) + \frac{1}{2}\left\{\sum_{s=1}^{N} c_{n,s}^{(1)}\, {}_sW_o\right\}^2 \cdot T^2(t)\right)\right\} \cdot \left(\left\{\sum_{s=1}^{N} c_{m,s}^{(2)}\, {}_sW_o\right\} T(t) + \left.\frac{d^2Z}{dx^2}\right|_{x=x_m}\right) - p_1\left({}_mW_o - {}_mW_i\right)\cdot T(t) - p_2\left({}_mW_o - {}_mW_i\right)^3 \cdot T^3(t) - k\, {}_mW_o T(t)$$

, (6.14)

where d_n is the weighting function which is calculated using Gauss–Lobatto integration rule. According to quadrature integration rule, integration value can be stated as a weighted sum of function values at specified points within the domain of integration (Eqs. (6.15) and (6.16)). The evaluation points are the roots of a polynomial belonging to a class of orthogonal polynomials which, in our case, is Gauss–Lobatto points which are as well used in the GDQM. It is worth noting that Gauss-Lobatto rule is accurate for polynomials up to the degree of $2n-3$, where n is the number of integration points [207].

$$\int_a^b f(x)dx \simeq \frac{b-a}{2}\left(d_1 \cdot f(a) + d_n \cdot f(b) + \sum_{i=2}^{n-1} d_i f\left(\frac{b-a}{2} z_i + \frac{b+a}{2}\right)\right), \tag{6.15}$$

$$d_i = \begin{cases} \dfrac{2}{n(n-1)\left[P_{n-1}(z_i)\right]^2}, & 2 \le i \le n-1 \\ \dfrac{2}{n(n-1)}, & i = 1, n \end{cases}, \tag{6.16}$$

where $P_n(z)$ is the n^{th} order Legendre polynomial.

Assuming a single harmonic solution in time, i.e. utilizing harmonic balance method (HBM) with a single harmonic Eqs. (6.13) and (6.14) become

$$E_i I_i \left\{\sum_{s=1}^{N} c_{m,s}^{(4)}\, {}_sW_i\right\} - \omega^2 \rho_i A_i\, {}_mW_i = \frac{EA_i}{L}\left\{\sum_{n=1}^{N} d_n \left(\left.\frac{dZ}{dx}\right|_{x=x_n} \left\{\sum_{s=1}^{N} c_{n,s}^{(1)}\, {}_sW_i\right\}\right)\right\} \left.\frac{d^2Z}{dx^2}\right|_{x=x_m} + \frac{3E_i A_i}{4L}\left\{\sum_{n=1}^{N} d_n \left(\frac{1}{2}\left\{\sum_{s=1}^{N} c_{n,s}\, {}_sW_i\right\}^2\right)\right\}\left\{\sum_{s=1}^{N} c_{m,s}^{(2)}\, {}_sW_i\right\}, + p_1\left({}_mW_o - {}_mW_i\right) + \frac{3p_2}{4}\left({}_mW_o - {}_mW_i\right)^3 \tag{6.17}$$

$$E_o I_o \left\{ \sum_{s=1}^{N} c_{m,s}^{(4)}\, {}_sW_o \right\} - \omega^2 \rho_o A_o\, {}_mW_o = \frac{E_o A_o}{L} \left\{ \sum_{n=1}^{N} d_n \left(\left. \frac{dZ}{dx} \right|_{x=x_n} \left\{ \sum_{s=1}^{N} c_{n,s}^{(1)}\, {}_sW_o \right\} \right) \right\} \left. \frac{d^2 Z}{dx^2} \right|_{x=x_m}$$
$$+ \frac{3E_o A_o}{4L} \left\{ \sum_{n=1}^{N} d_n \left(\frac{1}{2} \left\{ \sum_{s=1}^{N} c_{n,s}\, {}_sW_o \right\}^2 \right) \right\} \left\{ \sum_{s=1}^{N} c_{m,s}^{(2)}\, {}_sW_o \right\}. \qquad (6.18)$$
$$- p_1 \left({}_mW_o - {}_mW_i \right) - \frac{3p_2}{4} \left({}_mW_o - {}_mW_i \right)^3 - k\, {}_mW_o$$

The above equation can be written in matrix form as follows

$$\left(\mathbf{K_L} + \mathbf{K_{NL}} \right) \cdot \mathbf{x} - \omega^2 \mathbf{M} \cdot \mathbf{x} = \mathbf{0} \ , \qquad (6.19)$$

$$\mathbf{K_{NL}} = \mathbf{K_{NLg}} + \mathbf{K_{NLv}} \ , \qquad (6.20)$$

where $\mathbf{x}$ denotes the unknown dynamic displacement vector defined as

$$\mathbf{x} = \left\{ {}_1W_i \quad {}_2W_i \quad \cdots \quad {}_NW_i \ \middle| \ {}_1W_o \quad {}_2W_o \quad \cdots \quad {}_NW_o \right\}^T , \qquad (6.21)$$

and $\mathbf{M}$, $\mathbf{K_L}$, $\mathbf{K_{NLg}}$ and $\mathbf{K_{NLv}}$ represent mass matrix, linear stiffness matrix, and nonlinear stiffness matrices associated with geometric and vdW force nonlinearities of the system, respectively. These matrices are defined as

$$\mathbf{M}_{2N \times 2N} = identity \ , \qquad (6.22)$$

$$\mathbf{K_L} = \left[\begin{array}{c|c} \dfrac{E_i I_i}{\rho_i A_i} \cdot \mathbf{C}^{(4)} + \dfrac{p_1}{\rho_i A_i} \cdot \mathbf{I} - \dfrac{E_i e^2}{\rho_i L} \cdot \mathbf{E} & -\dfrac{p_1}{\rho_i A_i} \cdot \mathbf{I} \\ \hline -\dfrac{p_1}{\rho_o A_o} \cdot \mathbf{I} & \dfrac{E_o I_o}{\rho_o A_o} \cdot \mathbf{C}^{(4)} + \dfrac{\left(p_1 + k \right)}{\rho_o A_o} \cdot \mathbf{I} - \dfrac{E_o e^2}{\rho_o L} \cdot \mathbf{E} \end{array} \right], \qquad (6.23)$$

$$\mathbf{K_{NLg}} = \frac{3}{4L} \cdot \left[\begin{array}{c|c} \beta_i \dfrac{E_i}{\rho_i} \mathbf{C}^{(2)} & [0] \\ \hline [0] & \beta_o \dfrac{E_o}{\rho_o} \mathbf{C}^{(2)} \end{array} \right], \qquad (6.24)$$

$$\mathbf{K}_{\mathbf{NLv}} = \frac{3p_2}{4}\begin{bmatrix} \dfrac{1}{\rho_i A_i}\left[\mathbf{K}_1 \mid \mathbf{K}_2\right] \\ \hline \dfrac{-1}{\rho_o A_o}\left[\mathbf{K}_1 \mid \mathbf{K}_2\right] \end{bmatrix}. \tag{6.25}$$

$\mathbf{I}$ is identity matrix, $\mathbf{c}^{(n)}$ indicates weighting function matrix for the n^{th} order derivative using DQM, $\mathbf{E}$ stands for initial waviness matrix, $\beta_r\ (r = i, o)$ is a displacement dependent coefficient representing geometric nonlinearity, and $\mathbf{K}_1$, and $\mathbf{K}_2$ are displacement dependent matrices. The initial waviness matrix given in Eq. (6.23) is defined as follow

$$\mathbf{E} = \left\{\sum_{n=1}^{N} d_n \left(\phi'(x_n)\left\{\sum_{s=1}^{N} c_{n,s}^{(1)}\, {}_sW_o\right\}\right)\right\}\begin{bmatrix} \phi''(x_3) & & & 0 \\ & \phi''(x_4) & & \\ & & \ddots & \\ 0 & & & \phi''(x_{N-2}) \end{bmatrix}, \tag{6.26}$$

where $\phi'(x)$ and $\phi''(x)$ are first and second derivatives of the first linear eigenfunction of the system that is used to define the waviness, respectively; and $\beta_r\ (r = i, o)$, $\mathbf{K}_1$, and $\mathbf{K}_2$ given in Eqs. (6.24) and (6.25) are defined as follows:

$$\beta_r = \frac{1}{2}\left\{\sum_{n=1}^{N} d_n \left\{\sum_{s=1}^{N} c_{n,s}^{(1)}\, {}_sW_r\right\}^2\right\}, \tag{6.27}$$

$$\mathbf{K}_1 = \begin{bmatrix} {}_3W_i^2 + 3\,{}_3W_o^2 & & & 0 \\ & {}_4W_i^2 + 3\,{}_4W_o^2 & & \\ & & \ddots & \\ 0 & & & {}_{N-2}W_i^2 + 3\,{}_{N-2}W_o^2 \end{bmatrix}, \tag{6.28}$$

$$\mathbf{K}_2 = -\begin{bmatrix} {}_3W_o^2 + 3\,{}_3W_i^2 & & & 0 \\ & {}_4W_o^2 + 3\,{}_4W_i^2 & & \\ & & \ddots & \\ 0 & & & {}_{N-2}W_o^2 + 3\,{}_{N-2}W_i^2 \end{bmatrix}. \tag{6.29}$$

It should be noted that the higher order DQM weighting function matrix can as well be calculated through matrix multiplication, e.g. $\mathbf{C}^{(2)} = \mathbf{C} \times \mathbf{C}$, where the elements of $\mathbf{C}$ are given by Eq. (6.11).

In the present study, three common sets of boundary conditions namely as hinged-hinged (H-H), clamped–hinged (C-H), and clamped–clamped (C-C) are investigated. Boundary conditions for hinged and clamped ends are

$$w_r(x_s,t)=0, \quad \left.\frac{d^2 w_r}{dx^2}\right|_{x=x_s}=0, \tag{6.30}$$

$$w_r(x_s,t)=0, \quad \left.\frac{dw_r}{dx^2}\right|_{x=x_s}=0, \tag{6.31}$$

respectively. Where s=1 and $s=N$ represents the end points. Using the GDQM, the discretized counterparts of different boundary conditions given by Eqs. (6.30) and (6.31) can be written as follows

$$\begin{aligned} \mathbf{a}_s \cdot \left({}_1W_r \quad {}_2W_r \quad \cdots \quad {}_{N-1}W_r \quad {}_NW_r\right)^T &= \mathbf{0}, \\ \left(c_{s,1}^{(2)} \quad c_{s,2}^{(2)} \quad \cdots \quad c_{s,N-1}^{(2)} \quad c_{s,N}^{(2)}\right) \cdot \left({}_1W_r \quad {}_2W_r \quad \cdots \quad {}_{N-1}W_r \quad {}_NW_r\right)^T &= \mathbf{0}, \end{aligned} \tag{6.32}$$

$$\begin{aligned} \mathbf{a}_s \cdot \left({}_1W_r \quad {}_2W_r \quad \cdots \quad {}_{N-1}W_r \quad {}_NW_r\right)^T &= \mathbf{0}, \\ \left(c_{s,1}^{(1)} \quad c_{s,2}^{(1)} \quad \cdots \quad c_{s,N-1}^{(1)} \quad c_{s,N}^{(1)}\right) \cdot \left({}_1W_r \quad {}_2W_r \quad \cdots \quad {}_{N-1}W_r \quad {}_NW_r\right)^T &= \mathbf{0}, \end{aligned} \tag{6.33}$$

respectively. Where $\mathbf{a}_s = \left(1 \quad 0 \quad \cdots \quad 0 \quad 0\right)_{1\times N}$ for s=1 and $\mathbf{a}_s = \left(0 \quad 0 \quad \cdots \quad 0 \quad 1\right)_{1\times N}$ for $s=N$ Boundary conditions given by Eqs. (6.32) and (6.33) can as well be expressed in matrix form as follows

$$\left[\begin{array}{ccccc|c} 1 & 0 & \cdots & 0 & 0 & \\ c_{1,1}^{(n)} & c_{1,2}^{(n)} & \cdots & c_{1,N-1}^{(n)} & c_{1,N}^{(n)} & \\ c_{N,1}^{(n)} & c_{N,2}^{(n)} & \cdots & c_{N,N-1}^{(n)} & c_{N,N}^{(n)} & [0] \\ 0 & 0 & \cdots & 0 & 1 & \\ \hline & & & & & \\ & [0] & & & & \\ & & & & & \end{array} \begin{array}{ccccc} & & & & \\ & & & & \\ & & & & \\ & & & & \\ \hline 1 & 0 & \cdots & 0 & 0 \\ c_{1,1}^{(n)} & c_{1,2}^{(n)} & \cdots & c_{1,N-1}^{(n)} & c_{1,N}^{(n)} \\ c_{N,1}^{(n)} & c_{N,2}^{(n)} & \cdots & c_{N,N-1}^{(n)} & c_{N,N}^{(n)} \\ 0 & 0 & \cdots & 0 & 1 \end{array}\right]_{8\times 2N} \left\{\begin{array}{c} {}_1W_i \\ {}_2W_i \\ \vdots \\ {}_{N-1}W_i \\ {}_NW_i \\ \hdashline {}_1W_o \\ {}_2W_o \\ \vdots \\ {}_{N-1}W_o \\ {}_NW_o \end{array}\right\}_{2N\times 1} = \{0\} . \quad (6.34)$$

Where superscript n is assigned by the type of end conditions, where it is equal to 1 for the clamped end and 2 for the hinged end. By using matrix manipulation Eq. (6.34) can be written as

$$\mathbf{K_B}\cdot\mathbf{x_s}+\mathbf{K_S}\cdot\mathbf{x}^*=\mathbf{0}, \quad (6.35)$$

where

$$\mathbf{x_s}=\left\{ {}_1W_i, {}_2W_i, {}_{N-1}W_i, {}_NW \;\middle|\; {}_1W_o, {}_2W_o, {}_{N-1}W_o, {}_NW_o \right\}^T , \quad (6.36)$$

$$\mathbf{x}^*=\left\{ {}_3W_i \quad {}_4W_i \quad \cdots \quad {}_{N-2}W_i \;\middle|\; {}_3W_o \quad {}_4W_o \quad \cdots \quad {}_{N-2}W_o \right\}^T , \quad (6.37)$$

representing boundary and interior nodes and $\mathbf{K_B}$ and $\mathbf{K_S}$ are 8×8 and $8\times(2N-8)$ matrices related with boundary and interior nodes, respectively. Following a similar approach Eq. (6.19) can be written as

$$\mathbf{K_D}\cdot\mathbf{x_s}+\left(\mathbf{K_L^*}+\mathbf{K_{NL}^*}\right)\cdot\mathbf{x}^*-\omega^2\mathbf{M}^*\cdot\mathbf{x}^*=\mathbf{0}. \quad (6.38)$$

Here $\mathbf{K_L^*}$, $\mathbf{K_{NL}^*}$, and $\mathbf{M}^*$ are $(2N-8)\times(2N-8)$ matrices, representing the linear stiffness matrix, nonlinear stiffness matrix, and mass matrix for the interior nodes, respectively. It is worth noting that $\mathbf{K_L^*}$, $\mathbf{K_{NL}^*}$, and $\mathbf{M}^*$ are coefficient matrices for the non-boundary nodes, where $\mathbf{K_{NL}^*}$ is a displacement dependent matrix whose values

depend on the values of the boundary nodes in addition to the interior nodes. $\mathbf{K_D}$ is an $(2N-8)\times 8$ matrix, which contains coefficient of boundary nodes.

Solving $\mathbf{x}_s$ from Eq. (6.35) and substituting it in Eq. (6.38), equation of motion of the system is obtained as follows

$$\left[\left(\mathbf{K}_{\mathbf{L}}^{*}+\mathbf{K}_{\mathbf{NL}}^{*}\right)-\mathbf{K}_{\mathbf{D}}\mathbf{K}_{\mathbf{B}}^{-1}\mathbf{K}_{\mathbf{S}}\right]\cdot\mathbf{x}^{*}=\omega^{2}\mathbf{M}^{*}\cdot\mathbf{x}^{*}. \tag{6.39}$$

6.5. Solution method

The set of nonlinear algebraic equations given by Eq. (6.39) can be solved numerically by using Newton's method with Arc-length continuation. Newton's method converges to the correct solution quadratically, if the initial guess is sufficiently close to the actual solution. However, convergence problems arise when a solution is around a turning point since the Jacobian matrix becomes singular. Moreover, in order to follow the solution branch even it reverses its direction; continuation parameter has to be replaced with another parameter for which it is possible to follow the path (arc-length continuation). Details of Newton's method with arc-length continuation can be found in [121].

Another solution approach commonly used by a number of researchers is a direct iterative process (DIP) by using eigenvalue solvers. In this method [34, 122], vibration amplitude increases incrementally. At each step, nonlinear vibration dependent stiffness matrices are calculated based on the mode shape of the previous solution. The resultant linear system can be solved using an eigenvalue solver. This process is repeated until the difference between the assumed and calculated eigenmodes decreases to a predetermined tolerance. It should be noted that DIP method is established based on the assumption that variation of mode shapes along the solution path is small. However, due to strong nonlinearities existing in the problem, nonlinear system mode shape changes significantly along the solution path as shown in [121], where DIP fails in finding the correct solution and therefore it cannot be used directly. Moreover, the effect of each nonlinearity is different whether the in-phase vibration mode or out-of-phase vibration mode is considered. For

example, due to vdW force nonlinearity out-of-phase natural frequencies increase significantly as the maximum vibration amplitude increases; whereas, in-phase natural frequencies change slightly with respect to the maximum vibration amplitude. As a result of this, it is possible for the path of system natural frequencies to cross each other as presented in [121]. For instance, system can vibrate in the second mode (out-of-phase mode) with a nonlinear natural frequency higher than the nonlinear natural frequency of the third mode (in-phase mode) as vibration amplitude increases. Hence, in the present study, in order to overcome these two problems, a new method referred as "iterative path following method" is developed, which combines modal assurance criterion (MAC) and arc-length continuation method with DIP in order to improve its performance. In the iterative path following method (IPFM), by utilizing MAC it is possible to track the correct natural frequency and by using arc-length continuation it is possible to follow the solution path in the presence of multiple solutions.

The modal assurance criterion is outlined as a scalar constant relating the degree of consistency (linearity) between two vectors as follows

$$MAC = \frac{\left|\{\psi_A\}^T \{\psi_x\}\right|^2}{\left|\{\psi_A\}^T \{\psi_A\}\right|\left|\{\psi_x\}^T \{\psi_x\}\right|}, \tag{6.40}$$

where $\{\psi_A\}$ and $\{\psi_x\}$ are two vectors that are compared with each other. The modal assurance criterion takes values between 0 and 1, where 0 and 1 indicate two independent and identical vectors, respectively. Thus, if the modal vectors under study truly express a consistent, linear relationship, the modal assurance criterion approaches unity. This fact is utilized in finding the system eigenvalues. Additionally, instead of increasing incrementally the vibration amplitude, which may result in jump up or down in case of multiple solutions, arc-length continuation is utilized to follow the solution branch around turning points, in which the maximum vibration amplitude becomes an unknown and arc-length is the parameter used in path following.

The solution method consists of two major loops: the arc-length loop and direct iterative process loop which acts inside the arc-length loop. The step by step

description of the developed iterative path following method (IPFM) is given as follows:

Step 1:

The nonlinear equation of motion given in Eq. (6.39) can be written as a residual vector function as

$$\mathbf{f}(\mathbf{x}^*, \omega) = \left\{ \left(\mathbf{K}_{\mathbf{L}}^* + \mathbf{K}_{\mathbf{NL}}^* \right) - \mathbf{K}_{\mathbf{D}} \mathbf{K}_{\mathbf{B}}^{-1} \mathbf{K}_{\mathbf{S}} \right\} \cdot \mathbf{x}^* - \omega^2 \mathbf{M}^* \cdot \mathbf{x}^* = 0 \,, \tag{6.41}$$

$$\mathbf{x}^* = W_{\max} \cdot \left\{ \begin{array}{cccc|cccc} {}_3\tilde{W}_i & {}_4\tilde{W}_i & \cdots & {}_{N-2}\tilde{W}_i & {}_3\tilde{W}_o & {}_4\tilde{W}_o & \cdots & {}_{N-2}\tilde{W}_o \end{array} \right\}^T = W_{\max} \tilde{\mathbf{x}}^* \,, \tag{6.42}$$

where ${}_k\tilde{W}_i$ and ${}_k\tilde{W}_o$ represent the normalized vibration amplitudes of the mode shapes of inner and outer tubes with respect to the grid point of the innertube or outertube that result in the maximum absolute value. The arc length parameter is defined as the radius of a fictitious n-dimensional sphere centered at the previous converged solution point. It should be noted that in the first step, linear system eigenvector is considered as the reference mode. The new solution will be searched on the surface of this sphere rather than at the next vibration amplitude, where the amplitude become an unknown and the radius of the fictitious sphere is the parameter specified. Details about applying the arc-length method to a residual function can be found in [121]. Arc-length continuation is used to update the mode shapes obtained in the previous solution and predict the next vibration amplitude.

Step 2:

DIP loop starts here, where calculated eigenvectors are used to determine the nonlinear stiffness matrix, $\mathbf{K}_{\mathbf{NL}}^*$, and new eigenvalues and eigenvectors are calculated from the updated eigensystem. MAC is calculated based on the eigenvector of previous solution in order to select the correct eigenvector and the eigenvalue associated with it.

Step 3:

The calculated eigenvector is normalized and step 2 is repeated until the error in the residual function given by Eq. (6.41) is within predefined tolerance limit.

It should be noted that the maximum vibration amplitude does not occur at the same point on the CNTs; moreover, it can occur at points other than DQM points. Hence, in order to find the maximum vibration amplitude, after obtaining the nonlinear eigenvector, the full mode shape is reconstructed using Lagrange interpolation and the point of maximum amplitude is determined.

6.6. Results

In the following section, the effect of nonlinearities on the first in-phase and out-of-phase fundamental natural frequencies of a curved DWCNT is investigated. Firstly, the effect of geometric nonlinearity and initial curvature on the nonlinear natural frequency of a DWCNT is studied by presenting the variation of normalized nonlinear natural frequency with respect to the maximum vibration amplitude. Later, the same study is repeated considering the effect of vdW force nonlinearity together with the geometric nonlinearity. Finally, considering both nonlinearities medium stiffness on the nonlinear natural frequency of the DWCNTs are investigated. Meanwhile, the effects of different end conditions are as well considered in the studies performed. In order to present the results in a proper form, the nonlinear natural frequency is normalized with respect to the corresponding linear natural frequency of the curved DWCNT and vibration amplitudes are normalized with respect to $\sqrt{I_i/A_i}$.

The numerical values of the parameters used in this study are given in Table 6-2. Before proceeding into the nonlinear analysis, the effect of number of grid points is studied on the linear system (Table 6-1), where it is observed that the natural frequencies obtained for all types of boundary conditions considered are identical in case the number of grid points is larger or equal to 13. Therefore, in all the results presented, 18 grid points are utilized which is observed to be sufficient for the nonlinear cases as well.

Table 6-1 Effect of the Number of Grid Points on the Linear Fundamental Frequencies of the DWCNTs with Different Boundary Conditions

N	-	H-H (THz)	C-H (THz)	C-C (THz)
10	In-phase	0.46727276	0.72958103	1.05775816
	Out-of-phase	7.67867366	7.94739767	7.92494566
11	In-phase	0.46728898	0.72963714	1.05780658
	Out-of-phase	7.88518860	7.89901304	7.92495020
12	In-phase	0.46728882	0.72963963	1.05780510
	Out-of-phase	7.88518860	7.89901320	7.92495006
13	In-phase	0.46728867	0.72963869	1.05780414
	Out-of-phase	7.88518859	7.89901314	7.92494997
14	In-phase	0.46728868	0.72963868	1.05780415
	Out-of-phase	7.88518859	7.89901314	7.92494998
18	In-phase	0.46728868	0.72963869	1.05780416
	Out-of-phase	7.88518859	7.89901314	7.92494998

In Table 6-3, the fundamental natural frequency of the linear DWCNT with H-H end conditions are compared with the analytical solution and the results given in literature. It can be seen that the results of DQM and analytical solution are in very good agreement.

Table 6-2 Numerical Values of Tubes Parameters

Parameter	Value
Innertube diameter	$d_i = 0.7$ nm
Outertube diameter	$d_0 = 1.4$ nm
Young's modulus	$E = 1$ TPa
Poisson's ratio	$\nu = 0.25$
Thickness of each tube	$t = 0.34$ nm

Table 6-3 Fundamental Linear Natural Frequencies of a Simply Supported DWCNT

Natural frequencies	In-phase	Out-of-phase
Ref. [121]	0.4673	7.8852
Ref. [51]	0.46	7.71
Analytical solution	0.467289	7.885189
Present study, DQM	0.467289	7.885189

6.6.1. Geometric nonlinearity

In Figure 6-2, the variation of the normalized nonlinear natural frequency of the first in-phase vibration mode of a DWCNT is given for different types of end conditions in the presence of only geometric nonlinearity. A hardening stiffness behavior is observed for all types of boundary conditions, i.e. the nonlinear natural frequency increases as the vibration amplitude increases. Furthermore, it is observed that

although the clamped-clamped DWCNT have the highest fundamental linear natural frequencies, it has the lowest normalized nonlinear natural frequency at the same maximum vibration amplitude. This is an expected result, since the effect of geometric nonlinearity decreases due to the limited deformation obtained for stronger end supports

Figure 6-3 shows the variation of the normalized nonlinear natural frequency of a DWCNT vibrating in the first out-of-phase vibration mode where the effect of different boundary conditions is investigated. Results show that in contrast to in-phase vibration mode, the variation of nonlinear natural frequency increases as end conditions get stronger for the out-of-phase vibration mode. However, the amount of the increase in the nonlinear natural frequency is lower than the case of in-phase vibration mode and for H-H and C-C boundary conditions, it is negligible. Moreover, several turning points are observed for C-H end conditions, where at a single vibration amplitude multiple nonlinear natural frequencies exist.

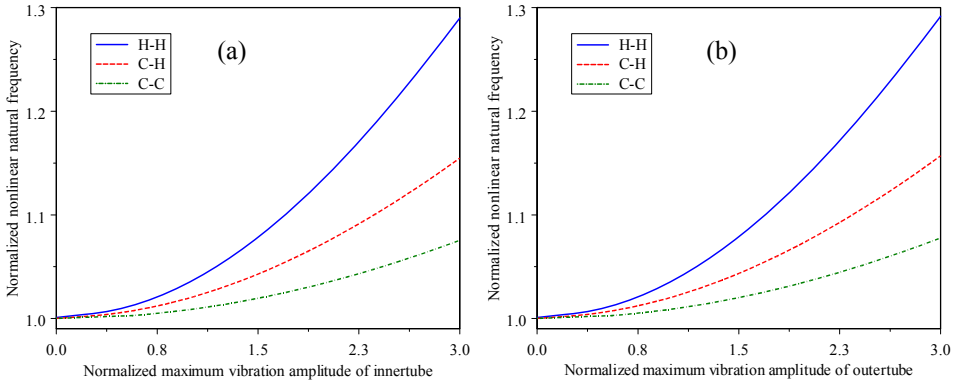

Figure 6-2 Variation of Normalized Nonlinear Natural Frequency of Inner and Outer Tubes Vibrating in the First in-Phase Mode for Different End Conditions ($e = 0$)

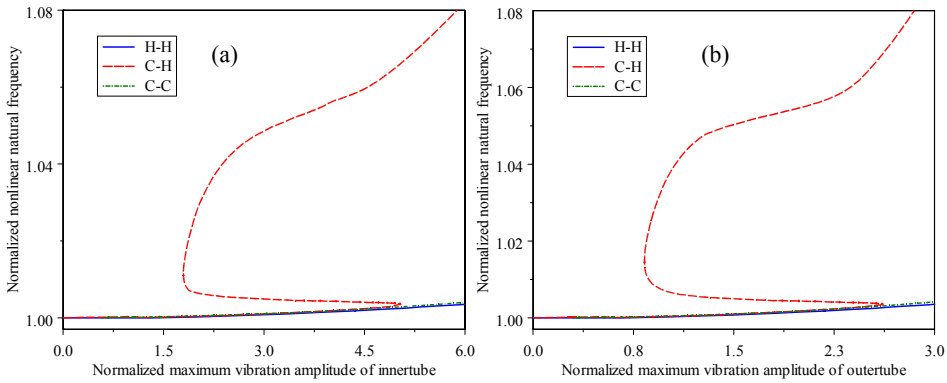

Figure 6-3 Variation of Normalized Nonlinear Natural Frequency of Inner and Outer Tubes Vibrating in the First out-of-Phase Mode for Different End Conditions ($e = 0$)

In Figure 6-4, the variation of nonlinear natural frequency for the C-H end conditions is re-plotted by dividing the plot into five regions where the corresponding mode shapes of the tubes at the center of each region is given as well. The regions are defined by considering the changes in the characteristics of the nonlinear mode shape, where, for some cases, it occurs around turning points. It can be seen that in the first region, the system vibrates in a mode shape similar to the fundamental out-of-phase mode shape of the linear system. However as the region number increases, the contribution of other linear modes become significant in the nonlinear solution. For instance, in the second region the system vibrates in a mode shape which can be identified as a combination of the first out-of-phase and the fourth in-phase linear vibration modes. In order to clearly study the contribution of each linear vibration mode to the nonlinear solution, variation of normalized modal contributions along the solution curve is plotted in Figure 6-5 for the first six modes that have the highest contributions. Normalized modal contributions are calculated using Eq. (6.40), where the nonlinear mode shape is compared with the linear modes of corresponding system. It can be seen that moving forward along the solution curve the contribution of the first out-of- phase mode decreases and at the same time the contribution of the forth in-phase mode increases and becomes maximum in the middle of the third region. Proceeding further contribution of the fourth in-phase mode decreases; whereas, the contribution of the second out-of-phase mode starts to increase and dominates the nonlinear solution. Our further studies show that system continues to vibrate in the second out-of-phase mode and does not return to the first out-of-phase vibration mode as vibration amplitude increases. This is due to the fact that, in the path following

method, the nonlinear vibration mode which is closer to the one at the previous amplitude step is followed; however, for H-H and C-C boundary conditions, which are symmetric, the first out-of-phase vibration mode is dominant in the nonlinear vibration mode.

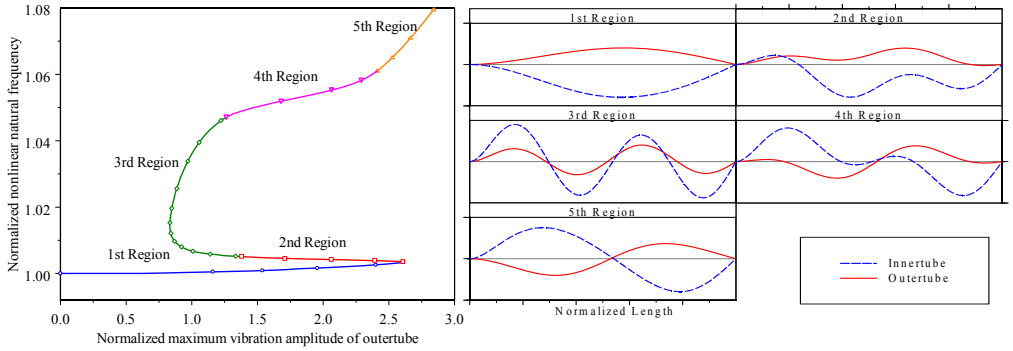

Figure 6-4 Variation of Normalized Nonlinear Natural Frequency of Outertube Vibrating in the First Out-of-Phase Mode and the Corresponding Mode Shapes in the Middle of Each Region

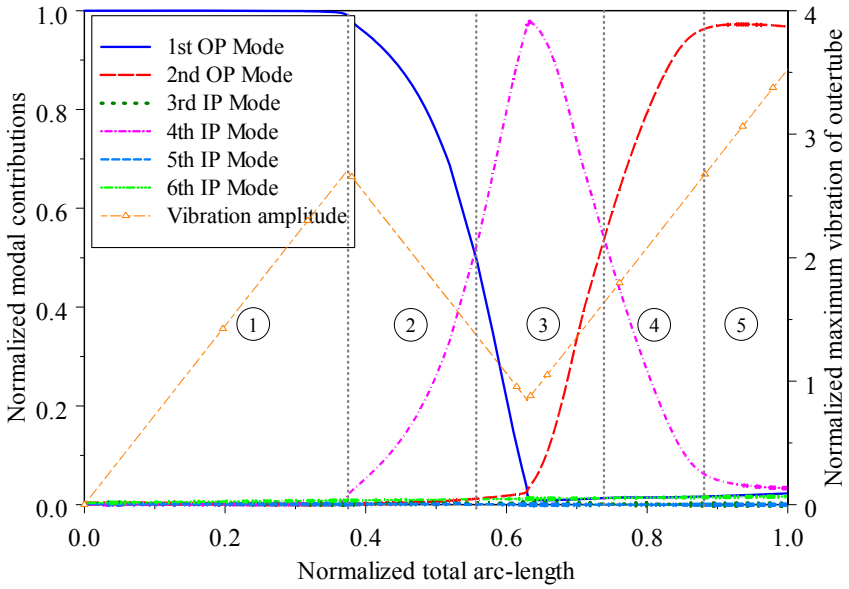

Figure 6-5 Variation of Normalized Modal Contributions vs. Normalized Total Arc-length

6.6.2. Effect of initial curvature on the fundamental natural frequencies of the DWCNT

In Figure 6-6, variation of normalized fundamental nonlinear natural frequency is given for different values of initial curvature (waviness) for hinged-hinged, clamped-hinged, and clamped-clamped DWCNT vibrating in the first in-phase vibration mode. It is observed that for all the cases normalized nonlinear natural frequency decreases as waviness increases and tends to approach to the linear one. It can be seen that as the end conditions get stronger, the effect of initial curvature on variation of nonlinear natural frequency decreases.

Figure 6-7 shows the effect of initial curvature on the nonlinear natural frequency of the DWCNT vibrating in the first out-of-phase vibration mode. It is observed that comparing to in-phase vibration mode the effect of initial curvature on the nonlinear natural frequency is insignificant in the out-of-phase vibration mode.

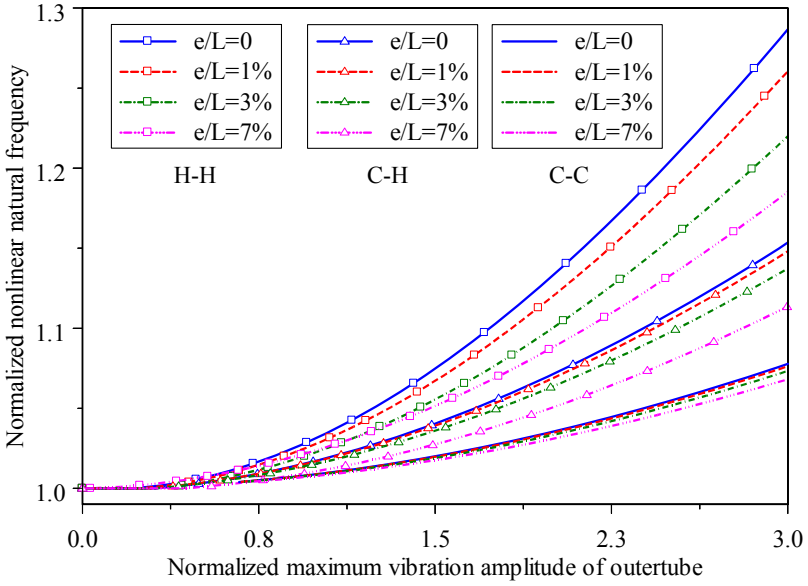

Figure 6-6 Effect of Initial Curvature on the Variation of Normalized Nonlinear Natural Frequency of Inner and Outer Tubes Vibrating in the First In-Phase Mode a) H-H b) C-H c) C-C

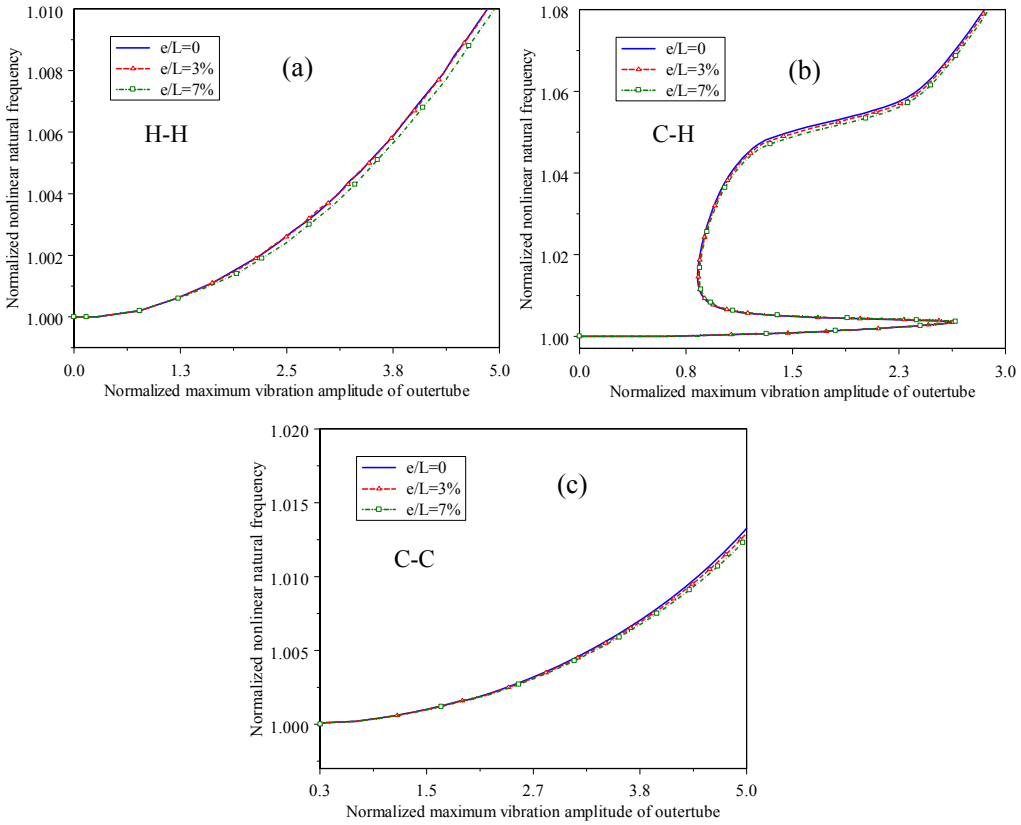

Figure 6-7 Effect of Initial Curvature on the Variation of Normalized Nonlinear Natural Frequency of Inner and Outer Tubes Vibrating in the First out-of-Phase Mode a) H-H b) C-H c) C-C

6.6.3. Van der Waals force nonlinearity together with geometric nonlinearity

In Figure 6-8, variation of normalized nonlinear natural frequency in the first in-phase vibration mode is given for different types of end conditions and initial curvature. Results show that in the in-phase vibration mode, nonlinear natural frequency majorly changes due to the geometric nonlinearity and considering the vdW force nonlinearity in addition to geometric nonlinearity does not affect the vibratory behavior of the DWCNT. Moreover, as initial curvature increases, a similar behavior as in Figure 6-6 is observed. This is an expected result, since vdW force nonlinearity depends on the relative motion between the inner and outer tubes and in the in-phase vibration modes, relative motion between the tubes changes slightly during free vibration. Furthermore, our studies show that, similar to the case of geometric nonlinearity, the effect of initial curvature is insignificant for the case of out-of-phase vibration mode. Hence, for

clarity, initial curvature is considered to be equal to zero for out-of-phase vibration modes presented from now on.

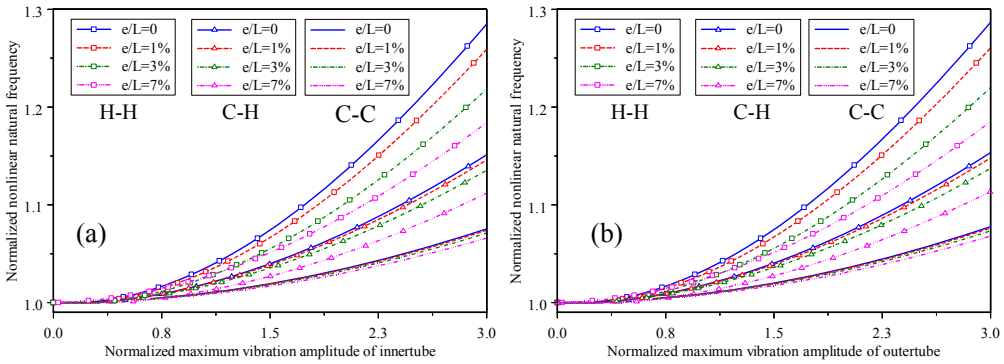

Figure 6-8 Variation of Normalized Nonlinear Natural Frequency of Inner and Outer Tubes Vibrating in the First In-Phase Mode for Different End Conditions in the Presence of both vdW Force and Geometric Nonlinearities

Figure 6-9 shows the variation of the normalized nonlinear natural frequency for the case of the first out-of-phase vibration mode considering different types of end conditions. Results show that due to the vdW force nonlinearity, nonlinear natural frequency changes considerably where several turning points are observed for all end conditions considered. The results obtained for the H-H DWCNT are the same as the ones presented by Cigeroglu and Samandari [121], where authors used a Galerkin based discretization method. In Figure 6-10, variation of the normalized nonlinear natural frequency for each end condition is given, where the curves are divided into seven different regions indicated by different markers and colors. In Figure 6-11, variation of the normalized contribution of each linear mode shape is plotted for the first seven modes that have the highest contributions, where different regions are indicated by numbers. It can be seen that for all the cases as total arc-length increases, or as the region number increases, the contribution of the first linear out-of-phase mode decreases and later increases again. Moreover, it is observed that for all the cases in the region for which the contribution of the first mode becomes a minimum (2^{nd} region for C-C and C-H, and 2^{nd}-4^{th} regions for H-H), CNTs vibrate as if it is vibrating in the fifth linear in-phase mode.

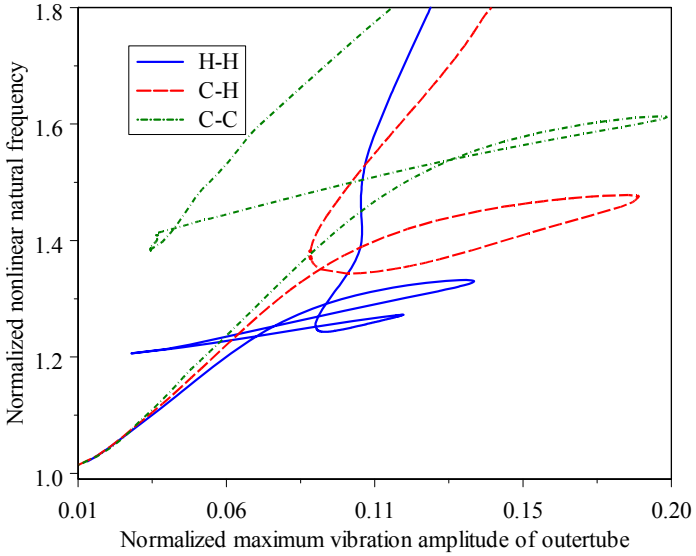

Figure 6-9 Variation of Normalized Nonlinear Natural Frequency of Inner and Outer Tubes Vibrating in the First Out-of-Phase Mode for Different End Conditions in the Presence of both vdW Force and Geometric Nonlinearities ($e = 0$)

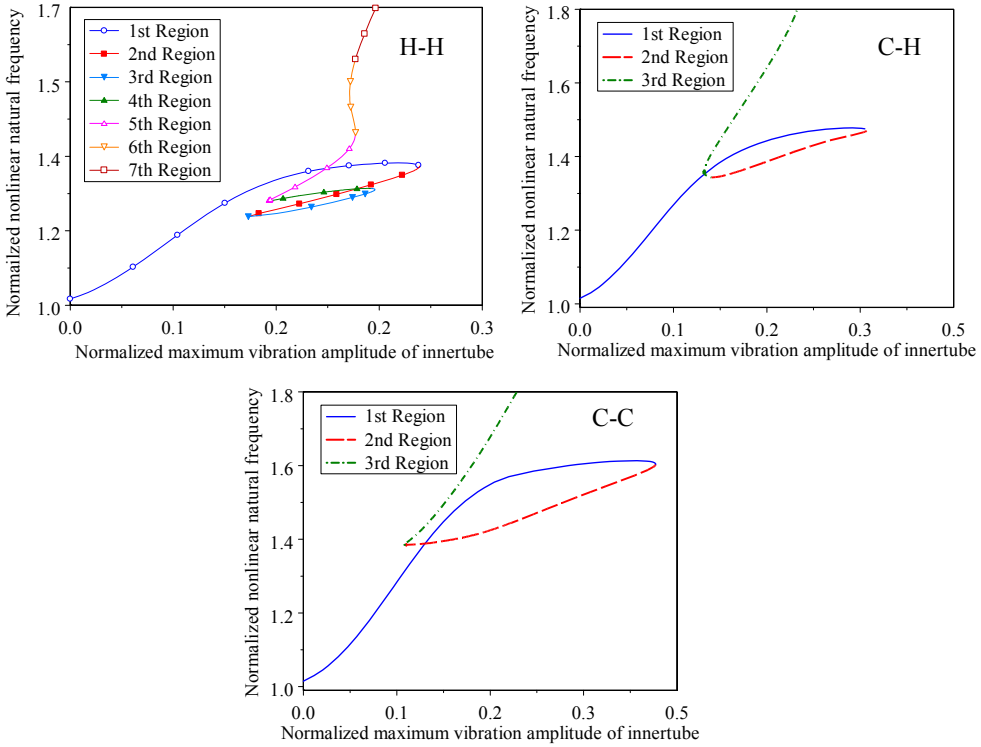

Figure 6-10 Variation of Normalized Nonlinear Natural Frequency of Innertube Vibrating in the First Out-of-Phase Mode a) H-H b) C-H c) C-C

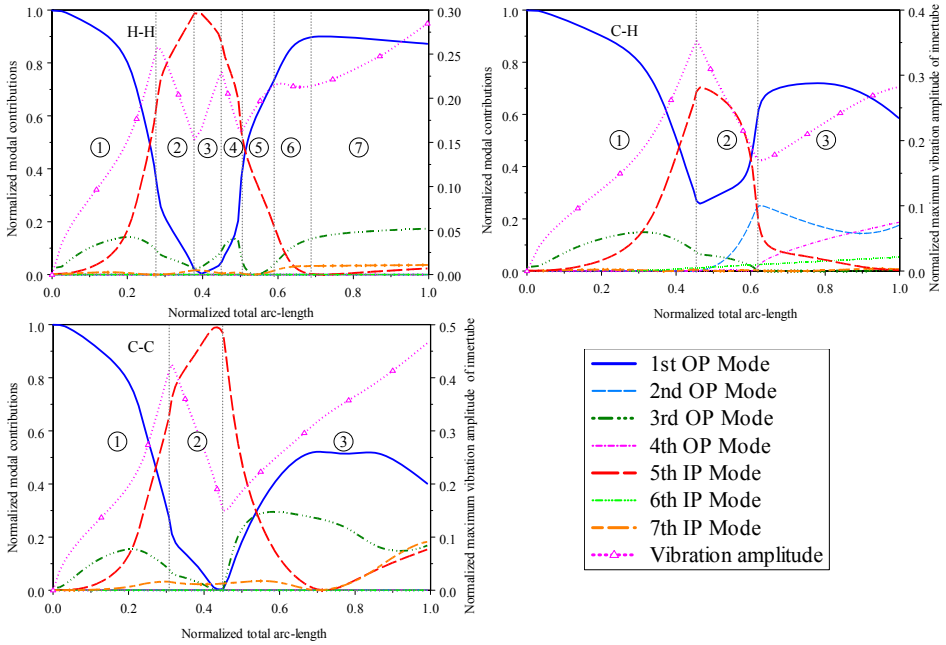

Figure 6-11 Variation of Normalized Modal Contributions vs. Total Arc-length a) H-H b) C-H c) C-C

Figure 6-12 shows a bar plot of normalized modal contributions of the system for H-H DWCNT at the end of each region, shown in Figure 6-10, in addition to the corresponding nonlinear mode shapes of the inner and outer tubes. It can be seen that at the end of the first region CNTs vibrate in a nonlinear mode shape completely different from the first linear out-of-phase mode shape where the contribution of the fifth in-phase mode passes the contribution of the first out-of-phase mode. It can be seen that at the end of the 2nd region, the contribution of the fifth in-phase mode reaches to its maximum, which starts to decrease and become zero at the end of the sixth region. It is worth noting that for the case of H-H DWCNT only the odd mode shapes are excited which verifies the results given in [121].

In Figure 6-13, normalized modal contribution of C-H DWCNT is given around the middle of each region in addition to the corresponding nonlinear mode shapes of the inner and outer tubes. It is observed that for the case of C-H DWCNT, in addition to odd modes, even modes are also excited. Moreover, it can be seen that asymmetric boundaries resulted in asymmetric mode shapes. Figure 6-14 shows a similar plot for C-C DWCNT. It is observed that, for the present case, only the odd modes are excited. Therefore, it can be concluded that for symmetric boundary conditions only the odd

mode shapes are present in the nonlinear modes whereas for asymmetrical end conditions in addition to the odd modes, even modes as well contribute to the nonlinear mode shapes.

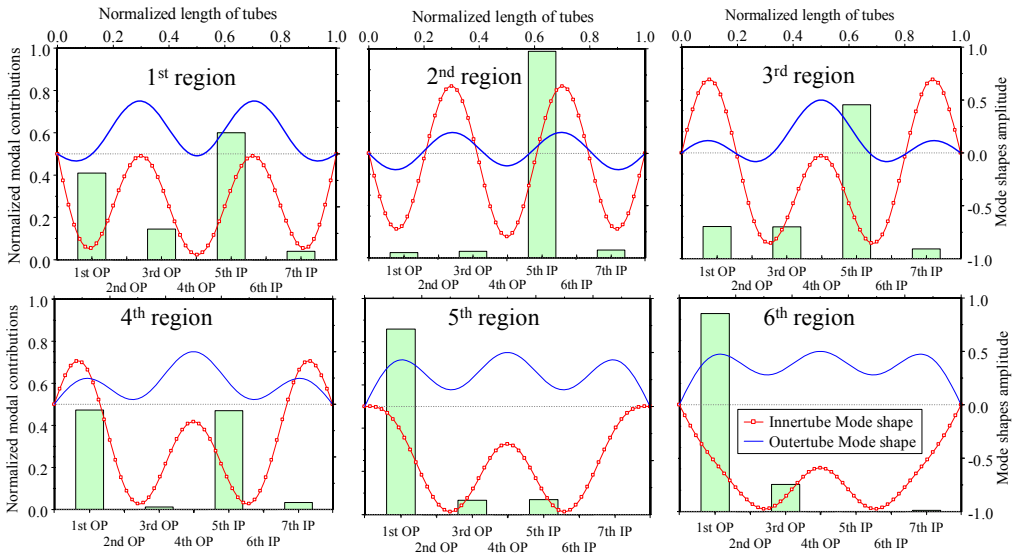

Figure 6-12 Normalized Modal Contribution of Innertube and the Mode Shapes of Inner and Outer Tubes at the End of each Region for H-H DWCNT

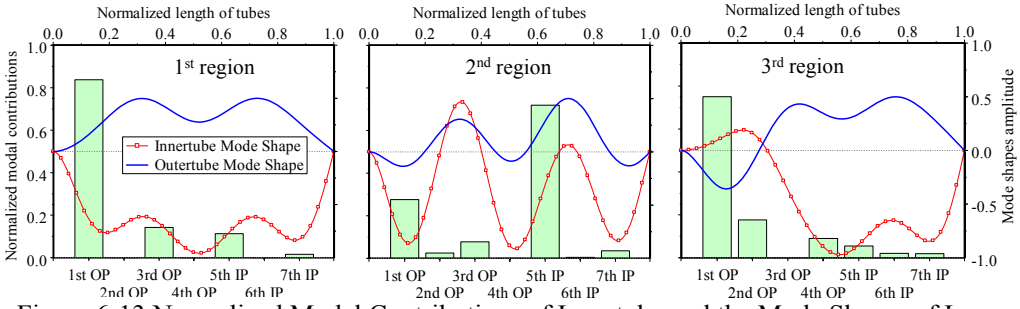

Figure 6-13 Normalized Modal Contributions of Innertube and the Mode Shapes of Inner and Outer Tubes around the Middle of each Region for C-H DWCNT

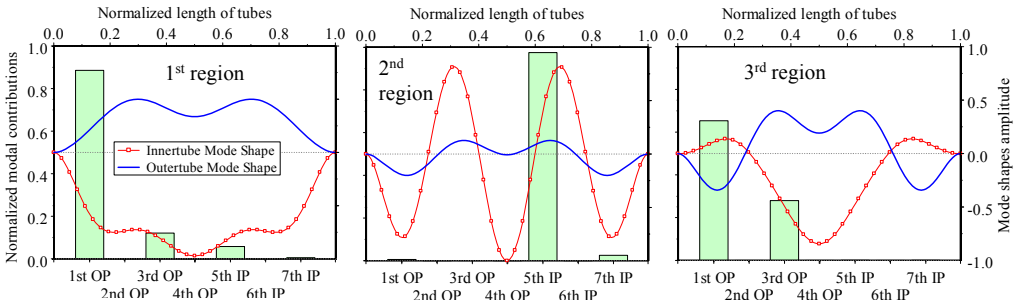

Figure 6-14 Normalized Modal Contributions of Innertube and the Mode Shapes of Inner and Outer Tubes around the Middle of each Region for C-C DWCNT

Figure 6-15 represents a comparison between the results of current study and available results in the literature. It is observed that the solutions obtained in the present study by utilizing DQM and the results given in literature by using multiple trail function and Galerkin method [121] are in good agreement. For the case of H-H DWCNT, the results at selected points obtained by the present study (DQM) and by Galerkin method [121] are tabulated in Table 6-4. It observed that both results are in good agreement and slight differences between the values are due to the nature of the two different methods compared.

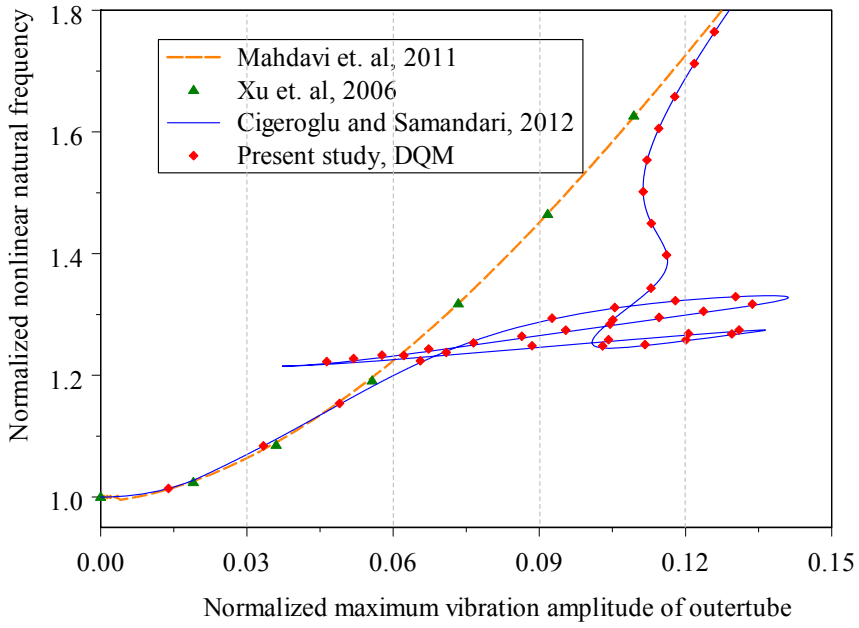

Figure 6-15 Comparison with Available Data in the Literature for a H-H DWCNT

Table 6-4 DQM and Galerkin Results at Selected Points for a H-H DWCNT

Normalized maximum vibration amplitude	0.03	0.06	0.09	0.12
Normalized nonlinear natural frequency (Present study, DQM)	1.0700	1.2022, 1.2314, 1.2355	1.2496, 1.2682, 1.2891	1.2583, 1.2682, 1.3011, 1.3242, 1.6890
Normalized nonlinear natural frequency (Galerkin) [121]	1.0700	1.1995, 1.2258, 1.2317	1.2460, 1.2652, 1.2875	1.2568, 1.2659, 1.2989, 1.3235, 1.6885

6.7. Effect of Medium stiffness

Table 6-5 shows the effect of medium stiffness on fundamental linear natural frequency of a DWCNT with hinged-hinged, clamped-hinged, and clamped-clamped end conditions. It can be seen that linear natural frequency of DWCNT increases slightly as medium stiffness increases for all type of boundary conditions. A similar pattern is detected in [34]; however, it can be seen that as medium stiffness increases beyond a certain limit (solid lines), in-phase natural frequencies increase significantly.

Table 6-5 Effect of Medium Stiffness on Fundamental Linear Natural Frequency of DWCNT

k	-	H-H (THz)	C-H (THz)	C-C (THz)
0	In-phase	0.4673	0.7296	1.0578
	Out-of-phase	7.8852	7.8990	7.9249
10^8	In-phase	0.4875	0.7427	1.0668
	Out-of-phase	7.8858	7.8996	7.9256
10^9	In-phase	0.6415	0.8514	1.1447
	Out-of-phase	7.8914	7.9052	7.9312
10^{10}	In-phase	1.4566	1.5586	1.7332
	Out-of-phase	7.9486	7.96272	7.9892

Figure 6-16 presents the effect of the medium stiffness, k, on the variation of normalized nonlinear natural frequency versus maximum vibration amplitude for H-H, C-H, and C-C DWCNT. It is observed that with an increase in the medium stiffness, k, the normalized nonlinear frequency tends to approach to the linear one for all end conditions. It is seen that for H-H end condition with medium stiffness less than 10^8 N/m^2, variation of normalized nonlinear natural frequency changes slightly; whereas, for medium stiffness larger than 10^8 N/m^2 significant changes in the normalized nonlinear natural frequency are observed. A similar behavior is observed formerly for variation of linear natural frequencies. This shows that the effect of geometric nonlinearity becomes negligible in the presence of sufficiently large medium stiffness. Moreover, it is observed that as boundary conditions get stiffer in addition to decreasing in variation of nonlinear natural frequency, the threshold value of medium stiffness increases. The results are tabulated in Table 6-6. A similar behavior is detected for the case of out-of-phase vibration modes. The results for the

case of H-H DWCNT vibrating in the first out of phase vibration mode can be found in chapter 4.

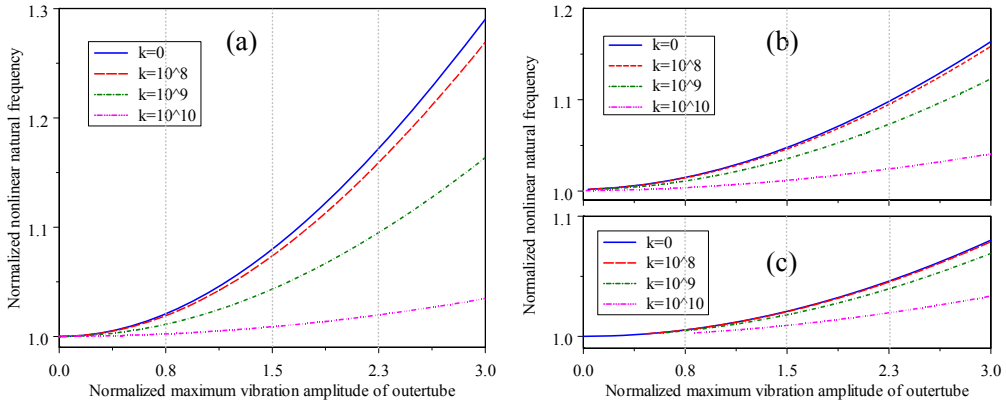

Figure 6-16 Effect of Medium Stiffness on the Nonlinear Fundamental Natural Frequency of DWCNT vibrating in the First in-phase Vibration Mode a) Hinged-Hinged b) Clamped-Hinged c) Clamped-Clamped ($e = 0$)

Table 6-6 Normalized Nonlinear Natural Frequencies at Selected Normalized Vibration Amplitudes of Outertube

Normalized Vibration Amplitude of Outertube	Normalized Nonlinear Natural Frequency											
	H-H				C-H				C-C			
	Medium Stiffness				Medium Stiffness				Medium Stiffness			
	0	10^8	10^9	10^{10}	0	10^8	10^9	10^{10}	0	10^8	10^9	10^{10}
0.8	1.0234	1.0216	1.0126	1.0025	1.0162	1.0156	1.0119	1.0039	1.0060	1.0059	1.0052	1.0025
1.5	1.0799	1.0736	1.0434	1.0089	1.0473	1.0457	1.0351	1.0115	1.0208	1.0204	1.0178	1.0091
2.3	1.1793	1.1658	1.0992	1.0206	1.1019	1.0985	1.0759	1.0251	1.0480	1.0472	1.0412	1.0203

6.8. Concluding remarks

In this chapter, nonlinear free vibration of a curved DWCNT embedded in elastic medium is studied by using differential quadrature method (DQM) where in addition to geometric nonlinearity, interlayer vdW force nonlinearity is also included. The effect of nonlinearities, end conditions, initial curvature, stiffness of the surrounding elastic medium, and vibrational modes on the nonlinear free vibration of DWCNTs is studied in detail.

Results show that nonlinear natural frequency increases as vibration amplitude increases in the presence of only geometric nonlinearity for all the type of end conditions. Moreover, it is observed that multiple solution at same vibration

amplitude can exist due to interaction of nonlinear in-phase and out-of-phase vibration modes.

Furthermore, application of DQM made it possible for the first time to study the effect of different boundary conditions in the presence of vdW force nonlinearity on the variation of the nonlinear natural frequencies of DWCNTs. Results show that due to the vdW force nonlinearity, nonlinear natural frequency changes considerably where several turning points are as well observed. It is been observed that the number of turning points is different for each boundary condition considered. Moreover, it is observed that for symmetric boundary conditions only the odd mode shapes are present in the nonlinear modes whereas for asymmetrical end conditions in addition to the odd modes, even modes as well contribute to the nonlinear mode shapes.

CHAPTER 7

NONLINEAR FREE VIBRATION OF NONUNIFORM ROTATING CARBON NANOTUBES BASES ON ERINGEN THEORY

The main objective of this chapter is to include and study the size effects in nonlinear equations of motion of CNTs. Size effects are emerged from the non-contact interactions of the atoms and molecules due to atomic potential forces. Classic continuum models fails to capture size effects because of their atomic origins. Hence, in this chapter based of Eringen nonlocal theory, nonlinear nonlocal equations of motion of CNTs are studied. Results show that boundary condition equations for nonlocal cantilever beam is totally different than classic beams where it includes nonlocal and nonlinear terms. It is worth mentioning that nonlinear nonlocal BCs are studied for the first time in this chapter.

7.1. Introduction

In recent years, there has been great interest in the application of nonlocal continuum mechanics for modeling and analysis of rotating nanobeams and nanotubes. It is worth noting that rotating structure will be inevitable part of the power transmission system of any future nano machines and nano robots. Pradhan and Murmu [208] used nonlocal Euler Bernoulli beam model to study the linear free vibration characteristics of a uniform rotating nano-cantilever. However, they failed to consider the nonlocal boundary conditions related to the free end of the nanobeams. Later, Murmu and Adhikari [209], investigated an initially pre-stressed single-walled carbon nanotube via nonlocal elasticity to analyze the effect of the initial preload. They show that vibration characteristic of CNTs is influenced by the existence of a preload. Narendar and Gopalakrishnan [210] studied the wave dispersion behavior of a rotating nanotube using the nonlocal Euler Bernoulli beam theory. Later, Narendar [211] used nonlocal

Timoshenko beam theory to investigate free vibration of uniform rotating nanotubes where shear deformation and rotary inertia are accounted. Aranda-Ruiz et al [212] studied natural frequencies of the transverse bending vibrations of a nonuniform rotating nano-cantilever. They have assumed that the nanobeam cross-section changes linearly.

It should be noted that in all of these studies CNTs have been assumed to behave linear; however, recent theoretical and experimental studies show that the deformation of CNTs is nonlinear in nature. Fu et al. [113] show that as vibration amplitude increases, the nonlinear natural frequency increases significantly for nonrotating simply supported single and double walled CNTs. In recent years, nonlinear vibration of CNTs have been studied by several researchers [51, 121, 184]. However, these studies are only limited to the case of nonrotating tubes. Therefore, it is important to study the behavior of rotating CNTs where effect of nonlinearities is considered.

Moreover, reviewing literature it can be seen that it is common assumption to use boundary condition equations of classic beam in studying the nonlocal beams. However, it should be noted that, in the case of cantilever beam, the system boundary condition equations are different than boundary conditions of a classic beam and they include nonlinear and nonlocal terms. Even though the effect of nonlocality on BCs have been reported for the first time by Lu et al. [213] and Wang et al [85] for nonrotating SWCNT, they have not been correctly incorporated in studies regarding the rotating nano structures. Furthermore, to the best of authors' knowledge, this is the first study that investigate the effect of nonlinear terms in boundaries on the variation of nonlinear natural frequencies.

7.2. Nonlocal constitutive relations

According to the nonlocal elastic stress theory developed by Eringen [41], stress, $\sigma_{ij}(\mathbf{x})$, at a reference point in a body, $\mathbf{x}$, is dependent not only on the strain at reference point but also on the strain at all other points, $\mathbf{x}^*$, of the body as follows

$$\sigma_{ij}(\mathbf{x}) = \int_V \alpha\left(\left|\mathbf{x}^* - \mathbf{x}\right|, \tau\right) t_{ij}(\mathbf{x}^*)\, dV(\mathbf{x}^*)\,, \tag{7.1}$$

where $t_{ij}(\mathbf{x}^*)$ are the components of the classic local stress tensor at point $\mathbf{x}^*$. The classic stress tensor for a Hookean material is

$$t_{ij}(\mathbf{x}^*) = C_{ijkl}\ \varepsilon_{ij}(\mathbf{x}^*)\,. \tag{7.2}$$

Equation (7.1) states that the nonlocal stress is given by spatial integration of weighted averages of local stress where spatial weight is represented by the specific nonlocal modulus $\alpha\left(\left|\mathbf{x}^* - \mathbf{x}\right|, \tau\right)$. τ is a constant given by

$$\tau = \frac{e_0 a}{l}\ , \tag{7.3}$$

where it represents the ratio between a characteristic internal length, a, (e.g. the lattice spacing, distance between the C--C bonds) and a characteristic external length, l, (e.g. wavelength and length of tube). Here, e_0 is a constant for calibrating the model and experimental results.

According to Eringen, Eq. (7.1) can be written in differential form as

$$\left(1 - \left(e_0 a\right)^2 \nabla^2\right)\sigma_{kl} = t_{kl}\,, \tag{7.4}$$

where ∇^2 is the Laplacian operator. For the case of one dimensional structures such as Euler beam, the Laplacian operator is reduced to one dimensional form and since the strains in the transverse directions are negligible, Eq. (7.4) can be expressed as

$$\sigma_{xx} - \left(e_0 a\right)^2 \frac{\partial^2 \sigma}{\partial x^2} = E\varepsilon_{xx}\ , \tag{7.5}$$

where σ_{xx} and ε_{xx} are nonlocal axial stress and strain accordingly.

7.3. Modeling

Consider a CNT of length L, cross-sectional area $A(x)$, area moment of inertia $I(x)$, Young's modulus E, and density ρ attached to a rotating molecular hub at $x=0$. The tube is clamped to the hub located at distance r from the axes of rotation. The structure rotates at a constant angular velocity Ω as shown in Figure 7-1-a.

Based on the Euler–Bernoulli beam theory and a nonlinear strain–displacement relationship of Von Karman type [153], the relation between displacement field and strain can be written as follows

$$\varepsilon(x,z)=\frac{\partial u(x,t)}{\partial x}+\frac{1}{2}\left(\frac{\partial w(x,t)}{\partial x}\right)^2-z\frac{\partial^2 w(x,t)}{\partial x^2}, \tag{7.6}$$

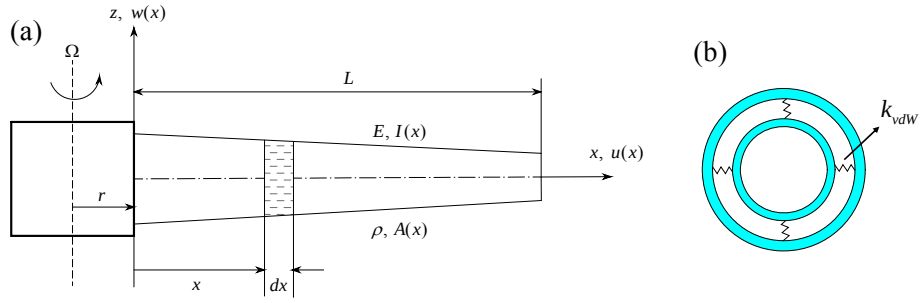

Figure 7-1 Schematic view of a rotating nanotube.

where x is the axial coordinate, t is the temporal variable, $u(x,t)$ and $w(x,t)$ denote the total axial and transverse displacements of the tube along the x coordinate directions, and $\varepsilon(x,z)$ is the corresponding total strain.

The potential energy V and the kinetic energy T stored in the tube can be written as follows

$$V=\frac{1}{2}\int_0^L\int_A \sigma\cdot\varepsilon(x,z)\,dA\,dx=\frac{1}{2}\int_0^L\int_A \sigma\cdot\left(\frac{\partial u}{\partial x}+\frac{1}{2}\left(\frac{\partial w}{\partial x}\right)-z\frac{\partial^2 w}{\partial x^2}\right)dA\,dx, \tag{7.7}$$

$$T=\frac{1}{2}\int_0^L\int_A \rho\cdot\left(\frac{\partial w}{\partial t}\right)^2 dA\,dx=\frac{1}{2}\int_0^L \rho\cdot A(x)\cdot\left(\frac{\partial w}{\partial t}\right)^2 dx, \tag{7.8}$$

where σ stands for stress on the section surface, and $A(x)$ is cross section area at distance x. It should be noted that, in writing the kinetic energy, rotary and axial kinetic energy of the beam are neglected. For the beam, the resultant normal force, and the bending moment are defined as:

$$N_x = \int_A \sigma \, dA \ , \tag{7.9}$$

$$M_x = \int_A z \cdot \sigma \, dA , \tag{7.10}$$

respectively. Therefore, Eq. (7.7) can be written as:

$$V = \frac{1}{2}\int_0^L \left\{ N_x \frac{\partial u}{\partial x} + N_x \frac{1}{2}\left(\frac{\partial w}{\partial x} \right)^2 - M_x \frac{\partial^2 w}{\partial x^2} \right\} dx \, . \tag{7.11}$$

The work done by the external forces in axial direction (such as centrifugal force) and transverse direction (such as medium force) can be calculated by

$$W_e = W_{e,m} + W_{e,c} = \int_0^L f(x,t) \cdot w dx + \int_0^L T(x) \cdot u \, dx , \tag{7.12}$$

$f(x,t)$ and $T(x)$ represent the medium stiffness force and average centrifugal force on the cross section at distance x, respectively. Here, $T(x)$ is equal to

$$T(x) = -\frac{\partial}{\partial x}\int_x^L \rho \cdot A(x) \cdot \Omega^2 \cdot \left(r + \zeta \right) d\xi , \tag{7.13}$$

where r is the molecular hub radius. The minus sign indicates that the force decreases as x increases. The equations of motion of the nonlocal rotating tube can be derived by using Hamilton's principle as

$$\delta \int_{t_1}^{t_2} \left(T - V + W_e \right) dt = 0 , \tag{7.14}$$

where δ stands for variation. Substituting Eqs. (7.8), (7.11), and (7.12) into Eq. (7.14) , applying integrating by parts and setting the coefficients of δu, δw equal to zero lead to the following equations of motion

$$T(x)+\frac{\partial N_x}{\partial x}=0\,, \tag{7.15}$$

$$-\rho A(x)\frac{\partial^2 w}{\partial t^2}+\frac{\partial}{\partial x}\left[N_x\frac{\partial w}{\partial x}\right]+\frac{\partial^2 M}{\partial x^2}+f(x,t)=0\,, \tag{7.16}$$

and the general form of boundary conditions as:

$$N_x\,\delta u\Big|_0^L=0\,, \tag{7.17}$$

$$N_x\frac{\partial w}{\partial x}\delta w\Big|_o^L+\frac{\partial M_x}{\partial x}\delta w\Big|_0^L=0\,, \tag{7.18}$$

$$-M_x\delta\frac{\partial w}{\partial x}\Big|_0^L=0\,. \tag{7.19}$$

Note that the expressions of the normal resultant force and bending moment in the nonlocal beam theory are different from those in the classical Euler Bernoulli beam theory due to the nonlocal constitutive relation. From Eqs. (7.5), (7.6), (7.12), and (7.13), the normal resultant force and bending moment can be expressed as

$$N_x-\left(e_0a\right)^2\frac{\partial^2 N_x}{\partial x^2}=EA(x)\cdot\left[\frac{\partial u}{\partial x}+\frac{1}{2}\left(\frac{\partial w}{\partial x}\right)^2\right], \tag{7.20}$$

$$M_x-\left(e_0a\right)^2\frac{\partial^2 M_x}{\partial x^2}=-EI(x)\frac{\partial^2 w}{\partial x^2}\,. \tag{7.21}$$

It is worth noting that, due to Eqs. (7.20) and (7.21), Eqs. (7.18) and (7.19) are nonlinear boundary conditions. By substituting Eqs. (7.15) and (7.16) into Eqs. (7.20) and (7.21), the expressions for nonlocal normal resultant force and bending moment can be obtained as

$$N_x=EA(x)\cdot\left[\frac{\partial u}{\partial x}+\frac{1}{2}\left(\frac{\partial w}{\partial x}\right)^2\right]-\left(e_0a\right)^2\frac{\partial T}{\partial x}\,, \tag{7.22}$$

$$M_x = -EI(x)\frac{\partial^2 w}{\partial x^2} - \left(e_0 a\right)^2 \left[-\rho A(x)\frac{\partial^2 w}{\partial t^2} + \frac{\partial}{\partial x}\left[N_x \frac{\partial w}{\partial x} \right] + f(x,t) \right]. \tag{7.23}$$

Even though N_x depends on axial elongation $u(x)$, it can be assumed that the tube total axial elongation is majorly due to the rotation. Therefore, by integrating Eq. (7.15) over the tube length and substituting Eq. (7.22), one can get the following equation for the normal force

$$N_x = \frac{1}{2L}\int_0^L EA(x)\cdot\left(\frac{\partial w}{\partial x}\right)^2 dx + \int_x^L \rho A(x)\Omega^2\left(r+\xi\right)d\xi\,. \tag{7.24}$$

Inserting Eq. (7.23) into Eq.(7.16), the nonlinear equations of motion for the nonlocal rotating tube can be obtained as

$$\begin{aligned} &\frac{\partial^2}{\partial x^2}\left[EI(x)\frac{\partial^2 w}{\partial x^2} \right] + \rho A(x)\frac{\partial^2 w}{\partial t^2} - \frac{\partial}{\partial x}\left[N_x \frac{\partial w}{\partial x} \right] - f(x,t) \\ &-\left(e_0 a\right)^2 \frac{\partial^2}{\partial x^2}\left(\rho A(x)\frac{\partial^2 w}{\partial t^2} - \frac{\partial}{\partial x}\left[N_x \frac{\partial w}{\partial x} \right] - f(x,t) \right) = 0 \end{aligned}, \tag{7.25}$$

where N_x is given by Eq. (7.24).

In the case of double walled CNT (DWCNT), two concentric tubes will interact with each other through the medium force due to the interlayer molecular van der Waals (vdW) pressure [80, 182]. This pressure acting on the two adjacent tubes depends on the difference between the transverse deflections of the inner and outer tubes and can be considered as an external force (Figure 7-1-b). The vdW force per unit area for two originally-concentric tubes is given in [168, 169] as

$$f\left(x,t\right) = p_1\left(w_o - w_i\right) + p_2\left(w_o - w_i\right)^3, \tag{7.26}$$

where $p_1 = 2r_i \left.\frac{\partial^2 U}{\partial \delta^2}\right|_{\delta=\delta_0}$, $p_2 = 2r_i \frac{1}{6}\left.\frac{\partial^4 U}{\partial \delta^4}\right|_{\delta=\delta_0}$. r_i is innertube radius, and U is potential energy expressed in terms of the interlayer spacing δ as follows [184, 197]

$$U(\delta) = K_{IL}\left[\left(\frac{\delta_0}{\delta}\right)^4 - 0.4\left(\frac{\delta_0}{\delta}\right)^{10}\right], \tag{7.27}$$

where $K_{IL} = 0.4089101874\ \text{J/m}^2$, and $\delta_0 = 0.34\ \text{nm}$ is the equilibrium interfacial spacing. It is worth noting that p_1 and p_2 are functions of the equilibrium interlayer spacing and innertube radius. However, since in the present study the equilibrium interlayer spacing is considered to be constant, they will only be functions of innertube radius and consequently functions of x.

The vdW force can be considered as external force acting in transverse direction; hence, the virtual work done by the vdW force is

$$\delta W_{e,m} = \delta W_{e,vdW} = \int_0^L \left[p_1(x)\cdot(w_o - w_i) + p_2(x)\cdot(w_o - w_i)^3 \right]\cdot(\delta w_o - \delta w_i)\,dx. \tag{7.28}$$

Adding the virtual work done by vdW force to Eq.(7.12), the equation of motion for a DWCNT can be derived by applying Hamilton's principle to the lagrangian of inner and outer tubes assuming that the tubes are vibrating in the same plane.

The coplanar transverse motion of an embedded DWCNT is described by the following coupled nonlinear partial differential equations.

$$\frac{\partial^2}{\partial x^2}\left[EI_o(x)\frac{\partial^2 w_o}{\partial x^2}\right] + \rho A_o(x)\frac{\partial^2 w_o}{\partial t^2} - \frac{\partial}{\partial x}\left[N_{x,o}\frac{\partial w_o}{\partial x}\right] + p_1(x)\cdot(w_o - w_i) + p_2(x)\cdot(w_o - w_i)^3$$
$$-(e_0 a)^2\frac{\partial^2}{\partial x^2}\left(\rho A_o(x)\frac{\partial^2 w_o}{\partial t^2} - \frac{\partial}{\partial x}\left[N_{x,o}\frac{\partial w_o}{\partial x}\right] + p_1(x)\cdot(w_o - w_i) + p_2(x)\cdot(w_o - w_i)^3\right) = 0$$

, (7.29)

$$\frac{\partial^2}{\partial x^2}\left[EI_i(x)\frac{\partial^2 w_i}{\partial x^2}\right] + \rho A_i(x)\frac{\partial^2 w_i}{\partial t^2} - \frac{\partial}{\partial x}\left[N_{x,\mathrm{i}}\frac{\partial w_i}{\partial x}\right] - p_1(x)\cdot(w_o - w_i) + p_2(x)\cdot(w_o - w_i)^3$$
$$-(e_0 a)^2\frac{\partial^2}{\partial x^2}\left(\rho A_i(x)\frac{\partial^2 w_i}{\partial t^2} - \frac{\partial}{\partial x}\left[N_{x,\mathrm{i}}\frac{\partial w_i}{\partial x}\right] - p_1(x)\cdot(w_o - w_i) + p_2(x)\cdot(w_o - w_i)^3\right) = 0$$

, (7.30)

where

$$N_{x,r} = \frac{1}{2L}\int_0^L EA_r(x)\cdot\left(\frac{\partial w_r}{\partial x}\right)^2 dx + \int_x^L \rho A_r(x)\Omega^2\left(r_h+\xi\right)d\xi\,, \tag{7.31}$$

and subscript r is equal to i and o indicating inner and outer tube, respectively.

7.4. Generalized differential quadrature method

Generalized differential quadrature method (GDQM) approximates the derivatives of a function with respect to a spatial variable at a given discrete point by a weighted linear summation of function values at all the discrete points in the computational domain [205]. For example, the n^{th} derivative of a function $W_r(x)$ at the m^{th} point, x_m, can be estimated by

$$W_r^{(n)}(x_m) = \sum_{s=1}^{N} c_{m,s}^{(n)} W_r(x_s), \qquad m = 1,2,...,N\,, \tag{7.32}$$

where $W_r^{(n)}(x_m)$ is the n^{th} order derivative of $W_r(x)$ at point x_m, and N is the number of grid points utilized in the discretization of the partial derivatives. In Eq. (7.32), $r = i,o$ refers to inner tube or outer tube, and $c_{m,s}^{(n)}(s = 1,...,N)$ are the weighting coefficients for the n^{th} derivative estimation of the m^{th} point, which can be pre-determined (given in previous chapter) [122]. Defining ${}_sW_r = W_r(x_s)$, Eq. (7.32) can be shorten as follows

$$\begin{aligned} {}_mW_r^{(n)} &= \sum_{s=1}^{N} c_{m,s}^{(n)}\,{}_sW_r = \left\{c_{s,1}^{(m)} \quad c_{s,2}^{(m)} \quad \cdots \quad c_{s,N-1}^{(m)} \quad c_{s,N}^{(m)}\right\}\cdot\left\{{}_1W_r \quad {}_2W_r \quad \cdots \quad {}_NW_r\right\}^T \\ &= \mathbf{c_m^{(n)T}}\cdot\mathbf{x}_r \end{aligned}\,. \tag{7.33}$$

where $\mathbf{c_m^{(n)}}$ represents the m^{th} column vector of matrix $\mathbf{C^{(n)}}$ formed by $c_{m,s}^{(n)}(s = 1,...,N)$. Superscript T stands for the matrix transport. It is worth noting that the higher order of the weighting coefficients can be calculated by using matrix multiplication as follows

$$\mathbf{C^{(n)} = C^{(n-1)}\,C}\,, \tag{7.34}$$

where $\mathbf{C}^{(n)}$ is the matrix of weighting coefficients at all points. Since the positions of the sampling points play a significant role in the accuracy of DQM [214], Gauss–Lobatto quadrature points are used in the present study which contains points at boundaries.

7.5. Utilizing DQM

Assuming a separable solution as $w_r(x,t) = W_r(x) \cdot T(t)$, the partial differential equation of motion given by Eqs. (7.29) and (7.30) can be expressed as

$$\begin{aligned}&\frac{\partial^2}{\partial x^2}\left[EI_o\frac{\partial^2 W_o}{\partial x^2}T\right]+\rho A_o\frac{\partial^2 T}{\partial t^2}W_o-\frac{\partial}{\partial x}\left[N_{x,o}\frac{\partial W_o}{\partial x}T\right]+p_1\cdot(W_o-W_i)T+p_2\cdot(W_o-W_i)^3T^3\\&-(e_0a)^2\frac{\partial^2}{\partial x^2}\left(\rho A_o\frac{\partial^2 T}{\partial t^2}W_o-\frac{\partial}{\partial x}\left[N_{x,o}\frac{\partial W_o}{\partial x}T\right]+p_1\cdot(W_o-W_i)T+p_2\cdot(W_o-W_i)^3T^3\right)=0\end{aligned}$$

, (7.35)

$$\begin{aligned}&\frac{\partial^2}{\partial x^2}\left[EI_i\frac{\partial^2 W_i}{\partial x^2}T\right]+\rho A_i\frac{\partial^2 T}{\partial t^2}W_i-\frac{\partial}{\partial x}\left[N_{x,\mathrm{i}}\frac{\partial W_i}{\partial x}T\right]-p_1\cdot(W_o-W_i)T-p_2\cdot(W_o-W_i)^3T^3\\&-(e_0a)^2\frac{\partial^2}{\partial x^2}\left(\rho A_i\frac{\partial^2 T}{\partial t^2}W_i-\frac{\partial}{\partial x}\left[N_{x,\mathrm{i}}\frac{\partial W_i}{\partial x}T\right]-p_1\cdot(W_o-W_i)T-p_2\cdot(W_o-W_i)^3T^3\right)=0\end{aligned}$$

, (7.36)

where

$$N_{x,\mathrm{r}} = G_{W_r}T^2 + F_{x,r} = \left(\frac{1}{2L}\int_0^L EA_r(x)\cdot\left(\frac{\partial W_r}{\partial x}\right)^2 dx\right)T^2 + \int_x^L \rho A_r(x)\Omega^2(r_h+\xi)\,d\xi\,. \tag{7.37}$$

Assuming a single harmonic solution in time, i.e. utilizing harmonic balance method (HBM) with a single harmonic, and applying the GDQM (Eq. (6.8)), the discrete nonlinear algebraic equation of motion at the m^{th} given point become

$$\left[\begin{array}{c|c} {}_m\mathbf{k}_o + {}_m\mathbf{k}_o^{NLg} + {}_m\mathbf{k}_1^{NLv} & {}_m\mathbf{k}_{oi} + {}_m\mathbf{k}_2^{NLv} \\ \hline {}_m\mathbf{k}_{oi} - {}_m\mathbf{k}_2^{NLv} & {}_m\mathbf{k}_i + {}_m\mathbf{k}_i^{NLg} - {}_m\mathbf{k}_1^{NLv} \end{array}\right]_{2\times 2N}\left\{\begin{array}{c}\mathbf{x_o}\\ \mathbf{x_i}\end{array}\right\} = \omega^2\left[\begin{array}{c|c} {}_m\mathbf{M}_o & 0 \\ \hline 0 & {}_m\mathbf{M}_i \end{array}\right]\left\{\begin{array}{c}\mathbf{x_o}\\ \mathbf{x_i}\end{array}\right\}, \tag{7.38}$$

where

$$
\begin{aligned}
{}_m\mathbf{k}_r = {} & \left.\frac{\partial^2 EI_r}{\partial x^2}\right|_{x_m} \mathbf{c}_\mathbf{m}^{(2)T} + 2\left.\frac{\partial EI_r}{\partial x}\right|_{x_m} \mathbf{c}_\mathbf{m}^{(3)T} + EI_r(x_m)\,\mathbf{c}_\mathbf{m}^{(4)T} + p_1\,\mathbf{a}_\mathbf{m}^{\mathbf{T}} - F_{x_m,r}\,\mathbf{c}_\mathbf{m}^{(2)T} - \frac{\partial F_{x_m,r}}{\partial x}\mathbf{c}_\mathbf{m}^{(1)T} \\
& -\left(e_0 a\right)^2 \left[\left.\frac{\partial^2 p_1}{\partial x^2}\right|_{x_m} \mathbf{a}_\mathbf{m}^{\mathbf{T}} + 2\left.\frac{\partial p_1}{\partial x}\right|_{x_m} \mathbf{c}_\mathbf{m}^{(1)T} + p_1\,\mathbf{c}_\mathbf{m}^{(2)T} - \frac{\partial^3 F_{x_m,r}}{\partial x^3}\mathbf{c}_\mathbf{m}^{(1)T} - 3\frac{\partial^2 F_{x_m,r}}{\partial x^2}\mathbf{c}_\mathbf{m}^{(2)T} \right. \\
& \left. -3\frac{\partial F_{x_m,r}}{\partial x}\mathbf{c}_\mathbf{m}^{(3)T} - F_{x_m,r}\,\mathbf{c}_\mathbf{m}^{(4)T} \right]
\end{aligned}, \tag{7.39}
$$

$$
{}_m\mathbf{k}_{oi} = -p_1\,\mathbf{a}_\mathbf{m}^{\mathbf{T}} + \left(e_0 a\right)^2 \left(\left.\frac{\partial^2 p_1}{\partial x^2}\right|_{x_m} \mathbf{a}_\mathbf{m}^{\mathbf{T}} + 2\left.\frac{\partial p_1}{\partial x}\right|_{x_m} \mathbf{c}_\mathbf{m}^{(1)T} + p_1\,\mathbf{c}_\mathbf{m}^{(2)T} \right), \tag{7.40}
$$

$$
{}_m\mathbf{k}_r^{NLg} = -\frac{3}{4} G_{W_r}\,\mathbf{c}_\mathbf{m}^{(2)T} + \frac{3}{4}\left(e_0 a\right)^2 \left(G_{W_r}\,\mathbf{c}_\mathbf{m}^{(4)T} \right), \tag{7.41}
$$

$$
\begin{aligned}
{}_m\mathbf{k}_1^{NLv} = {} & \frac{3}{4}\left[\left(p_2 - \left(e_0 a\right)^2 \left.\frac{\partial^2 p_2}{\partial x^2}\right|_{x_m} \right) \cdot \left(\mathbf{a}_\mathbf{m}^T \cdot \left(\mathbf{x_o} \cdot \mathbf{x_o} + 3\mathbf{x_i} \cdot \mathbf{x_i} \right) \right) - 6\left(e_0 a\right)^2 p_2 \left(\mathbf{c}_\mathbf{m}^{(1)T} \cdot \left(\mathbf{x_o} - \mathbf{x_i} \right) \right)^2 \right. \\
& -6\left(e_0 a\right)^2 \left.\frac{\partial p_2}{\partial x}\right|_{x_m} \left(\mathbf{c}_\mathbf{m}^{(1)T} \cdot \left(\mathbf{x_o} - \mathbf{x_i} \right) \right) \left(\mathbf{a}_\mathbf{m}^T \cdot \left(\mathbf{x_o} - \mathbf{x_i} \right) \right) \\
& \left. -3\left(e_0 a\right)^2 p_2 \left(\mathbf{c}_\mathbf{m}^{(2)T} \cdot \left(\mathbf{x_o} - \mathbf{x_i} \right) \right) \left(\mathbf{a}_\mathbf{m}^T \cdot \left(\mathbf{x_o} - \mathbf{x_i} \right) \right) \right] \mathbf{a}_\mathbf{m}^T
\end{aligned}, \tag{7.42}
$$

$$
\begin{aligned}
{}_m\mathbf{k}_2^{NLv} = -\frac{3}{4} & \left[\left(p_2 - \left(e_0 a\right)^2 \left.\frac{\partial^2 p_2}{\partial x^2}\right|_{x_m} \right) \cdot \left(\mathbf{a}_\mathbf{m}^T \cdot \left(\mathbf{x_i} \cdot \mathbf{x_i} + 3\,\mathbf{x_o} \cdot \mathbf{x_o} \right) \right) - 6\left(e_0 a\right)^2 p_2 \left(\mathbf{c}_\mathbf{m}^{(1)T} \left(\mathbf{x_o} - \mathbf{x_i} \right) \right)^2 \right. \\
& -6\left(e_0 a\right)^2 \left.\frac{\partial p_2}{\partial x}\right|_{x_m} \left(\mathbf{c}_\mathbf{m}^{(1)T} \left(\mathbf{x_o} - \mathbf{x_i} \right) \right) \left(\mathbf{a}_\mathbf{m}^T \cdot \left(\mathbf{x_o^T} - \mathbf{x_i^T} \right) \right) \\
& \left. -3\left(e_0 a\right)^2 p_2 \left(\mathbf{c}_\mathbf{m}^{(2)T} \left(\mathbf{x_o} - \mathbf{x_i} \right) \right) \left(\mathbf{a}_\mathbf{m}^T \cdot \left(\mathbf{x_o} - \mathbf{x_i} \right) \right) \right] \mathbf{a}_\mathbf{m}^T
\end{aligned}, \tag{7.43}
$$

$$
{}_m\mathbf{M}_r = \left[\rho A_r\big|_{x_m} - \left(e_0 a\right)^2 \left.\frac{\partial^2 \rho A_r}{\partial x^2}\right|_{x_m} \right] \mathbf{a}_\mathbf{m}^T - \left(e_0 a\right)^2 \left[2\left.\frac{\partial \rho A_r}{\partial x}\right|_{x_m} \mathbf{c}_\mathbf{m}^{(1)T} + \rho A_r\big|_{x_m}\,\mathbf{c}_\mathbf{m}^{(2)T} \right]. \tag{7.44}
$$

${}_m\mathbf{k}_r$, ${}_m\mathbf{k}_r^{NLg}$ ($r = i, o$), and ${}_m\mathbf{k}_s^{NLv}$ ($s = 1, 2$) represent the linear stiffness, geometric nonlinear stiffness, and vdW force nonlinear stiffness counterparts of equation of motion for inner and outer tubes. ${}_m\mathbf{M}_r$ stands for the system inertia. $\mathbf{a_m}$ is a unit vector which its m^{th} component is equal to unity. e.g. $\mathbf{a}_1 = \{1 \quad 0 \quad \cdots \quad 0 \quad 0\}_{1\times N}^T$. G_{W_r} is a nonlinear coefficient dependent on the system mode shape where it is calculated as follows

$$G_{W_r} = \frac{1}{2L}\sum_{n=1}^{N} d_n \left(EA_r\big|_{x_n} \left(\mathbf{c}_{\mathbf{n}}^{(1)T} \cdot \mathbf{x}_r \right)^2 \right) , \tag{7.45}$$

where d_n is the weighting function calculated using Gauss–Lobatto integration rule [207]. Adding and re-ordering equations for all point, equation of motion can be written in matrix form as follows

$$\left[\mathbf{K_L} + \mathbf{K_{NL}}\right] \times \mathbf{q} = \omega^2 \mathbf{M} \times \mathbf{q} \ , \tag{7.46}$$

where $\mathbf{q}$ denotes the unknown dynamic displacement vector defined as

$$\mathbf{q} = \begin{Bmatrix} \mathbf{x_o} \\ \cdots \\ \mathbf{x_i} \end{Bmatrix} = \left\{ \left\{ {}_1W_o \quad {}_2W_o \quad \cdots \quad {}_NW_o \right\} \vdots \left\{ {}_1W_i \quad {}_2W_i \quad \cdots \quad {}_NW_i \right\} \right\}^T . \tag{7.47}$$

$\mathbf{M}$, $\mathbf{K_L}$, and $\mathbf{K_{NL}}$ represent mass matrix, linear stiffness matrix, and nonlinear stiffness matrix including geometric and vdW force nonlinearities, respectively.

7.5.1. Nonlinear nonlocal boundary conditions

In the present study, free vibration of cantilever tubes is studied where they are clamped at $x = 0$. Hence, the boundary condition for the tubes will be

$$w_r(x_1, t) = 0, \quad \left.\frac{dw_r}{dx}\right|_{x=x_1} = 0 \ , \tag{7.48}$$

$$N_{x_N,r} \left.\frac{\partial w_r}{\partial x}\right|_{x=x_N} + \left.\frac{\partial M_{x,r}}{\partial x}\right|_{x=x_N} = 0, \quad -M_{x,r}\big|_{x=x_N} = 0 \, , \tag{7.49}$$

where x_1 and x_N represent the position of clamped and free ends, respectively. Using the DQM, the discretized counterparts of boundary conditions for inner and outer tubes at the end become

$$\mathbf{a}_1^T \cdot \mathbf{x_r} = 0, \quad \mathbf{c_1^{(1)T}} \cdot \mathbf{x_r} = 0 \, , \tag{7.50}$$

$$\left(\frac{3}{4}G_{W_r}\,\mathbf{c}_{\mathbf{N}}^{(1)}-\left.\frac{\partial EI}{\partial x}\right|_{x_N}\mathbf{c}_{\mathbf{N}}^{(2)}-EI_r\big|_{x_N}\mathbf{c}_{\mathbf{N}}^{(3)}-\left(e_0a\right)^2\left[\rho A_r\big|_{x_N}\omega^2\,\mathbf{c}_{\mathbf{N}}^{(1)}+\omega^2\left.\frac{\partial\rho A}{\partial x}\right|_{x_N}\mathbf{a}_{\mathbf{N}}+\frac{3}{4}G_{W_r}\,\mathbf{c}_{\mathbf{N}}^{(3)}\right]\right)^T\cdot\mathbf{x}_{\mathbf{r}}$$

$$\pm\left(e_0a\right)\frac{\partial}{\partial x}\left[-\mathbf{f}_{\mathbf{r}}\cdot\left(\mathbf{x}_{\mathbf{o}}-\mathbf{x}_{\mathbf{i}}\right)\right]=0,$$

$$\left(EI_r\big|_{x_N}\,\mathbf{c}_N^{(2)T}+\left(e_0a\right)^2\left[\rho A_r\big|_{x_N}\,\omega^2\,\mathbf{a}_{\mathbf{N}}^T+\frac{3}{4}G_{W_r}\,\mathbf{c}_N^{(2)T}\right]\right)\cdot\mathbf{x}_{\mathbf{r}}\pm\left(e_0a\right)^2\mathbf{f}_r\cdot\left(\mathbf{x}_{\mathbf{o}}-\mathbf{x}_{\mathbf{i}}\right)=0$$

. (7.51)

In the above equations, the first and second terms are added for the innertube and subtracted for the outertube and

$$\mathbf{f}_{\mathbf{r}}=\left[p_1+\frac{3}{4}p_2\cdot\left(\mathbf{a}_{\mathbf{N}}^T\cdot\left(\mathbf{x}_{\mathbf{o}}-\mathbf{x}_{\mathbf{i}}\right)\right)^2\right]\mathbf{a}_{\mathbf{N}}^T, \tag{7.52}$$

shows the value of vdW force for inner and outer tubes ($r=i,\mathrm{o}$) at the tip. It should be noted that the obtained boundaries are nonlinear and eigenvalue dependent boundaries due to nonlocality and geometric nonlinearity. Furthermore, it can be seen that boundary conditions are affected by linear and nonlinear counterparts of vdW interlayer force due to nonlocality. Considering the nonlocal effects equal to zero, the BCs, after simplifications, are become similar to the one reported in Ref [215].

7.6. Solution method

By using matrix manipulation, the boundary condition equations can be written in matrix form as follows

$$\left[\mathbf{K}_{\mathbf{B}}+\mathbf{K}_{\mathbf{B}}^{\mathbf{NL}}-\omega^2\mathbf{M}_{\mathbf{B}}\right]\mathbf{x}_{\mathbf{B}}+\left[\mathbf{K}_{\mathbf{s}}+\mathbf{K}_{\mathbf{s}}^{\mathbf{NL}}-\omega^2\mathbf{M}_{\mathbf{s}}\right]\mathbf{x}_{\mathbf{s}}=\mathbf{0}\ , \tag{7.53}$$

where $\mathbf{x}_{\mathbf{B}}$ and $\mathbf{x}_{\mathbf{s}}$ represent the boundaries and interior gird points, respectively, as follows

$$\mathbf{x}_{\mathbf{B}}=\left\{\ {}_1W_i,\ {}_2W_i,\ {}_{N-1}W_i,\ {}_NW\ \ \middle|\ {}_1W_o,\ {}_2W_o,\ {}_{N-1}W_o,\ {}_NW_o\right\}^T, \tag{7.54}$$

$$\mathbf{x}_{\mathbf{s}}=\left\{\ {}_3W_i\quad {}_4W_i\quad\cdots\quad {}_{N-2}W_i\ \middle|\ {}_3W_o\quad {}_4W_o\quad\cdots\quad {}_{N-2}W_o\right\}^T. \tag{7.55}$$

$\mathbf{K_B}$ and $\mathbf{K_B^{NL}}$ are 8×8 and $\mathbf{K_S}$ and $\mathbf{K_s^{NL}}$ are $8\times(2N-8)$ linear and nonlinear stiffness matrices of boundaries and interior gird points, and $\mathbf{M_B}$ and $\mathbf{M_S}$ are 8×8 and $8\times(2N-8)$ mass matrices of boundaries and interior gird points, respectively.

Furthermore, considering the interior and boundary grid points separately, the equation of motion (Eq. (7.46)) can be written as

$$\mathbf{K_D}\cdot\mathbf{x_B}+\left[\left(\mathbf{K_L^*}+\mathbf{K_{NL}^*}\right)-\omega^2\mathbf{M^*}\right]\cdot\mathbf{x_s}=\mathbf{0}. \tag{7.56}$$

Here, $\mathbf{K_L^*}$, $\mathbf{K_{NL}^*}$, and $\mathbf{M^*}$ are $(2N-8)\times(2N-8)$ matrices, representing the linear stiffness matrix, nonlinear stiffness matrix, and mass matrix for the interior nodes, respectively. It is worth noting that $\mathbf{K_L^*}$ and $\mathbf{M^*}$ are coefficient matrices for the non-boundary (interior) nodes whereas $\mathbf{K_{NL}^*}$ is a displacement dependent matrix whose values depend on the values of the boundary nodes in addition to the interior nodes. $\mathbf{K_D}$ is an $(2N-8)\times 8$ displacement dependent matrix which contains coefficients of boundary nodes.

Solving $\mathbf{x_B}$ from Eq. (7.53) and substituting it in Eq. (7.56), Eq. (7.56) can be simplified as follows

$$-\mathbf{K_D}\cdot\left[\mathbf{K_B}+\mathbf{K_B^{NL}}-\omega^2\mathbf{M_B}\right]^{-1}\cdot\left[\mathbf{K_s}+\mathbf{K_s^{NL}}-\omega^2\mathbf{M_s}\right]\cdot\mathbf{x_s}+\left[\left(\mathbf{K_L^*}+\mathbf{K_{NL}^*}\right)-\omega^2\mathbf{M^*}\right]\cdot\mathbf{x_s}=\mathbf{0}\ . \tag{7.57}$$

It should be noted since boundary conditions are nonlinear, it is almost impossible to use commonly eigenvalue solvers [34, 122]. Hence, the resulting nonlinear algebraic equation is solved using Arc-length method details of which are given in Ref [197] where the residual vector function is defined as follows

$$\mathbf{r}\left(\mathbf{x_s},\omega\right)=\left[\left[\left(\mathbf{K_L^*}+\mathbf{K_{NL}^*}\right)-\omega^2\mathbf{M^*}\right]-\mathbf{K_D}\left[\mathbf{K_B}+\mathbf{K_B^{NL}}-\omega^2\mathbf{M_B}\right]^{-1}\left[\mathbf{K_s}+\mathbf{K_s^{NL}}-\omega^2\mathbf{M_s}\right]\right]\cdot\mathbf{x_s}\ . \tag{7.58}$$

7.7. Results

In this section, first, the effect of nonlocal parameter, rotation speed, and variation of cross section on the linear natural frequencies of a non-uniform rotating DWCNT is studied. Later, the same study is repeated considering the effect of geometric and vdW force nonlinearities. The material and geometric parameters of the rotating DWCNT used in this study are given in Table 7-1. The hub radius and variation of cross section are considered to be equal to $r_h = 2$ nm and $\beta = 0$, respectively, unless they are mentioned. The effect of number of grid points is studied on the linear system, where it is detected that the natural frequencies obtained are identical when the number of grid points is larger or equal to 14. Therefore, in all the present results, 18 grid points are used which later it is observed to be sufficient for the nonlinear cases as well (Table 6-1 in previous chapter). The variation of the radius of the CNTs is assumed to change linearly along the axial direction with the following relation

$$r_r(x) = r_r^c - \left(\frac{r_r^c - r_r^F}{L}\right)x = r_r^c\left(1 - \beta\frac{x}{L}\right), \tag{7.59}$$

where r_r^c and r_r^F denote radius of the tube at clamped and free ends, respectively. β is the normalized slope of the variation of the radius (i.e. variation of cross section) along the axial direction.

Table 7-1 Numerical Values of tubes Parameters

Parameter	**Value**		
	Case 1 $\beta = 0$	**Case 2** $\beta = 0.3$	**Case 3** $\beta = 0.5$
Diameter of innertube at free end	0.7 nm	0.7 nm	0.7 nm
Diameter of innertube at clamped end	0.7 nm	1.0 nm	1.4 nm
Density of tubes	2.3 gr/cm^3	2.3 gr/cm^3	2.3 gr/cm^3
Young modulus of tubes	1 TPa	1 TPa	1 TPa
Thickness of tubes	0.34 nm	0.34 nm	0.34 nm
Interlayer space between tubes	0.35 nm	0.35 nm	0.35 nm

In order to present the results in a proper form, the linear and nonlinear natural frequencies are normalized with respect to the corresponding linear natural frequency of nonrotating uniform local DWCNT (Table 7-2). Furthermore, nonlocal parameter $e_0 a$ is normalized with respect to the tubes length. Normalized nonlocal parameter in

equation of motion is named as μ_2 whereas, in boundary equations, it is named as μ_1 . The naming scheme makes it possible to study the effect of nonlocality in equation of motion and boundary equations, separately.

Table 7-2 Linear natural frequencies of the non-rotating local DWCNT

Linear natural frequencies [THz]	Case 1	Case 2	Case 3
1st in-phase	0.1665	0.1417	0.1194
2nd in-phase	1.0418	0.8101	0.6220
3rd in-phase	2.8819	2.1933	1.6429
1st out-of-phase	7.8768	7.2130	6.4504

7.7.1. Linear vibration analysis and verifications

The validity of the present nonlocal model in anticipating vibration response of non-rotating CNT has been investigated in Figure 7-2. The nonlocal results are compared with the results reported by Lu et al. [213] and Wang et al [85] for SWCNTs. Furthermore, mode shapes of the system at selected nonlocal parameter are plotted in Figure 7-3 when nonlocality in boundaries are disregarded $\mu_1 = 0$ and included $\mu_1 = \mu_2$. A good agreement between the results is observed. It can be seen that, in the 1st in-phase vibration mode, the frequency parameter slightly increases as the nonlocal parameter increases. However, it is observed that even though disregarding the nonlocality in boundaries ($\mu_1 = 0$) does not change the variation of frequency parameter for a nonrotating tube, it has a considerable effect on the system mode shape as shown in Figure 7-3. It is worth noting that by setting vdW force coefficient equal to zero the DWCNT can be reduced to two SWCNT.

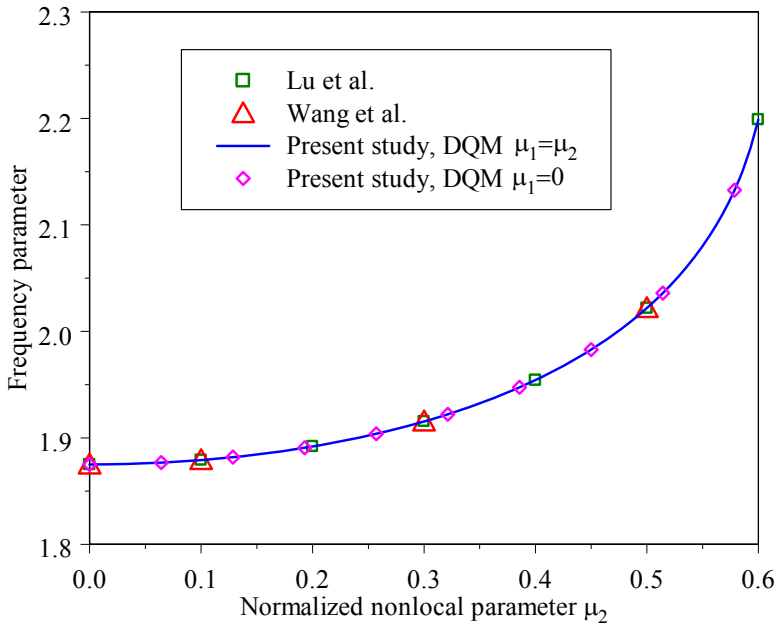

Figure 7-2 Validation of present study, DQM, with the results reported by Lu et al. [213] and Wang et al [85]

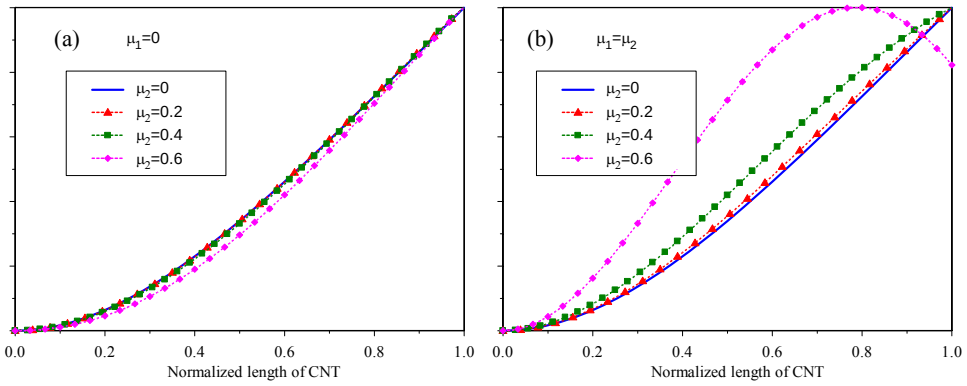

Figure 7-3 Variation of mode shape of CNT with normalized nonlocal parameter μ_2 a) $\mu_1 = 0$ i.e. disregarding the nonlocality effect in BCs b) $\mu_1 = \mu_2$ including the nonlocality effect in BCs

Figure 7-4-a presents a comparison between results of present study for a nonlocal rotating SWCNT with results reported in Pradhan and Murmu [208] where the hub radius is considered to be equal to the tube length. Rotation speed Ω is normalized with respect to $\sqrt{EI_1/\rho A_1 L^4}$ at clamped end. It should be noted that in [208] local BCs assumption is incorrectly used to study the variation of natural frequency of a nonlocal SWCNT. Hence, for the sake of comparison, μ_1 is considered to be equal to zero. A good agreement between results can be observed. However, disregarding nonlocality

effect in boundaries results in a considerable amount of error. Figure 7-4-b shows variation of normalized linear natural frequency when nonlocality effect in boundaries are included ($\mu_1 = \mu_2$). It can be seen that nonlocality effect in boundaries results in a faster increase of normalized linear natural frequency as rotation speed increases. Hence, it is important to consider nonlocal terms in boundaries. Therefore, in the following sections, $\mu_1 = \mu_2$ in order to present a correct application of theorem.

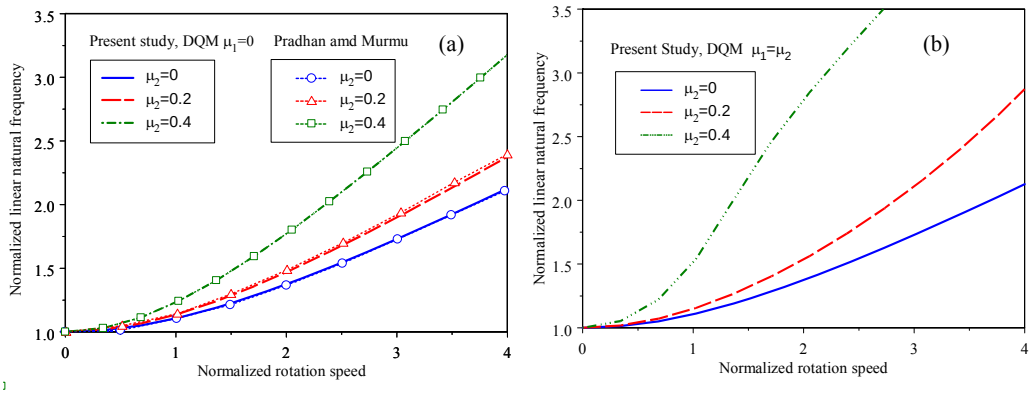

Figure 7-4 Variation of normalized linear natural frequency versus normalized rotation speed a) present study with $\mu_1 = 0$ comparing to Pradhan and Murmu [208] b) present study with $\mu_1 = \mu_2$

It is worth mentioning that in Ref. [211] linear free vibration of rotating nonlocal SWCNT is studied where nonlocal boundaries are correctly obtained (equation 31). However, following solution procedure and results, it is observed the matrix form of boundaries, equation 49 in [211] in comparison to Eq. (7.53) in present study, is reported incorrectly. Furthermore, since boundaries are eigenvalue dependent, an iterative procedure is required to obtain the correct values of system eigenvalues where it has not been specified in [211].

Table 7-3 shows the variation of the 1st and 2nd in-phase natural frequency of the nonlocal rotating DWCNT for different set of parameters. It is observed that no nontrivial real frequencies exist for some sets of rotation speeds and nonlocal parameters which we named them as unstable values. A similar phenomenon is reported by Lu et al. [213] and Wang et al. [85] for nonrotating SWCNT using Galerkin method. Results show that as nonlocal parameter increases, successive natural frequencies approach each other which results in no real frequencies.

Table 7-3 Variation of normalized 1st and 2nd linear in-phase vibration mode of DWCNT

	1st in-phase				**2nd in-phase**			
	$\beta = 0$				$\beta = 0$			
Ω [THz]	Nonlocal Parameter [nm]				Nonlocal Parameter [nm]			
	$e_0a = 0$	$e_0a = 2$	$e_0a = 4$	$e_0a = 6$	$e_0a = 0$	$e_0a = 2$	$e_0a = 4$	$e_0a = 6$
0	1.0000	1.0090	1.0389	1.1034	1.0000	0.8837	0.6654	-
0.1	1.1986	1.2422	1.5077	2.5328	1.0300	0.9358	0.8121	0.7807
0.2	1.6514	1.8792	3.1809	3.9834	1.1150	-	1.2204	1.1117
0.3	2.1918	-	8.3356	8.4143	1.2438	-	1.5728	1.4549
	$\beta = 0.3$				$\beta = 0.3$			
Ω [THz]	Nonlocal Parameter [nm]				Nonlocal Parameter [nm]			
	$e_0a = 0$	$e_0a = 2$	$e_0a = 4$	$e_0a = 6$	$e_0a = 0$	$e_0a = 2$	$e_0a = 4$	$e_0a = 6$
0	1.0000	1.0075	1.0323	1.0831	1.0000	0.9177	0.7401	-
0.1	1.3199	1.3655	1.6858	2.7664	1.0569	1.0045	0.9769	0.9640
0.2	1.9759	2.1814	3.7183	4.5862	1.2119	1.2681	1.5080	1.4086
0.3	2.7166	-	9.9821	10.448	1.4331	-	1.9852	1.9152
	$\beta = 0.5$				$\beta = 0.5$			
Ω [THz]	Nonlocal Parameter [nm]				Nonlocal Parameter [nm]			
	$e_0a = 0$	$e_0a = 2$	$e_0a = 4$	$e_0a = 6$	$e_0a = 0$	$e_0a = 2$	$e_0a = 4$	$e_0a = 6$
0	1.0000	1.0059	1.0260	1.0654	1.0000	0.9447	0.8113	0.6520
0.1	1.5100	1.5551	1.9517	3.0686	1.1102	1.0945	1.1907	1.1928
0.2	2.4324	2.6215	4.3572	5.3450	1.3895	1.5029	1.8892	1.8359
0.3	3.4172	3.9445	6.6563	7.7348	1.7572	2.1481	2.5708	2.5778

Figure 7-5 shows instability plots for a rotating DWCNT in the 1st and 2nd in-phase vibration mode. It is observed that instability region fade away as rotation speed increases for the 1st and 2nd in-phase vibration mode. However, as rotation speed increases more, a new unstable region takes form at lower nonlocal parameters. The observed phenomenon does not have any physical interpretation and it is a direct result of the application of Eringen theorem.

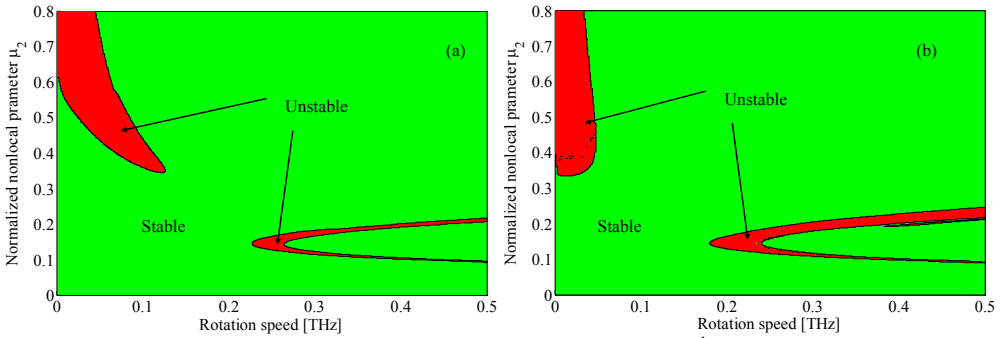

Figure 7-5 Instability plot a) 1st in-phase vibration mode b) 2nd in-phase vibration mode

7.7.2. Nonlinear vibrations

In the following section, nonlinear free vibration of a nonuniform rotating DWCNT is studied where the effect of nonlocal parameter, rotation speed, and normalized slope, β , on the nonlinear natural frequencies is investigated. It should be mentioned that the effect of nonlinearities in the boundaries on the variation of nonlinear natural frequency is investigated for the first time in present study.

In Figure 7-6, the variation of the normalized nonlinear natural frequency of the first in-phase vibration mode of a nonrotating uniform DWCNT is given for different values of nonlocal parameter disregarding and including the effects of nonlinear terms in boundary condition equations. Results show that the nonlinear terms in boundaries have a huge effect on the variation of normalized nonlinear natural frequency of the DWCNT. The effect is more detectable for the case of local DWCNT ($\mu_2 = 0$) where the behavior changes from a softening behavior to a hardening behavior as nonlinear terms in boundaries are included. It is observed that the nonlocal parameter has a hardening effect on the system. It is worth mentioning that boundary equation are affected by both nonlocal terms and nonlinear terms where the effect of nonlocal terms surpass the effect of nonlinear terms as nonlocal parameter increases. As a result, it can be seen that the difference between the variation of nonlinear frequency between the two cases in Figure 7-6 decreases as nonlocal parameter increases. Figure 7-7 shows the corresponding nonlinear mode shapes of the DWCNT at normalized vibration amplitude equal to 2.5 for local DWCNT $\mu_2 = 0$ and nonlocal DWCNT $\mu_2 = 0.4$. Results show that the mode shapes are more affected by nonlinearities for the case of nonlocal DWCNT in comparison to local DWCNT.

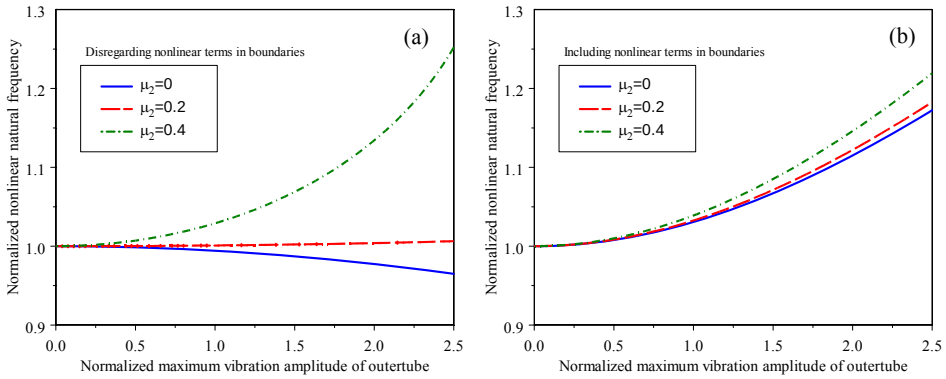

Figure 7-6 Variation of normalized nonlinear natural frequency of outertube vibrating in the first in-phase mode a) Disregarding nonlinear terms in boundaries b) Including the nonlinear terms

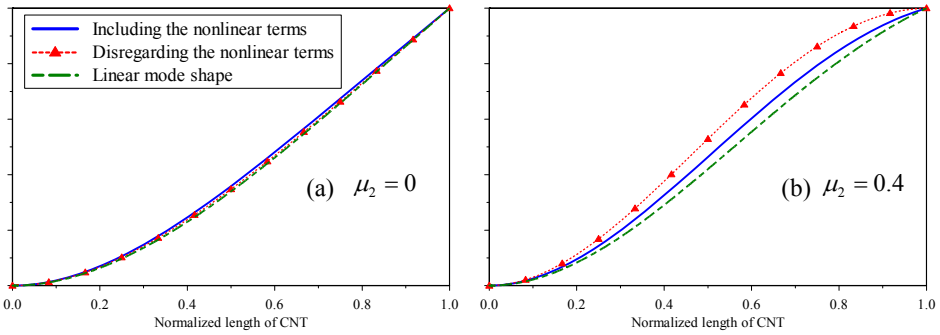

Figure 7-7 Variation of outer tube mode shape vibrating in the 1st in-phase vibration mode at normalized vibration amplitude equal to 2.5 a) Local DWCNT b) Nonlocal DWCNT $\mu_2 = 0.4$

In Figure 7-8, the variation of the normalized nonlinear natural frequency of the first in-phase vibration mode of uniform rotating DWCNT is given for different rotation speed and nonlocal parameter. It is observed that, with an increase in the rotation speed, the normalized nonlinear frequency tends to approach to the linear ones for the local DWCNT $\mu_2 = 0$. This shows that the effect of geometric nonlinearity becomes negligible in the presence of sufficiently large rotation speed. On the other hand, for the case of nonlocal DWCNT with $\mu_2 = 0.2$, for rotation speed larger than 0.3 THz significant changes in the normalized nonlinear natural frequency are observed. Moreover, for the case of rotation speed equal to 0.4 THz no real solution can be found for normalized vibration amplitude larger than 0.6 based on the Eringen theorem. Referring to Figure 7-5, it can be seen that, at $\mu_2 = 0.2$, these rotation speeds reside around second unstable region where successive natural frequencies with a

sudden increase approach each other and result in no real solution cases. The accuracy and validity of Eringen theorem in these regions is strictly questionable.

Figure 7-8-c shows the variation of the normalized nonlinear natural frequency for $\mu_2 = 0.4$. It is observed that the variation of the normalized nonlinear natural frequency decreases as rotation speed increases. However, as rotation speed increases beyond a certain value, the variation of the normalized nonlinear natural frequency suddenly increases and then decreases and settles down around rotation speed of 0.1 THz. The reason for this behavior can be found by studying the variation of mode shapes. Figure 7-9 shows the mode shapes of local and nonlocal DWCNT at normalized vibration amplitude equal to 2.5 for different rotation speeds. It is observed that the mode shapes of local DWCNT changes slightly as rotation speed increases whereas mode shape of nonlocal DWCNT changes significantly. Furthermore, results show that they take a shape similar to the clamped-hinged beam modes in large rotation speed due to eigenvalue dependent boundary conditions.

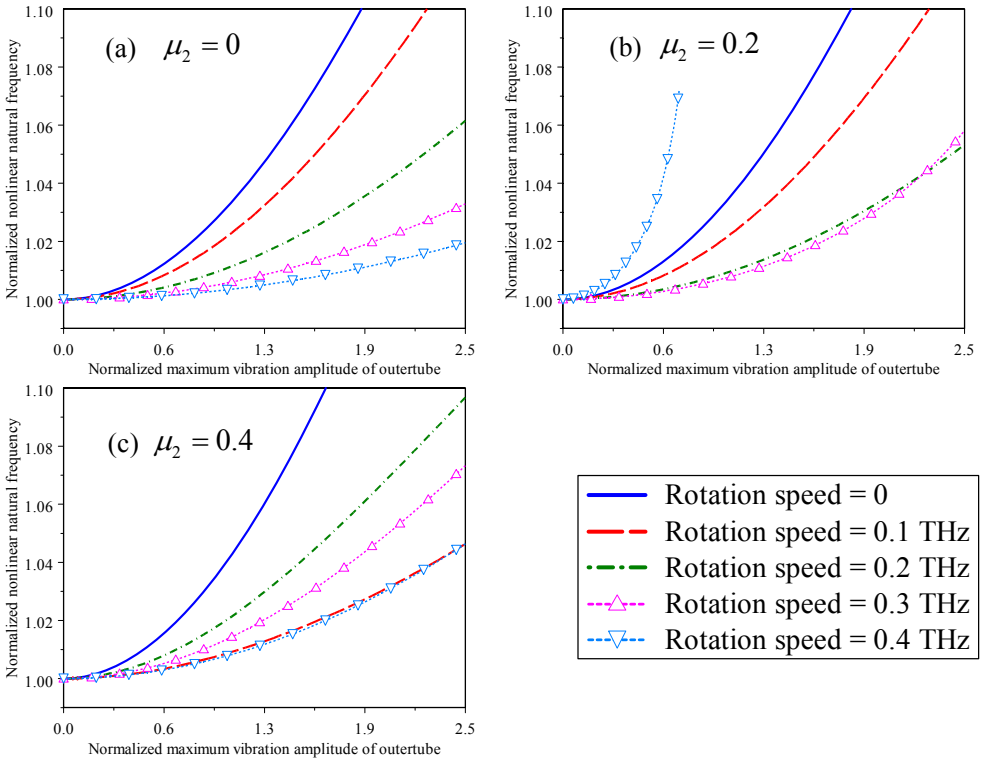

Figure 7-8 Variation of normalized nonlinear natural frequency of outertube vibrating in the first in-phase mode at different rotation speeds a) $\mu_2 = 0$ b) $\mu_2 = 0.2$ c) $\mu_2 = 0.4$

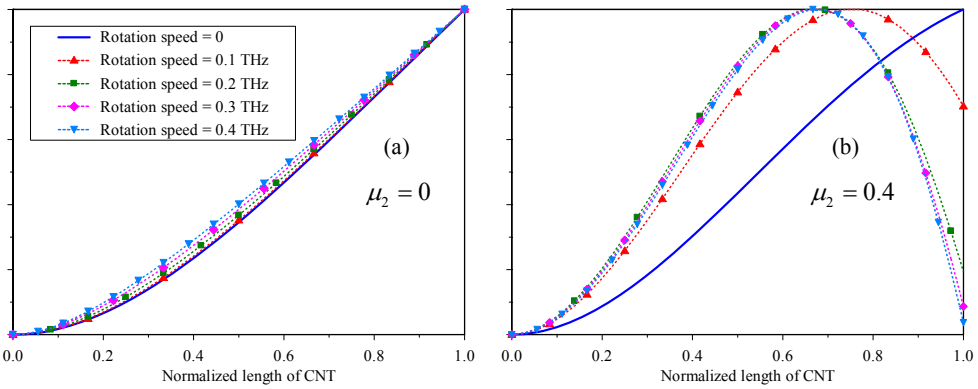

Figure 7-9 Variation of outer tube mode shape vibrating in the 1st in-phase vibration mode at different rotation speed a) local DWCNT $\mu_2 = 0$ b) nonlocal DWCNT $\mu_2 = 0.4$

Figure 7-10 presents the effect of the normalized slope, β , on the variation of normalized nonlinear natural frequency versus maximum vibration amplitude for the 1st and 2nd in-phase vibration modes. Results show that the normalized slope has a significant effect on the variation of normalized nonlinear natural frequency where it can changes its behavior from a hardening behavior to a softening behavior for the 1st in-phase vibration mode. On the other hand, it is observed that 2nd in-phase vibration mode are slightly affected by the normalized slope.

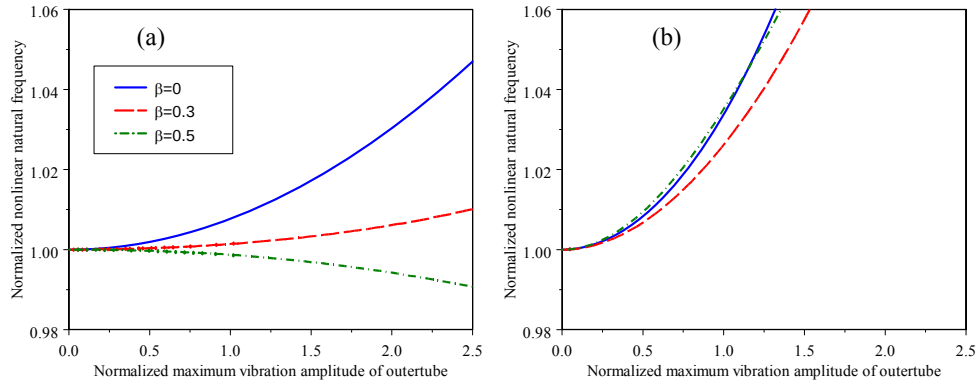

Figure 7-10 Variation of normalized nonlinear natural frequency of outertube with different cross sections at constant rotation speed of $\Omega = 0.4$ THz with $\mu_2 = 0.4$ vibrating in the a) 1st in-phase b) 2nd in-phase

In Figure 7-11, the variation of the normalized nonlinear natural frequency is given for different hub radius of local and nonlocal DWCNT at rotation speed $\Omega = 0.2$ THz for different β values. It is observed that the change in normalized nonlinear natural frequency decreases as hub radius increases in all the cases. Furthermore, the hardening effect of nonlocal parameter on normalized nonlinear natural frequency

decreases as β parameter increases and, as a result, local and nonlocal solutions approach each other.

Figure 7-12 shows the variation of the normalized nonlinear natural frequency of uniform and nonuniform nonlocal DWCNT vibrating in the first in-phase vibration mode where the effect of different length to diameter ratios is investigated. Results shows that as the length to diameter ratio increases, the variation of the normalized nonlinear natural frequency decreases even for some cases it changes from a hardening behavior to a softening behavior. Furthermore, for large ratios, the normalized nonlinear frequency approaches to the linear one due to increase in the rotation force. Moreover, results show that the variation of the normalized nonlinear natural frequency approaches to linear one faster for the nonuniform DWCNT.

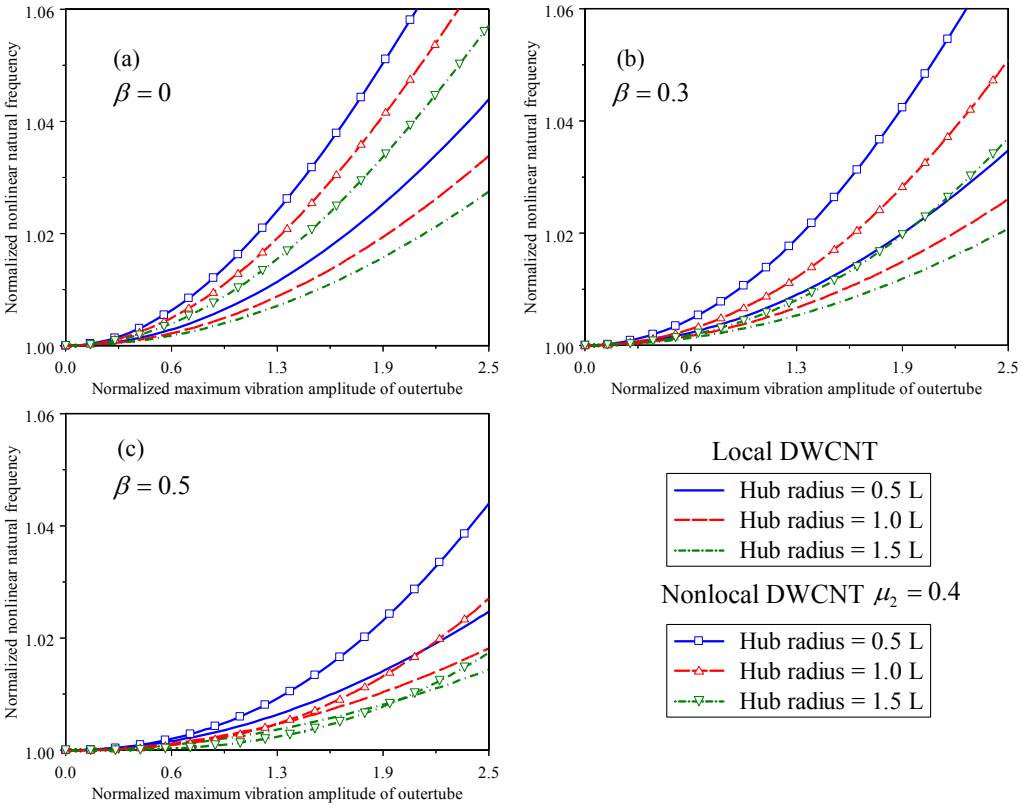

Figure 7-11 Variation of normalized nonlinear natural frequency of outertube vibrating in the first in-phase mode with different hub radius rotating at constant speed of $\Omega = 0.2$ THz a) $\beta = 0$ b) $\beta = 0.3$ c) $\beta = 0.5$

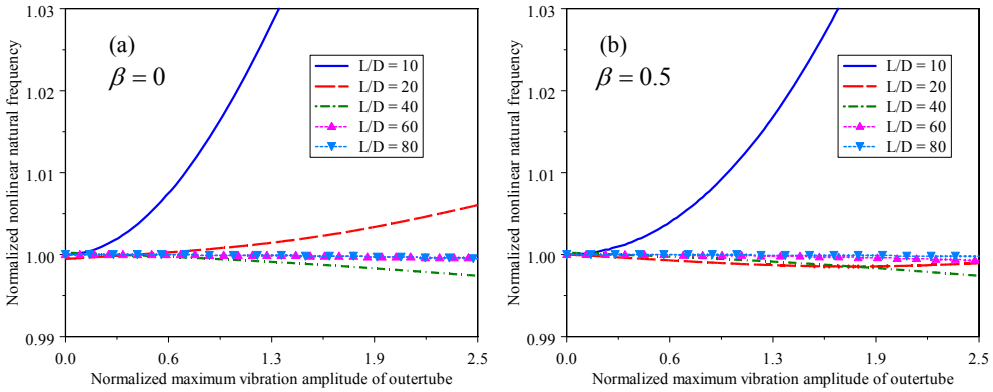

Figure 7-12 Variation of normalized nonlinear natural frequency of outertube vibrating in the first in-phase mode with different length to diameter ratio rotating at constant rotation speed of $\Omega = 0.2$ THz with $\mu_2 = 0.4$ a) $\beta = 0$ b) $\beta = 0.5$

7.8. Concluding remarks

In this chapter, linear and nonlinear free vibration of a rotating nonuniform DWCNT studied where equations of motion are derived based on Eringen theorem using Hamilton principle and Euler Bernoulli beam theory. The classic boundary conditions are widely used in studying nonlocal beams in literature. However, our study shows that boundary condition (BC) equations for a nonlocal cantilever beam is different than the classic beam where it includes nonlocal and nonlinear terms. It is observed that including the terms of nonlocal parameter in boundaries have significant effects on the system mode shape. Furthermore, it is observed that, in addition to mode shapes, the variation of linear natural frequency is also affected as rotation speed increases. The effect of nonlocality, rotation speed, normalized slope, and boundaries on the variation of linear natural frequency is studied and compared with existed results in literature for classic boundary assumptions.

Later, considering nonlinearities, similar studies are repeated where the effect of nonlinearities on the variation of normalized nonlinear natural frequency is studied in detail. Results show that nonlinear behavior of DWCNT in the 1st in-phase vibration mode is significantly affected by the nonlinear terms in boundaries where system behavior changes from a softening behavior to a hardening behavior as the nonlinear terms in boundaries are included in the solution expansion. It is observed that the variation of normalize nonlinear natural frequency decreases as rotation speed increases. Furthermore, our study shows that nonlocal mode shape of DWCNT takes

a form similar to mode shape of clamped-hinged beam in large rotation speeds due to nonlocal eigenvalue dependent terms in boundaries.

It should be mentioned that application of Eringen theorem for cantilever beam results in unstable solution for some set of system parameters. Instability of theorem is studied where unstable regions are determined. In unstable regions, successive natural frequency approach each other as nonlocal parameter changes which results in no real frequency cases. A similar phenomenon is observed by Lu et al. [213] and Wang et al. [85] for case of nonrotating SWCNTs.

CHAPTER 8

CONCLUSIONS, CONTRIBUTIONS AND FUTURE WORKS

In this thesis, nonlinear vibrations of curved single and double walled carbon nanotubes is investigated. In this chapter, the results of present study are summarized and the contributions are highlighted. Furthermore, several recommendations are provided for future works in this subject.

8.1. Introduction

In the past years, the subject area of nanotechnology has become the focus of attention of industries, scientists and researchers. Among nanomaterial, Carbon nanotubes (CNTs) have gained great amount of attention owing to their extraordinary strength, efficiency in heat conduction and unique electrical properties. CNTs have great potential in many applications such as nanotechnology, electrics, optics, sensors, materials science, and architecture. Nowadays, literally every day, a new application is proposed for CNTs. Among application areas, recently, considerable among of efforts have been given to comprehend the vibrational behavior of CNTs. A CNT resonator can oscillate at megahertz frequency. A resonator being able to oscillate at high frequency unfolds several applications for CNTs. In recent years, CNTs have been successfully fabricated and used as different parts in the new emerging nano-devices. CNTs are being used as nano-actuators, nano-motors, nano-sensors, nano-turbines, and nano shaft and gear systems. Several application areas of CNT were summarized in the second chapter.

However, in order to design a new efficient vibrating nano-scale device, detailed information about dynamic properties of such device are needed. In contrast to macro scale structures, atomic forces play an important role in the mechanical characteristics of nano-structures. Hence, a clear understanding of atomic interactions are required.

Furthermore, fabricating prototypes without having clear image of the structural properties can be very time consuming, misleading and sometimes impossible. Therefore, having a good insight of the dynamic behavior of such nano-structures is important in order to develop practical nanomachines.

In the second chapter, several well-known methods which are being used in the literature were studied. Molecular dynamics (MD) simulation is used by several researchers in studying the mechanical properties of CNTs. Although MD simulations provide considerable amount of information on mechanical properties of CNTs, they are limited by the size of such atomic systems due to highly time consuming computational requirements. Hence, in recent years, continuum mechanic models have been used by researchers in studying the free vibrations of CNTs. Using simple closed form equations of motion offered by the continuum models, key parameters that affect the free vibration of CNTs can be easily studied. Several continuum beam and shell models were summarized in the second chapter where advantages and dis-advantages of each model were also discussed in detail. However, majority of studies given in literature deal with linear free vibrations of CNTs while the nature of such structures is highly nonlinear. Nonlinear vibrational behavior of CNTs has recently become the interest of research. Recent developments in studying the effect of nonlinearity on vibration of CNT was investigated in the second chapter. It was observed that CNTs are affected by nonlinearities caused by large deflections (geometric nonlinearity), interlayer van der Waals force, and initial curvature of the tubes. Chapter two provides a detailed literature review on current state of studies regarding the effect of nonlinearity on nonlinear vibrations of CNTs whereas in the chapter's three to seven the effect of nonlinearities on the nonlinear vibrations of CNTs is investigate through several case studies. In each case, the structure was modeled accordingly and appropriate analyses were carried out to study the nonlinear free vibrations of CNTs.

8.2. Conclusions

In the chapter three of this thesis, nonlinear free vibration of a simply supported double walled carbon nanotube (DWCNT) with a concentrated-mass was investigated. The proposed model simulates behavior of nonlinear DWCNT mass

sensor where concentrated mass stands for the absorbed mass. The effect of nonlinearities and mass ratio of concentrated mass on the variation of nonlinear in-phase and out-of-phase natural frequency of the DWCNT was studied. Based on the numerical simulations, it was concluded that

- In the first in-phase vibration mode, the normalized nonlinear natural frequency of DWCNT is not affected by the concentrated-mass where only geometric nonlinearity exists. On the other hand, in the presence of the vdW force nonlinearity, the normalized nonlinear natural frequency is affected; but, this effect is very small.
- In the first out-of-phase vibration mode, it was observed that as the mass ratio increases, the slope of the normalized nonlinear frequency curves increases in the case of geometric and vdW force nonlinearities; however, the effect of vdW force nonlinearity is significantly higher than the effect of geometric nonlinearity.

It is worth mentioning that nano-sensors work based on the effect of nanoparticles on natural frequency shifts. However, the results provided in the chapter three show that the system natural frequency changes considerably as the vibration amplitude increases due to the inherent nonlinearity of CNTs. Hence in order to predict the shift in the natural frequency of the system accurately, one needs a comprehensive understanding of the nonlinear behavior of system. Moreover, in the presence of medium stiffness, it was concluded that due to nonlinearity, the rate of changes in the frequency increases suddenly after a certain value of vibration amplitudes. Provided results and the methods in this thesis can be used in development of future new nonlinear nano sensors.

In the chapter four, nonlinear free vibrations of a DWCNT was studied using describing function method (DFM) with multiple trial functions where geometric and interlayer vdW force nonlinearities were considered. Owing to DFM, the coupling between the trial functions used in the modal expansion process can be investigated. The nonlinearity matrices obtained using DFM showed that for simply supported CNTs considering geometric nonlinearity, a single trial function is sufficient to obtain the nonlinear natural frequencies; whereas, in case of vdW force nonlinearity,

multiple trial functions are necessary, especially for the out-of-phase modes in which the nonlinear effects are more significant. These findings were also verified with the numerical results obtained.

Within the chapter five, the effect of initial curvature on the variation of nonlinear natural frequencies was investigated. Galerkin method was used to discretize the equation of motion in spatial domain. Multiple harmonic balance method was utilized to convert the discretized ordinary differential equations of motion in time domain into nonlinear algebraic equations. On the basis of the number of harmonics used in the solution expansion, several case were studied in order to investigate the effect of higher harmonics on the nonlinear fundamental natural frequency in the presence of geometric and waviness nonlinearities. In each case, an analytical expression for the variation of the nonlinear fundamental natural frequency of CNTs was obtained. Results showed that the effect of initial curvature can be classified in two linear and nonlinear categories. It was observed that the higher harmonics should be considered in order to detect the nonlinear effect of initial curvature.

In the chapter six, nonlinear free vibrations of curved DWCNT was studied introducing a new accurate, efficient, and relatively fast technique for modeling the CNTs. Differential quadrature method (DQM), a solution method which does not require any pre-knowledge on the system comparison functions was developed in this chapter. The main advantage of DQM, compared to solution methods like variational approach or Galerkin method is its inherent simplicity in formulation, where different end conditions can be easily adopted. The effect of nonlinearities, end conditions, initial curvature, stiffness of the surrounding elastic medium, and vibrational modes on the nonlinear free vibration of DWCNTs was studied. Results showed that it is possible to detect different vibration modes occurring at a single vibration frequency when CNTs vibrate in the out-of-phase vibration mode. Moreover, it was concluded that the end conditions have significant effect on the nonlinear natural frequencies of the DWCNT including multiple solutions.

In the chapter seven, linear and nonlinear free vibration of a nonlocal rotating double walled carbon nanotube (DWCNT) was investigated. Based on Eringen theorem and Euler Bernoulli beam theory, Hamilton principle was used to obtain nonlinear and

nonlocal equations of motion and equation of boundaries. Results showed that the boundary condition equations for nonlocal cantilever beam is totally different than classic beams where it includes nonlocal and nonlinear terms. Nonlinear nonlocal BCs of CNTs were studied for the first time in this chapter. The effects of the nonlocal parameter and nonlinearities in boundary conditions and equation of motion on linear and nonlinear natural frequencies of the rotating carbon nanotubes were studied with respect to the rotation speed, variation of cross section, length to diameter ratio, hub radius, and vibration modes. It was concluded that the nonlinear behavior of DWCNT in the 1st in-phase vibration mode is significantly affected by the nonlinear terms in boundaries where system behavior changes from a softening behavior to a hardening behavior. It was observed that the variation of normalize nonlinear natural frequency decreases as rotation speed increases.

It is worth mentioning that in this thesis H-H, C-H, C-C, and C-F boundary conditions for the CNTs are studied. The F-F boundary condition is excluded since it does not represent any realistic case for a CNT resonator. C-C and C-F BCs are the realistic cases for the CNT resonators. However, in most of the studies H-H BC is considered for CNTs due to limits of methods such as Galerkin where it is easy to formulate and study.

It is worth mentioning that in this thesis H-H, C-H, C-C, and C-F boundary conditions for the CNTs are studied. The F-F boundary condition is excluded since it does not represent any realistic boundary condition for a CNT resonator while C-C and C-F BCs are the realistic ones. Moreover, it should be noted that in most of the studies in the literature H-H BC is considered for CNTs due to the limitations of numerical methods such as Galerkin as discussed in chapter 6.

8.3. Contributions

The following points outline the major contributions of this thesis:

- A comprehensive literature review is provided where shortfalls and advantageous of different methods in simulation of linear and nonlinear vibrations of CNTs are distinguished.

- Effect of geometric, vdW force, and initial curvature nonlinearities on the variation of nonlinear natural frequency of CNTs is investigated and a solid understanding of the effect of each nonlinearity and the interaction of nonlinearities with each other is provided.
- Describing function method with multiple trial functions is implemented for the first time in studying the vibrations of CNTs in order to get a better approximation of the system mode shape. DFM has the advantage of expressing the nonlinear force as a nonlinear stiffness matrix multiplied by a displacement vector, where the off-diagonal terms of the nonlinear stiffness matrix can provide a comprehensive knowledge about the coupling between the trial functions.
- Higher harmonic excitation of the system is studied using multiple balance harmonic method for the first time.
- Differential quadrature method, an accurate, efficient, and relatively fast techniques for modeling CNTs, is provided where in comparison to methods such as Galerkin does not require any pre-knowledge on the system comparison functions.
- In-phase and out-of-phase vibration of curved single and double walled carbon nanotubes are studied in detail using local and nonlocal beam models.
- Using Hamilton principle and Eringen nonlocal theorem, nonlinear nonlocal equations of motion and boundary conditions are obtained where the effect of nonlinear nonlocal boundary conditions on the variation of normalized nonlinear natural frequency of DWCNT is studied in detail.

All the goal of this thesis have been met to this end. However, the advancing area of nano structure has the potential for much deeper studies and there still exist several unsolved issues which need attention. Following section provides ideas for the possible future research areas.

8.4. Future works

In this thesis, the variation of nonlinear natural frequency of Carbon nanotube resonator is studied in detail. Several dynamic models are developed where effect of geometric, van der Waals force, and initial curvature nonlinearities are included in

equations of motion. Author believe that the accurate dynamic models which are developed in this thesis can be used as a practical tool in further developments of nano devices. Even though present study covers several aspect of nonlinear vibration of CNTs, there are still topics which need further investigations.

- Recent studies show that natural frequency of CNTs are affected by the temperature of their environment. Also experimental Studies have confirmed that the actual mass sensor performance is significantly affected by the variations of environment temperature. Hence, the effect of temperature on variation of natural frequency in the presence of nonlinearities can be a topic for future investigations.
- Recently, CNTs have been suggested to be used in fluid delivery nano mechanics. Therefore, another important subject can be the effect of conveying fluid on the system natural frequency.
- Eringen nonlocal theory was used in this thesis to model the size effects. Here it was shown that besides the plus points of using this theory, Eringen theory has its own shortfalls where the system natural frequency can become complex (unstable) as nonlocal parameter in Eringen theory increases more than a certain value. On the other hand, theories which include the atomic interactions are not limited to Eringen theory and there exist other theories such as couple stress elasticity theory, strain gradient theory, and modified couple stress theory which include nonlocality. Therefore, a thorough study to investigate and compare the advantages and shortfalls of these nonlocal theories can be a subject of a future investigation.
- In the present study, since the maximum vibration amplitude of the CNTs is limited to small vibration amplitudes, it is assumed that the cross section of CNTs remains circular during the nonlinear bending. It is worth mentioning that the present study studied the nonlinear bending up to the bending angle of 15 degree. However, Molecular dynamic simulations [69] concluded that for bending angles more than 30 degree the cross section of tube did not remain circular. Hence, a study using theorems where it consider the effect of cross section change can be a subject of a future investigation in studying the large bending angles.

- Last but not least, Euler Bernoulli beam theory was used in this thesis. However, for beams with length to diameter less than ten, Timoshenko beam or higher order beam theories can be used in future studies to get better responses.

REFERENCES

[1] R.H. Baughman, A.A. Zakhidov, W.A. de Heer, Carbon nanotubes - the route toward applications, Science, 297 (2002) 787-792.

[2] C. Li, E.T. Thostenson, T.W. Chou, Sensors and actuators based on carbon nanotubes and their composites: A review, Compos Sci Technol, 68 (2008) 1227-1249.

[3] R.F. Gibson, E.O. Ayorinde, Y.F. Wen, Vibrations of carbon nanotubes and their composites: A review, Compos Sci Technol, 67 (2007) 1-28.

[4] X.S. Wang, Q.Q. Li, J. Xie, Z. Jin, J.Y. Wang, Y. Li, K.L. Jiang, S.S. Fan, Fabrication of Ultralong and Electrically Uniform Single-Walled Carbon Nanotubes on Clean Substrates, Nano Lett, 9 (2009) 3137-3141.

[5] AlexanderAlUS, Graphene Sheet, in, Wikipedia, Wikipedia, 2010.

[6] A.K. Geim, K.S. Novoselov, The rise of graphene, Nat Mater, 6 (2007) 183-191.

[7] S. Iijima, Helical Microtubules of Graphitic Carbon, Nature, 354 (1991) 56-58.

[8] S. Bellucci, Carbon nanotubes: physics and applications, physica status solidi (c), 2 (2005) 34-47.

[9] M. Meo, M. Rossi, Prediction of Young's modulus of single wall carbon nanotubes by molecular-mechanics based finite element modelling, Compos Sci Technol, 66 (2006) 1597-1605.

[10] C.Y. Li, T.W. Chou, Elastic moduli of multi-walled carbon nanotubes and the effect of van der Waals forces, Compos Sci Technol, 63 (2003) 1517-1524.

[11] Wikipedia, Carbon nanotube; from Wikipedia, the free encyclopedia, in, Wikipedia, Web, 2014.

[12] P. Poncharal, Z.L. Wang, D. Ugarte, W.A. de Heer, Electrostatic deflections and electromechanical resonances of carbon nanotubes, Science, 283 (1999) 1513-1516.

[13] A.Y. Joshi, S.P. Harsha, S.C. Sharma, Vibration signature analysis of single walled carbon nanotube based nanomechanical sensors, Physica E, 42 (2010) 2115-2123.

[14] A.Y. Joshi, S.C. Sharma, S.P. Harsha, Dynamic Analysis of a Clamped Wavy Single Walled Carbon Nanotube Based Nanomechanical Sensors, Journal of Nanotechnology in Engineering and Medicine, 1 (2010) 031007-031007.

[15] C.T.C. Nguyen, Frequency-selective MEMS for miniaturized low-power communication devices, Ieee T Microw Theory, 47 (1999) 1486-1503.

[16] B.J. Aleman, A. Sussman, W. Mickelson, A. Zettl, A Carbon Nanotube-based NEMS Parametric Amplifier for Enhanced Radio Wave Detection and Electronic Signal Amplification, J Phys Conf Ser, 302 (2011).

[17] A. Cho, Physics - Researchers race to put the quantum into mechanics, Science, 299 (2003) 36-37.

[18] M.D. LaHaye, O. Buu, B. Camarota, K.C. Schwab, Approaching the quantum limit of a nanomechanical resonator, Science, 304 (2004) 74-77.

[19] V. Sazonova, Y. Yaish, H. Ustunel, D. Roundy, T.A. Arias, P.L. McEuen, A tunable carbon nanotube electromechanical oscillator, Nature, 431 (2004) 284-287.

[20] Q.S. Zheng, Q. Jiang, Multiwalled carbon nanotubes as gigahertz oscillators, Phys Rev Lett, 88 (2002).

[21] S.B. Legoas, V.R. Coluci, S.F. Braga, P.Z. Coura, S.O. Dantas, D.S. Galvao, Molecular-dynamics simulations of carbon nanotubes as gigahertz oscillators, Phys Rev Lett, 90 (2003).

[22] Y. Zhao, C.C. Ma, G.H. Chen, Q. Jiang, Energy dissipation mechanisms in carbon nanotube oscillators, Phys Rev Lett, 91 (2003).

[23] S.B. Legoas, V.R. Coluci, S.F. Braga, P.Z. Coura, S. Dantas, D.S. Galvao, Gigahertz nanomechanical oscillators based on carbon nanotubes, Nanotechnology, 15 (2004) S184-S189.

[24] J.W. Kang, O.K. Kwon, A molecular dynamics simulation study on resonance frequencies comparison of tunable carbon-nanotube resonators, Appl Surf Sci, 258 (2012) 2014-2016.

[25] H.J. Dai, J.H. Hafner, A.G. Rinzler, D.T. Colbert, R.E. Smalley, Nanotubes as nanoprobes in scanning probe microscopy, Nature, 384 (1996) 147-150.

[26] J. Tang, G. Yang, Q. Zhang, A. Parhat, B. Maynor, J. Liu, L.C. Qin, O. Zhou, Rapid and reproducible fabrication of carbon nanotube AFM probes by dielectrophoresis, Nano Lett, 5 (2005) 11-14.

[27] T. Rueckes, K. Kim, E. Joselevich, G.Y. Tseng, C.L. Cheung, C.M. Lieber, Carbon nanotube-based nonvolatile random access memory for molecular computing, Science, 289 (2000) 94-97.

[28] C.H. Ke, H.D. Espinosa, Feedback controlled nanocantilever device, Appl Phys Lett, 85 (2004) 681-683.

[29] K.E. Engstrom, J.M. Kinaret, Performance gain through dynamic control of device geometry: Nanoelectromechanical carbon nanotube-based switch, Ieee Electr Device L, 27 (2006) 988-991.

[30] K.E. Drexler, Nanosystems : molecular machinery, manufacturing, and computation, Wiley, New York, 1992.

[31] D. Srivastava, A phenomenological model of the rotation dynamics of carbon nanotube gears with laser electric fields, Nanotechnology, 8 (1997) 186-192.

[32] A.M. Fennimore, T.D. Yuzvinsky, W.Q. Han, M.S. Fuhrer, J. Cumings, A. Zettl, Rotational actuators based on carbon nanotubes, Nature, 424 (2003) 408-410.

[33] J. Yoon, C.Q. Ru, A. Mioduchowski, Vibration of an embedded multiwall carbon nanotube, Compos Sci Technol, 63 (2003) 1533-1542.

[34] L.L. Ke, Y. Xiang, J. Yang, S. Kitipornchai, Nonlinear free vibration of embedded double-walled carbon nanotubes based on nonlocal Timoshenko beam theory, Computational Materials Science, 47 (2009) 409-417.

[35] H. Fekrmandi, M. Rezaee, A Theoretical and Experimental Investigation on Free Vibration Behavior of a Cantilever Beam with a Breathing Crack, Shock and Vibration, 19 (2011) 175-186.

[36] R. Ansari, S. Sahmani, H. Rouhi, Axial buckling analysis of single-walled carbon nanotubes in thermal environments via the Rayleigh–Ritz technique, Computational Materials Science, 50 (2011) 3050-3055.

[37] M. Şimşek, Vibration analysis of a single-walled carbon nanotube under action of a moving harmonic load based on nonlocal elasticity theory, Physica E: Low-dimensional Systems and Nanostructures, 43 (2010) 182-191.

[38] C.Y. Wang, C.Q. Ru, A. Mioduchowski, Orthotropic elastic shell model for buckling of microtubules, Phys Rev E, 74 (2006) 1-4.

[39] Y. Yan, L.X. Zhang, W.Q. Wang, Dynamical mode transitions of simply supported double-walled carbon nanotubes based on an elastic shell model, J Appl Phys, 103 (2008) 1-6.

[40] M.S. Hoseinzadeh, S.E. Khadem, Thermoelastic vibration and damping analysis of double-walled carbon nanotubes based on shell theory, Physica E, 43 (2011) 1146-1154.

[41] A.C. Eringen, On Differential-Equations of Nonlocal Elasticity and Solutions of Screw Dislocation and Surface-Waves, J Appl Phys, 54 (1983) 4703-4710.

[42] R.F. Gibson, E.O. Ayorinde, Y.-F. Wen, Vibrations of carbon nanotubes and their composites: A review, Compos Sci Technol, 67 (2007) 1-28.

[43] K.B. Mustapha, Z.W. Zhong, Free transverse vibration of an axially loaded non-prismatic single-walled carbon nanotube embedded in a two-parameter elastic medium, Computational Materials Science, 50 (2010) 742-751.

[44] Y. Fu, J. Hong, X. Wang, Analysis of nonlinear vibration for embedded carbon nanotubes, J Sound Vib, 296 (2006) 746-756.

[45] M.H. Mahdavi, L.Y. Jiang, X. Sun, Nonlinear vibration of a single-walled carbon nanotube embedded in a polymer matrix aroused by interfacial van der Waals forces, Journal of Applied Physics, 106 (2009) 1-8.

[46] J. Yang, L.L. Ke, S. Kitipornchai, Nonlinear free vibration of single-walled carbon nanotubes using nonlocal Timoshenko beam theory, Physica E, 42 (2010) 1727-1735.

[47] Y. Lanir, Y.C.B. Fung, Fiber Composite Columns under Compression, J Compos Mater, 6 (1972) 387-401.

[48] L.Y. Jiang, Y. Huang, H. Jiang, G. Ravichandran, H. Gao, K.C. Hwang, B. Liu, A cohesive law for carbon nanotube/polymer interfaces based on the van der Waals force, J Mech Phys Solids, 54 (2006) 2436-2452.

[49] W.B. Lu, J. Wu, L.Y. Jiang, Y. Huang, K.C. Hwang, B. Liu, A cohesive law for multi-wall carbon nanotubes, Philos Mag, 87 (2007) 2221-2232.

[50] W.B. Lu, J. Wu, J. Song, K.C. Hwang, L.Y. Jiang, Y. Huang, A cohesive law for interfaces between multi-wall carbon nanotubes and polymers due to the van der Waals interactions, Comput Method Appl M, 197 (2008) 3261-3267.

[51] K.Y. Xu, X.N. Guo, C.Q. Ru, Vibration of a double-walled carbon nanotube aroused by nonlinear intertube van der Waals forces, J Appl Phys, 99 (2006) 1-7.

[52] A. Khosrozadeh, M.A. Hajabasi, Free vibration of embedded double-walled carbon nanotubes considering nonlinear interlayer van der Waals forces, Appl Math Model, 36 (2011) 997–1007.

[53] M.H. Mahdavi, L.Y. Jiang, X. Sun, Nonlinear vibration of a double-walled carbon nanotube embedded in a polymer matrix, Physica E: Low-dimensional Systems and Nanostructures, 43 (2011) 1813-1819.

[54] A.Y. Joshi, A. Bhatnagar, S.P. Harsha, S.C. Sharma, Vibration Response Analysis of Doubly Clamped Single Walled Wavy Carbon Nanotube Based Nanomechanical Sensors, Journal of Nanotechnology in Engineering and Medicine, 1 (2010) 031004-031004.

[55] P. Soltani, A. Kassaei, M. Taherian, A. Farshidianfar, Vibration of wavy single-walled carbon nanotubes based on nonlocal Euler Bernoulli and Timoshenko models, Int J Adv Struct Eng, 4 (2012) 1-10.

[56] S.W. Shaw, C. Pierre, Normal-Modes of Vibration for Nonlinear Continuous Systems, J Sound Vib, 169 (1994) 319-347.

[57] M.M.J. Treacy, T.W. Ebbesen, J.M. Gibson, Exceptionally high Young's modulus observed for individual carbon nanotubes, Nature, 381 (1996) 678-680.

[58] A. Krishnan, E. Dujardin, T.W. Ebbesen, P.N. Yianilos, M.M.J. Treacy, Young's modulus of single-walled nanotubes, Phys Rev B, 58 (1998) 14013-14019.

[59] E.W. Wong, P.E. Sheehan, C.M. Lieber, Nanobeam mechanics: Elasticity, strength, and toughness of nanorods and nanotubes, Science, 277 (1997) 1971-1975.

[60] M.F. Yu, O. Lourie, M.J. Dyer, K. Moloni, T.F. Kelly, R.S. Ruoff, Strength and breaking mechanism of multiwalled carbon nanotubes under tensile load, Science, 287 (2000) 637-640.

[61] D.E.H. Jones, Science of fullerenes and carbon nanotubes - Dresselhaus,MS, Dresselhaus,G, Eklund,PC, Nature, 381 (1996) 384-384.

[62] M.S. Dresselhaus, P. Avouris, Introduction to carbon materials research, Top Appl Phys, 80 (2001) 1-9.

[63] D. Qian, M.-F. Yu, R.S. Ruoff, G.J. Wagner, W.K. Liu, Mechanics of carbon nanotubes, Applied Mechanics Reviews, 55 (2002) 495-533.

[64] J.C. Charlier, Defects in carbon nanotubes, Accounts Chem Res, 35 (2002) 1063-1069.

[65] A.V. Krasheninnikov, K. Nordlund, Irradiation effects in carbon nanotubes, Nucl Instrum Meth B, 216 (2004) 355-366.

[66] K. Tada, S. Furuya, K. Watanabe, Ab initio study of hydrogen adsorption to single-walled carbon nanotubes, Phys Rev B, 63 (2001).

[67] V. Derycke, R. Martel, M. Radosvljevic, F.M.R. Ross, P. Avouris, Catalyst-free growth of ordered single-walled carbon nanotube networks, Nano Lett, 2 (2002) 1043-1046.

[68] I. Kaplan-Ashiri, S.R. Cohen, K. Gartsman, V. Ivanovskaya, T. Heine, G. Seifert, I. Wiesel, H.D. Wagner, R. Tenne, On the mechanical behavior of WS2 nanotubes under axial tension and compression, P Natl Acad Sci USA, 103 (2006) 523-528.

[69] S. Iijima, C. Brabec, A. Maiti, J. Bernholc, Structural flexibility of carbon nanotubes, J Chem Phys, 104 (1996) 2089-2092.

[70] J. Bernholc, C. Brabec, M.B. Nardelli, A. Maiti, C. Roland, B.I. Yakobson, Theory of growth and mechanical properties of nanotubes, Appl Phys a-Mater, 67 (1998) 39-46.

[71] B.I. Yakobson, C.J. Brabec, J. Bernholc, Nanomechanics of carbon tubes: Instabilities beyond linear response, Phys Rev Lett, 76 (1996) 2511-2514.

[72] C.Y. Li, T.W. Chou, Single-walled carbon nanotubes as ultrahigh frequency nanomechanical resonators, Phys Rev B, 68 (2003).

[73] C.Y. Li, T.W. Chou, Vibrational behaviors of multiwalled-carbon-nanotube-based nanomechanical resonators, Appl Phys Lett, 84 (2004) 121-123.

[74] M. Mir, A. Hosseini, G.H. Majzoobi, A numerical study of vibrational properties of single-walled carbon nanotubes, Computational Materials Science, 43 (2008) 540-548.

[75] J.N. Lu, H.B. Chen, P. Lu, P.Q. Zhang, Research of natural frequency of single-walled carbon nanotube, Chinese J Chem Phys, 20 (2007) 525-530.

[76] Z.L. Wang, R.P. Gao, Z.W. Pan, Z.R. Dai, Nano-scale mechanics of nanotubes, nanowires, and nanobelts, Adv Eng Mater, 3 (2001) 657-661.

[77] J. Yoon, C.Q. Ru, A. Mioduchowski, Noncoaxial resonance of an isolated multiwall carbon nanotube, Phys Rev B, 66 (2002).

[78] Y.Q. Zhang, G.R. Liu, X. Han, Transverse vibrations of double-walled carbon nanotubes under compressive axial load, Phys Lett A, 340 (2005) 258-266.

[79] Y.G. Hu, K.M. Liew, Q. Wang, Nonlocal elastic beam models for flexural wave propagation in double-walled carbon nanotubes, J Appl Phys, 106 (2009).

[80] J. Yoon, C.Q. Ru, A. Mioduchowski, Terahertz vibration of short carbon nanotubes modeled as Timoshenko beams, J Appl Mech-T Asme, 72 (2005) 10-17.

[81] Q. Wang, V.K. Varadan, Wave characteristics of carbon nanotubes, Int J Solids Struct, 43 (2006) 254-265.

[82] Y.Y. Zhang, C.M. Wang, V.B.C. Tan, Buckling of multiwalled carbon nanotubes using timoshenko beam theory, J Eng Mech-Asce, 132 (2006) 952-958.

[83] S. Timoshenko, D.H. Young, W. Weaver, Vibration problems in engineering, 4th ed., Wiley, New York,, 1974.

[84] I.H. Shames, C.L. Dym, Energy and finite element methods in structural mechanics, SI units ed., Taylor & Francis, New York, 1991.

[85] C.M. Wang, Y.Y. Zhang, X.Q. He, Vibration of nonlocal Timoshenko beams, Nanotechnology, 18 (2007).

[86] T.C. Chang, A molecular based anisotropic shell model for single-walled carbon nanotubes, J Mech Phys Solids, 58 (2010) 1422-1433.

[87] C.Y. Wang, C.Q. Ru, A. Mioduchowski, Applicability and limitations of simplified elastic shell equations for carbon nanotubes, J Appl Mech-T Asme, 71 (2004) 622-631.

[88] C.Y. Wang, C.Q. Ru, A. Mioduchowski, Axisymmetric and beamlike vibrations of multiwall carbon nanotubes, Phys Rev B, 72 (2005).

[89] C.Y. Wang, L.C. Zhang, An elastic shell model for characterizing single-walled carbon nanotubes, Nanotechnology, 19 (2008).

[90] S.S. Gupta, R.C. Batra, Continuum structures equivalent in normal mode vibrations to single-walled carbon nanotubes, Computational Materials Science, 43 (2008) 715-723.

[91] C.Y. Wang, C.F. Li, S. Adhikari, Axisymmetric vibration of single-walled carbon nanotubes in water, Phys Lett A, 374 (2010) 2467-2474.

[92] M. Cinefra, E. Carrera, S. Brischetto, Refined Shell Models for the Vibration Analysis of Multiwalled Carbon Nanotubes, Mech Adv Mater Struc, 18 (2011) 476-483.

[93] R. Ansari, H. Rouhi, S. Sahmani, Calibration of the analytical nonlocal shell model for vibrations of double-walled carbon nanotubes with arbitrary boundary conditions using molecular dynamics, Int J Mech Sci, 53 (2011) 786-792.

[94] C.M. Wang, Z.Y. Tay, A.N.R. Chowdhuary, W.H. Duan, Y.Y. Zhang, N. Silvestre, Examination of Cylindrical Shell Theories for Buckling of Carbon Nanotubes, Int J Struct Stab Dy, 11 (2011) 1035-1058.

[95] J. Peng, J. Wu, K.C. Hwang, J. Song, Y. Huang, Can a single-wall carbon nanotube be modeled as a thin shell?, J Mech Phys Solids, 56 (2008) 2213-2224.

[96] L.H. Donnell, Stability of thin-walled tubes under torsion, U. S. Govt. print. off., Washington,, 1933.

[97] J.L. SANDERS, Non-linear theories for thin shells, Quart J Appl Math, 21 (1963) 21–36.

[98] J. Peddieson, G.R. Buchanan, R.P. McNitt, Application of nonlocal continuum models to nanotechnology, Int J Eng Sci, 41 (2003) 305-312.

[99] L.J. Sudak, Column buckling of multiwalled carbon nanotubes using nonlocal continuum mechanics, J Appl Phys, 94 (2003) 7281-7287.

[100] Q. Wang, K.M. Liew, Application of nonlocal continuum mechanics to static analysis of micro- and nano-structures, Phys Lett A, 363 (2007) 236-242.

[101] Q. Wang, Wave propagation in carbon nanotubes via nonlocal continuum mechanics, J Appl Phys, 98 (2005).

[102] P. Lu, H.P. Lee, C. Lu, P.Q. Zhang, Application of nonlocal beam models for carbon nanotubes, Int J Solids Struct, 44 (2007) 5289-5300.

[103] S. Narendar, Terahertz wave propagation in uniform nanorods: A nonlocal continuum mechanics formulation including the effect of lateral inertia, Physica E, 43 (2011) 1015-1020.

[104] M.C. Ece, M. Aydogdu, Nonlocal elasticity effect on vibration of in-plane loaded double-walled carbon nano-tubes, Acta Mech, 190 (2007) 185-195.

[105] M. Simsek, Vibration analysis of a single-walled carbon nanotube under action of a moving harmonic load based on nonlocal elasticity theory, Physica E, 43 (2010) 182-191.

[106] C. Demir, O. Civalek, B. Akgoz, Free Vibration Analysis of Carbon Nanotubes Based on Shear Deformable Beam Theory by Discrete Singular Convolution Technique, Math Comput Appl, 15 (2010) 57-65.

[107] B. Arash, Q. Wang, A review on the application of nonlocal elastic models in modeling of carbon nanotubes and graphenes, Computational Materials Science, 51 (2012) 303-313.

[108] Y.G. Hu, K.M. Liew, Q. Wang, X.Q. He, B.I. Yakobson, Nonlocal shell model for elastic wave propagation in single- and double-walled carbon nanotubes, J Mech Phys Solids, 56 (2008) 3475-3485.

[109] N. Silvestre, Length dependence of critical measures in single-walled carbon nanotubes, Int J Solids Struct, 45 (2008) 4902-4920.

[110] R. Rafiee, R.M. Moghadam, On the modeling of carbon nanotubes: A critical review, Compos Part B-Eng, 56 (2014) 435-449.

[111] S.I. Lee, S.W. Howell, A. Raman, R. Reifenberger, C.V. Nguyen, M. Meyyappan, Nonlinear tapping dynamics of multi-walled carbon nanotube tipped atomic force microcantilevers, Nanotechnology, 15 (2004) 416-421.

[112] R.M.D. Stevens, N.A. Frederick, B.L. Smith, D.E. Morse, G.D. Stucky, P.K. Hansma, Carbon nanotubes as probes for atomic force microscopy, Nanotechnology, 11 (2000) 1-5.

[113] Y.M. Fu, J.W. Hong, X.Q. Wang, Analysis of nonlinear vibration for embedded carbon nanotubes, J Sound Vib, 296 (2006) 746-756.

[114] B. Lassagne, Y. Tarakanov, J. Kinaret, D. Garcia-Sanchez, A. Bachtold, Coupling Mechanics to Charge Transport in Carbon Nanotube Mechanical Resonators, Science, 325 (2009) 1107-1110.

[115] G.A. Steele, A.K. Huttel, B. Witkamp, M. Poot, H.B. Meerwaldt, L.P. Kouwenhoven, H.S.J. van der Zant, Strong Coupling Between Single-Electron Tunneling and Nanomechanical Motion, Science, 325 (2009) 1103-1107.

[116] I. Kozinsky, H.W.C. Postma, I. Bargatin, M.L. Roukes, Tuning nonlinearity, dynamic range, and frequency of nanomechanical resonators, Appl Phys Lett, 88 (2006).

[117] R.B. Karabalin, M.C. Cross, M.L. Roukes, Nonlinear dynamics and chaos in two coupled nanomechanical resonators, Phys Rev B, 79 (2009).

[118] J.S. Aldridge, A.N. Cleland, Noise-enabled precision measurements of a duffing nanomechanical resonator, Phys Rev Lett, 94 (2005).

[119] H.N. Cho, M.F. Yu, A.F. Vakakis, L.A. Bergman, D.M. McFarland, Tunable, Broadband Nonlinear Nanomechanical Resonator, Nano Lett, 10 (2010) 1793-1798.

[120] K.L. Ekinci, Y.T. Yang, M.L. Roukes, Ultimate limits to inertial mass sensing based upon nanoelectromechanical systems, J Appl Phys, 95 (2004) 2682-2689.

[121] E. Cigeroglu, H. Samandari, Nonlinear free vibration of double walled carbon nanotubes by using describing function method with multiple trial functions, Physica E, 46 (2012) 160-173.

[122] H. Samandari, E. Cigeroglu, Nonlinear Free Vibration of Curved Double Walled Carbon Nanotubes Using Differential Quadrature Method, in: G. Kerschen, D. Adams, A. Carrella (Eds.) Topics in Nonlinear Dynamics, Volume 1, Springer New York, 2013, pp. 269-279.

[123] I. Mehdipour, A. Barari, A. Kimiaeifar, G. Domairry, Vibrational analysis of curved single-walled carbon nanotube on a Pasternak elastic foundation, Adv Eng Softw, 48 (2012) 1-5.

[124] H. Samandari, E. Cigeroglu, Effect of waviness on the variation of nonlinear fundamental natural frequency of single wall carbon nanotube by using multiple harmonic

balance method, in: 2012 Space Elevator Conference, International Space Elevator Consortium, Museum of Flight, Seattle, Washington, USA, 2012, pp. 14.

[125] H. Mohammadi, M. Mahzoon, M. Mohammadi, M. Mohammadi, Postbuckling instability of nonlinear nanobeam with geometric imperfection embedded in elastic foundation, Nonlinear Dyn, 76 (2014) 2005-2016.

[126] F.N. Mayoof, M.A. Hawwa, Chaotic behavior of a curved carbon nanotube under harmonic excitation, Chaos Soliton Fract, 42 (2009) 1860-1867.

[127] X. Wang, X.Y. Wang, J. Xiao, A non-linear analysis of the bending modulus of carbon nanotubes with rippling deformations, Compos Struct, 69 (2005) 315-321.

[128] Y.M. Fu, R.G. Bi, P. Zhang, Nonlinear Dynamic Instability of Double-Walled Carbon Nanotubes under Periodic Excitation, Acta Mech Solida Sin, 22 (2009) 206-212.

[129] Y.D. Kuang, X.Q. He, C.Y. Chen, G.Q. Li, Analysis of nonlinear vibrations of double-walled carbon nanotubes conveying fluid, Computational Materials Science, 45 (2009) 875-880.

[130] A.K. Huttel, G.A. Steele, B. Witkamp, M. Poot, L.P. Kouwenhoven, H.S.J. van der Zant, Carbon Nanotubes as Ultrahigh Quality Factor Mechanical Resonators, Nano Lett, 9 (2009) 2547-2552.

[131] H.M. Ouakad, M.I. Younis, Nonlinear Dynamics of Electrically Actuated Carbon Nanotube Resonators, J Comput Nonlin Dyn, 5 (2010).

[132] L.L. Ke, J. Yang, S. Kitipornchai, Nonlinear free vibration of functionally graded carbon nanotube-reinforced composite beams, Compos Struct, 92 (2010) 676-683.

[133] M.A. Hawwa, H.M. Al-Qahtani, Nonlinear oscillations of a double-walled carbon nanotube, Computational Materials Science, 48 (2010) 140-143.

[134] R. Ansari, M. Hemmatnezhad, H. Ramezannezhad, Application of HPM to the Nonlinear Vibrations of Multiwalled Carbon Nanotubes, Numer Meth Part D E, 26 (2010) 490-500.

[135] H. Jannesari, H. Rafii-Tabar, M.D. Emami, Computational Modelling of Stability of a Single-Walled Carbon Nanotube Modelled as a Non-Linear Donnell Shallow Shell Conveying a Non-Viscous Flowing Fluid, J Comput Theor Nanos, 8 (2011) 51-59.

[136] H.S. Shen, C.L. Zhang, Nonlocal beam model for nonlinear analysis of carbon nanotubes on elastomeric substrates, Computational Materials Science, 50 (2011) 1022-1029.

[137] Y. Yan, W.Q. Wang, L.X. Zhang, Applied multiscale method to analysis of nonlinear vibration for double-walled carbon nanotubes, Appl Math Model, 35 (2011) 2279-2289.

[138] Z.X. Wang, H.S. Shen, Nonlinear vibration of nanotube-reinforced composite plates in thermal environments, Computational Materials Science, 50 (2011) 2319-2330.

[139] H.M. Ouakad, M.I. Younis, Natural frequencies and mode shapes of initially curved carbon nanotube resonators under electric excitation, J Sound Vib, 330 (2011) 3182-3195.

[140] A.Y. Joshi, S.C. Sharma, S.P. Harsha, Nonlinear Dynamic Analysis of Single-Walled Carbon Nanotube Based Mass Sensor, Journal of Nanotechnology in Engineering and Medicine, 2 (2012) 041008-041008.

[141] Y. Yang, C.W. Lim, Non-classical stiffness strengthening size effects for free vibration of a nonlocal nanostructure, Int J Mech Sci, 54 (2012) 57-68.

[142] H.M. Ouakad, M.I. Younis, Dynamic response of slacked single-walled carbon nanotube resonators, Nonlinear Dyn, 67 (2012) 1419-1436.

[143] R. Ansari, M. Hemmatnezhad, Nonlinear finite element analysis for vibrations of double-walled carbon nanotubes, Nonlinear Dyn, 67 (2012) 373-383.

[144] H. Samandari, E. Cigeroglu, Nonlinear Free Vibration Analysis of Double Walled Carbon Nanotubes with a Concentrated-Mass, in: 15th International Conference on Machine Design and Production Pamukkale, Denizli, Turkey, 2012, pp. 18.

[145] A. Farshidianfar, P. Soltani, Nonlinear flow-induced vibration of a SWCNT with a geometrical imperfection, Computational Materials Science, 53 (2012) 105-116.

[146] R. Ansari, H. Ramezannezhad, R. Gholami, Nonlocal beam theory for nonlinear vibrations of embedded multiwalled carbon nanotubes in thermal environment, Nonlinear Dyn, 67 (2012) 2241-2254.

[147] H.S. Shen, Y. Xiang, Nonlinear vibration of nanotube-reinforced composite cylindrical shells in thermal environments, Comput Method Appl M, 213 (2012) 196-205.

[148] A. Hajnayeb, S.E. Khadem, Nonlinear vibration and stability analysis of a double-walled carbon nanotube under electrostatic actuation, J Sound Vib, 331 (2012) 2443-2456.

[149] M. Rafiee, S. Mareishi, M. Mohammadi, An investigation on primary resonance phenomena of elastic medium based single walled carbon nanotubes, Mech Res Commun, 44 (2012) 51-56.

[150] R. Ansari, R. Gholami, M.A. Darabi, Nonlinear free vibration of embedded double-walled carbon nanotubes with layerwise boundary conditions, Acta Mech, 223 (2012) 2523-2536.

[151] A.G. Arani, M.S. Zarei, S. Amir, Z.K. Maraghi, Nonlinear nonlocal vibration of embedded DWCNT conveying fluid using shell model, Physica B, 410 (2013) 188-196.

[152] M. Rafiee, J. Yang, S. Kitipornchai, Large amplitude vibration of carbon nanotube reinforced functionally graded composite beams with piezoelectric layers, Compos Struct, 96 (2013) 716-725.

[153] B. Fang, Y.X. Zhen, C.P. Zhang, Y. Tang, Nonlinear vibration analysis of double-walled carbon nanotubes based on nonlocal elasticity theory, Appl Math Model, 37 (2013) 1096-1107.

[154] L.W. Zhang, Z.X. Lei, K.M. Liew, J.L. Yu, Large deflection geometrically nonlinear analysis of carbon nanotube-reinforced functionally graded cylindrical panels, Comput Method Appl M, 273 (2014) 1-18.

[155] P. Soltani, A. Kassaei, M.M. Taherian, Nonlinear and Quasi-Linear Behavior of a Curved Carbon Nanotube Vibrating in an Electric Force Field; an Analytical Approach, Acta Mech Solida Sin, 27 (2014) 97-110.

[156] S. Souayeh, N. Kacem, Computational models for large amplitude nonlinear vibrations of electrostatically actuated carbon nanotube-based mass sensors, Sensor Actuat a-Phys, 208 (2014) 10-20.

[157] Y.L. Kuo, Chaotic Analysis of the Geometrically Nonlinear Nonlocal Elastic Single-Walled Carbon Nanotubes on Elastic Medium, J Nanosci Nanotechno, 14 (2014) 2352-2360.

[158] E. Cigeroglu, H. Samandari, Nonlinear free Vibrations of curved double walled carbon Nanotubes using differential quadrature method, Physica E: Low-dimensional Systems and Nanostructures, DOI: 10.1016/j.physe.2014.07.010 (2014).

[159] M.H. Mahdavi, L.Y. Jiang, X. Sun, Nonlinear vibration of a single-walled carbon nanotube embedded in a polymer matrix aroused by interfacial van der Waals forces, Journal of Applied Physics, 106 (2009) 114309.

[160] Z.-B. Shen, X.-F. Li, L.-P. Sheng, G.-J. Tang, Transverse vibration of nanotube-based micro-mass sensor via nonlocal Timoshenko beam theory, Computational Materials Science, 53 (2012) 6.

[161] R. Chowdhury, S. Adhikari, J. Mitchell, Vibrating carbon nanotube based bio-sensors, Physica E: Low-dimensional Systems and Nanostructures, 42 (2009) 5.

[162] I. Mehdipour, A. Barari, G. Domairry, Application of a cantilevered SWCNT with mass at the tip as a nanomechanical sensor, Computational Materials Science, 50 (2011) 3.

[163] K.Y. Xu, X.N. Guo, C.Q. Ru, Vibration of a double-walled carbon nanotube aroused by nonlinear intertube van der Waals forces, Journal of Applied Physics, 99 (2006) 064303.

[164] M.E. Yumer, E. Cigeroglu, H.N. Ozguven, Mistuning Identification of Bladed Disks Utilizing Neural Networks, in: Proceedings of the Asme Turbo Expo 2010, Vol 6, Pts a and B, 2010, pp. 601-610.

[165] C. Boral, E. Cigeroglu, I. Korkmaz, Effect of Intentional Dry Friction Damping on the Performance of an Elastomeric Engine Mount, in: Proceedings of the Asme 10th Biennial Conference on Engineering Systems Design and Analysis, 2010, Vol 3, 2010, pp. 59-66.

[166] A.H. Nayfeh, B. Balachandran, Applied nonlinear dynamics : analytical, computational, and experimental methods, Wiley, New York, 1995.

[167] M. El-Mously, A Timoshenko-beam-on-Pasternak-foundation analogy for cylindrical shells, J Sound Vib, 261 (2003) 635-652.

[168] W. Burghard, Handbook for biologists, toxicologists, physicians and pharmacists, Kriminalistik, 54 (2000) 628-628.

[169] P. Soltani, P. Bahar, A. Farshidianfar, An efficient GDQ model for vibration analysis of a multiwall carbon nanotube on Pasternak foundation with general boundary conditions, P I Mech Eng C-J Mec, 225 (2011) 1730-1741.

[170] E. Budak, H.N. Özgüven, A new method for harmonic response of structures with symmetrical non-linearities, in: Fifteenth International Modal Analysis Seminar, Leaven, 1990.

[171] M.B. Ozer, H.N. Ozguven, T.J. Royston, Identification of structural non-linearities using describing functions and the Sherman-Morrison method, Mech Syst Signal Pr, 23 (2009) 30-44.

[172] E. Cigeroglu, H.N. Ozguven, Nonlinear vibration analysis of bladed disks with dry friction dampers, J Sound Vib, 295 (2006) 1028-1043.

[173] O. Tanrikulu, B. Kuran, H.N. Ozguven, M. Imregun, Forced Harmonic Response Analysis of Nonlinear Structures Using Describing Functions, Aiaa J, 31 (1993) 1313-1320.

[174] J.V. Ferreira, D.J. Ewins, Nonlinear receptance coupling approach based on describing functions, in: Proceedings of the 14th International Modal Analysis Conference, Vols I & Ii, 1996, pp. 1034-1040.

[175] R. Ansari, M. Hemmatnezhad, Nonlinear vibrations of embedded multi-walled carbon nanotubes using a variational approach, Math Comput Model, 53 (2011) 927-938.

[176] M. Janghorban, A. Zare, Free vibration analysis of functionally graded carbon nanotubes with variable thickness by differential quadrature method, Physica E: Low-dimensional Systems and Nanostructures, 43 (2011) 1602–1604.

[177] T. Murmu, S.C. Pradhan, Thermo-mechanical vibration of a single-walled carbon nanotube embedded in an elastic medium based on nonlocal elasticity theory, Computational Materials Science, 46 (2009) 854-859.

[178] Z.H. Yang, An Acceleration Method in the Homotopy Newton Continuation for Nonlinear Singular Problems, J Comput Math, 6 (1988) 1-6.

[179] T.M. Wu, A study of convergence on the Newton-homotopy continuation method, Appl Math Comput, 168 (2005) 1169-1174.

[180] G. von Groll, D.J. Ewins, The harmonic balance method with arc-length continuation in rotor/stator contact problems, J Sound Vib, 241 (2001) 223-233.

[181] P.M. Jelf, N.A. Fleck, Compression Failure Mechanisms in Unidirectional Composites, J Compos Mater, 26 (1992) 2706-2726.

[182] A.A. Abrikosov, L.P. Gorkov, I.E. Dzyaloshinskii, On the Application of Quantum-Field-Theory Methods to Problems of Quantum Statistics at Finite Temperatures, Sov Phys Jetp-Ussr, 9 (1959) 636-641.

[183] M.B. Ozer, H.N. Özgüven, T.J. Royston, Identification of structural non-linearities using describing functions and Sherman–Morrison method, in: Proceedings of the 23rd International Modal Analysis Conference, Orlando, Florida, 2005.

[184] M.H. Mahdavi, L.Y. Jiang, X. Sun, Nonlinear vibration of a double-walled carbon nanotube embedded in a polymer matrix, Physica E, 43 (2011) 1813-1819.

[185] K.Y. Xu, X.N. Guo, C.Q. Ru, Vibration of a double-walled carbon nanotube aroused by nonlinear intertube van der Waals forces, J Appl Phys, 99 (2006).

[186] I. Mehdipour, D.D. Ganji, M. Mozaffari, Application of the energy balance method to nonlinear vibrating equations, Current Applied Physics, 10 (2010) 104-112.

[187] J.H. He, Preliminary report on the energy balance for nonlinear oscillations, Mech Res Commun, 29 (2002) 107-111.

[188] M. Bayat, A. Barari, M. Shahidi, Dynamic response of axially loaded Euler-Bernoulli beams, Mechanika, (2011) 172-177.

[189] A.H. Nayfeh, D.T. Mook, Nonlinear oscillations, Wiley, New York, 1979.

[190] G. Hummer, J.C. Rasaiah, J.P. Noworyta, Water conduction through the hydrophobic channel of a carbon nanotube, Nature, 414 (2001) 188-190.

[191] J. Liu, A.G. Rinzler, H.J. Dai, J.H. Hafner, R.K. Bradley, P.J. Boul, A. Lu, T. Iverson, K. Shelimov, C.B. Huffman, F. Rodriguez-Macias, Y.S. Shon, T.R. Lee, D.T. Colbert, R.E. Smalley, Fullerene pipes, Science, 280 (1998) 1253-1256.

[192] M. Ali-Asgari, H.R. Mirdamadi, M. Ghayour, Coupled effects of nano-size, stretching, and slip boundary conditions on nonlinear vibrations of nano-tube conveying fluid by the homotopy analysis method, Physica E, 52 (2013) 77-85.

[193] A. Lohrasebi, H. Raffii-Tabar, Computational modeling of an ion-driven nanomotor, J Mol Graph Model, 27 (2008) 116-123.

[194] H.L. Tang, D.K. Li, S.M. Zhou, Vibration of horn-shaped carbon nanotube with attached mass via nonlocal elasticity theory, Physica E, 56 (2014) 306-311.

[195] Z.B. Shen, L.P. Sheng, X.F. Li, G.J. Tang, Nonlocal Timoshenko beam theory for vibration of carbon nanotube-based biosensor, Physica E, 44 (2012) 1169-1175.

[196] M.B. Panchal, S.H. Upadhyay, Cantilevered single walled boron nitride nanotube based nanomechanical resonators of zigzag and armchair forms, Physica E, 50 (2013) 73-82.

[197] E. Cigeroglu, H. Samandari, Nonlinear free vibration of double walled carbon nanotubes by using describing function method with multiple trial functions, Physica E: Low-dimensional Systems and Nanostructures, 46 (2012) 160–173.

[198] R. Bellman, J. Casti, Differential Quadrature and Long-Term Integration, J Math Anal Appl, 34 (1971) 235-&.

[199] C.W. Bert, M. Malik, Free vibration analysis of thin cylindrical shells by the differential quadrature method, J Press Vess-T Asme, 118 (1996) 1-12.

[200] O. Civalek, C. Demir, B. Akgoz, Free Vibration and Bending Analyses of Cantilever Microtubules Based on Nonlocal Continuum Model, Math Comput Appl, 15 (2010) 289-298.

[201] L. Wang, Q. Ni, On vibration and instability of carbon nanotubes conveying fluid, Computational Materials Science, 43 (2008) 399-402.

[202] Y.X. Zhen, B. Fang, Thermal-mechanical and nonlocal elastic vibration of single-walled carbon nanotubes conveying fluid, Computational Materials Science, 49 (2010) 276-282.

[203] M. Janghorban, A. Zare, Free vibration analysis of functionally graded carbon nanotubes with variable thickness by differential quadrature method, Physica E, 43 (2011) 1602-1604.

[204] R. Ansari, S. Sahmani, Small scale effect on vibrational response of single-walled carbon nanotubes with different boundary conditions based on nonlocal beam models, Commun Nonlinear Sci, 17 (2012) 1965-1979.

[205] C. Shu, B.E. Richards, Application of Generalized Differential Quadrature to Solve 2-Dimensional Incompressible Navier-Stokes Equations, Int J Numer Meth Fl, 15 (1992) 791-798.

[206] M. Danesh, A. Farajpour, M. Mohammadi, Axial vibration analysis of a tapered nanorod based on nonlocal elasticity theory and differential quadrature method, Mech Res Commun, 39 (2012) 23-27.

[207] M. Abramowitz, I.A. Stegun, Handbook of mathematical functions with formulas, graphs, and mathematical tables, U.S. Govt. Print. Off., Washington,, 1964.

[208] S.C. Pradhan, T. Murmu, Application of nonlocal elasticity and DQM in the flapwise bending vibration of a rotating nanocantilever, Physica E, 42 (2010) 1944-1949.

[209] T. Murmu, S. Adhikari, Scale-dependent vibration analysis of prestressed carbon nanotubes undergoing rotation, J Appl Phys, 108 (2010).

[210] S. Narendar, S. Gopalakrishnan, Nonlocal wave propagation in rotating nanotube, Results in Physics, 1 (2011) 17-25.

[211] S. Narendar, Differential quadrature based nonlocal flapwise bending vibration analysis of rotating nanotube with consideration of transverse shear deformation and rotary inertia, Appl Math Comput, 219 (2012) 1232-1243.

[212] J. Aranda-Ruiz, J. Loya, J. Fernandez-Saez, Bending vibrations of rotating nonuniform nanocantilevers using the Eringen nonlocal elasticity theory, Compos Struct, 94 (2012) 2990-3001.

[213] P. Lu, H.P. Lee, C. Lu, P.Q. Zhang, Dynamic properties of flexural beams using a nonlocal elasticity model, J Appl Phys, 99 (2006).

[214] C. Ng, Y. Zhao, Y. Xiang, G. Wei., On the accuracy and stability of a variety of differential quadrature formulations for the vibration analysis of beams International Journal of Engineering & Applied Sciences, 1(4) (2009) 1-25.

[215] S. Adali, Variational principles for multi-walled carbon nanotubes undergoing non-linear vibrations by semi-inverse method, Micro Nano Lett, 4 (2009) 198-203

APPENDIX A. Nonlinear equations of motion

The mid-plan stretching relation of a beam which goes through of large deformation can be determined using Figure A.1. Figure A.1 shows how a point A_i with coordinates of x_i and z_i in the axial and transverse directions respectively moves to a point A_f with coordinates of x_f and z_f during deformation. The relation between the coordinates of A_f and A_i and the elongation of differential element are expressed as

$$x_f = x_i + u = x + u\,, \tag{A.1}$$

$$z_f = z_i + w = Z + w\,, \tag{A.2}$$

$$ds = \sqrt{\left(dx_f\right)^2 + \left(dz_f\right)^2} = \sqrt{\left(dx + du\right)^2 + \left(dZ + dw\right)^2} = \sqrt{\left(1 + u'\right)^2 + \left(Z' + w'\right)^2}\,dx\,, \tag{A.3}$$

where $'$ stands for the derivative with respect to x. The slope of the initial rise of the curved beam is smaller than unity according to the shallow arch approximations i.e. $\left(Z'\right)^2 \ll 1$; hence, Eq. (A.3) reduces to

$$ds = \sqrt{1 + 2u' + u'^2 + w'^2 + 2w'Z'}\,dx\,. \tag{A.4}$$

The strain for the differential element is obtained as follows

$$\varepsilon = \frac{ds - dx}{dx} = \sqrt{1 + 2u' + u'^2 + w'^2 + 2w'Z'} - 1\,, \tag{A.5}$$

Expanding Eq. (A.5) up to quadratic terms using Taylor series expansion for small u' and w', the mid-plan stretching is obtained as

$$\varepsilon \simeq u' + \frac{w'^2}{2} + w'Z'\,. \tag{A.6}$$

Now, the total strain at a point at distance z from the mid-plan us given by

$$\varepsilon_z \simeq \varepsilon - zw'' = u' + \frac{w'^2}{2} + w'Z' - zw'' . \tag{A.7}$$

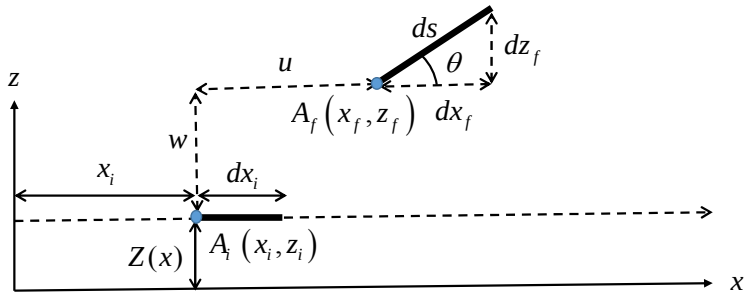

Figure A.1 Segment of the beam before and after deformation

Consider a thin tube of length L, cross-sectional area A, area moment of inertia I, Young's modulus E, and density ρ, the potential energy V and the kinetic energy T stored in the tube can be written as follows

$$\begin{aligned} V &= \frac{1}{2}\iiint_{Volume}\left(E\varepsilon_z^2\right)dydzdx \\ &= \frac{1}{2}\iiint_{Volume}\left(E\left[\left(u' + \frac{w'^2}{2} + w'Z'\right)^2 - zw''\left(u' + \frac{w'^2}{2} + w'Z'\right) + z^2 w''^2\right]\right)dydzdx , \\ &= \frac{EA}{2}\int_0^L\left(u' + \frac{w'^2}{2} + w'Z'\right)^2 dx + \frac{EI}{2}\int_0^L w''^2 dx \end{aligned} \tag{A.8}$$

$$T = \frac{\rho A}{2}\int_0^L \dot{w}^2 dx , \tag{A.9}$$

where the dot stands for the partial derivative with respect to the time variable.

The equations of motion of the tube can be derived by using Hamilton's principle as

$$\delta\int_{t_1}^{t_2}\left(T - V + W_e\right)dt = 0 , \tag{A.10}$$

where W_e is the work done by external loads on the system. Here, W_e is considered to be equal to zero. t_1 and t_2 are the initial and final times, respectively. Applying

integrating by parts and setting the coefficients of δu, δw equal to zero lead to the following equations of motion

$$\left(u' + \frac{w'^2}{2} + w'Z'\right)' = 0, \tag{A.11}$$

$$\rho A\ddot{w} + EIw'''' - EA\left(u' + \frac{w'^2}{2} + w'Z'\right)'\left(w' + Z'\right) - EA\left(u' + \frac{w'^2}{2} + w'Z'\right)\left(w'' + Z''\right) = 0, \tag{A.12}$$

respectively. Eq. (A.11) can be integrated over beam domain to obtain the beam elongation in axial direction as follows

$$u(L,t) - u(0,t) = \left(u' + \frac{w'^2}{2} + w'Z'\right)L - \int_0^L \left(\frac{w'^2}{2} + w'Z'\right)dx \tag{A.13}$$

Assuming small elongation in axial direction, Eq. (A.13) reduces to

$$\left(u' + \frac{w'^2}{2} + w'Z'\right) = \frac{1}{L}\int_0^L \left(\frac{w'^2}{2} + w'Z'\right)dx. \tag{A.14}$$

Substituting Eqs. (A.11) and (A.14) into Eq. (A.12), the nonlinear equation of motion in transverse direction can be obtained as follows

$$\rho A\ddot{w} + EIw'''' = \left[\frac{EA}{L}\int_0^L \left(\frac{w'^2}{2} + w'Z'\right)dx\right]\left(w'' + Z''\right). \tag{A.15}$$

APPENDIX B. Nonlinear vdW force terms

The nonlinearity matrix for the interlayer vdW force nonlinearity, considering three trial functions, is given in Eq. (4.33) where k_{ni} are defined as follow

$$k_{n1} = \left\|a_{i,1}^2\right\| + \left\|a_{i,1}a_{o,3}\right\| - 2\left\|a_{i,1}a_{o,1}\right\| - 4\left\|a_{i,3}a_{o,3}\right\| - 2\left\|a_{i,1}a_{i,3}\right\| + 2\left\|a_{i,3}^2\right\| - 4\left\|a_{i,3}a_{o,3}\right\| + \left\|a_{o,1}^2\right\| + \left\|a_{i,3}a_{o,1}\right\| - \left\|a_{o,1}a_{o,3}\right\| + 2\left\|a_{i,3}^2\right\| + 2\left(\left\|a_{i,2}\right\| - \left\|a_{o,2}\right\|\right)^2, \quad \text{(B.1)}$$

$$k_{n2} = \left\|a_{i,2}^2\right\| - 2\left\|a_{i,2}a_{o,2}\right\| - 2\left\|a_{i,3}a_{o,1}\right\| + 2\left\|a_{i,3}^2\right\| - 2\left\|a_{i,1}a_{o,3}\right\| + 2\left\|a_{i,3}a_{i,1}\right\| + \left\|a_{o,2}^2\right\| + 2\left\|a_{o,1}^2\right\| + 2\left\|a_{i,1}^2\right\| + 2\left\|a_{o,3}^2\right\| - 4\left\|a_{i,1}a_{o,1}\right\| + 2\left\|a_{o,1}a_{o,3}\right\| - 4\left\|a_{i,3}a_{o,3}\right\|, \quad \text{(B.2)}$$

$$k_{n3} = \left\|a_{i,3}^2\right\| - 3\left\|a_{i,3}a_{o,3}\right\| + 2\left\|a_{i,1}^2\right\| - 4\left\|a_{i,1}a_{o,1}\right\| + 2\left\|a_{o,1}^2\right\| + 2\left(\left\|a_{i,2}\right\| - \left\|a_{o,2}\right\|\right)^2, \quad \text{(B.3)}$$

$$k_{n4} = \left(\left\|a_{i,2}\right\| - \left\|a_{o,2}\right\|\right)^2, \quad \text{(B.4)}$$

$$k_{n5} = -\left\|a_{i,1}^2\right\| + 3\left\|a_{i,1}a_{o,1}\right\| + \left(\left\|a_{i,2}\right\| - \left\|a_{o,2}\right\|\right)^2. \quad \text{(B.5)}$$

APPENDIX C. Permissions

This thesis is prepared in integrated format where each chapter is a standalone article. Permissions have been given to the author to include the articles in this thesis. Copyright permissions are brought in this appendix.

C.1. Permission for Chapter 4: NONLINEAR FREE VIBRATION OF DOUBLE WALLED CARBON NANOTUBES BY USING DESCRIBING FUNCTION METHOD WITH MULTIPLE TRIAL FUNCTIONS

A version of this chapter is published in the Physica E: Low-dimensional Systems and Nanostructures as "Nonlinear Free Vibration of Double Walled Carbon Nanotubes by Using Describing Function Method with Multiple Trial Functions"

ELSEVIER LICENSE
TERMS AND CONDITIONS

Jun 07, 2014

This is a License Agreement between Hamed Samandari ("You") and Elsevier ("Elsevier") provided by Copyright Clearance Center ("CCC"). The license consists of your order details, the terms and conditions provided by Elsevier, and the payment terms and conditions.

All payments must be made in full to CCC. For payment instructions, please see information listed at the bottom of this form.

Supplier	Elsevier Limited The Boulevard,Langford Lane Kidlington,Oxford,OX5 1GB,UK
Registered Company Number	1982084
Customer name	Hamed Samandari
Customer address	ODTU Makina Muh Bolumi Ankara, 06800
License number	3403761380729
License date	Jun 07, 2014
Licensed content publisher	Elsevier
Licensed content publication	Physica E: Low-dimensional Systems and Nanostructures
Licensed content title	Nonlinear free vibration of double walled carbon nanotubes by using describing function method with multiple trial functions
Licensed content author	Ender Cigeroglu,Hamed Samandari
Licensed content date	September 2012
Licensed content volume number	46
Licensed content issue number	None
Number of pages	14
Start Page	160
End Page	173
Type of Use	reuse in a thesis/dissertation
Portion	full article
Format	both print and electronic
Are you the author of this Elsevier article?	Yes
Will you be translating?	No
Title of your thesis/dissertation	NONLINEAR VIBRATIONS OF CURVED SINGLE AND DOUBLE WALLED CARBON NANOTUBES
Expected completion date	Jul 2014

C.2. Permission for Chapter 6: DIFFERENTIAL QUADRATURE METHOD, A NOVEL METHOD TO STUDY NONLINEAR VIBRATIONS OF CNTS

A version of this chapter is published in the Physica E: Low-dimensional Systems and Nanostructures as “Nonlinear free Vibrations of curved double walled carbon Nanotubes using differential quadrature method”

ELSEVIER LICENSE
TERMS AND CONDITIONS

Jul 21, 2014

This is a License Agreement between Hamed Samandari ("You") and Elsevier ("Elsevier") provided by Copyright Clearance Center ("CCC"). The license consists of your order details, the terms and conditions provided by Elsevier, and the payment terms and conditions.

All payments must be made in full to CCC. For payment instructions, please see information listed at the bottom of this form.

Supplier	Elsevier Limited The Boulevard,Langford Lane Kidlington,Oxford,OX5 1GB,UK
Registered Company Number	1982084
Customer name	Hamed Samandari
Customer address	ODTU Makina Muh Bolumi Ankara, 06800
License number	3433540107082
License date	Jul 21, 2014
Licensed content publisher	Elsevier
Licensed content publication	Physica E: Low-dimensional Systems and Nanostructures
Licensed content title	Nonlinear free Vibrations of curved double walled carbon Nanotubes using differential quadrature method
Licensed content author	Ender Cigeroglu,Hamed Samandari
Licensed content date	16 July 2014
Licensed content volume number	None
Licensed content issue number	None
Number of pages	1
Start Page	0
End Page	0
Type of Use	reuse in a thesis/dissertation
Intended publisher of new work	other
Portion	full article
Format	both print and electronic
Are you the author of this Elsevier article?	Yes
Will you be translating?	No
Title of your thesis/dissertation	NONLINEAR VIBRATIONS OF CURVED SINGLE AND DOUBLE WALLED CARBON NANOTUBES
Expected completion date	Jul 2014

CURRICULUM VITAE

➢ PERSONAL INFORMATION

Mr. Hamed Samandari
Nationality: Iranian
Mobile: (+90) 537-5081365
hamed.samandari@gmail.com

➢ EDUCATION

- Ph.D. Mechanical Engineering, 2011-2014
  Middle East Technical University, Ankara, Turkey
- MSc. Mechanical Engineering, 2008-2011
  University of Tabriz, Tabriz, Iran
- BSc. Mechanical Engineering, 2004-2008
  Isfahan University of Technology (IUT), Isfahan, Iran

➢ PUBLICATIONS

- ✓ Cigeroglu E. and Samandari H., 2014, "Nonlinear Free Vibrations of Curved Double Walled Carbon Nanotubes Using Differential Quadrature Method", *Journal of Physica E*
- ✓ Cigeroglu E., and Samandari H., 2012, "Nonlinear Free Vibration of Double Walled Carbon Nanotubes by Using Describing Function Method with Multiple Trial Functions", *Journal of Physica E*.
- ✓ Hamed Samandari, Mousa Rezaee, 2011, "Chaotic behavior and resonances of a nonlinear vehicle suspension system" Published in *Journal of Applied and computational Sciences in Mechanics* 2010 (In Persian).
- ✓ Samandari H., and Cigeroglu E., 2013, "Nonlinear Free Vibration of Curved Double Walled Carbon Nanotubes Using Differential Quadrature Method", Proceeding of the *IMAC XXXI A Conference and Exposition on Structural Dynamics*, February 11 - 14, 2013, California, USA.

- ✓ H. Samandari, M. Rezaee, 2011, "The Influence of Shock absorber parameters on the Aircraft Dynamics during Landing on a bumpy runway", presented at the *10th Conference of Iranian aerospace society*, March 1-3, 2011, Tehran, Iran (In Persian).
- ✓ H. Hajkarami, H. Samandari, S. Ziaei-Rad, 2009, "Analysis of chaotic vibration of a Nonlinear Seven Degrees of Freedom Full Vehicle model", *3rd International Conference on Integrity, Reliability and Failure*, Porto, 20-24 July 2009.

➢ PRESENTATIONS

- ✓ Samandari H., and Cigeroglu E., 2014, "Nonlinear Free Vibration Analysis of Nonuniform Rotating Double Walled Carbon Nanotubes", Presented and published in the *16th International Conference on Machine Design and Production*, June 30 - July 3, 2014, Izmir, Turkey.
- ✓ Samandari H., and Cigeroglu E., 2012, "Effect of Waviness on the Variation of Nonlinear Fundamental Natural Frequency of Single Wall Carbon Nanotube by Using Multiple Harmonic Balance Method", Presented and published in proceeding of the *2012 Space Elevator Conference*, August 25-27, 2012, Seattle, Washington, USA.
- ✓ Sadeghi M.H., Soleimanian P., Samandari H. , 2012, "Model Updating of Complex Assembly Structures Based on Substructures-joint Parameters ",Presented and published in proceeding of *IMAC XXX A Conference and Exposition on Structural Dynamics*, January 30 – February 2, 2012, Jacksonville, Florida USA.
- ✓ Samandari H., and Cigeroglu E., 2012, "Nonlinear Free Vibration Analysis of Double Walled Carbon Nanotubes with a Concentrated-Mass", Presented and published in proceeding of the *15th International Conference on Machine Design and Production*, June 19 - 22, 2012, Pamukkale, Denizli, Turkey.
- ✓ Hamed Samandari, Mousa Rezaee, 2010, "The Stability and Chaos Analysis of a Nonlinear Wheeled Vehicle Under Road Excitation", Presented and published in proceeding of the *ASME 2010 10th Biennial Conference on Engineering Systems Design and Analysis*, July 12-14, 2010, Istanbul, Turkey